



**UNIVERSITY OF
KWAZULU-NATAL** TM

**INYUVESI
YAKWAZULU-NATALI**

**AN INVESTIGATION INTO THE MOLECULAR AND EPIGENETIC
ALTERATIONS ASSOCIATED WITH FUMONISIN B₁-INDUCED
TOXICITY IN HUMAN LIVER (HEPG2) CELLS**

By

THILONA ARUMUGAM

B. Med. Sc. (Hons), M. Med Sc (Medical Biochemistry)

**Submitted in fulfilment for the degree of
Doctor of Philosophy (Medical Biochemistry),
School of Laboratory Medicine and Medical Science,
College of Health Sciences,
University of KwaZulu-Natal**

Supervisors

Prof. Anil A. Chuturgoon

Dr. Terisha Ghazi

2020

DECLARATION

I, **Thilona Arumugam**, declare that:

- i. The research reported in this thesis, except where otherwise indicated, is my original work.
- ii. This thesis has not been submitted for any degree or examination at another university.
- iii. This thesis does not contain other persons' data, pictures, graphs, or other information, unless specifically acknowledged as being sourced from other persons.
- iv. This thesis does not contain other person's writing, unless specifically acknowledged as being sourced from other researchers. Where other written sources have been quoted, then:
 - a. their words have been re-written but the general information sourced has been referenced to the authors;
 - b. where their exact words have been used, their writing has been placed within quotation marks, and referenced.
- v. Where I have reproduced a publication of which I am an author, co-author, or editor, I have indicated in detail which part of the publication was written by myself alone and have fully referenced such publications.
- vi. This thesis does not contain text, graphics, or tables copied and pasted from the internet, unless specifically acknowledged, and the source being detailed in the thesis and reference section.

The research described in this study was carried out in the Discipline of Medical Biochemistry, School of Laboratory Medicine and Medical Science, College of Health Sciences, University of Kwa-Zulu Natal, under the supervision of Professor A.A. Chuturgoon, and Dr T. Ghazi.


Miss Thilona Arumugam

02/12/2020

Date

DEDICATION

To my parents, **Imantha** and **Erwin Arumugam**, for always believing in me and encouraging me to strive for excellence.

ACKNOWLEDGEMENTS

My family

Thank you for your guidance, support and allowing me every opportunity to further my education and knowledge. I appreciate everything that you have done for me, your continuous encouragement, support and patience is deeply appreciated.

Prof Anil Chuturgoon

Thank you for the opportunity to not only grow as a scientist but to be inspired and motivated. I will always be grateful to you for your guidance, encouragement during difficult times and never allowing me to lose sight of my own worth. It is an honour to learn from a great and dedicated scientist such as yourself.

Dr Terisha Ghazi

I cannot thank you enough for all your patience, advice, corrections, suggestions and contributions that enabled me to complete this thesis and become a better scientist. You are an amazing mentor and friend.

Friends and Colleagues of Medical Biochemistry

Thank you for your friendship and help throughout the years. A special thanks to Mr. Theolan Adimulam for always being someone I could count on.

Funding Sources

I would like to thank the National Research Foundation (Grant no.: SFH170627245272) and the University of KwaZulu-Natal College of Health Sciences for financially supporting this study.

PUBLICATIONS

1. Arumugam, T., Pillay, Y., Ghazi, T., Nagiah, S., Abdul, N. S., and Chuturgoon, A. A. (2019). Fumonisin B₁-induced oxidative stress triggers Nrf2-mediated antioxidant response in human hepatocellular carcinoma (HepG2) cells. **Mycotoxin Research**, 35 (1), 99-109. DOI: [10.1007/s12550-018-0335-0](https://doi.org/10.1007/s12550-018-0335-0)
2. Arumugam T., Ghazi T., Chuturgoon A.A. (2020). Fumonisin B₁ Epigenetically Regulates PTEN Expression and Modulates DNA Damage Checkpoint Regulation in HepG2 Liver Cells. **Toxins**, 12(10):625. DOI: [10.3390/toxins12100625](https://doi.org/10.3390/toxins12100625).
3. Arumugam T., Ghazi T., Chuturgoon A.A. (2020). Fumonisin B₁ Alters Global m6A RNA Methylation and Epigenetically Regulates Keap1-Nrf2 Signaling in Human Hepatoma (HepG2) Cells. **Archives of Toxicology** (*In Review*). Manuscript ID: ATOX-D-20-00996.
4. Arumugam T., Ghazi T., Chuturgoon A.A. (2020). Fumonisin B₁ inhibits p53-dependent apoptosis via HOXA11-AS/miR-124/DNMT axis in human hepatoma (HepG2) cells. **Archives of Toxicology** (*In Review*). Manuscript ID: ATOX-D-20-00999.
5. Arumugam T., Ghazi T., Chuturgoon A.A. (2020). Molecular and Epigenetic Modes of Fumonisin B₁-Mediated Toxicity and Carcinogenesis and Detoxification Strategies. **Critical Reviews in Toxicology** (*In Review*). Manuscript ID: BTXC-2020-0101
6. Arumugam T., Ghazi T., Abdul N.S., Chuturgoon A.A. (2020). A review on the oxidative effects of the fusariotoxins: Fumonisin B₁ and fusaric acid. **In Toxicology**, Chapter 19, 181-190. Academic Press. DOI: [10.1016/B978-0-12-819092-0.00019-4](https://doi.org/10.1016/B978-0-12-819092-0.00019-4).
7. Ghazi, T., Arumugam, T., Foolchand, A., & Chuturgoon, A. A. (2020). The Impact of Natural Dietary Compounds and Food-Borne Mycotoxins on DNA Methylation and Cancer. **Cells**, 9(9):2004. DOI: [10.3390/cells9092004](https://doi.org/10.3390/cells9092004)

PRESENTATIONS

1. Arumugam, T., Nagiah, S., Pillay, Y., Chuturgoon, A.A. (2017), Fumonisin B1 induced oxidative stress in human liver (HepG2) cells- an alternate mechanism of carcinogenesis. College of Health Sciences Research Symposium, University of Kwa-Zulu Natal, Durban, South Africa – 2nd Prize Oral Presentation.
2. Arumugam, T., Nagiah, S., Pillay, Y., Chuturgoon, A.A. (2018), Fumonisin B1 induced oxidative stress in human liver (HepG2) cells- an alternate mechanism of carcinogenesis. PathCape Congress 2018, Rejuvenating Pathology - Stellenbosch, South Africa.
3. Arumugam, T., Ghazi T., Chuturgoon, A.A. (2019), Fumonisin B₁ Epigenetically Regulates PTEN Expression and Modulates DNA Damage Checkpoint Regulation in HepG2 Liver Cells. College of Health Sciences Research Symposium, University of Kwa-Zulu Natal, Durban, South Africa.

Table of Contents

DECLARATION	ii
DEDICATION	iii
ACKNOWLEDGEMENTS	iv
PUBLICATIONS	v
PRESENTATIONS	vi
LIST OF FIGURES	ix
LIST OF TABLES	xi
ABBREVIATIONS	xii
ABSTRACT	xvi
CHAPTER 1: Introduction	1
CHAPTER 2: Literature Review	13
2.1. <i>Fusarium</i> Mycotoxins	13
2.1.1. Fumonisin B ₁	14
2.1.1.1. Structure and Biosynthesis	15
2.1.1.2. Primary mechanism of toxicity	16
2.1.1.3. Impact of FB1 on human and animal health	17
2.2. Epigenetics	18
2.2.1. DNA Methylation	19
2.2.1.1. Regulation of DNA Methylation	20
2.2.2. Histone Modifications	23
2.2.2.1. H3K4me3	25
2.2.3. RNA methylation: N6-methyladenosine	26
2.2.4. NcRNA	28
2.2.4.1. MiRNAs	29
2.2.4.1.1. Biogenesis	30
2.2.4.1.2. Regulation of gene expression	31
2.2.4.2. LncRNAs	31
2.2.4.2.1. Biogenesis	32
2.2.4.2.2. Functions	33
2.2.4.3. Regulation of miRNA by lncRNAs	35
2.2.5. The role of epigenetics in <i>Fusarium</i> mycotoxin induced toxicities	35
2.3. Cellular Response to stress	37
2.3.1. The DNA damage response	37
2.3.1.1. CHK1	38

2.3.2. Keap-1/Nrf2 anti-oxidant signalling	39
2.3.2.1. Epigenetic regulation of Keap1/Nrf2.....	40
2.3.3. Apoptosis	41
2.3.3.1. Caspase	43
2.3.3.2.. Pathways of apoptosis.....	43
2.3.3.2.1. Intrinsic apoptotic program.....	43
2.3.3.2.2. Extrinsic Apoptotic program.....	44
2.3.3.2.3. Execution of apoptosis.....	45
2.3.3.3. p53.....	45
2.3.3.3.1. p53-mediated apoptosis	47
2.4. References.....	48
CHAPTER 3: Molecular and Epigenetic Modes of Fumonisin B ₁ -Mediated Toxicity and Carcinogenesis and Detoxification Strategies	64
CHAPTER 4: Fumonisin B ₁ Epigenetically Regulates PTEN Expression and Modulates DNA Damage Checkpoint Regulation in HepG2 Liver Cells.....	107
CHAPTER 5: Fumonisin B ₁ Alters Global m ⁶ A RNA Methylation and Epigenetically Regulates Keap1-Nrf2 Signaling in Human Hepatoma (HepG2) Cells	133
CHAPTER 6: Fumonisin B ₁ inhibits p53-dependent apoptosis via HOXA11-AS/miR- 124/DNMT axis in human hepatoma (HepG2) cells.	156
CHAPTER 7: Conclusion	182
ADDENDUM A	187
ADDENDUM B.....	200

LIST OF FIGURES

Figure 2.1. Chemical structure of the main <i>Fusarium</i> mycotoxins (Ferrigo et al., 2016)	14
Figure 2.2. FUM mediated biosynthesis of FB ₁	16
Figure 2.3. The complex epigenetic landscape (Aristizabal et al., 2020)	19
Figure 2.4. Regulation of gene expression via DNA methylation	20
Figure 2.5: Regulation of DNA methylation	23
Figure 2.6. Schematic representation of some of the modifications found on histone tails of core histones (H2A, H2B, H3, H4) (Ueda and Seki, 2020)	24
Figure 2.7. m6A modification machinery (prepared by author)	27
Figure 2.8. The canonical pathway of miRNA biogenesis	30
Figure 2.9. Classification of lncRNA based on the location in the genome (Choudhari et al., 2020).	32
Figure 2.10. General mechanism by which lncRNA function	34
Figure 2.11. Interaction between ncRNA and mRNA	35
Figure 2.12. DNA damage response network	38
Figure 2.13. (A) Nrf2 promotes the transcription of antioxidants as well as phase II and III detoxifying enzymes. (B) Oxidative stress triggers Nrf2 dissociation from Keap1 and induces transcription of ARE genes (Arumugam et al., 2020).	40
Figure 2.14. Morphological changes that occur during apoptosis	42
Figure 2.15. Intrinsic and extrinsic signalling of apoptosis (Glowacki et al., 2013).	45
Figure 2.16. p53 responds to a plethora of stress signals and regulates diverse responses (Biegging and Attardi, 2012).	46
Figure 2.17. Mechanisms of p53-mediated apoptosis via Bcl2-regulated pathway (Aubrey et al., 2018).	48
Figure 3.1. The molecular structure of FB ₁ , HFB ₁ and the sphingoid bases, Sa and So.	72
Figure 3.2. An overview of the effect of FB ₁ and its metabolites on sphingolipid metabolism.	75
Figure 3.3. FB ₁ disrupts redox homeostasis.	78
Figure 3.4. FB ₁ -induced ER stress mediates autophagy.	81
Figure 3.5. An overview of the toxic and carcinogenic modes of action by FB ₁ as well as strategies involved in its detoxification	89
Figure 4.1. Fumonisin B ₁ (FB ₁) significantly increased the oxidative DNA damage biomarker, 8-OHdG, in human hepatoma G2 (HepG2) cells	113

Figure 4.2. The effect of FB ₁ on miR-30c levels in HepG2 cells and potential miR-30c targets.	114
Figure 4.3. The effect of FB ₁ on KDM5B and H3K4me3 levels in HepG2 cells.	115
Figure 4.4. FB ₁ -induced KDM5B and miR-30c modulates PTEN expression.	116
Figure 4.5. The effect of FB ₁ on the PI3K/AKT signaling cascade.	117
Figure 4.6. The effect of FB ₁ on CHK1 expression.	118
Figure 4.7. FB ₁ induces oxidative DNA damage and epigenetically regulates PTEN/PI3K/AKT/CHK1 axis by epigenetically regulating PTEN.	121
Supplementary Figure 4.1. The cytotoxic effects of FB ₁ on HepG2 cells.	122
Supplementary Figure 4.2. FB ₁ induced 8-OHdG levels in HepG2 cells.	122
Supplementary Figure 4.3: FB ₁ altered miR-30c expression in HepG2 cells	123
Supplementary Figure 4.4: The effect of FB ₁ on KDM5B and H3K4me3 expression in HepG2 cells.	123
Supplementary Figure 4.5: FB ₁ induced KDM5B and miR-30c modulates PTEN expression.	124
Supplementary Figure 4.6: The effect of FB ₁ on the PI3K/AKT signalling cascade.	125
Supplementary Figure 4.7: The influence of FB ₁ on CHK1 expression in HepG2 cells.	125
Figure 5.1. FB ₁ -induced intracellular ROS generation and LDH leakage	140
Figure 5.2. Aberrant m ⁶ A modification induced by FB ₁ in HepG2 cells.	141
Figure 5.3. The epigenetic effects of FB ₁ on Keap1 expression in HepG2 cells.	142
Figure 5.4. FB ₁ epigenetically regulates Nrf2 expression in HepG2 cells.	144
Figure 5.5. FB ₁ alters global m ⁶ A RNA methylation and epigenetically regulates Keap1-Nrf2 signaling.	148
Supplementary Figure S5.1. TargetScan analyses of miR-27b to the 3' UTR of <i>NFE2L2</i> (<i>Nrf2</i>) in humans. MiR-27b has complementary base pairs with the 3' UTR of <i>Nrf2</i> at positions 62-68 in humans.	150
Figure 6.1. Effect of FB ₁ on HOXA11-AS, miR-124, DNMT3B and SP1	164
Figure 6.2. Effect of FB ₁ on DNMT1.	165
Figure 6.3. Effect of FB ₁ on DNMT3A and global DNA methylation	166
Figure 6.4. Effect of FB ₁ on the methylation of p53 promoters and p53 expression	167
Figure 6.5. Effect of FB ₁ on caspase activity	167
Figure 6.6. FB ₁ inhibits p53 via HOXA11-AS/miR-124/DNMT axis.	171

Supplementary Figure S6.1. FB ₁ alters lncRNA profiles in HepG2 cells.	174
Supplementary Figure S6.2. starBase v2.0 analyses of HOXA11-AS interaction humans.	174
Supplementary Figure S6.3. TargetScan analyses of miR-124 to the 3' UTR of <i>SPI</i> and <i>DNMT3B</i> in humans.	175

LIST OF TABLES

Table 2.1: The localization and function of YTH domain containing m6A-readers	28
Table 2.2: Characteristics and functioning of regulatory ncRNAs	29
Table 2.3: Classification of lncRNA	32
Table 2.4: Epigenetic regulation of Keap-1 and Nrf2	41
Table 3.1: Studies evaluating the development of neoplastic lesions in <i>in vivo</i> models exposed to <i>F. verticillioides</i> and/or FB ₁	67
Table 4.1: The annealing temperatures (°C) and primer sequences for the genes of interest.	111
Supplementary Table S5.1: Primer sequences and annealing temperatures used in qPCRs	149
Supplementary Table S6.1: Antibodies with dilutions used for western blotting	172
Supplementary Table S6.2: Primer sequences and annealing temperatures used in qPCRs	173

ABBREVIATIONS

1-deoxySa	1-deoxysphinganine
2-AAF/PH	2-acetylaminofluorene/partial hepatectomy
5-Aza-2-dc	5-Aza-2-deoxycytidine
5caC	5-carboxylcytosine
5fC	5-formylcytosine
5hmC	5-hydroxymethylcytosine
5hmU	5-hydroxymethyluracil
5mC	5-methylcytosine
8-OHdG	8-hydroxy-2'-deoxyguanosine
A	Adenosine
AFB ₁	Aflatoxin B1
AGO	Argonaute
AID/APOBEC	Activation-induced cytidine deaminase/apolipoprotein B mRNA-editing catalytic polypeptides
AKT	Protein kinase B
Apaf-1	apoptotic protease activating factor-1
ATP	Adenosine triphosphate
CAD	Caspase-activated deoxyribonuclease
CCM	Complete culture media
cDNA	Complementary DNA
ceRNA	Competing endogenous RNA
CERT	Ceramide transport protein
ChIP	Chromatin immunoprecipitation
CpG	Cytosine phosphate guanine
CS	Ceramide synthase
Ct	Comparative threshold cycle
Cul3	Cullin-3 E3-ubiquitin ligase
DDR	DNA damage response
DEHP	di-(2-ethylhexyl) phthalate
DEN	Diethylnitrosamine
DGCR8	DiGeorge Syndrome Critical Region 8
DISC	Death-inducing signalling complex
DNA	Deoxyribonucleic acid
DNMT	DNA methyltransferase
DON	Deoxynivalenol

DR3	Death receptor 3
EDTA	Ethylenediaminetetraacetic acid
ELEM	Equine leukoencephalomalacia
EMEM	Eagles minimum essentials medium
ER	Endoplasmic reticulum
ERAD	ER-associated degradation
ETC	Electron transport chain
EZH2	Enhancer of zeste homolog 2
F6A	N6-formyladenosine
FADD	Fas-associated death domain
FasR	Fas receptor
FB ₁	Fumonisin B ₁
GSTP ⁺	Glutathione-S-transferase-positive
GGT ⁺	Gamma-glutamyl-transpeptidase-positive
H	Histone
H2DCF-DA	2,7-dichlorodihydrofluorescein-diacetate
H3K4me3	Histone 3 lysine 4 tri-methylation
HAT	Histone acetyl transferase
HepG2	Human liver cell line
HDAC	Histone deacetylase
HFB ₁	Hydrolysed FB ₁
hm6A	N6-hydroxymethyladenosine
HOTAIR	HOX transcript antisense RNA
HOX11-AS	Homeobox A11 antisense RNA
IARC	International Agency of Research on Cancer
IL	Interleukin
INF- γ	Interferon gamma
JAK/STAT	Janus kinase/Signal transducer and activator of transcription
K	Lysine
KDM	Histone lysine demethylase
Keap1	Kelch-like ECH-associated protein 1
KMT2	Histone lysine methyltransferase
LDH	Lactose dehydrogenase
lncRNA	Long non-coding RNA
LHX8	LIM Homeobox 8
m6A	N-6-methyladenosine

MAPK	Mitogen activated protein kinase
MBD	Methyl-CpG binding domain
MDM2	Murine double minute 2
MeCP2	Methyl CpG binding protein 2
METTL3	Methyltransferase-like-3
METTL14	Methyltransferase-like-14
miRISC	RNA induced silencing complex
miRNA	MicroRNA
MRE	MiRNA Response Element
MRN	MRe11-Rad 50-Nbs1
mRNA	Messenger RNA
ncRNA	Non-coding Ribonucleic acid
NF κ B	Nuclear factor kappa B
NIC	Nivalenol
Nrf2	Nuclear factor erythroid 2-related factor 2
nt	Nucleotide
NTD	Neural tube defects
qPCR	Quantitative Polymerase Chain Reaction
PANDA	p21-associated ncRNA DNA damage -activated
PBS	Phosphate buffered saline
PH	Partial hepatectomy
PHFB ₁	Partially hydrolysed FB $\bar{1}$
PI3K	Phosphatidylinositol 3-kinase
PIP3	Phosphatidylinositol-3,4,5-triphosphate
ppm	Part per million
PRC2	Polycomb repressive complex 2
pre-miRNA	Precursor-miRNA
pri-miRNA	Primary-miRNA
PTEN	Phosphatase and tensin homolog
R	Arginine
RBD	Relative band density
RBM	RNA binding protein
RIP	RNA immunoprecipitation
RNA	Ribonucleic acid
RNAP	RNA Polymerase
ROS	Reactive oxygen species

rRNA	ribosomal RNA
RT	Room temperature
Sa	Sphinganine
Sa1p	Sphinganine-1-phosphate
SAM	S-adenosylmethionine
SD	Standard deviation
SDS	Sodium dodecyl sulphate
SET	Su(var)3-9, Enhancer-of-zester and Trithorax
shRNA	Small hairpin RNA
siRNA	Silencing RNA
siR-NC	Negative control siRNA
snRNA	Small nuclear RNAs
snoRNA	Small nucleolar RNAs
So	Sphingosine
So1P	Sphingosine-1-phosphate
SPK1	Sphingosine kinase 1
SPT	Serine palmitoyltransferase
START	Steroidogenic acute regulatory protein-related lipid transfer
TET	Ten-eleven translocation
TDG	Thymine DNA glycolase
TNF	Tumor necrosis factor
TNFR	Tumor necrosis factor receptor
TRADD	TNFR-associated death domain
TRAILR	TNF-related apoptosis inducing ligand receptor
tRNA	Transfer RNA
TTBS	Tween 20-Tris buffer saline
UHRF	Ubiquitin-like and ring finger domain 1
UPR	Unfolded protein response
UTR	Untranslated region
WHO	World Health Organization
WTAP	Wilm's tumour 1-associated protein
YTHDC	YT521-B homology domain containing
YTHDF	YT521-B homology domain family

ABSTRACT

The contamination of agricultural commodities with *Fusarium* mycotoxins is a global issue in food safety, with fumonisin B₁ (FB₁) being the most prevalent contaminant. FB₁ is not only phytotoxic, but it induces a wide range of toxic effects in animals and humans and is associated with carcinogenesis in animals and humans. Intense research has uncovered several mechanisms by which FB₁ induces toxicity. Recent evidence suggests that epigenetic mechanisms may also contribute to the toxic effects of FB₁. Epigenetic modifications including DNA methylation, histone methylation, N⁶-methyladenosine (m⁶A) RNA methylation, and non-coding RNAs such as microRNAs (miRNA) and long non-coding RNA (lncRNA) are central mediators of cellular function and cellular stress responses and disruption may be pertinent in FB₁-induced toxicities. This study aimed to determine the epigenetic mechanisms of FB₁-induced hepatotoxicity by specifically investigating changes in DNA methylation, histone 3 lysine 4 trimethylation (H3K4me₃), m⁶A RNA modification, and noncoding RNA in human hepatoma (HepG2) cells. The effect of these FB₁-induced epigenetic modifications on stress responses was further investigated.

FB₁ impairs DNA repair processes via epigenetic mechanism. FB₁ reduced the expression of histone demethylase, KDM5B, which subsequently increased the total H3K4me₃ and the enrichment of H3K4me₃ at the *PTEN* promoter region; this led to an increase in *PTEN* transcript levels. However, miR-30c inhibited PTEN translation. Thus, PI3K/AKT signaling was activated, inhibiting CHK1 activity via phosphorylation of its serine 280 residue. This hampered the repair of oxidative DNA damage that occurred as a result of FB₁ exposure.

Exposure to FB₁ not only induced oxidative DNA damage but elevated levels of intracellular ROS triggering cell injury. In response to oxidative injury, cells induce Keap1/Nrf2 signaling which is regulated by epigenetic mechanisms. FB₁ elevated global m⁶A RNA levels which were accompanied by an increase in m⁶A “writers”: *METTL3* and *METTL14*, and “readers”: *YTHDF1*, *YTHDF2*, *YTHDF3* and *YTHDC2* and a decrease in m⁶A “erasers”: *ALKBH5* and *FTO*. Hypermethylation occurred at the *Keap1* promoter, resulting in a reduction of *Keap1* transcripts. The hypomethylation of *Nrf2* promoters and decrease in miR-27b expression led to an increase in *Nrf2* mRNA expression. m⁶A-*Keap1* and m⁶A-*Nrf2* levels were both elevated; however, protein expression of Keap1 was reduced whereas Nrf2 was increased. Collectively, these epigenetic modifications (promoter methylation, miRNA-27b and m⁶A RNA) activated antioxidant signaling by reducing Keap1 expression and increasing Nrf2 expression.

If cells are unable to cope with stress, p53-mediated apoptosis is activated. Crosstalk between the lncRNA, HOXA11-AS, miR-124 and DNA methylation can influence p53 expression and apoptosis. FB₁ upregulated HOXA11-AS leading to the subsequent decrease in miR-124 and increase in *SP1* and DNA methyltransferases (DNMT1, DNMT3A, and DNMT3B). This promoted global DNA

methylation and hypermethylation of *p53* promoters, thereby reducing p53 expression and caspase activity. Taken together, the data suggests that FB₁ inhibits p53-dependent apoptosis via HOXA11-AS/miR-124/DNMT axis.

Collectively, this study provides novel insights into additional mechanisms of FB₁-induced toxicities by epigenetically modulating stress response mechanisms.

1
2
3
4
5
6
7
8
9
10
11
12
13
14
15
16
17
18
19
20
21
22
23
24
25
26
27
28
29
30
31
32
33
34
35

CHAPTER 1

INTRODUCTION

One of the United Nations sustainable development goals is achieving food safety and security in developing countries. However, almost 30% of global agricultural crops are contaminated by toxic fungal secondary metabolites referred to as mycotoxins (Nesic, Ivanovic et al. 2014, Gbashi, Madala et al. 2018). Annually, over one billion tons of crops are lost due to mycotoxin contamination and it reduces the quality of an already limited food supply (Gbashi, Madala et al. 2018). Contamination frequently occurs in dietary staples that rural and developing communities heavily rely on. These staples include cereal grains such as maize, rice, wheat, oats and sorghum as well as ground nuts, fruit, and their byproducts (Fernández-Cruz, Mansilla et al. 2010, Tolosa, Font et al. 2013, Ferrigo, Raiola et al. 2016, Lee and Ryu 2017). Moreover, the eminent reality of climate change further exacerbates the situation as fungal growth and mycotoxin production thrive during weather extremes and plant stress (Magan, Medina et al. 2011). The ingestion of mycotoxin contaminated crops has enormous public health significance because these toxins are usually nephrotoxic, hepatotoxic, immunotoxic, teratogenic and mutagenic (Zain 2011). Over 300 chemically distinct mycotoxins with diverse biological activities have been identified (Nesic, Ivanovic et al. 2014). Among them, fumonisin B₁ (FB₁) is one of the most important in terms of prevalence, contamination levels and toxic effects (Rheeder, Marasas et al. 2002). FB₁ is a diester that arises from the condensation of two molecules of propane-1,2,3-tricarboxylic acid and 2-amino-12,16-dimethylcosane-3,5,10,14,15-pentol (Alexander, Proctor et al. 2009). *Fusarium verticillioides* and *Fusarium proliferatum* are major FB₁ producers with contamination occurring globally (Rheeder, Marasas et al. 2002). FB₁ is found in abundance in maize, wheat, rice, oats, barley, and millets and has been reported to contaminate numerous food products including vine fruit, asparagus, cornflakes, beers, beef, egg, and milk and canned foods (Gazzotti, Lugoboni et al. 2009, Lee and Ryu 2017, Farhadi, Nowrozi et al. 2019). FB₁ contamination occurs at various points in the food chain including storage and is resistant to many food processing techniques making it difficult to control contamination of foods and feeds as well as human and animal exposure (Kamle, Mahato et al. 2019). Currently, several countries employ strict regulations to keep levels of FB₁ low in food. Acceptable limits of FB₁ in maize intended for human consumption range from 1 to 2 parts per million (ppm). The Scientific Committee on Food (SCF) and the joint Food and Agriculture Organization (FAO)/ World Health Organisation (WHO) Expert Committee for Food Additives (JECFA) independently established a provisional maximum tolerable daily intake (TDI) of 2 µg/kg body weight/day for FB₁, which was later expanded to include FB₁ alone or in combination with FB₂ and FB₃. This was based on a no-observable-adverse-effects level (NOAEL) in the liver and kidney of rodent models (SCF/EC 2000, FOA/WHO 2002, SCF/EC 2003). Since mycotoxins can be altered by plant defense mechanisms which

36 often masks their presence during analysis, the European Food Safety Authority (EFSA) established a
37 TDI of 1.0 µg/kg bw per day of FB₁ alone or in combination with FB₂, FB₃, and FB₄ (EFSA 2018).
38 Food that does not reach regulatory limits for human consumption are either used as animal feed or
39 discarded completely. This leads to large annual losses in the agricultural industry (Gbashi, Madala et
40 al. 2018). In many developing countries with a high-cereal consumption, regulation is either lacking or
41 not enforced (Gbashi, Madala et al. 2018). Furthermore, FB₁ contamination and exposure is higher in
42 low income countries, where rural subsistence farming communities are common (Mngqawa, Shephard
43 et al. 2016, Alberts, Rheeder et al. 2019). Young children weaned on maize-based food are also
44 vulnerable to FB₁ exposure that exceed the TDI (Shirima, Kimanya et al. 2013, Chen, Riley et al. 2018).

45 FB₁ is responsible for several pathological states in humans and animals. It is known to induce
46 leukoencephalomalacia in equine, oedema in porcine and liver and renal toxicities in equine, porcine
47 and rodents (Klarić and Pepeljnjak 2001, Voss, Smith et al. 2007, EFSA 2018). The International
48 Agency for Research on Cancer (IARC) has classified FB₁ as a group 2 carcinogen as it is known to
49 initiate and promote the development of renal, hepatocellular and cholangiocarcinoma in rodents, and
50 is associated with the development of human esophageal (and in one case hepatocellular) carcinomas
51 in regions that have a high maize consumption (Sydenham, Thiel et al. 1990, Dragan, Bidlack et al.
52 2001, IARC 2002, Sun, Wang et al. 2007, Alizadeh, Roshandel et al. 2012). Due to its structural
53 similarity to sphingoid bases, the primary mechanism by which FB₁ induces its toxicity is through the
54 disruption of sphingolipid metabolism. This inhibitory action interferes with signal transduction, cell
55 cycle regulation and the functioning of lipid containing molecules such as cell membranes (Wang,
56 Norred et al. 1991). FB₁ is known to trigger a host of other toxic responses such as oxidative stress,
57 endoplasmic reticulum (ER) stress, disrupts cell cycle and alterations in immune responses
58 (Chuturgoon, Phulukdaree et al. 2015, Yin, Guo et al. 2016, Arumugam, Pillay et al. 2019, Arumugam,
59 Ghazi et al. 2020, Liu, Zhang et al. 2020). It also disrupts anti-oxidant signaling and cell death
60 mechanisms (Chuturgoon, Phulukdaree et al. 2015, Arumugam, Pillay et al. 2019).

61 It has become increasingly clear that epigenetic mechanisms may also be exacerbate FB₁ induced
62 toxicities. Epigenetics involves phenotypic variations that are brought about by regulating gene
63 expression rather than altering DNA sequences (Bollati and Baccarelli 2010). Epigenetic modifications
64 are essential for the normal cellular processes and maintenance of gene expression patterns; however,
65 aberrant modifications can affect genome stability or have toxic and carcinogenic effects (Ho, Johnson
66 et al. 2012, Shamsi, Firoz et al. 2017). Epigenetic modifications include changes in DNA methylation,
67 RNA methylation [such as N⁶-Methyladenosine (m⁶A)], histone modifications and non-coding RNAs
68 (ncRNA) such as microRNA (miRNA) and long-noncoding RNA (lncRNA) (Bannister and Kouzarides
69 2011, Moore, Le et al. 2013, Zaccara, Ries et al. 2019, Yang, Liu et al. 2020).

70 Several studies have investigated the impact of FB₁ on DNA methylation and histone modifications;
71 however, the results are often conflicting. FB₁ induced global hypermethylation of DNA in rat C6

72 glioma cells and human Caco-2 cells; however, hypomethylation was observed in HepG2 cells and no
73 significant changes occurred in rat liver (Clone 9 cells) and kidney epithelial cells (NRK-52E) (Mobio,
74 Anane et al. 2000, Kouadio, Dano et al. 2007, Chuturgoon, Phulukdaree et al. 2014, Demirel,
75 Alpertunga et al. 2015). Furthermore, FB₁ induced methylation of CpG islands found on the promoter
76 regions of tumor suppressor genes (Demirel, Alpertunga et al. 2015). With regards to histone
77 modification, FB₁ induced H3K9me3 and repressed H4K20me3 (Pellanda, Forges et al. 2012, Sancak
78 and Ozden 2015). FB₁ had little effect on H4K16 and H3K18 acetylation; however, promoted
79 acetylation of H2NK12, H3K9 and H3K23 (Pellanda, Forges et al. 2012, Gardner, Riley et al. 2016).
80 Only one study has evaluated changes in miRNA profiles upon FB₁ exposure (Chuturgoon, Phulukdaree
81 et al. 2014). Thus far, no study has evaluated the impact of FB₁ on m6A modifications and lncRNAs
82 and little is known on the downstream implications of these epigenetic changes. In this study, the impact
83 of FB₁ on DNA methylation, histone methylation (H3K4), m6A RNA methylation, miRNAs and
84 lncRNAs were evaluated. The effect of these changes on response mechanisms to cellular stress were
85 further investigated.

86 It was previously shown that FB₁ enhanced ROS production, resulting in oxidative stress in HepG2
87 cells (Arumugam, Pillay et al. 2019). Oxidative stress induced by FB₁ has also been observed in several
88 other *in vivo* and *in vitro* models [extensively reviewed by Arumugam, Ghazi et al. (2020)]. A major
89 consequence of excessive ROS level is oxidative injury to DNA which results in modification to
90 nitrogenous bases and single- and double-stranded DNA breaks. The lesions incurred on DNA are often
91 deleterious or have mutagenic effects (Loft, Høgh Danielsen et al. 2008). Cells are safe guarded by a
92 complex network of DNA damage responses (DDR) with the tumor suppressor, PTEN and checkpoint
93 signaling at the forefront (Dai and Grant 2010). Checkpoint kinase 1 (CHK1), a key transducer in this
94 signaling networking, halts the cell cycle allowing for repair of damaged DNA to occur (Dai and Grant
95 2010, Patil, Pabla et al. 2013). Loss of the tumor suppressor PTEN generates DNA damage and prevents
96 DNA repair via the inappropriate inactivation of CHK1 (Puc, Keniry et al. 2005, Puc and Parsons 2005).
97 It is possible that PTEN expression is affected by epigenetic changes such as histone modifications and
98 miRNA. Tri-methylation of the fourth lysine residue of histone 3 (H3K4me3) found on the promoter
99 region of PTEN activates its transcription, whereas demethylation has the opposing effect (Shen, Cheng
100 et al. 2018). Furthermore, miRNA, such as microRNA-30c (miR-30c), binds to the 3' untranslated
101 region (3'UTR) of *PTEN* mRNA and inhibits its translation (Hu, Duan et al. 2019). FB₁ is known to
102 affect both miR-30c and H3K4me regulation and may therefore affect DNA damage checkpoint
103 regulation by epigenetically modulating PTEN (Chuturgoon, Phulukdaree et al. 2014, Chuturgoon,
104 Phulukdaree et al. 2014, Sancak and Ozden 2015).

105 Oxidative stress not only induces oxidative lesions in DNA but it may also induce chemical
106 modifications in RNA (Li, Li et al. 2017, Zhao, Li et al. 2019, Wu, Gan et al. 2020). Over a hundred
107 covalent modifications are known to occur on the various classes of RNA with the most prevalent being

108 the methylation of the sixth nitrogen of adenosine (m6A) residues found on mRNA and lncRNA
109 (Cantara, Crain et al. 2011, Machnicka, Milanowska et al. 2013, Yue, Liu et al. 2015). m6A marks are
110 installed by “writers” (methyltransferases: METTL3 and METTL14), removed by “erasers”
111 (demethylases: FTO and ALKBH5) and recognized by “readers” [YTH21-B homology (YTH) domain
112 family proteins: YTHDF1, YTHDF2, YTHDF3, YTHDC1 and YTHDC2]. M6A “readers” control the
113 fate of m6A modified transcripts by regulating its export, degradation, splicing, and protein translation
114 (Zaccara, Ries et al. 2019). M6A modifications are also influenced by cellular stress and can influence
115 stress responses (Dominissini, Moshitch-Moshkovitz et al. 2012, Engel, Eggert et al. 2018). Global
116 m6A levels are increased in response to oxidative stress; however, m6A modifications to certain
117 transcripts have been shown to influence oxidative stress responses (Li, Li et al. 2017, Zhao, Li et al.
118 2019, Wu, Gan et al. 2020, Zhao, Wang et al. 2020). For instance, oxidative stress that occurred due to
119 colistin exposure altered m6A levels; however, colistin-induced oxidative stress was diminished by
120 m6A modifications on pri-miR-873. This promoted the generation of mature miR-873-5p and
121 subsequently inhibited Keap1 expression and promoted Nrf2 antioxidant responses (Wang, Ishfaq et al.
122 2019). It was previously shown that Keap1/Nrf2 signaling is activated in response to FB₁-mediated
123 oxidative stress (Arumugam, Pillay et al. 2019). The activation of Keap1/Nrf2 signaling promotes the
124 transcription of anti-oxidants and other detoxifying enzymes to combat excess ROS (Ray, Huang et al.
125 2012). It is possible that FB₁-mediated oxidative stress affects global m6A levels and that m6A
126 modifications are a potential factor contributing to Keap1/Nrf2 activation. Furthermore, Keap1 and
127 Nrf2 are also regulated by promoter methylation and microRNA-27b (miR-27b).

128 When cells are unable to overcome genotoxic and oxidative stress, they initiate p53 mediated apoptosis.
129 While *p53* is considered the most mutated gene in cancer, its expression may also be influenced by
130 epigenetic factors such as lncRNA, miRNA and DNA methylation (Saldaña-Meyer and Recillas-Targa
131 2011, Chmelarova, Krepinska et al. 2013, Anbarasan and Bourdon 2019). Epigenetic modifications
132 may also work in concert to regulate gene expression. For instance, the lncRNA, homeobox A11
133 antisense (HOXA11-AS) functions as circulating endogenous RNA (ceRNA) and molecular scaffold
134 to alter DNA methylation patterns (Sun, Nie et al. 2016, Yu, Peng et al. 2017). As a ceRNA, HOXA11-
135 AS binds to miRNAs and inhibits the regulatory interaction between the miRNA and its target mRNA
136 (Khandelwal, Bacolla et al. 2015). By acting as a molecular scaffold, HOXA11-AS modulates the
137 transcription of target genes by recruiting proteins including DNA methyltransferases (DNMTs) to the
138 promoter regions of genes (Wang and Chang 2011). HOXA11-AS sequesters miR-124, which in turn
139 upregulates DNMT3B and SP1, a DNMT1 transcription factor (Chen, Liu et al. 2015). HOXA11-AS
140 may also act as a scaffold for DNMT1 (Sun, Nie et al. 2016). DNMTs are responsible for the
141 methylation of gene promoters and thus inhibition of gene expression (Lyko 2018). It was previously
142 shown that FB₁ impairs the transcription of tumor suppressors via methylation of their promoter regions

143 (Demirel, Alpertunga et al. 2015). It is possible that p53 expression may be downregulated by
144 methylation of its promoter via the HOXA11-AS/miR-124/DNMT axis.

145 In this study, the human hepatoma (HepG2) cell line was used to identify epigenetic mechanisms that
146 may contribute to FB₁ induced hepatotoxicity. The liver is the initial site for the metabolism and
147 detoxification of food contaminants and is one of the primary organs in which FB₁ accumulates and
148 exerts toxicity (Martinez-Larranaga, Anadon et al. 1999, Kammerer and Küpper 2018). The use of
149 primary hepatocyte cell lines as a toxicity model has many limitations. When primary hepatocytes are
150 cultured they undergo morphological, phenotypic and functional changes in a process known as de-
151 differentiation. Furthermore, liver specific functions such as cytochrome P450 metabolism also declines
152 (Soldatow, Lecluyse et al. 2013). It is for these reasons that the HepG2 cell line was used instead.
153 HepG2 cells have similar physiological functions to primary hepatocytes; however, it retains its
154 functions and morphology in culture. It also displays a metabolic capacity and epigenetic profile similar
155 to intact hepatocytes (Ruoff, Damm et al. 2019). Moreover, no mutations have been found in the *PTEN*
156 or *p53* gene of the HepG2 cell line, making it a reliable model for testing epigenetic changes as a result
157 of FB₁ exposure (Ma, Xu et al. 2005, Lee and Park 2015).

158 **1.1. Aim**

159 The aim of this study was to determine the epigenetic effects of FB₁ and the downstream implications
160 of these epigenetic alterations to stress response pathways in human liver (HepG2) cells.

161

162 **1.2. Hypothesis**

163 FB₁ modifies the epigenome of HepG2 cells and alters cellular responses to stress which further
164 contributes to its' toxicity.

165

166 **1.3. Objectives**

167 The objectives of this study were to determine the effects of FB₁ in HepG2 cells by assessing:

- 168 - genome integrity, epigenetic regulation of PTEN by miR-30c and H3K4me3 and CHK1.
- 169 - ROS levels, global m6A levels and the epigenetic regulation of Keap1/Nrf2 via m6A RNA
170 methylation, miR-27b and promoter methylation.
- 171 - epigenetic regulation of p53 via the HOXA11-AS/miR-124/DNMT axis and its effect on
172 apoptosis.

173 Ethical approval for this study was obtained from the University of Kwazulu-Natal Biomedical
174 Research Ethics Committee (Ethical approval number: BE322/19; Addendum B, Page 209).

175

176 **References**

- 177 Alberts, J., J. Rheeder, W. Gelderblom, G. Shephard and H.-M. Burger (2019). "Rural Subsistence
178 Maize Farming in South Africa: Risk Assessment and Intervention models for Reduction of Exposure
179 to Fumonisin Mycotoxins." Toxins **11**(6): 334.
- 180 Alexander, N. J., R. H. Proctor and S. P. McCormick (2009). "Genes, gene clusters, and biosynthesis
181 of trichothecenes and fumonisins in *Fusarium*." Toxin Reviews **28**(2-3): 198-215.
- 182 Alizadeh, A. M., G. Roshandel, S. Roudbarmohammadi, M. Roudbary, H. Sohanaki, S. A. Ghiasian,
183 A. Taherkhani, S. Semnani and M. Aghasi (2012). "Fumonisin B1 contamination of cereals and risk of
184 esophageal cancer in a high risk area in northeastern Iran." Asian Pacific journal of cancer prevention
185 **13**(6): 2625-2628.
- 186 Anbarasan, T. and J.-C. Bourdon (2019). "The Emerging Landscape of p53 Isoforms in Physiology,
187 Cancer and Degenerative Diseases." International Journal of Molecular Sciences **20**(24): 6257.
- 188 Arumugam, T., T. Ghazi, N. Sheik Abdul and A. A. Chuturgoon (2020). A review on the oxidative
189 effects of the fusariotoxins: Fumonisin B1 and fusaric acid. Toxicology. V. B. Patel and V. R. Preedy,
190 Academic Press: 181-190.
- 191 Arumugam, T., Y. Pillay, T. Ghazi, S. Nagiah, N. S. Abdul and A. A. Chuturgoon (2019). "Fumonisin
192 B(1)-induced oxidative stress triggers Nrf2-mediated antioxidant response in human hepatocellular
193 carcinoma (HepG2) cells." Mycotoxin Res **35**(1): 99-109.
- 194 Bannister, A. J. and T. Kouzarides (2011). "Regulation of chromatin by histone modifications." Cell
195 Research **21**(3): 381-395.
- 196 Bollati, V. and A. Baccarelli (2010). "Environmental epigenetics." Heredity **105**(1): 105-112.
- 197 Cantara, W. A., P. F. Crain, J. Rozenski, J. A. McCloskey, K. A. Harris, X. Zhang, F. A. P. Vendeix,
198 D. Fabris and P. F. Agris (2011). "The RNA Modification Database, RNAMDB: 2011 update." Nucleic
199 acids research **39**(Database issue): D195-D201.
- 200 Chen, C., R. T. Riley and F. Wu (2018). "Dietary Fumonisin and Growth Impairment in Children and
201 Animals: A Review." Comprehensive Reviews in Food Science and Food Safety **17**(6): 1448-1464.
- 202 Chen, Z., S. Liu, L. Tian, M. Wu, F. Ai, W. Tang, L. Zhao, J. Ding, L. Zhang and A. Tang (2015).
203 "miR-124 and miR-506 inhibit colorectal cancer progression by targeting DNMT3B and DNMT1."
204 Oncotarget **6**(35): 38139-38150.
- 205 Chmelarova, M., E. Krepinska, J. Spacek, J. Laco, M. Beranek and V. Palicka (2013). "Methylation in
206 the p53 promoter in epithelial ovarian cancer." Clinical and Translational Oncology **15**(2): 160-163.
- 207 Chuturgoon, A., A. Phulukdaree and D. Moodley (2014). "Fumonisin B1 induces global DNA
208 hypomethylation in HepG2 cells - An alternative mechanism of action." Toxicology **315**: 65-69.

209 Chuturgoon, A. A., A. Phulukdaree and D. Moodley (2014). "Fumonisin B1 modulates expression of
210 human cytochrome P450 1b1 in human hepatoma (HepG2) cells by repressing Mir-27b." Toxicology
211 Letters **227**(1): 50-55.

212 Chuturgoon, A. A., A. Phulukdaree and D. Moodley (2015). "Fumonisin B1 inhibits apoptosis in
213 HepG2 cells by inducing Birc-8/ILP-2." Toxicology Letters **235**(2): 67-74.

214 Dai, Y. and S. Grant (2010). "New insights into checkpoint kinase 1 in the DNA damage response
215 signaling network." Clinical cancer research : an official journal of the American Association for Cancer
216 Research **16**(2): 376-383.

217 Demirel, G., B. Alpertunga and S. Ozden (2015). "Role of fumonisin B1 on DNA methylation changes
218 in rat kidney and liver cells." Pharmaceutical Biology **53**(9): 1302-1310.

219 Dominissini, D., S. Moshitch-Moshkovitz, S. Schwartz, M. Salmon-Divon, L. Ungar, S. Osenberg, K.
220 Cesarkas, J. Jacob-Hirsch, N. Amariglio, M. Kupiec, R. Sorek and G. Rechavi (2012). "Topology of
221 the human and mouse m6A RNA methylomes revealed by m6A-seq." Nature **485**(7397): 201-206.

222 Dragan, Y. P., W. R. Bidlack, S. M. Cohen, T. L. Goldsworthy, G. C. Hard, P. C. Howard, R. T. Riley
223 and K. A. Voss (2001). "Implications of apoptosis for toxicity, carcinogenicity, and risk assessment:
224 fumonisin B1 as an example." Toxicological Sciences **61**(1): 6-17.

225 EFSA (2018). "Risks for animal health related to the presence of fumonisins, their modified forms and
226 hidden forms in feed." EFSA journal. European Food Safety Authority **16**(5): e05242-e05242.

227 Engel, M., C. Eggert, P. Kaplick, M. Eder, S. Roeh, L. Tietze, C. Namendorf, J. Knauer-Arloth, P.
228 Weber, M. Rex-Haffner, S. Geula, M. Jakovcevski, J. Hanna, D. Leshkowitz, M. Uhr, C. Wotjak, M.
229 Schmidt, J. Deussing, E. Binder and A. Chen (2018). "The Role of m6A/m-RNA Methylation in Stress
230 Response Regulation." Neuron **99**: 389-403.

231 Farhadi, A., H. Nowrozi and R. Kachuei (2019). "Metabolism, Toxicity, Detoxification, Occurrence,
232 Intake and Legislations of Fumonisins-A Review." Journal of Pharmaceutical Research International:
233 1-35.

234 Fernández-Cruz, M., M. Mansilla and J. Tadeo (2010). "Mycotoxins in fruits and their processed
235 products: Analysis, occurrence and health implications." Journal of Advanced Research **1**: 113-122.

236 Ferrigo, D., A. Raiola and R. Causin (2016). "Fusarium Toxins in Cereals: Occurrence, Legislation,
237 Factors Promoting the Appearance and Their Management." Molecules (Basel, Switzerland) **21**(5): 627.

238 FOA/WHO (2002). Evaluation of certain mycotoxins in food : fifty-sixth report of the Joint FAO/WHO
239 Expert Committee on Food Additives. Geneva, World Health Organization.

240 Gardner, N. M., R. T. Riley, J. L. Showker, K. A. Voss, A. J. Sachs, J. R. Maddox and J. B. Gelineau-
241 van Waes (2016). "Elevated nuclear sphingoid base-1-phosphates and decreased histone deacetylase

242 activity after fumonisin B1 treatment in mouse embryonic fibroblasts." Toxicol Appl Pharmacol **298**:
243 56-65.

244 Gazzotti, T., B. Lugoboni, E. Zironi, A. Barbarossa, A. Serraino and G. Pagliuca (2009). "Determination
245 of fumonisin B1 in bovine milk by LC–MS/MS." Food Control **20**(12): 1171-1174.

246 Gbashi, S., N. E. Madala, S. De Saeger, M. De Boevre, I. Adekoya, O. A. Adebo and P. B. Njobeh
247 (2018). The socio-economic impact of mycotoxin contamination in Africa. Mycotoxins-Impact and
248 Management Strategies, IntechOpen.

249 Ho, S.-M., A. Johnson, P. Tarapore, V. Janakiram, X. Zhang and Y.-K. Leung (2012). "Environmental
250 epigenetics and its implication on disease risk and health outcomes." ILAR journal **53**(3-4): 289-305.

251 Hu, W., Z. Duan, Q. Wang and D. Zhou (2019). "The suppression of ox-LDL-induced inflammatory
252 response and apoptosis of HUVEC by lncRNA XIAT knockdown via regulating miR-30c-5p/PTEN
253 axis." European review for medical and pharmacological sciences **23**(17): 7628-7638.

254 IARC (2002). "Some traditional herbal medicines, some mycotoxins, naphthalene and styrene." IARC
255 Monogr Eval Carcinog Risks Hum **82**: 1-556.

256 Kamle, M., D. K. Mahato, S. Devi, K. E. Lee, S. G. Kang and P. Kumar (2019). "Fumonisin: Impact
257 on Agriculture, Food, and Human Health and their Management Strategies." Toxins **11**(6): 328.

258 Kammerer, S. and J.-H. Küpper (2018). "Human hepatocyte systems for in vitro toxicology analysis."
259 Journal of Cellular Biotechnology **3**: 85-93.

260 Khandelwal, A., A. Bacolla, K. Vasquez and A. Jain (2015). "Long non-coding RNA: A new paradigm
261 for lung cancer." Molecular carcinogenesis **54**.

262 Klarić, M. and S. Pepeljnjak (2001). "Fumonisin and their effects on animal health - A brief review."
263 Veterinarski Arhiv **71**: 299-323.

264 Kouadio, J. H., S. D. Dano, S. Moukha, T. A. Mobio and E. E. Creppy (2007). "Effects of combinations
265 of Fusarium mycotoxins on the inhibition of macromolecular synthesis, malondialdehyde levels, DNA
266 methylation and fragmentation, and viability in Caco-2 cells." Toxicol **49**(3): 306-317.

267 Lee, H. J. and D. Ryu (2017). "Worldwide Occurrence of Mycotoxins in Cereals and Cereal-Derived
268 Food Products: Public Health Perspectives of Their Co-occurrence." Journal of Agricultural and Food
269 Chemistry **65**(33): 7034-7051.

270 Lee, Y. R. and S. Y. Park (2015). "P53 expression in hepatocellular carcinoma: influence on the
271 radiotherapeutic response of the hepatocellular carcinoma." Clinical and molecular hepatology **21**(3):
272 230-231.

273 Li, Q., X. Li, H. Tang, B. Jiang, Y. Dou, M. Gorospe and W. Wang (2017). "NSUN2-Mediated m5C
274 Methylation and METTL3/METTL14-Mediated m6A Methylation Cooperatively Enhance p21
275 Translation." J Cell Biochem **118**(9): 2587-2598.

276 Liu, X., E. Zhang, S. Yin, C. Zhao, L. Fan and H. Hu (2020). "Activation of the IRE1 α Arm, but not
277 the PERK Arm, of the Unfolded Protein Response Contributes to Fumonisin B1-Induced
278 Hepatotoxicity." Toxins **12**(1): 55.

279 Loft, S., P. Høgh Danielsen, L. Mikkelsen, L. Risom, L. Forchhammer and P. Møller (2008).
280 "Biomarkers of oxidative damage to DNA and repair." Biochem Soc Trans **36**(Pt 5): 1071-1076.

281 Lyko, F. (2018). "The DNA methyltransferase family: a versatile toolkit for epigenetic regulation."
282 Nature Reviews Genetics **19**(2): 81-92.

283 Ma, D.-Z., Z. Xu, Y.-L. Liang, J.-M. Su, Z.-X. Li, W. Zhang, L.-Y. Wang and X.-L. Zha (2005). "Down-
284 regulation of PTEN expression due to loss of promoter activity in human hepatocellular carcinoma cell
285 lines." World journal of gastroenterology **11**(29): 4472-4477.

286 Machnicka, M. A., K. Milanowska, O. Osman Oglou, E. Purta, M. Kurkowska, A. Olchowik, W.
287 Januszewski, S. Kalinowski, S. Dunin-Horkawicz, K. M. Rother, M. Helm, J. M. Bujnicki and H.
288 Grosjean (2013). "MODOMICS: a database of RNA modification pathways--2013 update." Nucleic
289 acids research **41**(Database issue): D262-D267.

290 Magan, N., A. Medina and D. Aldred (2011). "Possible climate-change effects on mycotoxin
291 contamination of food crops pre- and postharvest." Plant Pathology **60**(1): 150-163.

292 Martinez-Larranaga, M. R., A. Anadon, M. J. Diaz, M. L. Fernandez-Cruz, M. A. Martinez, M. T. Frejo,
293 M. Martinez, R. Fernandez, R. M. Anton, M. E. Morales and M. Tafur (1999). "Toxicokinetics and oral
294 bioavailability of fumonisin B1." Vet Hum Toxicol **41**(6): 357-362.

295 Mngqawa, P., G. S. Shephard, I. R. Green, S. H. Ngobeni, T. C. de Rijk and D. R. Katerere (2016).
296 "Mycotoxin contamination of home-grown maize in rural northern South Africa (Limpopo and
297 Mpumalanga Provinces)." Food Addit Contam Part B Surveill **9**(1): 38-45.

298 Mobio, T. A., R. Anane, I. Baudrimont, M. R. Carratú, T. W. Shier, S. D. Dano, Y. Ueno and E. E.
299 Creppy (2000). "Epigenetic properties of fumonisin B(1): cell cycle arrest and DNA base modification
300 in C6 glioma cells." Toxicol Appl Pharmacol **164**(1): 91-96.

301 Moore, L. D., T. Le and G. Fan (2013). "DNA Methylation and Its Basic Function."
302 Neuropsychopharmacology **38**(1): 23-38.

303 Nestic, K., S. Ivanovic and V. Nestic (2014). "Fusarial toxins: secondary metabolites of Fusarium fungi."
304 Rev Environ Contam Toxicol **228**: 101-120.

305 Patil, M., N. Pabla and Z. Dong (2013). "Checkpoint kinase 1 in DNA damage response and cell cycle
306 regulation." Cellular and molecular life sciences : CMLS **70**(21): 4009-4021.

307 Pellanda, H., T. Forges, A. Bressenot, A. Chango, J. P. Bronowicki, J. L. Guéant and F. Namour (2012).
308 "Fumonisin FB1 treatment acts synergistically with methyl donor deficiency during rat pregnancy to
309 produce alterations of H3- and H4-histone methylation patterns in fetuses." Mol Nutr Food Res **56**(6):
310 976-985.

311 Puc, J., M. Keniry, H. S. Li, T. K. Pandita, A. D. Choudhury, L. Memeo, M. Mansukhani, V. V. V. S.
312 Murty, Z. Gaciong, S. E. M. Meek, H. Piwnica-Worms, H. Hibshoosh and R. Parsons (2005). "Lack of
313 PTEN sequesters CHK1 and initiates genetic instability." Cancer Cell **7**(2): 193-204.

314 Puc, J. and R. Parsons (2005). "PTEN loss inhibits CHK1 to cause double stranded-DNA breaks in
315 cells." Cell Cycle **4**(7): 927-929.

316 Ray, P. D., B.-W. Huang and Y. Tsuji (2012). "Reactive oxygen species (ROS) homeostasis and redox
317 regulation in cellular signaling." Cellular signalling **24**(5): 981-990.

318 Rheeder, J. P., W. F. O. Marasas and H. F. Vismer (2002). "Production of Fumonisin Analogs by
319 *Fusarium* Species." Applied and Environmental Microbiology **68**(5): 2101-2105.

320 Ruöß, M., G. Damm, M. Vosough, L. Ehret, C. Grom-Baumgarten, M. Petkov, S. Naddalin, R.
321 Ladurner, D. Seehofer, A. Nussler and S. Sajadian (2019). "Epigenetic Modifications of the Liver
322 Tumor Cell Line HepG2 Increase Their Drug Metabolic Capacity." Int J Mol Sci **20**(2).

323 Saldaña-Meyer, R. and F. Recillas-Targa (2011). "Transcriptional and epigenetic regulation of the p53
324 tumor suppressor gene." Epigenetics **6**(9): 1068-1077.

325 Sancak, D. and S. Ozden (2015). "Global histone modifications in Fumonisin B1 exposure in rat kidney
326 epithelial cells." Toxicol In Vitro **29**(7): 1809-1815.

327 SCF/EC (2000). Opinion of the Scientific Committee on Food on Fusarium Toxins, Part 3: Fumonisin
328 B1 (FB1), European Commission Brussels.

329 SCF/EC (2003). Updated opinion of the Scientific Committee on Food on Fumonisin B1, B2 and B3,
330 European Commission Brussels.

331 Shamsi, M. B., A. S. Firoz, S. N. Imam, N. Alzaman and M. A. Samman (2017). "Epigenetics of human
332 diseases and scope in future therapeutics." Journal of Taibah University Medical Sciences **12**(3): 205-
333 211.

334 Shen, X., G. Cheng, L. Xu, W. Wu, Z. Chen and P. Du (2018). "Jumonji AT-rich interactive domain
335 1B promotes the growth of pancreatic tumors via the phosphatase and tensin homolog/protein kinase B
336 signaling pathway." Oncol Lett **16**(1): 267-275.

337 Shirima, C. P., M. E. Kimanya, J. L. Kinabo, M. N. Routledge, C. Srey, C. P. Wild and Y. Y. Gong
338 (2013). "Dietary exposure to aflatoxin and fumonisin among Tanzanian children as determined using
339 biomarkers of exposure." Molecular nutrition & food research **57**(10): 1874-1881.

340 Soldatow, V. Y., E. L. Lecluyse, L. G. Griffith and I. Rusyn (2013). "In vitro models for liver toxicity
341 testing." Toxicology research **2**(1): 23-39.

342 Sun, G., S. Wang, X. Hu, J. Su, T. Huang, J. Yu, L. Tang, W. Gao and J.-S. Wang (2007). "Fumonisin
343 B1 contamination of home-grown corn in high-risk areas for esophageal and liver cancer in China."
344 Food Additives & Contaminants **24**(2): 181-185.

345 Sun, M., F. Nie, Y. Wang, Z. Zhang, J. Hou, D. He, M. Xie, L. Xu, W. De, Z. Wang and J. Wang
346 (2016). "LncRNA HOXA11-AS Promotes Proliferation and Invasion of Gastric Cancer by Scaffolding
347 the Chromatin Modification Factors PRC2, LSD1, and DNMT1." Cancer Res **76**(21): 6299-6310.

348 Sydenham, E. W., P. G. Thiel, W. F. Marasas, G. S. Shephard, D. J. Van Schalkwyk and K. R. Koch
349 (1990). "Natural occurrence of some Fusarium mycotoxins in corn from low and high esophageal cancer
350 prevalence areas of the Transkei, Southern Africa." Journal of Agricultural and Food Chemistry **38**(10):
351 1900-1903.

352 Tolosa, J., G. Font, J. Mañes and E. Ferrer (2013). "Nuts and dried fruits: Natural occurrence of
353 emerging Fusarium mycotoxins." Food Control **33**(1): 215-220.

354 Voss, K. A., G. W. Smith and W. M. Haschek (2007). "Fumonisin: Toxicokinetics, mechanism of
355 action and toxicity." Animal Feed Science and Technology **137**(3): 299-325.

356 Wang, E., W. P. Norred, C. W. Bacon, R. T. Riley and A. H. Merrill, Jr. (1991). "Inhibition of
357 sphingolipid biosynthesis by fumonisins. Implications for diseases associated with Fusarium
358 moniliforme." J Biol Chem **266**(22): 14486-14490.

359 Wang, J., M. Ishfaq, L. Xu, C. Xia, C. Chen and J. Li (2019). "METTL3/m(6)A/miRNA-873-5p
360 Attenuated Oxidative Stress and Apoptosis in Colistin-Induced Kidney Injury by Modulating
361 Keap1/Nrf2 Pathway." Frontiers in pharmacology **10**: 517-517.

362 Wang, K. C. and H. Y. Chang (2011). "Molecular mechanisms of long noncoding RNAs." Molecular
363 cell **43**(6): 904-914.

364 Wu, J., Z. Gan, R. Zhuo, L. Zhang, T. Wang and X. Zhong (2020). "Resveratrol Attenuates Aflatoxin
365 B(1)-Induced ROS Formation and Increase of m(6)A RNA Methylation." Animals (Basel) **10**(4).

366 Yang, X., M. Liu, M. Li, S. Zhang, H. Hiju, J. Sun, Z. Mao, M. Zheng and B. Feng (2020). "Epigenetic
367 modulations of noncoding RNA: a novel dimension of Cancer biology." Molecular Cancer **19**(1): 64.

368 Yin, S., X. Guo, J. Li, L. Fan and H. Hu (2016). "Fumonisin B1 induces autophagic cell death via
369 activation of ERN1-MAPK8/9/10 pathway in monkey kidney MARC-145 cells." Archives of
370 Toxicology **90**(4): 985-996.

371 Yu, W., W. Peng, H. Jiang, H. Sha and J. Li (2017). "LncRNA HOXA11-AS promotes proliferation
372 and invasion by targeting miR-124 in human non-small cell lung cancer cells." Tumour Biol **39**(10):
373 1010428317721440.

374 Yue, Y., J. Liu and C. He (2015). "RNA N6-methyladenosine methylation in post-transcriptional gene
375 expression regulation." Genes Dev **29**(13): 1343-1355.

376 Zaccara, S., R. J. Ries and S. R. Jaffrey (2019). "Reading, writing and erasing mRNA methylation."
377 Nat Rev Mol Cell Biol **20**(10): 608-624.

378 Zain, M. E. (2011). "Impact of mycotoxins on humans and animals." Journal of Saudi Chemical Society
379 **15**(2): 129-144.

380 Zhao, T., X. Li, D. Sun and Z. Zhang (2019). "Oxidative stress: One potential factor for arsenite-induced
381 increase of N6-methyladenosine in human keratinocytes." Environmental Toxicology and
382 Pharmacology **69**: 95-103.

383 Zhao, T., J. Wang, L.-J. Shen, C.-L. Long, B. Liu, Y. Wei, L.-D. Han, Y.-X. Wei and G.-H. Wei (2020).
384 "Increased m6A RNA modification is related to the inhibition of the Nrf2-mediated antioxidant
385 response in di-(2-ethylhexyl) phthalate-induced prepubertal testicular injury." Environmental Pollution
386 **259**: 113911.

387

388

389

390

391

392

393

394

395

396

397

398

399

CHAPTER 2

400

LITERATURE REVIEW

401

2.1. *Fusarium* Mycotoxins

402

Among numerous fungal genera, those belonging to *Fusarium* are considered the most significant. *Fusarium* species invade important agricultural crops such as small grain cereals and maize (Escrivá et al., 2015). Under optimal conditions, many of these fungi produce an array of structurally diverse and toxic secondary metabolites. These metabolites are known as mycotoxins and the quantity and type produced is dependent upon factors such as moisture, temperature and insect stress (Nesic et al., 2014, Bakker et al., 2018). Mycotoxins are related to the development of plant diseases resulting in the reduction of global crops by almost 30% (Nesic et al., 2014). Of significant concern is the acute and chronic implications of the consumption of *Fusarium* contaminated commodities on human and animal health (Escrivá et al., 2015). Some *Fusarium* mycotoxins co-contaminate crops and elicit a broad variety of toxic and carcinogenic effects in both humans and animals. Co-exposure to multiple *Fusarium* mycotoxins results in possibly synergistic or additive toxic effects (Grenier and Oswald, 2011). The most relevant *Fusarium* mycotoxins in terms of toxicology and distribution include fumonisins, trichothecenes and zearalenone (Figure 1) (Bakker et al., 2018).

415

Trichothecenes consist of metabolites containing an epoxide moiety (Figure 2.1A). They are produced by a wide variety of *Fusarium* species, including *F. sporotrichioides*, *F. poae*, *F. equiseti*, and *F. acuminatum* (Chain, 2011). More than 150 trichothecenes have been identified and classified into 4 types (A-D) based on substitutions on the core structure of 12,13-epoxytrichothec-9-ene (Escrivá et al., 2015). Toxicologically relevant trichothecenes consist of T-2 toxin, HT-2 toxin, nivalenol (NIV) and deoxynivalenol (DON). Trichothecenes are potent inhibitors of DNA, RNA and protein synthesis and have been associated with damage to the gastrointestinal system, dermatitis, immune suppression and hematologic disorders (Chain, 2011, Nesic et al., 2014).

423

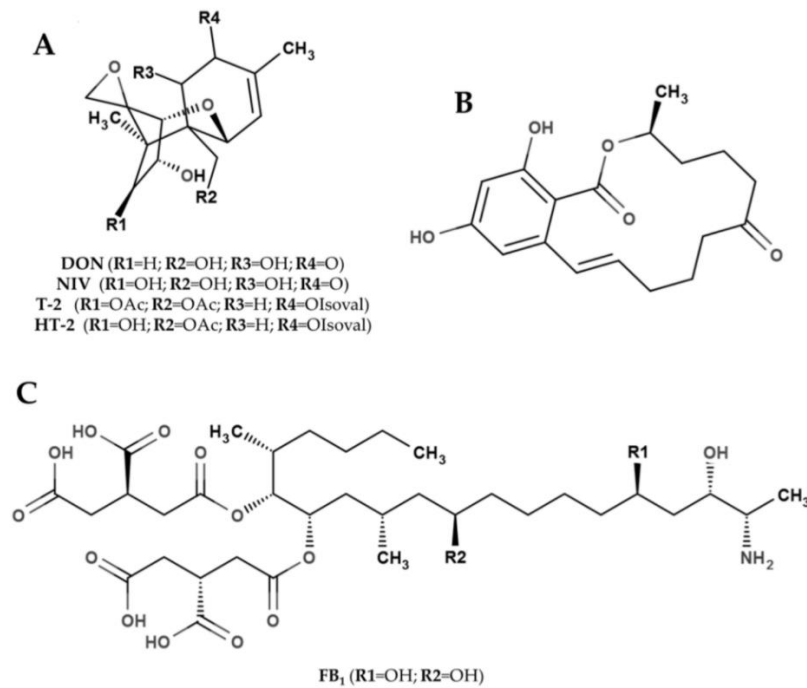
Zearalenones (Figure 2.1B) are predominantly produced by *F. graminearum*, and *F. cerealis*, in temperate climates with cool temperatures and high humidity (EFSA, 2011). Zearalenones are classified as myco-oestrogens as they bind to cytosolic oestrogen receptors in the uterus, hypothalamus, mammary and pituitary glands resulting in strong hyper-oestrogenic effects (Abbès et al., 2006). Therefore, zearalenones exert their toxicity on the reproductive system by inducing morphological changes to the reproductive tract such as vaginal swelling, testicular atrophy and enlargement of mammary glands; as well as decreased fertility, higher embryo lethal resorptions and precocious puberty (EFSA, 2011, Escrivá et al., 2015). In addition, zearalenone also induces hepatotoxic, immunotoxic, and carcinogenic effects (EFSA, 2011, Escrivá et al., 2015).

432

Fumonisin are polyketide derived mycotoxins predominantly produced by *F. verticillioides* and *F. proliferatum*. Fumonisin have carcinogenic potential and have been associated with neuro-, hepato-

433

434 and renal toxicities (EFSA, 2018). Currently, 28 fumonisins have been identified and categorized into
435 four groups (A, B, C and P). Among these analogues, fumonisin B₁ (FB₁; Figure 2.1C) is regarded as
436 the most relevant due to its wide spread distribution and potent toxicity (Rheeder et al., 2002).



437

438 **Figure 2.1.** Chemical structure of the main *Fusarium* mycotoxins. (A) Trichothecenes; (B)
439 Zearalenone; (C) Fumonisin; OAc = acetyl group; Olsoval = isovalerate group (Ferrigo et al., 2016).

440 2.1.1. Fumonisin B₁

441 Approximately 61% of global cereal grains are contaminated with fumonisins (Lee and Ryu, 2017).
442 FB₁ accounts for 70-80% of total fumonisins that naturally infect food and feed samples, making it the
443 most relevant fumonisin analogue (Rheeder et al., 2002). Due to their wide geographical distribution
444 and frequent occurrence on maize, *F. verticillioides* and *F. proliferatum* are considered the most
445 important FB₁ producers (Rheeder et al., 2002). Furthermore, *F. verticillioides* and *F. proliferatum*
446 produce the highest levels of FB₁ reaching levels as high as 17,900 and 31,000 mg/kg of FB₁. 13
447 additional *Fusariums* have been found to produce FB₁, however, to a much lower extent (7-7,200
448 mg/kg) (Rheeder et al., 2002).

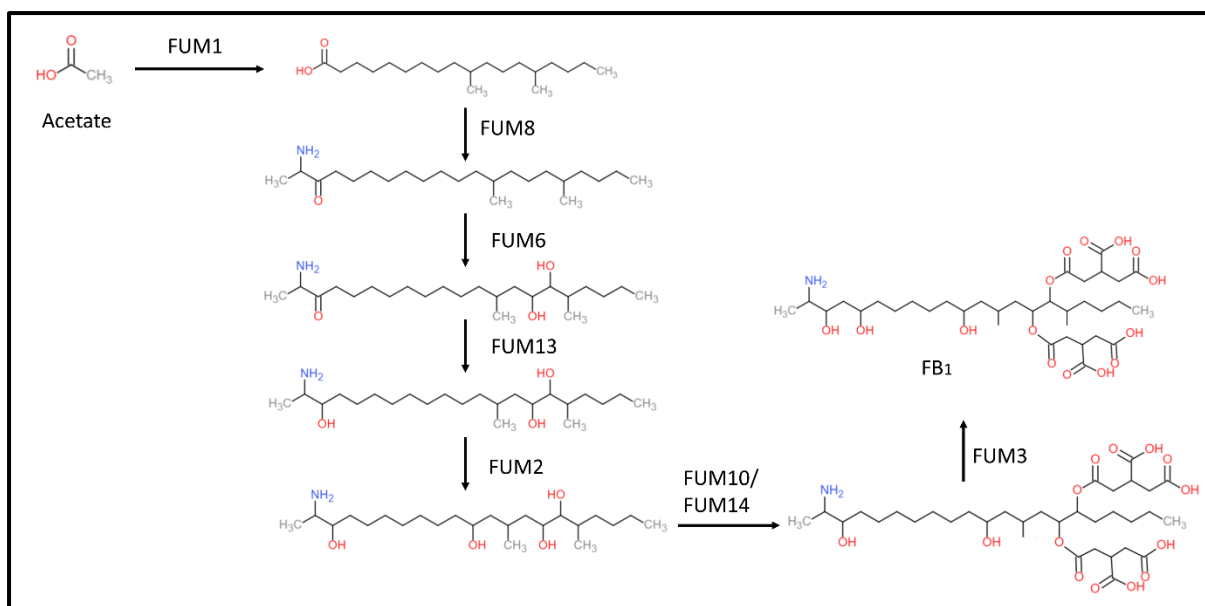
449 The production of FB₁ occurs preharvest and during storage and is heavily dependent on agroclimatic
450 conditions. Production is favoured in temperate regions where temperatures are warm and humidity is
451 high. Heat stress, insect damage and drought stress also influence FB₁ production (Ferrigo et al., 2016).
452 It is found in abundance in maize and maize-based products such as corn flakes, flour and oil as well as
453 in small cereal grains such as wheat, rice and oats (Lee and Ryu, 2017). Maize and cereals are dietary
454 staples and developing countries are heavily reliant on them. Moreover, FB₁ production is prominent in
455 rural regions that rely on subsistence farming. Most subsistence farmers do not have the resources to

456 implement the same agronomic practices seen in commercial settings. Poor agronomic practices
457 exacerbate the incidence of *Fusarium* infection and FB₁ production (Shephard et al., 2019). Due to the
458 high incidence of FB₁ in crops and its resistance to food processing, several countries and organisations
459 have set regulations to limit FB₁ contamination in food and feed. The Joint FAO-WHO Expert
460 Committee (JECFA) have also declared the provisional maximum tolerable intake of FB₁ alone or in
461 combination with FB₂ and FB₃ should be 2 µg/kg bw/day (FOA/WHO, 2002); however, FB₁ intake is
462 exceeded in many developing countries that rely heavily on cereal grains (Sun et al., 2007, Torres et
463 al., 2007).

464 2.1.1.1. Structure and Biosynthesis

465 The structure of FB₁ (C₃₄H₅₉NO₁₅), consists of linear 20 carbon (C) aminopentol backbone which is
466 substituted with an amine, three hydroxyl, two methyl, and two tricarboxylic acid groups at various
467 positions (Alexander et al., 2009). Genes involved in the biosynthesis of fumonisin have been mapped
468 to one locus in the genome of *F. verticillioides* and *F. proliferatum*. This region is regarded as the FUM
469 cluster and consists of 17 genes (Khaldi and Wolfe, 2011). Genes belonging to the FUM cluster are co-
470 regulated and its expression is influenced by abiotic factors such as water availability and temperature
471 which in turn influence fumonisin production (Medina et al., 2013).

472 The biosynthesis of FB₁ is initiated by the condensation of nine acetate and two methyl groups to form
473 a linear 18-C long polyketide. This reaction is catalysed by polyketide synthase (FUM 1) (Du et al.,
474 2008, Alexander et al., 2009). Thereafter, the aminotransferase, FUM 8, mediates the condensation of
475 the polyketide to alanine, resulting in a 20-C long backbone with an amine group at C-2, carbonyl group
476 at C-3 and methyl groups at C-12 and C-16 (Du et al., 2008). The resulting polyketide amino acid
477 undergoes hydroxylation at C-14 and C-15 by FUM 6. Thereafter, the carbonyl group is removed at C-
478 3, C-10 is hydroxylated and two tricarboxylic acids are esterified to C-14 and C-15. These three
479 reactions are catalysed by FUM 13, FUM 2 and FUM 10/14, respectively (Alexander et al., 2009). The
480 addition of a hydroxyl group at C-5 by the dioxygenase FUM 3 is responsible for the final step of FB₁
481 biosynthesis (Figure 2.2) (Ding et al., 2004).



482

483 **Figure 2.2.** FUM mediated biosynthesis of FB₁ (prepared by author).

484 *2.1.1.2. Primary mechanism of toxicity*

485 The primary mechanism by which FB₁ exerts its toxicity is via the disruption of sphingolipid
 486 metabolism (Riley and Merrill, 2019). Ceramide synthase (CS) plays a central role in sphingolipid
 487 metabolism by catalysing the N-acylation of sphinganine (Sa) during sphingolipid synthesis and the N-
 488 acylation of sphingosine (So) during sphingolipid turnover (Futerman and Riezman, 2005). The
 489 aminopentol backbone of FB₁ bears close structural resemblance to the sphingoid bases: Sa and So,
 490 thus, FB₁ competes with sphingoid bases for CS binding. CS recognizes and binds both the amino group
 491 and the tricarboxylic acid side chains of FB₁, thereby inhibiting both *de novo* synthesis and degradation
 492 pathways of sphingolipid metabolism (Wang et al., 1991). This results in the reduction in the formation
 493 of complex sphingolipids such as sphingomyelin and glycosphingolipids. The toxic effects of FB₁ are
 494 only partially due to the reduction of complex sphingolipids. The rapid accumulation of sphingoid bases
 495 and their phosphorylated counter parts can also trigger cell injury and membrane degradation (Wang et
 496 al., 1991, Riley and Merrill, 2019). Reduction of ceramide and the accumulation of
 497 phosphosphingolipids disrupt signalling pathways and in turn trigger several toxicologically relevant
 498 perturbations such endoplasmic reticulum (ER) stress, accumulation of reactive oxygen species (ROS),
 499 altered mitochondrial and immune functioning, and disruption to developmental regulation (Riley and
 500 Merrill, 2019). Furthermore, FB₁-induced fluctuations in the levels of sphingoid bases alter rates of cell
 501 death and regeneration, which may play a major role in FB₁-mediated tumorigenesis (Wang et al., 1991,
 502 Soriano et al., 2005). For a detailed discussion on the impact of FB₁ on disruption of sphingolipid
 503 metabolism and the molecular implications, see chapter 3: Molecular and Epigenetic Mechanisms of
 504 FB₁ Mediated Toxicity and Carcinogenesis and Detoxification Strategies, pages 74-86.

505

506 2.1.1.3. *Impact of FB₁ on human and animal health*

507 The 1970 field outbreak of equine leukoencephalomalacia (ELEM) in South Africa prompted the
508 discovery and characterization of fumonisins. The disease was associated with the consumption of
509 maize contaminated with *F. verticillioides* (formally *F. moniliforme*); later it was discovered that FB₁
510 was the main aetiological agent in the outbreak (Marasas, 2001). ELEM affects the central nervous
511 system and is characterized by liquefactive lesions in the subcortical white matter of the cerebrum.
512 Lesions may also develop in the brain stem, spinal cord and cerebellum (Klarić and Pepeljnjak, 2001).
513 This leads to depression, pharyngeal paralysis, lethargy, blind staggering and seizures in affected horses
514 (EFSA, 2018). Death can occur within a week after consuming of contaminated feed and can occur
515 without prior signs (Klarić and Pepeljnjak, 2001). Moreover, hepatic and renal lesions and cardiac
516 defects may develop independently or concurrently with ELEM (Klarić and Pepeljnjak, 2001, EFSA,
517 2018).

518 Along with horses, swine are considered the most sensitive domestic animals to FB₁. Swine exposed to
519 FB₁ develop a syndrome termed porcine pulmonary oedema (Haschek et al., 2001). Within 4 to 7 days
520 of exposure, swine present with respiratory distress, cyanosis, hydrothorax and pulmonary oedema.
521 Death occurs rapidly within hours of respiratory distress; however, long term exposure to low doses of
522 FB₁ results in non-lethal oedema (Voss et al., 2007). Pulmonary oedema induced by FB₁ may result
523 from acute left-side heart failure due to changes in So/Sa concentrations which regulate L-type calcium
524 channels. As a result, decreased heart rate, cardiac output and contractility also occur (Haschek et al.,
525 2001). Aside from the pulmonary and cardiac effects, acute liver injury, pancreatic necrosis, formation
526 of oesophageal plaques and depressed immune responses have also been observed (Voss et al., 2007).

527 The pathological effects of FB₁ have been well established in experimental rodent models. FB₁
528 predominantly targets the liver and kidney of rat and mouse models however the extent of toxicity is
529 dependent on the species and sex of the animals as well as the dose of FB₁ received (Klarić and
530 Pepeljnjak, 2001). Hepatotoxicity is minimal in Sprague Dawley and Fischer 344 rats, whereas the liver
531 is a major target in BD IX rats. However, male rats are more sensitive to the nephrotoxic effects of FB₁
532 than female rats; while mice are less sensitive to nephrotoxicity than rats (Voss et al., 2007). FB₁-
533 induced hepatotoxicity consisted of necrosis accompanied by changes in the lipid ratios, distortion of
534 liver lobules, and the development of hyperplastic nodules. Nephrotoxicity was characterised by
535 hyperplasia, necrosis of tubules, fatty changes and pyknosis (Klarić and Pepeljnjak, 2001). Impairment
536 of development and congenital malformations in the embryo and foetus are common in dams exposed
537 to FB₁. FB₁ further retards growth and induces developmental abnormalities in these offspring
538 (Lumsankul et al., 2019). FB₁ has been implicated in the initiation and promotion of carcinogenesis.
539 Cholangiocarcinomas, hepatocellular carcinomas and renal tubular tumours have been observed in male
540 rats; while female mice present with hepatocellular carcinomas and adenomas (Dragan et al., 2001).
541 Tumours tend to be aggressive and often metastasize (Voss et al., 2007). Epigenetic changes in

542 conjunction with compensatory cell proliferation and apoptosis are the proposed mechanisms by which
543 FB₁ exerts its carcinogenic effects (Dragan et al., 2001, Demirel et al., 2015).

544 While the carcinogenicity of FB₁ in experimental animals have been well established, evidence of FB₁-
545 carcinogenicity in humans are limited. Therefore, the International Agency for Research on Cancer
546 (IARC) has classified FB₁ as a class 2B carcinogen (IARC, 2002). Epidemiological studies have shown
547 an association between the high incidence of oesophageal cancer and, in one instance, hepatocellular
548 carcinomas in regions with high consumption of FB₁ contaminated maize. Regions of major concern
549 include South Africa, Iran and China (Sydenham et al., 1990, Sun et al., 2007, Alizadeh et al., 2012).
550 Epidemiological studies have also linked the high incidence of neural tube defects along the Mexican-
551 Texan border to the maternal consumption of maize based products contaminated with FB₁ (Missmer
552 et al., 2006). The inhibition of sphingolipid synthesis disturbs cellular membranes and receptors. FB₁
553 inhibits folate uptake, leading to neural tube defects such as spinal bifida and anencephaly with
554 extremely high exposure leading to foetal death (Marasas et al., 2004). Furthermore, evidence linking
555 fumonisin exposure to the stunting of growth in Sub-Saharan infants and children that consume maize-
556 based weaning foods has been increasing (Shirima et al., 2013, Chen et al., 2018). Finally, only one
557 outbreak of acute mycotoxicosis caused by the consumption of FB₁-contaminated sorghum and corn
558 has been recorded. The outbreak occurred in South India after 2 cyclonic storms which promoted growth
559 of mould. The outbreak affected 27 villages and 1,412 people. Affected individuals reported transient
560 abdominal pain, borborygmus and diarrhoea (Reddy and Raghavender, 2008).

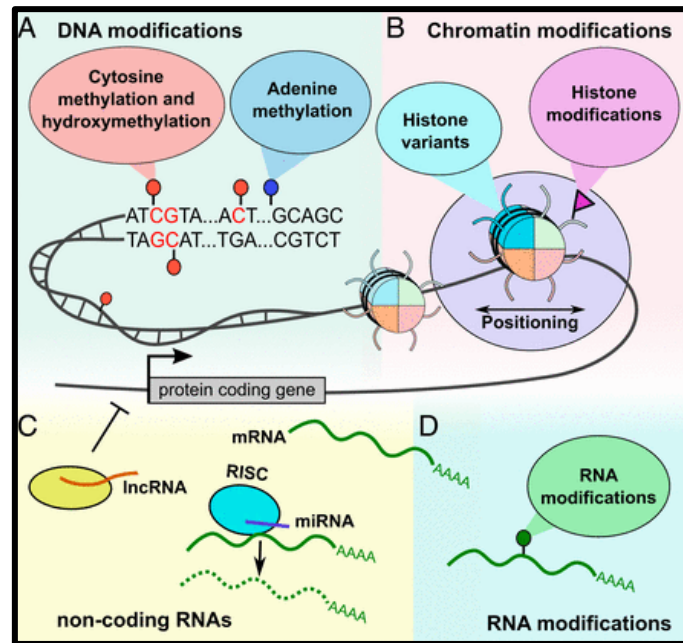
561 While the disruption of sphingolipid metabolism by FB₁ has been ruled as the primary mechanism for
562 its adverse effects; several emerging evidences suggests that mycotoxins induce epigenetic changes that
563 play a key role in their toxicity. It is plausible to assume that epigenetic changes may also contribute to
564 FB₁-mediated toxicities and pathologies.

565 **2.2. Epigenetics**

566 Although virtually all cells in an organism contain identical DNA sequence, not all cell types share the
567 same phenotype at the same time (Moore et al., 2013). Conard Waddington found that environmental
568 changes during development could induce an alternative phenotype despite their identical sequence. He
569 further observed that these environmentally induced changes could be inherited. He termed this
570 phenomenon as “epigenetics” (Waddington, 1956, Holliday, 2006). Epigenetics encompasses heritable
571 modifications that regulate gene expression and are not associated with changes in DNA sequence
572 (Bollati and Baccarelli, 2010). The complete description of all epigenetic modifications of a cell at any
573 given time is termed the epigenome. Interactions between the epigenome, genome and environment
574 play a critical role in shaping the development and health of an individual (Marczylo et al., 2016).

575 Several types of epigenetic modifications have been identified. These modifications include: DNA
576 methylation, covalent histone modifications, RNA methylation and non-coding RNAs (ncRNA) (Figure

577 2.3). DNA methylation and histone modifications influence transcription by altering chromatin
 578 structure and accessibility of transcriptional machinery to nucleotide sequences (Bannister and
 579 Kouzarides, 2011, Moore et al., 2013). On the other hand, RNA methylation targets posttranscriptional
 580 regulation; whereas, ncRNA influence transcriptional and posttranscriptional regulation of genes
 581 (Zaccara et al., 2019, Yang et al., 2020).



582

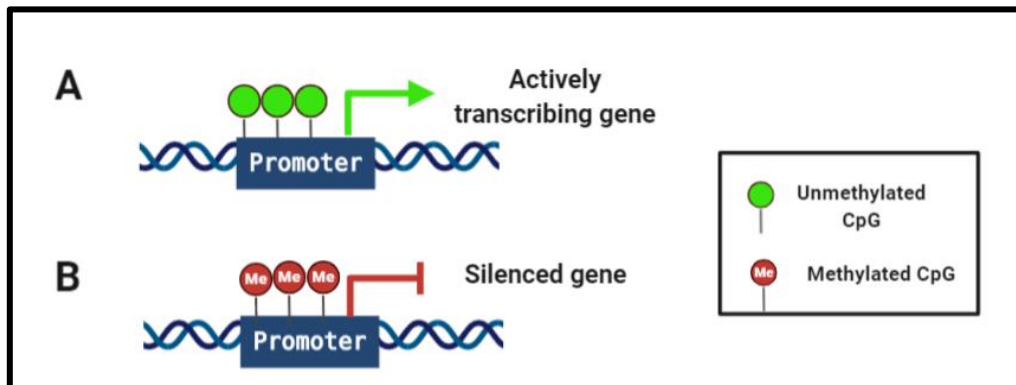
583 **Figure 2.3.** The complex epigenetic landscape involves: (A) DNA methylation, (B) histone
 584 modifications, (C) ncRNA such as miRNA and lncRNA and (D) RNA modifications such as RNA
 585 methylation (Aristizabal et al., 2020)

586 While the epigenome is stable, it is dynamic and can be influenced by a number of environmental factors
 587 (Marczylo et al., 2016). Aberrant changes to the epigenome can induce abnormalities in gene expression
 588 and disrupt cellular processes (Kanherkar et al., 2014). Therefore, aberrations in the epigenome have
 589 been identified to precede various diseases such as metabolic disorders, autoimmune diseases,
 590 neurological disorders and cancers (Shamsi et al., 2017). However, unlike genetic defects, epigenetic
 591 deviations are reversible and are thus potential therapeutic targets (Kelly et al., 2010).

592 **2.2.1. DNA Methylation**

593 DNA methylation is the most studied epigenetic mark that involves the covalent transfer of methyl
 594 groups from S-adenosylmethionine (SAM) to the fifth carbon in the nitrogenous base of cytosine (5mC)
 595 in DNA (Robertson, 2005). It usually occurs on cytosine bases adjacent to guanine bases (CpG site)
 596 (Robertson, 2005). Approximately 70% of CpG sites in mammalian DNA are methylated (Cooper and
 597 Krawczak, 1989); however, the distribution of CpG sites are not random. Multiple repeats of CpG sites,
 598 known as CpG islands, are usually found on gene promoters (Saxonov et al., 2006). CpG islands found
 599 on gene promoters are usually unmethylated and are associated with actively transcribing genes (Bird,

600 1986, Antequera, 2003, Saxonov et al., 2006). In contrast, methylation of promoter associated CpG
 601 islands results in the silencing of gene expression (Figure 2.4) (Mohn et al., 2008, Payer and Lee, 2008).
 602 Methylation can also occur on intergenic regions, where it prevents the expression of potentially
 603 harmful genetic elements (Moore et al., 2013), as well as within the gene body, where a positive
 604 correlation with gene expression occurs (Hellman and Chess, 2007, Aran et al., 2011, Jjingo et al.,
 605 2012).
 606



607
 608 **Figure 2.4.** Regulation of gene expression via DNA methylation. (A) Genes are actively transcribed
 609 when CpG islands are unmethylated; however, (B) methylation of CpG islands on the gene promoter
 610 inhibits transcription (prepared by author).

611 It is clear that DNA methylation is strongly involved in the physiological control of gene expression
 612 (Moore et al., 2013). It plays a key role in normal development (Li et al., 1992), compaction of
 613 chromatin (Geiman et al., 2004), genomic imprinting (Li et al., 1993), X chromosome inactivation
 614 (Csankovszki et al., 2001) and the bulk silencing of viral and transposable elements (Schulz et al.,
 615 2006). However, aberrant methylation patterns are associated with a multitude of diseases especially,
 616 cancer (Laird and Jaenisch, 1996, Ehrlich, 2002, Robertson, 2005, Jin and Liu, 2018, Kader et al., 2018).
 617 For example, CpG sites especially, those found in the promoter region of tumour suppressor genes are
 618 hot spots for somatic mutations (Rideout et al., 1990, Greenblatt et al., 1994). DNA methylation can
 619 promote increases in mutation rates and forms part of Knudson’s two-hit model for tumour formation
 620 by causing the heritable silencing of growth regulating genes (Jones, 1996, Moore et al., 2013, Zhou et
 621 al., 2020). Furthermore, global hypomethylation accompanied with hypermethylation of tumour
 622 suppressor genes are considered a hallmark of cancer and have been observed in several types of cancers
 623 (Lin et al., 2001, Yang et al., 2003, Saito et al., 2010, Wu et al., 2010, Hon et al., 2012, Pfeifer, 2018).

624 *2.2.1.1. Regulation of DNA Methylation*

625 DNA methylation is dynamic and involves enzymes that install (methyltransferases), recognize
 626 (readers) and remove (demethylases) methyl marks on DNA. DNA methylation is established by the
 627 DNA methyltransferase (DNMT) family which includes: DNMT1, DNMT3A, DNMT3B and

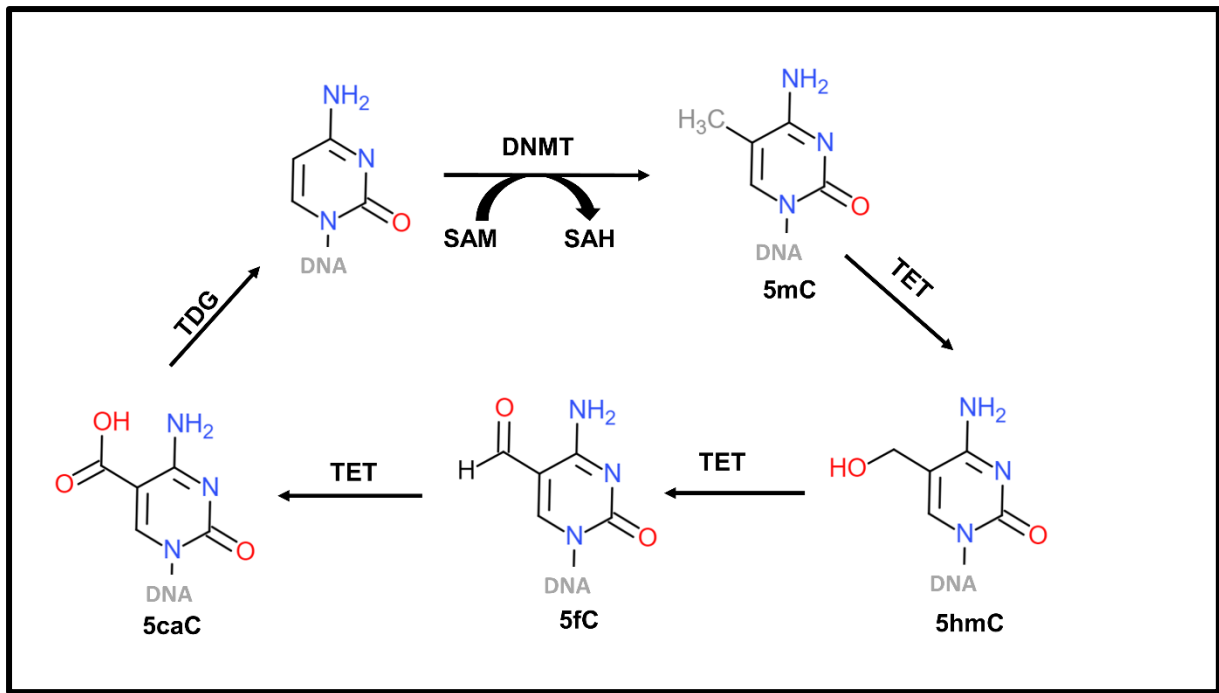
628 DNMT3L (Cheng and Blumenthal, 2008). The DNMT family are structurally similar with large
629 regulatory N-terminal domains and catalytic C-terminal domains; however, they vary in functionality
630 (Lyko, 2018).

631 DNMT1 is known as the maintenance DNMT as it maintains methylation patterns in a cell lineage
632 (Moore et al., 2013). A unique feature of its N-terminal is the replication foci targeting sequence which
633 allows DNMT1 to localize to the replication fork during DNA synthesis (Leonhardt et al., 1992). Here,
634 DNMT1 copies methylation patterns to hemi-methylated daughter strands to precisely mimic the
635 methylation pattern of the parent strand (Hermann et al., 2004). Moreover, DNMT1 accumulates at
636 DNA repair sites and is associated with mismatch repair and DNA damage response machinery
637 (Mortusewicz et al., 2005, Eades et al., 2011, Loughery et al., 2011). Silencing of DNMT1 leads to the
638 significant reduction in DNA methylation, aberrant imprinting and embryonic lethality suggesting that
639 it plays a critical role in dividing cells and cellular differentiation (Li et al., 1992, Li et al., 1993). While
640 DNMT1 maintains methylation patterns, DNMT3A and DNMT3B are responsible for the *de novo*
641 methylation of DNA (Figure 2.5) (Okano et al., 1998). DNMT3A and DNMT3B bare close structural
642 resemblance with the key difference being their expression pattern. DNMT3A is ubiquitously expressed
643 while DNMT3B is poorly expressed in most differentiated tissue (Xie et al., 1999). Furthermore,
644 DNMT3B is essential for early development as knockout of DNMT3B results in embryonic lethality in
645 mice, whereas growth is stunted when DNMT3A is silenced (Okano et al., 1998). The final member of
646 the DNMT3 family, DNMT3L, lacks catalytic activity however it supports *de novo* DNMTs by
647 enhancing their ability to bind to SAM and by stimulating their activity (Kareta et al., 2006). DNMT3L
648 is mainly present during early development where it is required for imprinting, compaction of the X
649 chromosome and methylation of retrotransposons (Bourc'his et al., 2001, Hata et al., 2002, Bourc'his
650 and Bestor, 2004, Zamudio et al., 2011). The exact mechanism by which *de novo* methyltransferases
651 target specific gene sequences is unknown; however, two hypotheses exist. The first suggests that RNA
652 interference directs DNMTs to specific sequences. While this mechanism occurs in plants, the evidence
653 observed in the mammalian genome is insufficient (Morris et al., 2004). The second suggests that
654 transcription factors regulate DNA methylation by either recruiting or blocking DNMTs to specific
655 DNA sequences (Brenner et al., 2005, Straussman et al., 2009). Binding of transcription factors seems
656 to primarily protect CpG islands from methylation and deletion or mutations to transcription factor
657 binding sites results in the *de novo* methylation of CpG islands (Brandeis et al., 1994, Macleod et al.,
658 1994).

659 While DNA methylation prevents the binding of transcription factors and thus switched off
660 transcription, DNA methylation “readers” are able to recognize and bind to 5mC bases, further
661 inhibiting transcription factor binding (Moore et al., 2013). Three classes of DNA methylation readers
662 exist: methyl-CpG-binding domain (MBD), ubiquitin-like containing PHD and RING-finger domain
663 (UHRF) and zinc-finger proteins. MBD family consists of Methyl CpG binding protein 2 (MeCP2),

664 MBD1, MBD2, MBD3, and MBD4. (Fatemi and Wade, 2006). MeCP2, MBD1 and MBD2 contain a
665 transcriptional repression domain that allows them to recruit corepressor complexes such as histone
666 deacetylases to methylated DNA to further silence gene transcription (Nan et al., 1998, Ng et al., 1999,
667 Villa et al., 2006). MeCP2 also plays a role in methylation maintenance by recruiting DNMT1 to hemi-
668 methylated DNA (Kimura and Shiota, 2003). MBD4 has DNA *N*-glycosylase enzymatic activity and is
669 able to recognize and repair guanine : thymine, uracil, or 5-fluorouracil mismatches that occur due to
670 5mC demethylation processes (Hendrich et al., 1999). Zinc finger proteins (Kaiso, ZBTB4, and
671 ZBTB38) are able to bind to 5mC and act in a similar way to the MBD family by repressing transcription
672 in a DNA methylation-dependent manner (Prokhortchouk et al., 2001, Fillion et al., 2006). UHRF
673 promotes DNMT1-targeted methylation of hemi-methylated DNA during DNA synthesis by tethering
674 DNMT1 to chromatin (Bostick et al., 2007).

675 DNA demethylation is the process of removing methyl marks from 5mC residues in either a passive or
676 active manner. Passive demethylation is the loss of DNA methylation patterns during successive rounds
677 of replication (Kohli and Zhang, 2013). It usually occurs due to loss of DNA methylation maintenance
678 in actively dividing cells (von Meyenn et al., 2016). Active demethylation occurs in both dividing and
679 non-dividing cells and is dependent on three enzyme families (Bhutani et al., 2011, Kohli and Zhang,
680 2013): (i) ten-eleven translocation (TET) family which can either hydroxylate 5mC to 5-
681 hydroxymethylcytosine (5hmC) or further oxidize it to 5-formylcytosine (5fC) and 5-carboxylcytosine
682 (5caC) (Tahiliani et al., 2009, Ito et al., 2011), (ii) Activation-induced cytidine
683 deaminase/apolipoprotein B mRNA-editing catalytic polypeptides (AID/APOBEC) family which is
684 responsible for the deamination of 5mC to thymine or 5hmC to 5-hydroxymethyluracil (5hmU)
685 (Morgan et al., 2004, Guo et al., 2011) and (iii) base excision repair glycosylases such as thymine DNA
686 glycosylase (TDG) which cleaves the products of TET and AID/APOBEC demethylation (5fC, 5caC,
687 thymine, and 5hmU) from the DNA backbone and replaces it with an unmethylated cytosine (Figure
688 2.5) (Cortellino et al., 2011, He et al., 2011).

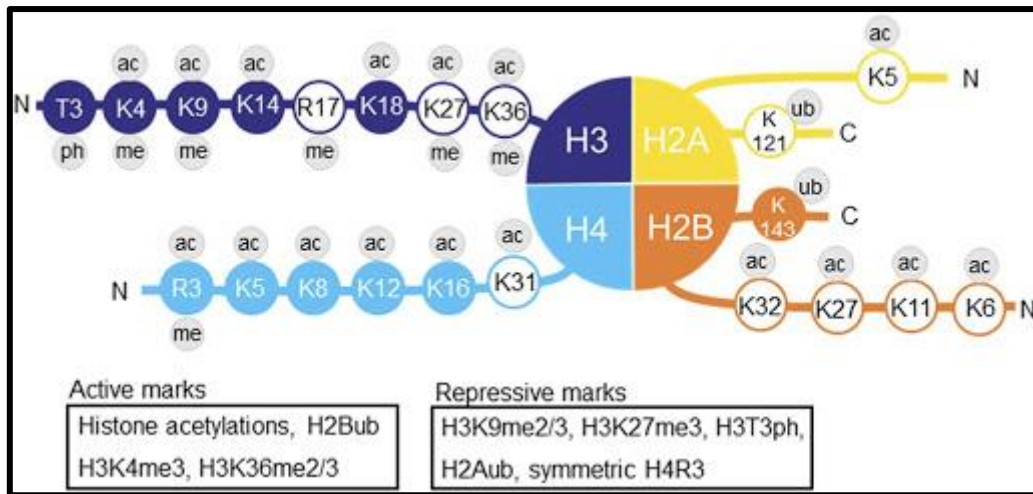


689

690 **Figure 2.5.** Regulation of DNA methylation. DNMT1 maintains DNA methylation patterns via
 691 methylation, while DNMT3A and DNMT3B are required for *de novo* methylation by catalysing the
 692 transfer of a methyl group from SAM to cytosine forming 5mC. TET plays a central role in DNA
 693 demethylation by oxidizing 5mC to hmC and further to 5fC and 5caC. 5caC is excised by TDG and
 694 replaced with an unmethylated cytosine (prepared by author).

695 **2.2.2. Histone Modifications**

696 The eukaryotic genome is tightly packaged into chromatin whose functional and structural unit is
 697 referred to as the nucleosome. Each nucleosome consists of four core histone proteins (H2A, H2B, H3
 698 and H4) arranged as an octamer around which approximately 200 base pairs of DNA is wrapped (Luger
 699 et al., 1997). The tight packaging of DNA by the nucleosome imposes a barrier to protein machinery
 700 required for its replication, repair and transcription (Ehrenhofer-Murray, 2004, Eaton et al., 2010,
 701 Chambers and Downs, 2012, Voss and Hager, 2014, Li and Zhu, 2015). Like DNA, histones can be
 702 modified by the addition or removal of chemical groups to control gene expression; however, histone
 703 modifications are not limited to methylation (Bannister and Kouzarides, 2011, Jambhekar et al., 2019).
 704 The N-terminal of histone tails can be subjected to several post-translational modifications. Such
 705 modifications include the methylation of arginine (R) and lysine (K), phosphorylation of serine and
 706 threonine and acetylation, ribosylation, sumoylation or ubiquitination of K (Figure 2.6). These covalent
 707 modifications, alter chromatin state, affect nucleosome positioning and influence accessibility to
 708 nucleotide base sequences (Bannister and Kouzarides, 2011, Chron et al., 2017, Jambhekar et al., 2019).



709

710 **Figure 2.6.** Schematic representation of some of the modifications found on histone tails of core
 711 histones (H2A, H2B, H3, H4) (Ueda and Seki, 2020).

712 The most common and well-studied histone marks are acetylation and methylation. Acetylation usually
 713 occurs on histone 3 (H3) and histone 4 (H4) and is a dynamic process regulated by histone
 714 acetyltransferases (HATs) and histone deacetylases (HDACs) (Verdone et al., 2006). The *N*-terminal
 715 tail of histones contain highly conserved positively charged K residues that have high affinity to the
 716 negatively charged DNA backbone, resulting in a condensed chromatin structure (Müller and Muir,
 717 2015). Acetylation of K residues neutralizes the positive charge; reducing the affinity between histone
 718 tail and DNA backbone. This leaves the DNA exposed and more accessible to transcription factors
 719 (Müller and Muir, 2015, Zhao and Shilatifard, 2019). Acetylation not only contributes to gene
 720 expression by influencing histone-DNA interactions but it is also recognized and bound by
 721 bromodomain containing enzymes that can influence transcription and other chromatin-templated
 722 processes (Zhao and Shilatifard, 2019).

723 Histone methylation primarily occurs on K and R residues found on H3 and H4 and is more complex
 724 than acetylation (Jambhekar et al., 2019). Methylation does not alter the charge of histone tails, instead
 725 histone methylation generates motifs that recruit bromo-, chromo-, and PHD domains of protein
 726 containing complexes that regulate gene expression (Strahl and Allis, 2000, Jenuwein and Allis, 2001).
 727 The outcome of methylation on gene expression is dependent on the specific residue that is methylated,
 728 the degree of methylation and the location of the methylated nucleosome in the genome (Jambhekar et
 729 al., 2019). There are three major forms of methylated R: mono-methyl-R, symmetrical di-methyl-R,
 730 and asymmetric-di-methyl-R, which are regulated by protein arginine N-methyltransferases (PRMTs)
 731 and the demethylase – Jumonji Domain-Containing Protein 6 (Jmjd6) (Chang et al., 2007, Guccione
 732 and Richard, 2019). Several methylation sites have been identified to alter gene expression. The
 733 following R modifications have been associated with active transcription: H4R3me2a, H3R2me2s,
 734 H3R17me2a, H3R26me2a; while H3R2me2a, H3R8me2a, H3R8me2s, whereas H4R3me2s marks
 735 repression of transcription (Blanc and Richard, 2017). On the other hand, K residues of histones can be

736 mono-, di- or tri- methylated (Jenuwein and Allis, 2001). Di- or tri- methylation of H3K4 at promoters,
737 H3K36 and K3K79 on gene body is typically associated with active transcription (Bernstein et al., 2002,
738 Bannister et al., 2005, Steger et al., 2008), whereas methylation of H3K9, H3K27, and H4K20 is
739 generally gene repressive (Karachentsev et al., 2005, Brykczynska et al., 2010, Ninova et al., 2019).

740 In this study, the interest is focussed on histone 3 lysine 4 trimethylation (H3K4me3) due to its distinct
741 presence at transcriptional start sites and promoters of actively transcribing genes as well as its possible
742 susceptibility to alteration by genotoxic agents.

743 2.2.2.1. *H3K4me3*

744 H3K4me3 is a highly conserved histone mark occurring in organisms as simple as protozoan to complex
745 organisms such as humans (Woo and Li, 2012, Song et al., 2017). In mammals, H3K4 methylation is
746 facilitated by histone lysine methyltransferase 2 family (KMT2) which consists of six members. Each
747 member contains a catalytic Su(var)3-9, Enhancer-of-zester and Trithorax (SET) domain that is
748 responsible for the transfer of methyl groups from SAM to the fourth lysine residue of H3 (Collins et al.,
749 2019). Each histone methyltransferase operates within a multiprotein complex that produces distinct
750 enzymatic responses (Hyun et al., 2017). Histone methylation functions by recruiting effector proteins
751 that function in chromatin remodelling and regulate gene expression. Interestingly, some H3K4
752 effectors reside within the enzymatic writer complexes (Collins et al., 2019). For example, H3K4me3
753 recruits bromodomain PHD finger transcription factor (BPTF), a subunit of the chromatin remodelling
754 complex – nucleosome remodelling factor (NURF), through its PHD fingers. This promotes the
755 accessibility of transcriptional machinery to the chromatin template (Mizuguchi et al., 1997). On the
756 other hand, demethylation of H3K4 makes the chromatin template inaccessible to transcription factors
757 and inhibits transcription (Hyun et al., 2017). This process is regulated by two families of histone lysine
758 demethylases: KDM1 and KDM5. KDM1 family (KDM1A and KDM1B) removes methyl groups from
759 H3K4me1 and H3K4me2 while the KDM5 family (KDM5A, KDM5B, KDM5C and KDM5D) removes
760 methyl groups from H3K4me1, H3K4me2 and H3K4me3 (Collins et al., 2019).

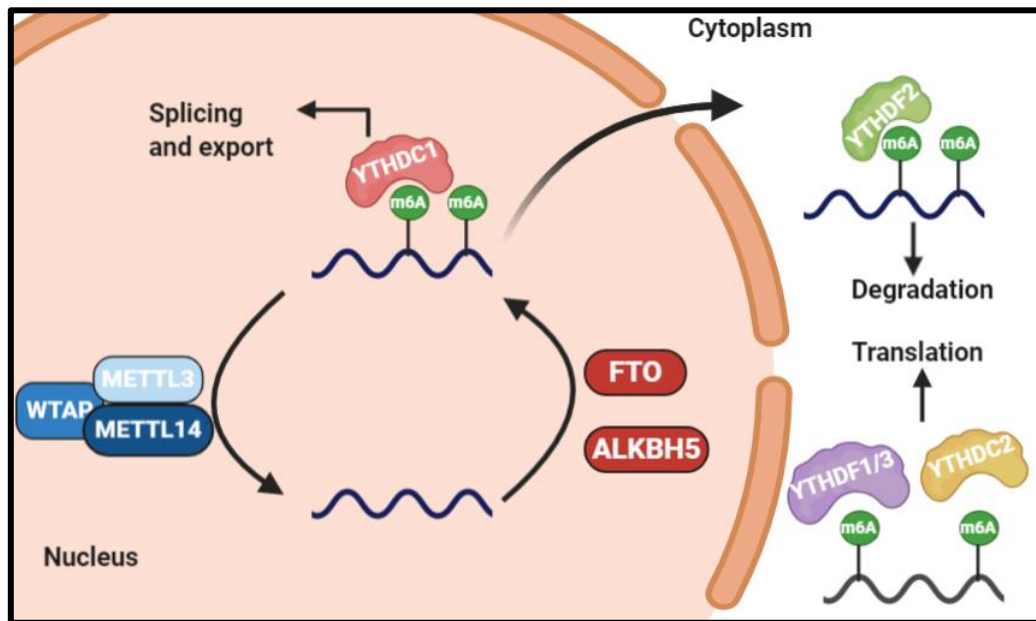
761 Aside from its role in transcriptional activation, H3K4me3 has been implicated in other nuclear
762 processes, including pre-mRNA splicing (Davie et al., 2015), meiotic DNA recombination (Borde et
763 al., 2009), and DNA repair (Pena et al., 2008, Faucher and Wellinger, 2010). H3K4me3 is essential for
764 cell cycle regulation, development and differentiation (Cui et al., 2009, Grandy et al., 2016, Zhang et
765 al., 2016, Huang et al., 2019b). Dysregulation of H3K4me3 has been associated with intellectual
766 disabilities and developmental disorders (Singh et al., 2016, Zamurrad et al., 2018, Larizza and Finelli,
767 2019). Moreover, aberrant H3K4me3 and mutations in H3K4 methyltransferases highly increases an
768 individual's susceptibility to various cancers (Rao and Dou, 2015).

769 **2.2.3. RNA methylation: N6-methyladenosine**

770 Chemical modifications are not limited to histones and DNA as over a hundred structurally distinct
771 chemical modifications are known to occur on the various classes of RNA (Cantara et al., 2011,
772 Machnicka et al., 2013). The most prevalent of these RNA modifications is the methylation of the sixth
773 nitrogen of adenosine (m6A) residues found on mRNA as well as lncRNA (Yue et al., 2015). M6A
774 modifications were first identified in the 1970s by researchers evaluating 5' cap structure of mammalian
775 mRNA (Desrosiers et al., 1974, Perry and Kelley, 1974). However, research in the field subsided shortly
776 after due to the lack of methods for detecting m6A sites in RNA. With the establishment of high
777 throughput sequencing methods, interest in the field has now resurfaced. These mapping approaches
778 has revealed that m6A modifications are dynamic, widespread, conserved and occur primarily in
779 DRACH (where D = A/G/U, R= A/G, H=A/C/U) sequence consensus motifs that are located near stop
780 codons, long exonic regions and 3' untranslated regions (3' UTR) (Dominissini et al., 2012, Meyer et
781 al., 2012, Ke et al., 2015). M6A modifications are conserved amongst eukaryotes (Dominissini et al.,
782 2012) but have also been identified in the mRNA of replicating viruses (Krug et al., 1976), and several
783 classes of RNA in bacteria and archaea (Deng et al., 2015, Couturier and Lindås, 2018). The
784 modification functions by affecting mRNA stability, translation, splicing and nuclear export, miRNA
785 biogenesis and lncRNA metabolism (Wang et al., 2014a, Alarcón et al., 2015, Ma et al., 2019, Zaccara
786 et al., 2019).

787 The m6A epitranscriptome is shaped by m6A writers, readers and erasers (Figure 2.7) (Zaccara et al.,
788 2019). m6A marks are installed during transcription by a multicomponent methyltransferase complex
789 which selectively methylates RNA substrates exhibiting the DRACH consensus (Bokar et al., 1997, Liu
790 et al., 2014, Ping et al., 2014). The complex consists of methyltransferase like 3 (METTL3) (Bokar et
791 al., 1997), methyltransferase like 14 (METTL14) (Liu et al., 2014) and Wilms' tumor 1-associating
792 protein (WTAP) (Ping et al., 2014). METTL3 serves as the catalytic subunit and facilitates the transfer
793 of methyl groups from SAM to adenosine (A) of RNA (Bokar et al., 1997) while METTL14 acts as a
794 support for METTL3 by recognizing RNA substrates and allowing binding to RNA (Wang et al., 2016).
795 Liu et al. (2014) have demonstrated that METTL14 may have catalytic activity as well. Studies have
796 shown that knockdown of either METTL3 or METTL14 led to a concurrent decrease in m6A levels of
797 polyadenylated RNA (Liu et al., 2014). Surprisingly, the knockdown of METTL14 led to a more
798 pronounced decrease in global m6A transcript levels (Place et al., 2008); however, a combination of
799 both methyltransferases drastically enhances methylation efficiency (Wang et al., 2014b). WTAP is the
800 third crucial component; it does not possess catalytic methyltransferase activity, but coordinates the
801 localization of the METTL3-METTL14 heterodimer into nuclear speckles (Liu et al., 2014, Ping et al.,
802 2014). WTAP may also interact with other components such as RNA binding motif protein 15 (RBM15)
803 and RBM15B which bind to uridine-enriched regions and then recruit WTAP/METTL3 complexes to

804 methylate nearby DRACH motifs (Patil et al., 2016) and Zinc Finger CCCH-Type Containing 13
 805 (Zc3H13) which also plays a role in the nuclear localization (Wen et al., 2018).



806

807 **Figure 2.7:** m6A modification machinery. The m6A methyltransferase complex (METTL13,
 808 METTL14 and WTAP) serves as an m6A “writer”, demethylases (e.g., FTO and ALKBH5) serve as
 809 m6A “erasers”, and a set of m6A “readers” (e.g., YTHDF1/2/3, YTHDC1/2) serve to determine the
 810 fate of target m6A-modified mRNA transcripts (prepared by author).

811 Seeing that m6A modifications are dynamic, demethylation of m6A to adenosine (A) is catalysed by
 812 the m6A “erasers” (Jia et al., 2011). Thus far, only two m6A demethylases have been identified, i.e.,
 813 fat mass and obesity associated protein (FTO) and its homologue ALKBH5 (Jia et al., 2011, Zheng et
 814 al., 2013). Both proteins belong to the ALKB subfamily of Fe(II)/ α -ketoglutarate-dependent
 815 dioxygenases which repair DNA alkylation damage by demethylating DNA and RNA nucleotides that
 816 have been alkylated (Fedele et al., 2015). FTO has been shown to oxidatively demethylate m6A to A
 817 in a stepwise manner with N6-hydroxymethyladenosine (hm6A) and N6-formyladenosine (f6A) as
 818 intermediates (Fu et al., 2013). In contrast, ALKBH5 directly and oxidatively removes methyl marks
 819 with no detected intermediates (Zheng et al., 2013). FTO and ALKBH5 knockout and overexpression
 820 have been shown to increase and reduce m6A levels, respectively (Jia et al., 2011, Zheng et al., 2013).
 821 Both demethylases are tissue specific and have diverse intracellular localization, thus demethylation in
 822 some tissue may be facilitated solely by FTO or ALKBH5 (Zhang et al., 2019).

823 While writer and eraser proteins are responsible for installing and removing m6A marks, readers
 824 control the fate of m6A modified transcripts (Liao et al., 2018). The m6A readers consist of the YTH
 825 B homology (YTH) domain family proteins: YTHDF1, YTHDF2, YTHDF3 and YHT domain
 826 containing proteins: YTHDC1 and YTHDC2, which preferentially recognize and bind to m6A sites and
 827 confer downstream functions (Liao et al., 2018). Nuclear readers regulate mRNA splicing and other

828 nuclear processes (Xiao et al., 2016) whereas cytoplasmic readers affect mRNA stability, translation
 829 and localization (Zaccara et al., 2019). The localization and function of all known YTH domain
 830 containing m6A readers are summarized in Table 2.1.

831 **Table 2.1: The localization and function of YTH domain containing m6A-readers**

m6A Reader	Cellular Localization	Effects of Binding to m6A RNA
YTHDC1	Nucleus	Affects splicing and export Preferably binds to ncRNA, may bind to mRNA
YTHDC2	Nucleus and cytoplasm	Implicated in mRNA degradation and initiation of translation
YTHDF1	Cytoplasm	Promotes translation
YTHDF2	Cytoplasm	Promotes degradation
YTHDF3	Cytoplasm	Promotes translation

832

833 **2.2.4. ncRNA**

834 Although early studies have reported the occurrence of transcription in regions not coding for proteins,
 835 it is only recently that researchers have realized that while a vast majority of the genome is transcribed
 836 (62.1%); only 2-3% constitute of protein coding genes (Panzeri et al., 2016). Areas of the genome that
 837 do not encode for protein, are transcribed to ncRNA. Since ncRNA do not function in protein coding,
 838 it was long regarded that ncRNAs were “junk RNAs” or “transcriptional noise”. However, through the
 839 development of high-throughput technologies, this idea has been rejected as we now know that ncRNAs
 840 play a key role in regulating cellular events and gene expression (Kapranov et al., 2002, Kapranov et
 841 al., 2007).

842 ncRNAs are classified based on their function into housekeeping ncRNAs and regulatory ncRNAs
 843 (Wei et al., 2017). Housekeeping ncRNAs include ribosomal RNAs (rRNAs), transfer RNAs (tRNAs),
 844 small nuclear RNAs (snRNAs) and small nucleolar RNAs (snoRNAs). They are usually short (~20-200
 845 nucleotides; nt), constitutively expressed and necessary for the maintenance of normal cellular functions
 846 and are involved in protein translation, splice regulation, RNA modifications as well as the transport
 847 and insertion of proteins into membranes (Morey and Avner, 2004). On the other hand, regulatory
 848 ncRNA consists of both short and long (22 nt to ~100 kilobases) ncRNAs that are involved in regulating
 849 gene expression through various mechanisms (Table 2.2). Transcriptional silencing by ncRNA has been
 850 implicated in several diseases including cancer predisposition or status. Among the ever-increasing
 851 types of ncRNAs being deciphered, microRNAs (miRNAs) and long non-coding RNAs (lncRNAs) are
 852 the most intensively studied and play a prominent role in epigenetic control (Dai et al., 2019).

853 **Table 2.2: Characteristics and functioning of regulatory ncRNAs.**

Type	Symbol	Source	Size (nt)	Function
microRNA	miRNA	pri-miRNA	~22	Gene silencing
Small interfering RNA	siRNA	Long double stranded RNA	19-25	Gene silencing
Piwi interacting RNA	piRNA	Long single chain precursor transcripts	26-31	Transposon silencing and DNA methylation
Long non-coding RNA	lncRNA	Multiple	>200	Transcriptional activation Post-transcriptional regulation X chromosome inactivation Regulation of chromatin remodelling, imprinting, miRNA, methylation and RNA binding proteins

854

855 **2.2.4.1. MiRNAs**

856 The discovery of miRNAs has revolutionized the field of molecular biology. In 1993, Lee and
 857 Whiteman identified the first miRNA, *lin-4* in *Caenorhabditis elegans* (Lee et al., 1993, Wightman et
 858 al., 1993). Although miRNAs were identified in the early 1990s, it took almost 10 years until their
 859 fundamental roles in gene regulation were recognized (Lagos-Quintana et al., 2001). The field of
 860 miRNA research has since grown with over 17,000 miRNAs discovered to date in 142 species (Dwivedi
 861 et al., 2019). Today, we know that these small regulatory RNAs, play key roles in developmental and
 862 physiological processes in most eukaryotes and are even encoded by some viruses (Pfeffer et al., 2004,
 863 Vidigal and Ventura, 2015). However, aberrant expression of miRNAs is associated with many human
 864 diseases. Aberrant miRNA profiles have been observed in numerous cancers where they act as either
 865 tumour suppressors or oncogenes depending on their mRNA targets (Cui et al., 2019). Therefore, the
 866 evaluation of extracellular miRNAs profiles are used as potential biomarkers for a variety of diseases
 867 (Paul et al., 2018).

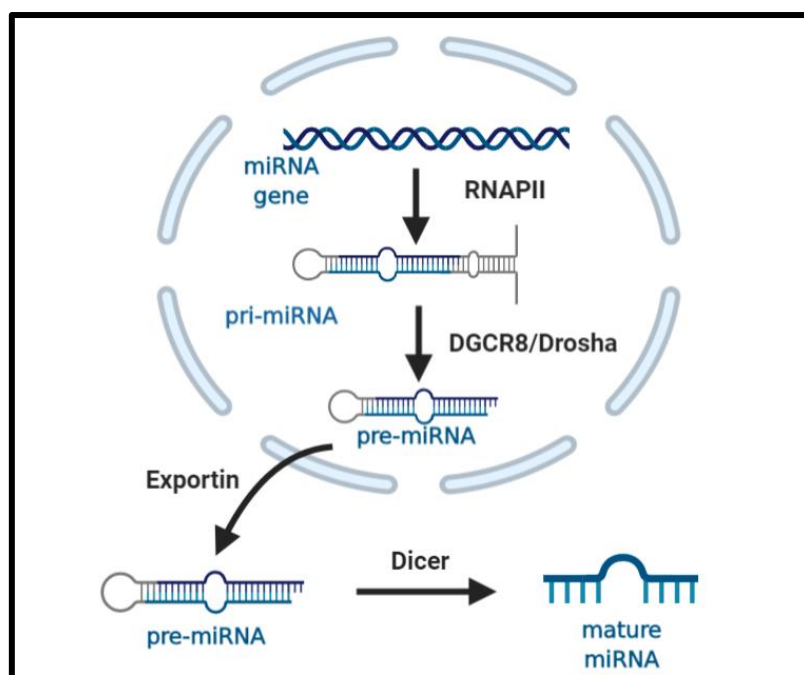
868

869

870 2.2.4.1.1. Biogenesis

871 The biogenesis of miRNAs begins with its transcription from the host gene (intragenic miRNAs) or
872 independently of the host gene with the use of their own promoter (intergenic miRNAs). miRNAs can
873 be transcribed individually as monocistronic transcripts or as one long transcript (polycistronic
874 transcripts) called clusters which are later processed to individual mature miRNAs. The biogenesis of
875 miRNAs can occur via the canonical or noncanonical pathways (O'Brien et al., 2018).

876 Processing of miRNAs usually occurs via the canonical biogenesis pathway which involves two ordered
877 endonucleolytic cleavages by RNase III enzymes (Figure 2.8) (Davis and Hata, 2009). Most miRNAs
878 are transcribed from DNA sequences by RNA polymerase II (RNAP II) as capped and polyadenylated
879 primary miRNAs (pri-miRNA), which undergo processing by the microprocessor complex to form a
880 single hairpin structure termed precursor miRNA (pre-miRNA) (Treiber et al., 2019). The
881 microprocessor complex consists of DiGeorge Syndrome Critical Region 8 (DGCR8), an RNA binding
882 protein that recognizes an N6-methyladenylated GGAC motif within the pri-miRNA and RNase III
883 enzyme Drosha, which cleaves the pri-miRNA duplex. Once pre-miRNA is generated, exportin-5 and
884 Ran-GTP exports it to the cytoplasm where it undergoes cleavage by the RNase III enzyme, Dicer
885 (O'Brien et al., 2018). Processing by Dicer removes the terminal loop giving rise to a double stranded
886 22 nt product consisting of the mature miRNA guide strand and passenger strand. The double stranded
887 miRNA product is transferred onto RNA binding proteins known as Argonaute (AGO) protein. The
888 passenger strand is usually discarded whereas the guide strand is incorporated into the RNA-induced
889 silencing complex (miRISC) and mediates mRNA degradation or translational inhibition. (Treiber et
890 al., 2019).



891

892 **Figure 2.8.** The canonical pathway of miRNA biogenesis (prepared by author).

893 Biogenesis of miRNAs can also occur via several non-canonical pathways. Non-canonical pathways
894 are generally classified into Drosha/DGCR8-independent pathway and Dicer-independent pathways.
895 One class of Drosha/DGCR8-independent miRNAs are known as mitrons which originate from spliced
896 introns and function as pre-miRNAs that do not require cleavage by Drosha/DGCR8 complex. They
897 are immediately exported to the cytoplasm for Dicer processing (Treiber et al., 2019). On the other
898 hand, Dicer-independent miRNAs are relatively rare. They are processed by Drosha from endogenous
899 short hairpin RNA (shRNA) transcripts and are directly recognized by Ago proteins. Therefore, they
900 are produced independently of Dicer (Dai et al., 2019).

901 2.2.4.1.2. Regulation of gene expression

902 Generally, miRNAs guide miRISC to recognize a specific complementary seed sequence in the 3'UTR
903 region of the target mRNA and downregulates gene expression by either translational repression or
904 mRNA degradation (Wahid et al., 2010). miRNA binding sites have also been detected in other mRNA
905 regions. miRNA binding to 5' UTR and coding sequences have been reported to have silencing effects
906 whereas binding within promoter regions induces transcription (Place et al., 2008). The mechanism of
907 gene silencing by miRISC depends on the degree of complementarity between the miRNA and a
908 specific sequence on the target mRNA known as the miRNA response element (MRE). A high degree
909 of sequence complementarity enables AGO degradation of target mRNA (Jo et al., 2015). Other
910 mechanisms such as deadenylation, decapping, and exonucleolytic digestion of mRNA are also
911 involved in mRNA degradation (Wahid et al., 2010). However, most miRNA-MRE interactions are not
912 entirely complementary and result in translational repression. The exact mechanism is not well
913 understood but miRNAs are involved in either the inhibition of initiation or elongation stages of
914 translation (Kong et al., 2008).

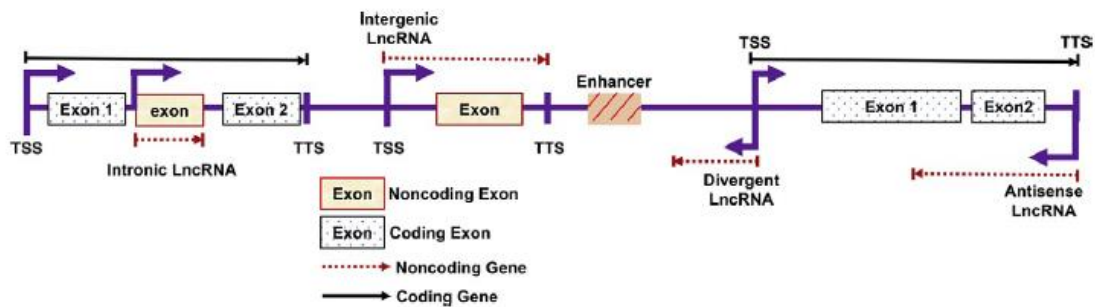
915 2.2.4.2. *LncRNAs*

916 The first lncRNA, H19, was discovered in the late 1980s during studies investigating genomic
917 imprinting (Jarroux et al., 2017). Since then tens of thousands of lncRNAs have been identified;
918 however, less than 1% of loci identified lncRNA have been experimentally validated (Kopp and
919 Mendell, 2018). lncRNAs share several characteristics with mRNA such as poly-adenylation, 5'-
920 capping and exon-intron splicing. Despite these similarities, lncRNAs tend to have fewer exons and
921 lack open reading frames which prevent its translation (Wang et al., 2017a, DiStefano, 2018). Although
922 lncRNA lack protein coding abilities, they have a broad functional repertoire which include regulation
923 of gene expression, embryonic development, imprinting, chromosomal dynamics, telomere biology,
924 and immune responses (Amaral and Mattick, 2008, Ouyang et al., 2016, Liu et al., 2017, Oliva-Rico
925 and Herrera, 2017). Due to its diverse role in regulating molecular pathways, dysregulation of lncRNA
926 have been implicated in the aetiology of more than 200 diseases including cancer (Bao et al., 2018,

927 DiStefano, 2018). Therefore, significant research endeavours are being exercised to study the role of
 928 lncRNAs in biological processes, and to apply lncRNAs as biomarkers or therapeutic targets.

929 2.2.4.2.1. Biogenesis

930 The synthesis of most lncRNA, like mRNA and miRNA, begins with its transcription by RNAP II.
 931 They can be transcribed from several different genomic loci and are classified accordingly (Figure 2.9
 932 and Table 2.3) (Khandelwal et al., 2015). Similar to protein coding regions, lncRNA promoters are
 933 enriched for active histone modifications (Quinn and Chang, 2016). Many lncRNA transcripts are not
 934 end products. To reach their mature forms, they undergo extensive co- and post-transcriptional
 935 processing which include 5'capping, 3'-polyadenylation, splicing and RNA editing (Dhanao et al.,
 936 2018). Some lncRNAs undergo alternative processing to distinguish them from other transcripts. For
 937 example, back-splicing of linear transcripts produces stable circular RNAs (circRNAs) consisting of
 938 non-sequential exon-exon junctions (Lasda and Parker, 2014).



939

940 **Figure 2.9.** Classification of lncRNA based on the location in the genome (Choudhari et al., 2020).

941 **Table 2.3: Classification of lncRNA**

Type	Origin	RNA polymerase	Direction of transcription	Additional information
Intergenic lncRNA	Large intervening regions flanked by two protein coding genes	RNAP II or III	Sense or anti-sense	Is 5'-capped and contains 3'-end poly(A) tail. Serves as a precursor to other ncRNAs such as miRNA.
Intronic lncRNA	Intronic regions of protein coding genes	RNAP III or RNAP IV	Sense or anti-sense	Undergoes alternative splicing and contains some exonic sequences and 3'-end poly(A) tail.

Sense lncRNA (exonic/divergent lncRNA)	Protein coding portions of genes, with exons overlapping those of the companion mRNAs	RNAP II	Sense	Undergoes splicing and lacks open reading frames preventing protein translation
Natural antisense transcripts (NATs)	Antisense strand of proteins coding genes	RNAP III	Antisense	NATs are categorized as cis (occurs on opposite strand of coding gene) or trans (occurs on the opposite strands of the pseudogene)
Bidirectional	(<1 000 bps) to the transcriptional start sites of protein-coding genes	RNAP II	Anti-sense to the protein coding gene	

942

943 2.2.4.2.2. Functions

944 Unlike miRNAs, the functioning of lncRNA cannot be inferred from its sequence or structure. The exact
945 functioning and mechanism of these RNA molecules calls for extensive research; however, we do know
946 that the dynamic functional repertoire of lncRNA includes gene silencing, cell cycle regulation,
947 splicing, chromatin modifications, and differentiation and that lncRNA implement these functions by
948 serving as signalling molecules, molecular decoys, guides or scaffolds (Wang and Chang, 2011, Dhanoa
949 et al., 2018).

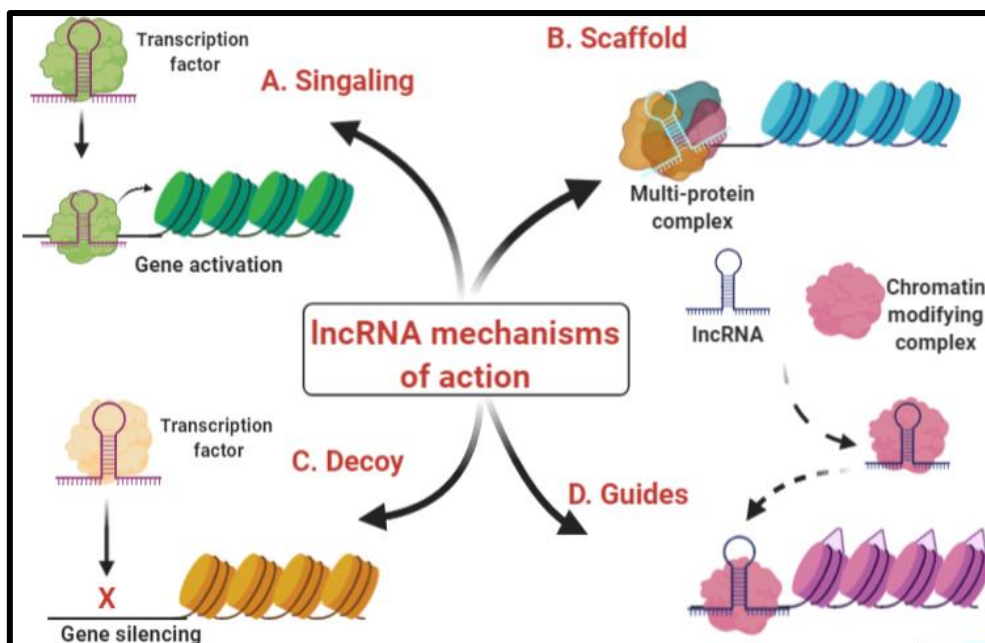
950 The belief that some lncRNA act as signalling molecules stems from the finding that their transcription
951 is tightly controlled and fluctuates in a cell specific manner and is dependent on diverse stimuli and
952 biological events (Figure 2.9A). Signalling lncRNA serve as molecular indicators that reversibly
953 regulate transcriptional and post-transcriptional processes in response to various stimuli (Wang and
954 Chang, 2011). lincRNA-p21 promotes p21 transcription, thereby signalling the repression of p53-
955 dependent genes and the initiation of apoptosis. The main function of a signal lncRNA is to serve as a

956 molecular signal to regulate transcription in response to various stimuli. Thus, its production and
957 presence can serve as an indicator of transcriptional activity (Huarte et al., 2010).

958 Recent evidence suggests that like proteins, lncRNA are major players involved in various scaffolding
959 complexes. lncRNAs can also serve as platforms upon which relevant molecular components may be
960 assembled. lncRNA that act as scaffolds are complex and possess different domains that bind to multiple
961 effectors concurrently to regulate gene expression. These effectors can achieve either transcriptional
962 activation or repression in a time and space restricted manner (Figure 2.9B) (Wang and Chang, 2011).
963 For example, the 5'-end of the lncRNA, HOX transcript antisense RNA (HOTAIR) binds to polycomb
964 repressive complex 2 (PRC2) which methylate H3K27 while its 3'-end binds to LSD1 which results in
965 H3K4 demethylation and subsequently gene repression (Tsai et al., 2010).

966 lncRNA that act as decoys can regulate transcription in a positive and negative manner. Decoy lncRNAs
967 mimic the target binding site of effector molecules on DNA. This prevents the effectors such as
968 transcription factors and chromatin modifiers from gaining access to DNA (Figure 2.9C) (Khandelwal
969 et al., 2015). The lncRNA, p21-associated ncRNA DNA damage activated (PANDA) binds and
970 sequesters the transcription factor NF-YA to limit the expression of pro-apoptotic genes and promote
971 cell survival in response to low levels of DNA damage (Hung et al., 2011).

972 As molecular guides, lncRNAs bind to proteins and chaperones them to specific targets (Figure 2.9D).
973 This activity can cause changes in gene expression either in cis (on neighbouring genes) or in trans
974 (distantly located genes). For example, the lncRNA, Air recruits the histone methyltransferase, G9a and
975 leads it to their target site where gene silencing is achieved through H3K9 methylation (Nagano et al.,
976 2008).

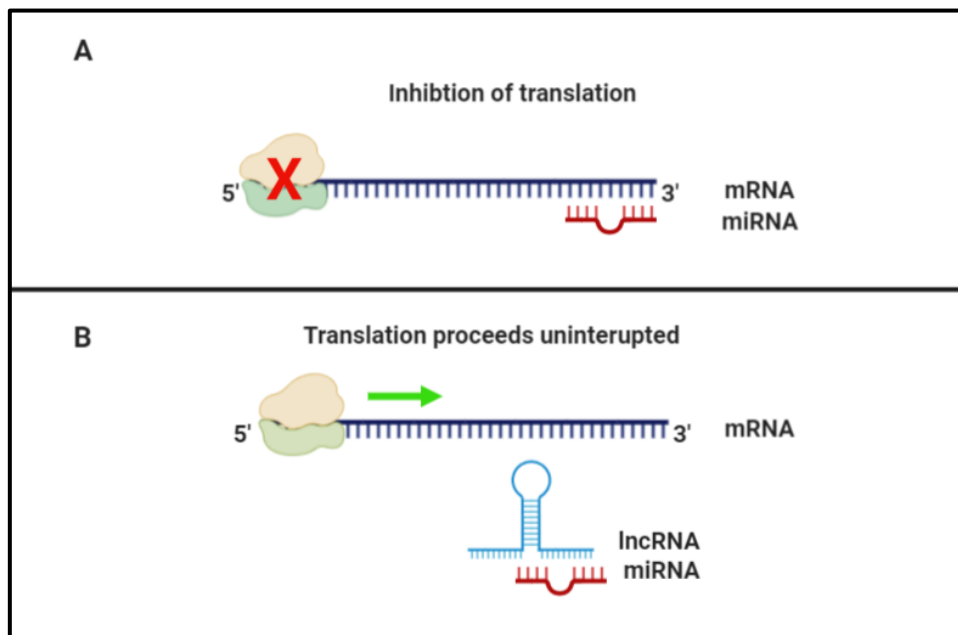


977

978 **Figure 2.10.** General mechanism by which lncRNA function. lncRNAs can act as (A) molecular
979 signals, (B) dynamic scaffolds, (C) decoys and (D) guides (prepared by author).

980 *2.2.4.3. Regulation of miRNA by lncRNAs*

981 As previously discussed, miRNAs sequester their target mRNA through binding of MRE to inhibit
982 translation. lncRNA are able to compete with MRE for miRNA binding. These lncRNA are known as
983 competing endogenous RNAs (ceRNAs) (Wang and Chang, 2011, Tay et al., 2014). They are able to
984 mimic miRNA targets which results in the sequestering of miRNAs at their 3' UTR. This reduces
985 miRNA availability within cells and promotes the translation of their target mRNA (Figure 2.10)
986 (Khandelwal et al., 2015). An example of a lncRNA that functions as a ceRNA is HOXA 11 antisense
987 RNA (HOXA11-AS). HOXA11-AS ceRNA abilities have been observed in various cancers. In non-
988 small-cell lung cancer, HOXA11-AS sequester miR-124 and miR-454, which promotes SP1 and
989 STAT3 expression, respectively (Yu et al., 2017, Zhao et al., 2018). This, in turn, promotes
990 proliferation, invasion and migration of cancer cells. In addition, HOXA11-AS targets miR-125a-5p,
991 miR-130a, miR-140-5p, miR-146-5p, miR-214-3p, miR-215a-5p, miR-241-3p, miR-1297 in various
992 cancers such as hepatocellular, gastric, renal, colorectal cancers and glioma (Wei et al., 2020).
993 Furthermore, HOXA11-AS-miR-124 interactions are involved in fracture healing by inhibiting
994 osteoblast proliferation and enhancing apoptosis (Wang et al., 2017b).



995 **Figure 2.11.** Interaction between ncRNA and mRNA. (A) miRNA prevents translation by binding to
996 mRNA. (B) lncRNA sequesters miRNA which allows translation to occur (prepared by author).

998 *2.2.5. The role of epigenetics in Fusarium mycotoxin induced toxicities*

999 The molecular mechanisms by which *Fusarium* mycotoxins induces toxicity have been well
1000 documented, however emerging evidence suggests that crosstalk between molecular and epigenetic

1001 modifications play an important role in *Fusarium*-induced toxicities (Huang et al., 2019a, Ghazi et al.,
1002 2020a).

1003 It has been suggested that epigenetic modifications may be responsible for Zearalenone's oestrogenic
1004 effects. Zearalenone induces the expression of DNMTs and increases global levels of DNA methylation,
1005 H3K4me3, H3K9me3 and H3K27me3. These changes have been associated with the disruption of
1006 oocyte maturation and early embryonic development associated with zearalenone exposure (Han et al.,
1007 2015). Moreover, zearalenone induces CpG methylation of the *LIM Homeobox 8 (LHX8)* gene,
1008 repressing its transcription. LHX8 is the transcription factor responsible for ovarian follicle formation,
1009 therefore its downregulation disrupts primordial follicle formation (Zhang et al., 2017). Changes in
1010 miRNA profiles have also been attributed to zearalenone's effect on the reproductive system.
1011 Zearalenone induces miR-7 expression via protein kinase C and p38. Zearalenone-induced
1012 overexpression of miR-7 inhibits follicle stimulating hormone synthesis and secretion (He et al., 2018).

1013 The trichothecenes, T-2 toxin and HT-2 have been shown to induce epigenetic modifications. HT-2
1014 toxin-induced disruption of mouse oocyte maturation via increased global 5mC levels, and decreased
1015 H3K9me2 and H3K27me3 levels (Zhu et al., 2016). T-2 toxin induces toxicity through proinflammatory
1016 mechanisms. While T-2 toxin increased global DNA methylation, it demethylated the promoters of
1017 proinflammatory cytokines which induced cytokine production which in turn induced hepatotoxicity (Liu
1018 et al., 2019). Furthermore T-2 toxin induces miR-155 expression which disrupts cytokine suppressors
1019 (Guo et al., 2020).

1020 Like zearalenone and trichothecenes, the effect of FB₁ on DNA methylation and histone modifications
1021 have been thoroughly researched while little research has focused on the role of miRNAs in FB₁-
1022 induced toxicity. For instance, several studies have evaluated the effects of FB₁ on DNA methylation.
1023 Chuturgoon et al. (2014a) demonstrated that FB₁ induces DNA hypomethylation in HepG2; however,
1024 DNA hypermethylation occurred in rat C6 glioma cells and human Caco-2 cells (Mobio et al., 2000,
1025 Kouadio et al., 2007). Furthermore, Demirel et al. (2015) found no significant changes in global DNA
1026 methylation but hypermethylation occurred at the promoter regions of the tumor suppressors: *c-myc*,
1027 *p15*, *p16*, and *e-cadherin*. With regards to histone modification, FB₁ induced H3K9me3 and acetylation
1028 of H2NK12, H3K9 and H3K23 and repressed H4K20me3 (Pellanda et al., 2012, Sancak and Ozden,
1029 2015, Gardner et al., 2016). The only study to investigate the effect of FB₁ on miRNA found that FB₁
1030 downregulated miR-27b which subsequently increased cytochrome P450 1B1; which may play a role
1031 in FB₁-induced hepatic neoplastic transformation (Chuturgoon et al., 2014b). For a detailed discussion
1032 on epigenetic mechanisms involved in FB₁ toxicity, see Chapter 3: Molecular and Epigenetic
1033 Mechanisms of FB₁ Mediated Toxicity and Carcinogenesis and Detoxification Strategies; pages 86-89.

1034 Little is known on the relationship between *Fusarium* mycotoxins and lncRNA and RNA modifications
1035 with the exception of two independent studies that demonstrated that exposure to the mycotoxins fusaric

1036 acid and DON alters the m6A transcriptome (Ghazi et al., 2020b, Zhengchang et al., 2020). While the
1037 above-mentioned studies demonstrate that epigenetic modifications play an important role in
1038 mycotoxin-induced toxicities, further research should be dedicated to ncRNA and RNA modifications.
1039 Moreover, our understanding on the downstream effects of FB₁-induced epigenetic changes is
1040 insufficient. Further research should be done to assess the downstream effects of FB₁-induced
1041 epigenetic modifications. For instance, epigenetic mechanisms may exacerbate toxicity by
1042 dysregulating response mechanism to the stress induced by FB₁. Such stress response mechanisms
1043 include DNA damage checkpoint signalling, Keap1/Nrf2 anti-oxidant responses and apoptosis as it well
1044 established that FB₁ induces DNA damage and oxidative stress.

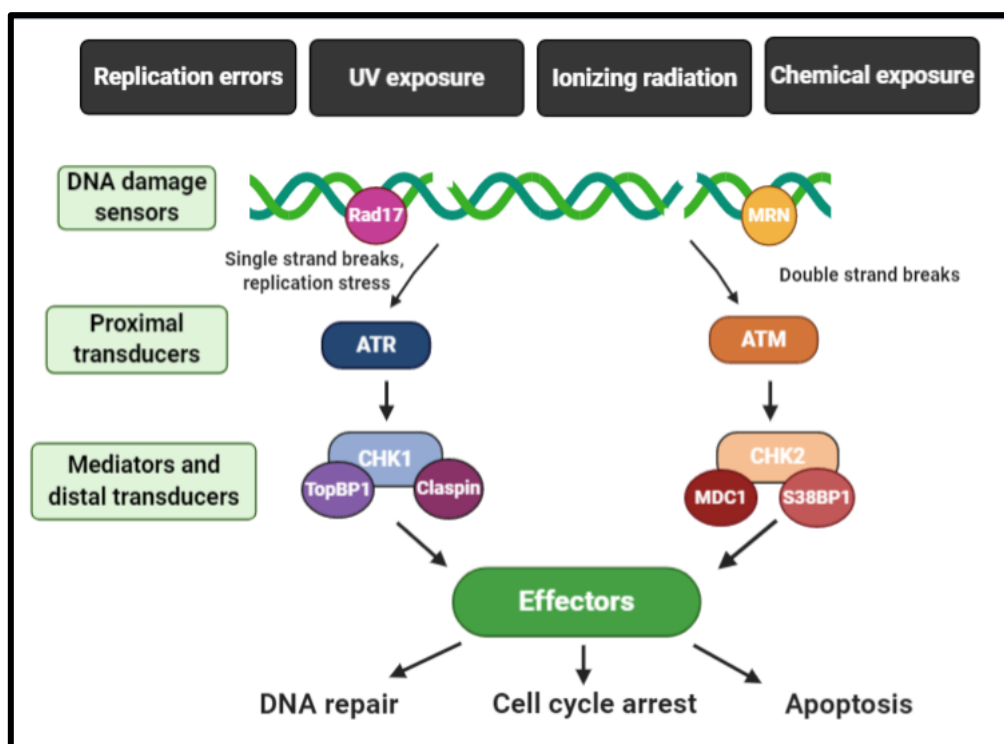
1045 **2.3. Cellular Response to stress**

1046 ***2.3.1. The DNA damage response***

1047 The survival of organisms depends on the preservation of genetic information between cell lineages
1048 during replication (Zhou and Elledge, 2000). However, DNA is highly susceptible to damage by
1049 endogenous and exogenous agents and mistakes during replication can occur (Chatterjee and Walker,
1050 2017). It is estimated that approximately 10⁵ DNA lesions occur in each cell per day. These lesions
1051 severely affect important genomic processes such as transcription and replication of damaged DNA
1052 result in mutations that induce and propagate carcinogenesis (Giglia-Mari et al., 2011). The timely
1053 clearance of genomic injuries is therefore, essential. Cells are equipped with a complex network of
1054 DNA damage responses (DDR) which monitor the structure and integrity of the genome, co-ordinate
1055 cell cycle arrest and initiate DNA repair (Zhou and Elledge, 2000).

1056 DNA damage checkpoint signalling is a central orchestrator of the DDR network. Checkpoints stall cell
1057 division so that effective DNA repair can occur (Dai and Grant, 2010). This signalling network consists
1058 of sensors, transducers, mediators and effectors (Figure 2.11) (Zhou and Elledge, 2000). Sensors are
1059 multiprotein complexes that detect aberrant DNA structures and initiate the signalling response. The
1060 MRe11-Rad 50-Nbs1 (MRN) sensor complex detects double stranded DNA breaks and recruit's ATM
1061 to the DNA damage site, while Rad17 and Rad9-Rad1-Hus1/9-1-1 complex generally recognise single
1062 strand breaks and localizes ATR to the lesion (Dai and Grant, 2010). ATR and ATM are proximal
1063 transducers that have kinase activity. The activation of ATR and ATM phosphorylates and activates
1064 mediators (such as 53BP1, MDC1, TopBP1, and claspin etc.) at DNA damage sites which in turn
1065 activates the distal transducers: checkpoint kinase 1 (CHK1) and checkpoint kinase 2 (CHK2) (Dai and
1066 Grant, 2010). Ultimately, ATR transduces signals to CHK1 whereas ATM transduces signals to CHK2.
1067 Activated “distal transducers” phosphorylate, degrade or sequester “effectors” Cdc25s (e.g., Cdc25A,
1068 B, and C), which in turn inhibit cyclin-dependent kinases (e.g., Cdk1/cdc2 and Cdk2) that are
1069 responsible for cell cycle progression (Patil et al., 2013).

1070 This process prevents S-phase entry (G1/S-phase checkpoint), delay S-phase progression (S-phase
 1071 checkpoint), or halts mitotic entry (G2/M-phase checkpoint) (Dai and Grant, 2010). DNA repair is now
 1072 able to occur and the type of repair is dependent on the type of DNA damage that occurred (Chatterjee
 1073 and Walker, 2017). If the damage is irreversible CHK1 and CHK2 trigger p53-dependent or -
 1074 independent apoptosis (Dai and Grant, 2010).



1075

1076 **Figure 2.12.** DNA damage response network (prepared by author).

1076

1077 *2.3.1.1. CHK1*

1078 As a central regulator in DNA damage checkpoint signalling, the role of CHK1 is not limited to the
 1079 interphase of the cell cycle. CHK1 enables spindle checkpoint which delays anaphase onset in cells
 1080 with mitotic spindle defects (Dai and Grant, 2010). CHK1 facilitates DNA damage-induced
 1081 transcriptional repression via the phosphorylation of threonine residues on histone 3 and loss of histone
 1082 acetylation (Patil et al., 2013). In addition to its regulation of p53, CHK1 suppresses caspase-3-
 1083 dependent apoptosis and blocks caspase-2-dependent apoptotic responses. Furthermore, CHK1
 1084 mediates DNA repair by targeting repair kinases (e.g., DNA-PK) important for the repair double
 1085 stranded DNA breaks, homologous repair and Fanconi Anemia(FA)/BRCA-mediated DNA repair
 1086 pathway (Patil et al., 2013).

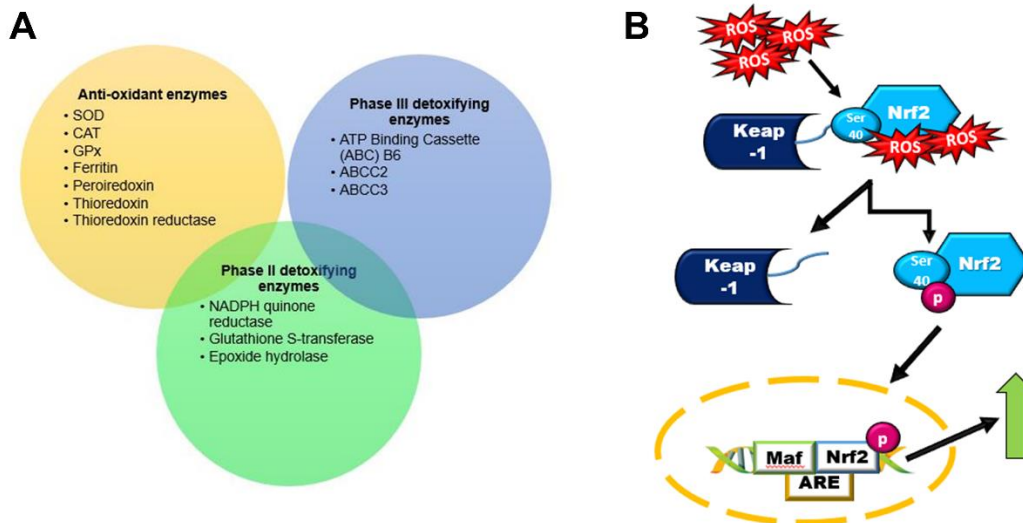
1087 Diminished activity or expression of CHK1 abrogates its essential function and therefore it should be
 1088 tightly regulated. As discussed previously, CHK1 is activated via mediators in response to DNA damage
 1089 (Dai and Grant, 2010). Activation occurs via the phosphorylation of two conserved sites, serine-317
 1090 and serine-345; however, it's not well understood how exactly phosphorylation activates CHK1 (Patil

1091 et al., 2013). One model suggests that the C-terminal domain of CHK1 interacts with its kinase domain
1092 to mask the active site, and that the phosphorylation at serine-317 and serine-345 dissociates these two
1093 domains leading to CHK1 activation (Chen et al., 2000). Phosphorylation of CHK1 can also have
1094 inhibitory effects. Downregulation of the tumour suppressor, phosphatase and tensin homolog (PTEN),
1095 inactivates CHK1 activity and promotes the accumulation of DNA damage due to its loss of control
1096 over phosphatidylinositol 3-kinase (PI3K)/protein kinase B (AKT) signalling. PI3K/AKT signalling
1097 induces phosphorylation of the serine-280 residue of CHK1 which subsequently impairs CHK1
1098 activation by DNA damage and promotes genomic instability (King et al., 2004, Puc et al., 2005).

1099 ***2.3.2. Keap1/Nrf2 anti-oxidant signalling***

1100 ROS are produced during normal physiological reactions and are involved in a number of signalling
1101 pathways (Finkel, 2011). The rapid accumulation of ROS by dysfunctional endogenous or exogenous
1102 sources overwhelms the antioxidant system of cells and oxidative stress ensues (Thannickal and
1103 Fanburg, 2000). This results in cellular injury in the form of lipid peroxidation, protein carbonylation
1104 and DNA damage and eventually, the development of cancer, neurodegeneration, and diabetes. It is,
1105 therefore, necessary that cellular redox signalling is tightly controlled (Thannickal and Fanburg, 2000,
1106 Finkel, 2011).

1107 The Kelch-like ECH-associated protein 1 (Keap1)/ Nuclear factor erythroid 2-related factor 2 (Nrf2)
1108 signalling pathway is the master regulator of cytoprotective responses to oxidative and electrophilic
1109 stress. The key players are the redox sensitive transcription factor, Nrf2 and the cysteine rich repressor
1110 protein Keap1 (Kansanen et al., 2013). In a redox balanced environment Keap1 interacts with the cullin-
1111 3 E3-ubiquitin ligase (Cul3) which serves as a platform for the ubiquitination and proteasomal
1112 degradation of Nrf2 by 26S. (Baird and Yamamoto, 2020). On exposure to oxidative or xenobiotic
1113 stress, excess ROS interacts with the redox sensitive cysteine residues on Keap1 resulting in
1114 conformational changes to Keap1. The binding affinity between Nrf2 and Keap1 is reduced and the
1115 ubiquitination system of Nrf2-Cul3 is disrupted (Kansanen et al., 2013). The stabilized Nrf2 translocates
1116 to the nucleus where it dimerizes with small maf proteins and subsequently binds to the anti-oxidant
1117 response element (ARE) found on genes involved phase II and III detoxification, cellular regeneration,
1118 xenobiotic metabolism, and ROS detoxification (antioxidants) (Figure 2.12) (Ray et al., 2012). On
1119 recovery of the redox balance, Nrf2 is dissociated from the ARE sequence. Keap1 enters into the
1120 nucleus and escorts Nrf2 to the cytoplasm for degradation (Kansanen et al., 2013).



1121

1122 **Figure 2.13.** (A) Nrf2 promotes the transcription of antioxidants as well as phase II and III detoxifying
 1123 enzymes. (B) Oxidative stress triggers Nrf2 dissociation from Keap1 and induces transcription of ARE
 1124 genes (Arumugam et al., 2020).

1125 Although the cytoprotective effects offered by Nrf2 is essential in cancer prevention, the constitutive
 1126 activation of Nrf2 promotes the development and chemoresistance of various cancers. Nrf2
 1127 hyperactivity incites new characteristics to cancer cells such as avoidance of apoptosis, excessive
 1128 proliferation and chemoresistance. There are several mechanisms by which Nrf2 signalling is activated
 1129 in cancer cells: i) somatic mutations in *Keap1*, *Cul3* or *Nrf2* disrupting Keap1/Nrf2 interactions, (ii)
 1130 Nrf2 transcription facilitated by the oncogenes *Myc*, *K-Ras*, and *B-Raf* mutation via mitogen-activated
 1131 protein kinases (MAPKs), (iii) Keap1 competing proteins that disrupt Keap1/Nrf2 interactions and (iv)
 1132 epigenetic changes that amplify Nrf2 levels and reduce Keap1 (Wu et al., 2019).

1133 *2.3.2.1. Epigenetic regulation of Keap1/Nrf2*

1134 Research into Epigenetic modifications involved in Keap1/Nrf2 regulation have only recently become
 1135 wide spread. Interest in the field was initiated by Guo et al. (2012) who observed that hypermethylation
 1136 of *Keap1* promoters in lung cancer prevented SP1 binding and thus *Keap1* transcription. Since then,
 1137 several studies have evaluated the effect of DNA methylation, histone modifications, and ncRNA on
 1138 Keap1 and Nrf2 (Cheng et al., 2016, Bhattacharjee and Dashwood, 2020). Table 2.4 summarizes the
 1139 effects of these epigenetic mechanisms on Keap1 and Nrf2.

1140

1141

1142

1143

1144 **Table 2.4: Epigenetic regulation of Keap-1 and Nrf2**

Target	Epigenetic modification	Effect on target	Reference
Nrf2	DNA methylation	Gene silencing	(Khor et al., 2014)
	DNA demethylation	Transcriptional activation	(Kang et al., 2014)
	H3k27me3	Gene silencing	(Li et al., 2014)
	miR-27a, 34, 93 153, 142-5p, 144	Degrade Nrf2 mRNA	(Bhattacharjee and Dashwood, 2020)
	lncRNA: UCA1, MEG3, NRA2	Promotes Nrf2 translation by sponging miRNA that targets Nrf2	(Bhattacharjee and Dashwood, 2020)
Keap1	DNA methylation	Gene silencing	(Guo et al., 2012)
	DNA demethylation	Transcriptional activation	(Palsamy et al., 2012)
	H3K4me3	Transcriptional activation	(Mishra et al., 2014)
	miR-7, 141, 200, 432, 455, 873	Degrades Keap1 mRNA	(Bhattacharjee and Dashwood, 2020)
	lncRNA: MALAT	Downregulates Keap1	(Bhattacharjee et al., 2020)

1145

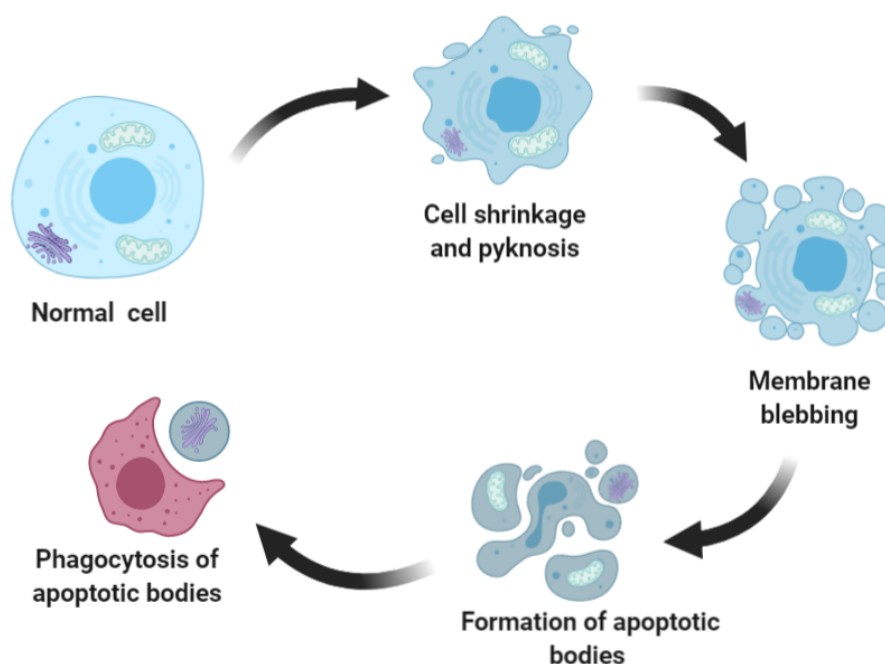
1146 The role of m6A modifications in Keap1/Nrf2 regulation have also been investigated but not as
 1147 thoroughly as other epigenetic modifications. One study showed that colistin-induced oxidative stress
 1148 was attenuated by the accumulation of m6A modifications on pri-miR-873. This promoted the
 1149 generation of mature miR-873-5p which in turn inhibited Keap1 expression and promoted Nrf2
 1150 antioxidant responses (Wang et al., 2019). Oxidative stress was also shown to elevate m6A-*Nrf2* levels
 1151 in di-(2-ethylhexyl) phthalate (DEHP) exposed rats; however, the authors hypothesized that m6A-*Nrf2*
 1152 inhibits Nrf2 signalling (Zhao et al., 2020).

1153 **2.3.3. Apoptosis**

1154 Apoptosis is a form of cell death that involves the controlled dismantling of intracellular components
 1155 while avoiding inflammation and damage to neighbouring tissue (McIlwain et al., 2013). It is a
 1156 homeostatic process that secures normal development and aging and controls cell populations by
 1157 removing surplus, damaged, and cancerous cells (Shen and White, 2001). Apoptosis is also a defence

1158 mechanism that responds to various noxious stimuli and stresses such as DNA damage, cell cycle
1159 dysfunctions and oncogene activation (Shen and White, 2001, Elmore, 2007). Considering that
1160 apoptosis responds to both physiological and pathophysiological stimuli, aberrant regulation of
1161 apoptosis can result in Alzheimer's disease, rheumatoid arthritis, defects in embryonic development
1162 and cancer.

1163 Various morphological changes occur during apoptosis (Figure 2.13). The onset apoptosis is
1164 characterized by cell shrinkage followed by pyknosis – chromatin condensation and nuclear shrinkage;
1165 while the latter stages are typified by membrane blebbing, karyorrhexis (nuclear and DNA
1166 fragmentation) and the containment of cell fragments into apoptotic bodies (Saraste and Pulkki, 2000,
1167 Elmore, 2007). The apoptotic bodies are tightly packed with intact organelles and nuclear fragments of
1168 the apoptotic cells. These bodies are subsequently engulfed by phagocytes such as macrophages and
1169 parenchyma (Saraste and Pulkki, 2000). Degradation occurs within phagolysosomes; however, if
1170 phagocytosis does not occur cells will undergo degradation which resembles necrosis (cell death via
1171 rapid swelling and rupturing of cells) in a process called secondary necrosis (Saraste and Pulkki, 2000)
1172 The containment of apoptotic cells in apoptotic bodies and rapid engulfment by phagocytes prevents
1173 apoptotic cells from releasing their cellular content into the neighbouring tissue. This prevents the
1174 occurrence of inflammation and necrosis to the surrounding tissue (Elmore, 2007).



1175

1176 **Figure 2.14.** Morphological changes that occur during apoptosis (prepared by author).

1177 These morphological hallmarks of apoptosis are dependent on highly complex and sophisticated
1178 molecular and biochemical events necessary for the proper execution of apoptosis (Shen and White,
1179 2001). Apoptosis occurs via two main pathways: intrinsic or mitochondrial pathway and extrinsic or

1180 death receptor pathway (Elmore, 2007). Both pathways rely on the activation of a family of endo-
1181 proteases known as caspases (McIlwain et al., 2013).

1182 2.3.3.1. Caspase

1183 Caspases are a family of evolutionary conserved cysteinyl aspartate proteinases that are responsible for
1184 the morphological changes that occur during apoptosis. Presently, 14 caspases have been identified and
1185 have been broadly classified according to their functions in apoptosis and inflammation (McIlwain et
1186 al., 2013). All caspases consist of an active site cysteine and can cleave substrates after an aspartic acid
1187 residue. Caspases are initially expressed as inert monomeric proenzymes or procaspases (McIlwain et
1188 al., 2013). Procaspsases consist of an N-terminal prodomain, p10 and p20 domains and activation of
1189 caspases can occur via three general mechanisms: induced proximity, formation of a holoenzyme or
1190 processing by an upstream caspase (Hengartner, 2000).

1191 Induced proximity involves the aggregation of multiple procaspases resulting in their cross-activation;
1192 while activation by holoenzyme is mediated by conformational changes rather than proteolytic
1193 cleavage. These two mechanisms are involved in the activation of short domain initiator caspase-8 and
1194 caspase-9, respectively (Hengartner, 2000). The activation of procaspase by an upstream caspase is
1195 responsible for the activation of most caspases and is the most effective method for executioner caspase
1196 (caspase-3, -6, and -7) activation. Initiator caspases cleave executioner procaspases at the aspartate
1197 residue between the N-terminal prodomain and p20 and between p20 and p10 domains. These
1198 executioner caspases are workhorses of the caspase family. Once activated, an executioner caspase can
1199 activate other executioner procaspases (McIlwain et al., 2013). The activation of procaspases by mature
1200 caspases is known as the caspase cascade and is an effective method of amplifying apoptotic signalling
1201 resulting in rapid cell death (Elmore, 2007).

1202 2.3.3.2. Pathways of apoptosis

1203 Various pathways exist to execute apoptotic cell death. They are easily distinguished by their adaptors
1204 and initiator caspases. However, there are two distinct yet converging pathways that play a key role in
1205 the apoptotic program of mammals. These pathways are referred to as the intrinsic and extrinsic
1206 pathways and both pathways rely on the activation of the caspase cascade to execute apoptosis.

1207 2.3.3.2.1. Intrinsic apoptotic program

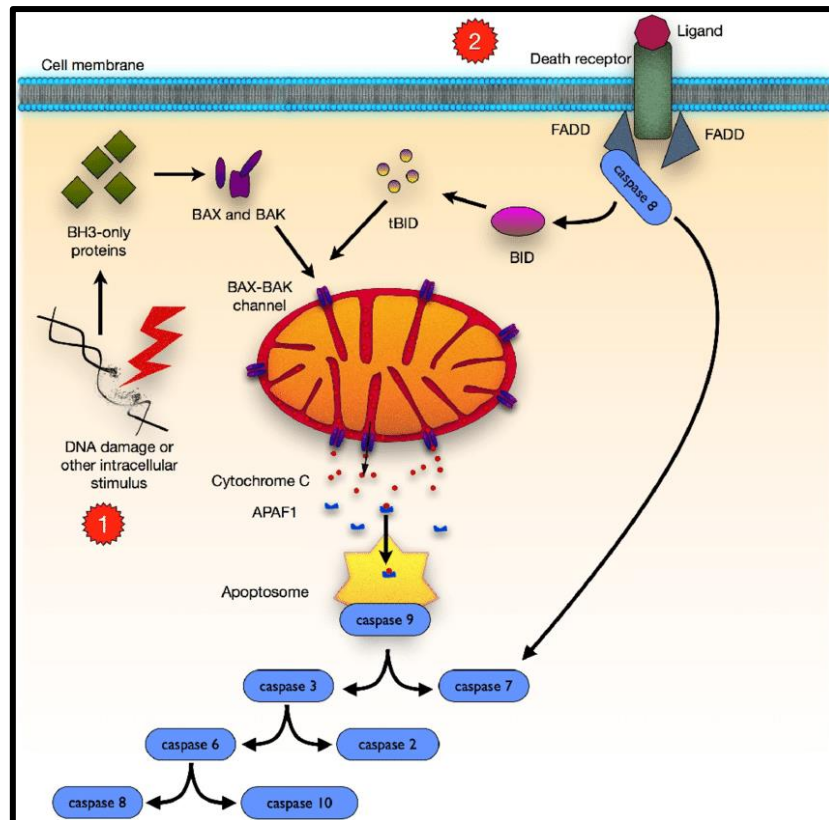
1208 The intrinsic pathway of apoptosis is also known as the mitochondrial pathway as it depends on factors
1209 released from the mitochondria. It is activated by an array of cellular stresses such as toxins, free
1210 radicals, radiation and viral factors or via developmental signals such as the absence of growth factors
1211 or hormones that usually suppress death programs (Elmore, 2007).

1212 These stimuli trigger the activation of the proapoptotic protein, Bim. Bim sequesters the antiapoptotic
1213 protein Bcl-2 and promotes the formation of Bak-Bax oligomers within the outer membrane of the

1214 mitochondria (Nakajima and Kuranaga, 2017). This results in the opening of the mitochondrial
1215 permeability transition pore and the release of cytochrome c from the mitochondria (Elmore, 2007).
1216 The release of cytochrome c into the cytosol promotes the formation of the signalling platform known
1217 as the apoptosome (Nakajima and Kuranaga, 2017). The binding of cytochrome c and subsequent
1218 binding of deoxyATP to apoptotic protease activating factor-1 (Apaf-1) induces conformational
1219 changes that activate Apaf-1 (McIlwain et al., 2013). Seven activated Apaf-1 monomers oligomerize
1220 and recruit procaspase-9. This complex is known as the apoptosome and its formation induces
1221 conformational changes required for the activation of procaspase-9, which consequently activates
1222 executioner caspases, resulting in apoptotic cell death (Figure 2.14) (McIlwain et al., 2013).

1223 2.3.3.2.2. Extrinsic Apoptotic program

1224 The extrinsic pathway or death receptor pathway is triggered by extracellular signals in the form of
1225 ligands binding to death receptors. Death receptors involved in apoptosis include tumor necrosis factor
1226 (TNF) receptor 1 (TNFR1), TNF-related apoptosis inducing ligand receptor 1 (TRAILR1), TRAILR2,
1227 Fas receptor (FasR) and death receptor 3 (DR3) (McIlwain et al., 2013). The binding of ligands to their
1228 respective death receptors triggers the multimerization of death receptors and recruitment of adapter
1229 proteins [TNFR-associated death domain (TRADD) and Fas-associated death domain (FADD)] via
1230 their death domains, forming an intracellular death-inducing signalling complex known as DISC (Li
1231 and Yuan, 2008). The N-terminal of procaspase-8 also contains a death domain, thus DISC can recruit
1232 procaspase-8 to the complex. An accumulation of procaspase-8 results in its dimerization and activation
1233 (McIlwain et al., 2013). Depending on the cell type, caspase-8 can directly cleave and activate
1234 executioner caspases (type I cells) or activate intrinsic apoptosis (type II cells). To activate intrinsic
1235 apoptosis, caspase-8 cleaves and activates the proapoptotic protein bid to tBid. tBid localizes to the
1236 mitochondria to activate downstream intrinsic pathways (Figure 2.14) (Li and Yuan, 2008).



1237

1238 **Figure 2.15.** Intrinsic and extrinsic signalling of apoptosis (Glowacki et al., 2013).

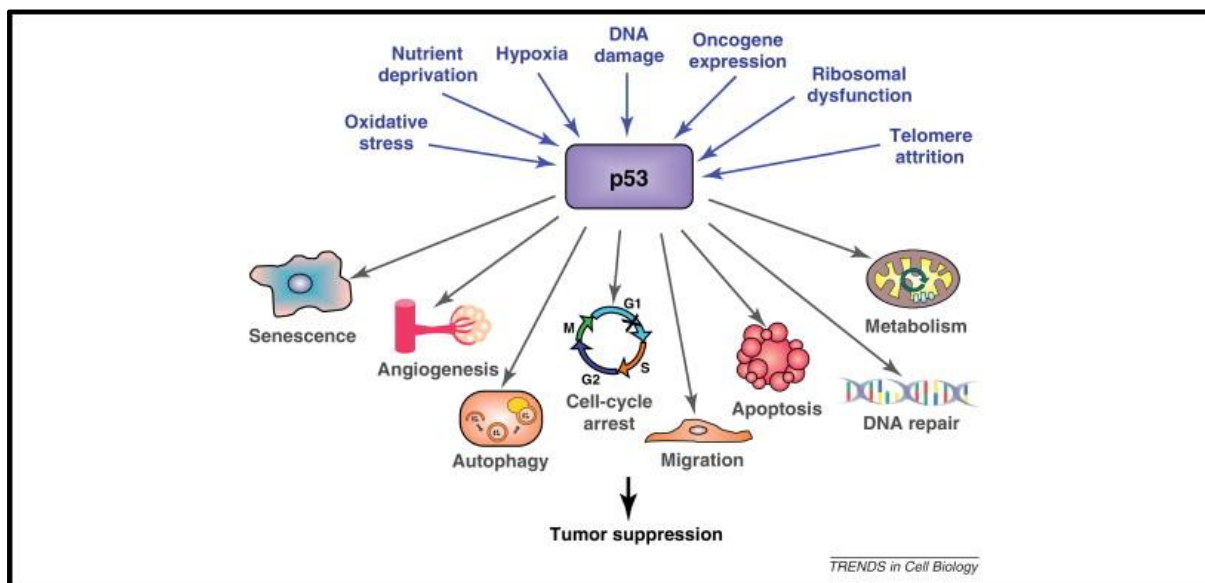
1239 2.3.3.2.3. Execution of apoptosis

1240 Both intrinsic and extrinsic apoptosis terminate with the activation of executioner caspases (Caspases-
 1241 3, -6 and -7) (McIlwain et al., 2013). Executioner caspases execute apoptosis via the cleavage and
 1242 subsequent activation of substrates such as cytoplasmic endonucleases and proteases, which degrade
 1243 nuclear material and cytoskeletal proteins respectively (Elmore, 2007). The cleavage of various
 1244 substrates results in the morphological changes that occur in apoptotic cells. For example, caspase-
 1245 activated deoxyribonuclease (CAD) is responsible for chromatin condensation and degradation of
 1246 chromosomal DNA during apoptosis. In proliferating cells, CAD is inactivated as it is complexed to the
 1247 inhibitor, ICAD. Caspase-3 cleaves ICAD thereby activating CAD and chromatin condensation (Enari
 1248 et al., 1998).

1249 2.3.3.3. *p53*

1250 The tumour suppressor, *p53* is widely regarded as the guardian of the genome and is the master regulator
 1251 of cellular stress responses (Anbarasan and Bourdon, 2019). *p53* is responsible for maintaining tissue
 1252 homeostasis and responds to a variety of stress signals (such as DNA damage, nutrient deprivation and
 1253 oncogenic activation) by mediating surveillance of genome integrity, cell cycle checkpoint regulation,
 1254 DNA repair and apoptosis (Figure 2.15). Loss of *p53* expression or function promotes checkpoint
 1255 defects, genomic instability and the continued proliferation of damaged cells (Fridman and Lowe,

1256 2003). Unfortunately, almost 50% of cancers have been reported to contain a mutated or inactive p53
 1257 (Anbarasan and Bourdon, 2019). On the other hand, chronic activation of p53 is associated with
 1258 degenerative disorders such as arthritis and sclerosis. It is, therefore, imperative that expression and
 1259 activity of p53 should be tightly regulated (Fierabracci and Pellegrino, 2016).



1260
 1261 **Figure 2.16.** p53 responds to a plethora of stress signals and regulates diverse responses (Bieging and
 1262 Attardi, 2012).

1263 As the central player in stress response, p53 needs to be tightly regulated. During homeostatic
 1264 conditions, p53 is maintained in an inactive state via proteasomal degradation by Mouse double minute
 1265 2 homolog (MDM2). Cellular stress signals inhibit MDM2 degradation of p53 or induce
 1266 posttranslational modifications (such as acetylation, proliferation) to p53. These changes allow for the
 1267 accumulation and activation of p53 (Aubrey et al., 2018).

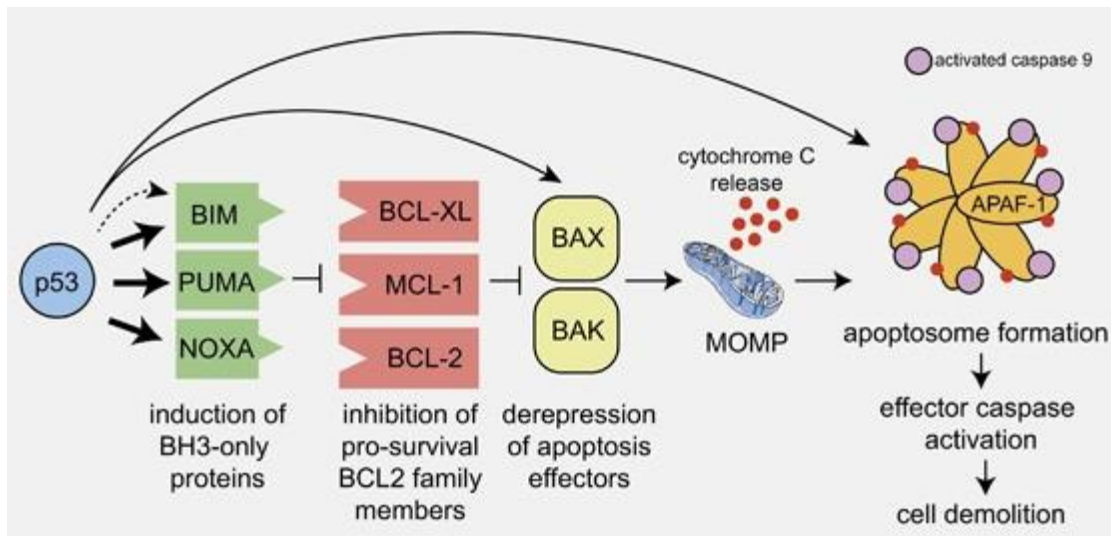
1268 p53 is also regulated via epigenetic mechanisms such as promoter methylation. At the transcriptional
 1269 level, hypermethylation of the *p53* gene promoter prevents the binding of transcriptional machinery and
 1270 reduces *p53* transcription. However, hypomethylation of the p53 promoter, enables the binding of
 1271 transcriptional machinery, and promotes p53 expression (Chmelarova et al., 2013). *In vitro* studies
 1272 using reporter gene constructs found that DNA methylation reduced *p53* gene expression by 90% in
 1273 mice and by 85% in rats (Saldaña-Meyer and Recillas-Targa, 2011). In cancer cells tumour suppressor
 1274 genes are frequently silenced via epigenetic mechanisms Hypermethylation of the *p53* gene promoter
 1275 and subsequent loss of p53 function was observed in the majority of patients with hepatocellular
 1276 carcinomas, 51.5% of patients with ovarian cancer, 40% of patients with chronic lymphocytic
 1277 leukaemia and 30% of patients with acute lymphoblastic leukaemia (Saldaña-Meyer and Recillas-
 1278 Targa, 2011, Chmelarova et al., 2013). At the post-transcriptional level, p53 is regulated by a variety of
 1279 miRNAs. miRNAs such as miR-125a, miR-125b, miR-504, miRNA-25 are responsible for the
 1280 degradation of p53 (Saldaña-Meyer and Recillas-Targa, 2011).

1281 2.3.3.3.1. p53-mediated apoptosis

1282 p53 is a transcription factor that has the ability to transactivate genes involved in promoting apoptosis
1283 (Aubrey et al., 2018). The Bcl2 family are important players in regulating apoptosis. The Bcl2 family
1284 consists of both pro-apoptotic (Bax, Bak, Bim, Bid, Noxa, Puma and Bcl-x_s) and anti-apoptotic (Bcl-2
1285 and Bcl-x_L) members that interact with one another to control apoptosis especially intrinsic apoptosis
1286 (Shen and White, 2001). Such interaction includes the binding and inactivation of anti-apoptotic Bcl2
1287 by proapoptotic Bim (Nakajima and Kuranaga, 2017). Genes encoding for several pro-apoptotic Bcl2
1288 members (Bax, Bid, Puma, and Noxa) harbour consensus p53 response elements which allows for p53
1289 binding. p53 binding to these sequences promotes the transcription of these apoptotic genes (Figure
1290 2.16) (Fridman and Lowe, 2003).

1291 Furthermore, p53 is also involved in the transactivation of apoptotic machinery involved in the extrinsic
1292 pathway (DR5, FasR, Fas ligand) and the intrinsic pathway (Apaf-1) and executioner caspase-6. While
1293 most studies focus on p53 transactivation function, p53 also suppresses transcription. The inhibitor of
1294 apoptosis, survivin is one of the targets of p53-transrepression (Fridman and Lowe, 2003).

1295 p53 can drive the expression of several other genes to inhibit survival pathways. For example, the
1296 PI3K/AKT pathway is involved in the phosphorylation and subsequent activation of proteins that
1297 promote survival. p53 induces PTEN expression which in turn negatively regulates PI3K/AKT and
1298 survival signals (Fridman and Lowe, 2003). p53 induces miR-34 expression, which in turn represses
1299 proapoptotic Bcl2 translation (Aubrey et al., 2018). p53 may also regulate apoptosis via transcription-
1300 independent mechanisms, however it is not as established as transcriptional-dependent mechanisms.
1301 p53 accumulates in the mitochondria in response to DNA damage and this redistribution may play a
1302 role in cytochrome c release and caspase activation (Fridman and Lowe, 2003). p53 plays an essential;
1303 role in co-ordinating apoptosis. While it may not induce apoptosis directly; it sensitizes cells so that
1304 apoptosis can be triggered more easily in response to stimuli that activates cell death (Aubrey et al.,
1305 2018).



1306

1307 **Figure 2.17.** Mechanisms of p53-mediated apoptosis via Bcl2-regulated pathway (Aubrey et al., 2018).

1308 Recently, changes to the epigenome have been associated with exposure to FB₁. However current
 1309 research on the association between FB₁ and epigenetic modifications are often conflicting.
 1310 Furthermore, the downstream effects of these FB₁-induced epigenetic changes have not been adequately
 1311 assessed. It is well established that FB₁ induces oxidative stress and DNA damage. FB₁-induced
 1312 epigenetic changes may dysregulate responses (checkpoint signalling, Keap1/Nrf2 and apoptosis) to
 1313 oxidative stress and/or DNA damage. This may further exacerbate toxicity induced by FB₁. Therefore,
 1314 this study aimed to determine the epigenetic effects of FB₁ and the downstream implications of these
 1315 epigenetic alterations to stress response in human liver (HepG2) cells.

1316 2.4. References

- 1317 Abbès S, Salah-Abbès JB, Ouanes Z, Houas Z, Othman O, Bacha H, Abdel-Wahhab MA & Oueslati R
 1318 2006. Preventive role of phyllosilicate clay on the Immunological and Biochemical toxicity of
 1319 zearalenone in Balb/c mice. *International Immunopharmacology*, 6, 1251-1258.
- 1320 Alarcón CR, Lee H, Goodarzi H, Halberg N & Tavazoie SF 2015. N6-methyladenosine marks primary
 1321 microRNAs for processing. *Nature*, 519, 482-485.
- 1322 Alexander NJ, Proctor RH & McCormick SP 2009. Genes, gene clusters, and biosynthesis of
 1323 trichothecenes and fumonisins in *Fusarium*. *Toxin Reviews*, 28, 198-215.
- 1324 Alizadeh AM, Roshandel G, Roudbarmohammadi S, Roudbary M, Sohanaki H, Ghiasian SA,
 1325 Taherkhani A, Semnani S & Aghasi M 2012. Fumonisin B1 contamination of cereals and risk of
 1326 esophageal cancer in a high risk area in northeastern Iran. *Asian Pacific journal of cancer prevention*,
 1327 13, 2625-2628.
- 1328 Amaral PP & Mattick JS 2008. Noncoding RNA in development. *Mammalian genome*, 19, 454-492.
- 1329 Anbarasan T & Bourdon J-C 2019. The Emerging Landscape of p53 Isoforms in Physiology, Cancer
 1330 and Degenerative Diseases. *Int J Mol Sci*, 20, 6257.
- 1331 Antequera F 2003. Structure, function and evolution of CpG island promoters. *Cell Mol Life Sci*, 60,
 1332 1647-1658.
- 1333 Aran D, Toperoff G, Rosenberg M & Hellman A 2011. Replication timing-related and gene body-
 1334 specific methylation of active human genes. *Hum Mol Genet*, 20, 670-680.

- 1335 Aristizabal MJ, Anreiter I, Halldorsdottir T, Odgers CL, McDade TW, Goldenberg A, Mostafavi S,
1336 Kobor MS, Binder EB, Sokolowski MB, et al. 2020. Biological embedding of experience: A primer on
1337 epigenetics. *Proceedings of the National Academy of Sciences*, 117, 23261-23269.
- 1338 Arumugam T, Ghazi T, Sheik Abdul N & Chaturgoon AA 2020. A review on the oxidative effects of
1339 the fusariotoxins: Fumonisin B1 and fusaric acid. In: PATEL, V. B. & PREEDY, V. R. (eds.)
1340 *Toxicology*. Academic Press.
- 1341 Aubrey BJ, Kelly GL, Janic A, Herold MJ & Strasser A 2018. How does p53 induce apoptosis and how
1342 does this relate to p53-mediated tumour suppression? *Cell Death & Differentiation*, 25, 104-113.
- 1343 Baird L & Yamamoto M 2020. The Molecular Mechanisms Regulating the KEAP1-NRF2 Pathway.
1344 *Mol Cell Biol*, 40, e00099-00020.
- 1345 Bakker MG, Brown DW, Kelly AC, Kim H-S, Kurtzman CP, McCormick SP, O'Donnell KL, Proctor
1346 RH, Vaughan MM & Ward TJ 2018. Fusarium mycotoxins: a trans-disciplinary overview. *Canadian*
1347 *Journal of Plant Pathology*, 40, 161-171.
- 1348 Bannister AJ, Schneider R, Myers FA, Thorne AW, Crane-Robinson C & Kouzarides T 2005. Spatial
1349 distribution of di- and tri-methyl lysine 36 of histone H3 at active genes. *J Biol Chem*, 280, 17732-
1350 17736.
- 1351 Bannister AJ & Kouzarides T 2011. Regulation of chromatin by histone modifications. *Cell Research*,
1352 21, 381-395.
- 1353 Bao Z, Yang Z, Huang Z, Zhou Y, Cui Q & Dong D 2018. LncRNADisease 2.0: an updated database
1354 of long non-coding RNA-associated diseases. *Nucleic Acids Res*, 47, D1034-D1037.
- 1355 Bernstein BE, Humphrey EL, Erlich RL, Schneider R, Bouman P, Liu JS, Kouzarides T & Schreiber
1356 SL 2002. Methylation of histone H3 Lys 4 in coding regions of active genes. *Proc Natl Acad Sci U S*
1357 *A*, 99, 8695-8700.
- 1358 Bhattacharjee S, Li J & Dashwood RH 2020. Emerging crosstalk between long non-coding RNAs and
1359 Nrf2 signaling. *Cancer Letters*, 490, 154-164.
- 1360 Bhattacharjee S & Dashwood RH 2020. Epigenetic Regulation of NRF2/KEAP1 by Phytochemicals.
1361 *Antioxidants*, 9, 865.
- 1362 Bhutani N, Burns DM & Blau HM 2011. DNA demethylation dynamics. *Cell*, 146, 866-872.
- 1363 Biegging KT & Attardi LD 2012. Deconstructing p53 transcriptional networks in tumor suppression.
1364 *Trends Cell Biol*, 22, 97-106.
- 1365 Bird AP 1986. CpG-rich islands and the function of DNA methylation. *Nature*, 321, 209-213.
- 1366 Blanc RS & Richard S 2017. Arginine Methylation: The Coming of Age. *Molecular cell*, 65, 8-24.
- 1367 Bokar JA, Shambaugh ME, Polayes D, Matera AG & Rottman FM 1997. Purification and cDNA
1368 cloning of the AdoMet-binding subunit of the human mRNA (N6-adenosine)-methyltransferase. *RNA*,
1369 3, 1233-1247.
- 1370 Bollati V & Baccarelli A 2010. Environmental epigenetics. *Heredity*, 105, 105-112.
- 1371 Borde V, Robine N, Lin W, Bonfils S, Geli V & Nicolas A 2009. Histone H3 lysine 4 trimethylation
1372 marks meiotic recombination initiation sites. *The EMBO journal*, 28, 99-111.
- 1373 Bostick M, Kim JK, Estève P-O, Clark A, Pradhan S & Jacobsen SE 2007. UHRF1 Plays a Role in
1374 Maintaining DNA Methylation in Mammalian Cells. *Science (New York, N.Y.)*, 317, 1760-1764.
- 1375 Bourc'his D, Xu GL, Lin CS, Bollman B & Bestor TH 2001. Dnmt3L and the establishment of maternal
1376 genomic imprints. *Science (New York, N.Y.)*, 294, 2536-2539.
- 1377 Bourc'his D & Bestor TH 2004. Meiotic catastrophe and retrotransposon reactivation in male germ cells
1378 lacking Dnmt3L. *Nature*, 431, 96-99.

- 1379 Brandeis M, Frank D, Keshet I, Siegfried Z, Mendelsohn M, Nemes A, Temper V, Razin A & Cedar H
1380 1994. Sp1 elements protect a CpG island from de novo methylation. *Nature*, 371, 435-438.
- 1381 Brenner C, Deplus R, Didelot C, Loriot A, Viré E, De Smet C, Gutierrez A, Danovi D, Bernard D, Boon
1382 T, et al. 2005. Myc represses transcription through recruitment of DNA methyltransferase corepressor.
1383 *Embo j*, 24, 336-346.
- 1384 Brykczynska U, Hisano M, Erkek S, Ramos L, Oakeley EJ, Roloff TC, Beisel C, Schübeler D, Stadler
1385 MB & Peters AHFM 2010. Repressive and active histone methylation mark distinct promoters in human
1386 and mouse spermatozoa. *Nature Structural & Molecular Biology*, 17, 679-687.
- 1387 Cantara WA, Crain PF, Rozenski J, McCloskey JA, Harris KA, Zhang X, Vendeix FAP, Fabris D &
1388 Agris PF 2011. The RNA Modification Database, RNAMDB: 2011 update. *Nucleic Acids Res*, 39,
1389 D195-D201.
- 1390 Chain EPoCitF 2011. Scientific Opinion on the risks for animal and public health related to the presence
1391 of T-2 and HT-2 toxin in food and feed. *EFSA Journal*, 9, 2481.
- 1392 Chambers AL & Downs JA 2012. The RSC and INO80 chromatin-remodeling complexes in DNA
1393 double-strand break repair. *Prog Mol Biol Transl Sci*, 110, 229-261.
- 1394 Chang B, Chen Y, Zhao Y & Bruick RK 2007. JMJD6 Is a Histone Arginine Demethylase. *Science*
1395 (*New York, N.Y.*), 318, 444-447.
- 1396 Chatterjee N & Walker GC 2017. Mechanisms of DNA damage, repair, and mutagenesis.
1397 *Environmental and Molecular Mutagenesis*, 58, 235-263.
- 1398 Chen C, Riley RT & Wu F 2018. Dietary Fumonisin and Growth Impairment in Children and Animals:
1399 A Review. *Comprehensive Reviews in Food Science and Food Safety*, 17, 1448-1464.
- 1400 Chen P, Luo C, Deng Y, Ryan K, Register J, Margosiak S, Tempczyk-Russell A, Nguyen B, Myers P,
1401 Lundgren K, et al. 2000. The 1.7 Å crystal structure of human cell cycle checkpoint kinase Chk1:
1402 implications for Chk1 regulation. *Cell*, 100, 681-692.
- 1403 Cheng D, Wu R, Guo Y & Kong A-NT 2016. Regulation of Keap1–Nrf2 signaling: The role of
1404 epigenetics. *Current Opinion in Toxicology*, 1, 134-138.
- 1405 Cheng X & Blumenthal RM 2008. Mammalian DNA methyltransferases: a structural perspective.
1406 *Structure*, 16, 341-350.
- 1407 Chmelarova M, Krepinska E, Spacek J, Laco J, Beranek M & Palicka V 2013. Methylation in the p53
1408 promoter in epithelial ovarian cancer. *Clinical and Translational Oncology*, 15, 160-163.
- 1409 Choudhari R, Sedano MJ, Harrison AL, Subramani R, Lin KY, Ramos EI, Lakshmanaswamy R, Gadad
1410 SS 2020. Long noncoding RNAs in cancer: From discovery to therapeutic targets. *Advances in Clinical*
1411 *Chemistry*, 95, 105-147.
- 1412 Chrun ES, Modolo F & Daniel FI 2017. Histone modifications: A review about the presence of this
1413 epigenetic phenomenon in carcinogenesis. *Pathology - Research and Practice*, 213, 1329-1339.
- 1414 Chuturgoon A, Phulukdaree A & Moodley D 2014a. Fumonisin B1 induces global DNA
1415 hypomethylation in HepG2 cells - An alternative mechanism of action. *Toxicology*, 315, 65-69.
- 1416 Chuturgoon AA, Phulukdaree A & Moodley D 2014b. Fumonisin B1 modulates expression of human
1417 cytochrome P450 1b1 in human hepatoma (Hepg2) cells by repressing Mir-27b. *Toxicology Letters*,
1418 227, 50-55.
- 1419 Collins BE, Greer CB, Coleman BC & Sweatt JD 2019. Histone H3 lysine K4 methylation and its role
1420 in learning and memory. *Epigenetics Chromatin*, 12, 7.
- 1421 Cooper DN & Krawczak M 1989. Cytosine methylation and the fate of CpG dinucleotides in vertebrate
1422 genomes. *Hum Genet*, 83, 181-188.

- 1423 Cortellino S, Xu J, Sannai M, Moore R, Caretti E, Cigliano A, Le Coz M, Devarajan K, Wessels A,
1424 Soprano D, et al. 2011. Thymine DNA glycosylase is essential for active DNA demethylation by linked
1425 deamination-base excision repair. *Cell*, 146, 67-79.
- 1426 Couturier M & Lindås A-C 2018. The DNA Methylome of the Hyperthermoacidophilic Crenarchaeon
1427 *Sulfolobus acidocaldarius*. *Front Microbiol*, 9, 137-137.
- 1428 Csankovszki G, Nagy A & Jaenisch R 2001. Synergism of Xist RNA, DNA methylation, and histone
1429 hypoacetylation in maintaining X chromosome inactivation. *Journal of Cell Biology*, 153, 773-784.
- 1430 Cui K, Zang C, Roh T-Y, Schones DE, Childs RW, Peng W & Zhao K 2009. Chromatin signatures in
1431 multipotent human hematopoietic stem cells indicate the fate of bivalent genes during differentiation.
1432 *Cell stem cell*, 4, 80-93.
- 1433 Cui M, Wang H, Yao X, Zhang D, Xie Y, Cui R & Zhang X 2019. Circulating MicroRNAs in Cancer:
1434 Potential and Challenge. *Frontiers in Genetics*, 10.
- 1435 Dai X, Kaushik AC & Zhang J 2019. The Emerging Role of Major Regulatory RNAs in Cancer Control.
1436 *Frontiers in Oncology*, 9.
- 1437 Dai Y & Grant S 2010. New insights into checkpoint kinase 1 in the DNA damage response signaling
1438 network. *Clin Cancer Res*, 16, 376-383.
- 1439 Davie JR, Xu W & Delcuve GP 2015. Histone H3K4 trimethylation: dynamic interplay with pre-mRNA
1440 splicing. *Biochemistry and Cell Biology*, 94, 1-11.
- 1441 Davis BN & Hata A 2009. Regulation of MicroRNA Biogenesis: A miRiad of mechanisms. *Cell*
1442 *Communication and Signaling*, 7, 18.
- 1443 Demirel G, Alpertunga B & Ozden S 2015. Role of fumonisin B1 on DNA methylation changes in rat
1444 kidney and liver cells. *Pharmaceutical Biology*, 53, 1302-1310.
- 1445 Deng X, Chen K, Luo G-Z, Weng X, Ji Q, Zhou T & He C 2015. Widespread occurrence of N6-
1446 methyladenosine in bacterial mRNA. *Nucleic Acids Res*, 43, 6557-6567.
- 1447 Desrosiers R, Friderici K & Rottman F 1974. Identification of methylated nucleosides in messenger
1448 RNA from Novikoff hepatoma cells. *Proc Natl Acad Sci U S A*, 71, 3971-3975.
- 1449 Dhanoa JK, Sethi RS, Verma R, Arora JS & Mukhopadhyay CS 2018. Long non-coding RNA: its
1450 evolutionary relics and biological implications in mammals: a review. *J Anim Sci Technol*, 60, 25.
- 1451 Ding Y, Bojja RS & Du L 2004. Fum3p, a 2-Ketoglutarate-Dependent Dioxygenase Required for C-5
1452 Hydroxylation of Fumonisin in *Fusarium verticillioides*. *Applied and Environmental*
1453 *Microbiology*, 70, 1931-1934.
- 1454 DiStefano JK 2018. The Emerging Role of Long Noncoding RNAs in Human Disease. *Methods Mol*
1455 *Biol*, 1706, 91-110.
- 1456 Dominissini D, Moshitch-Moshkovitz S, Schwartz S, Salmon-Divon M, Ungar L, Osenberg S, Cesarkas
1457 K, Jacob-Hirsch J, Amariglio N, Kupiec M, et al. 2012. Topology of the human and mouse m6A RNA
1458 methylomes revealed by m6A-seq. *Nature*, 485, 201-206.
- 1459 Dragan YP, Bidlack WR, Cohen SM, Goldsworthy TL, Hard GC, Howard PC, Riley RT & Voss KA
1460 2001. Implications of apoptosis for toxicity, carcinogenicity, and risk assessment: fumonisin B1 as an
1461 example. *Toxicological Sciences*, 61, 6-17.
- 1462 Du L, Zhu X, Gerber R, Huffman J, Lou L, Jorgenson J, Yu F, Zaleta-Rivera K & Wang Q-M 2008.
1463 Biosynthesis of sphinganine-analog mycotoxins. *Journal of industrial microbiology & biotechnology*,
1464 35, 455-464.
- 1465 Dwivedi S, Purohit P & Sharma P 2019. MicroRNAs and Diseases: Promising Biomarkers for
1466 Diagnosis and Therapeutics. *Indian Journal of Clinical Biochemistry*, 34, 243-245.
- 1467 Eades G, Yang M, Yao Y, Zhang Y & Zhou Q 2011. miR-200a regulates Nrf2 activation by targeting
1468 Keap1 mRNA in breast cancer cells. *J Biol Chem*, 286, 40725-40733.

- 1469 Eaton ML, Galani K, Kang S, Bell SP & MacAlpine DM 2010. Conserved nucleosome positioning
1470 defines replication origins. *Genes Dev*, 24, 748-753.
- 1471 EFSA 2011. Scientific Opinion on the risks for public health related to the presence of zearalenone in
1472 food. *EFSA Journal*, 9, 2197.
- 1473 EFSA 2018. Risks for animal health related to the presence of fumonisins, their modified forms and
1474 hidden forms in feed. *EFSA J*, 16, e05242-e05242.
- 1475 Ehrenhofer-Murray AE 2004. Chromatin dynamics at DNA replication, transcription and repair. *Eur J*
1476 *Biochem*, 271, 2335-2349.
- 1477 Ehrlich M 2002. DNA methylation in cancer: too much, but also too little. *Oncogene*, 21, 5400-5413.
- 1478 Elmore S 2007. Apoptosis: a review of programmed cell death. *Toxicol Pathol*, 35, 495-516.
- 1479 Enari M, Sakahira H, Yokoyama H, Okawa K, Iwamatsu A & Nagata S 1998. A caspase-activated
1480 DNase that degrades DNA during apoptosis, and its inhibitor ICAD. *Nature*, 391, 43-50.
- 1481 Escrivá L, Font G & Manyes L 2015. In vivo toxicity studies of fusarium mycotoxins in the last decade:
1482 A review. *Food and Chemical Toxicology*, 78, 185-206.
- 1483 Fatemi M & Wade PA 2006. MBD family proteins: reading the epigenetic code. *J Cell Sci*, 119, 3033-
1484 3037.
- 1485 Faucher D & Wellinger RJ 2010. Methylated H3K4, a Transcription-Associated Histone Modification,
1486 Is Involved in the DNA Damage Response Pathway. *PLOS Genetics*, 6, e1001082.
- 1487 Fedeles BI, Singh V, Delaney JC, Li D & Essigmann JM 2015. The AlkB Family of Fe(II)/ α -
1488 Ketoglutarate-dependent Dioxygenases: Repairing Nucleic Acid Alkylation Damage and Beyond. *J*
1489 *Biol Chem*, 290, 20734-20742.
- 1490 Ferrigo D, Raiola A & Causin R 2016. Fusarium Toxins in Cereals: Occurrence, Legislation, Factors
1491 Promoting the Appearance and Their Management. *Molecules*, 21, 627.
- 1492 Fierabracci A & Pellegrino M 2016. The Double Role of p53 in Cancer and Autoimmunity and Its
1493 Potential as Therapeutic Target. *Int J Mol Sci*, 17, 1975.
- 1494 Filion GJP, Zhenilo S, Salozhin S, Yamada D, Prokhortchouk E & Defossez P-A 2006. A family of
1495 human zinc finger proteins that bind methylated DNA and repress transcription. *Mol Cell Biol*, 26, 169-
1496 181.
- 1497 Finkel T 2011. Signal transduction by reactive oxygen species. *Journal of Cell Biology*, 194, 7-15.
- 1498 FOA/WHO 2002. Evaluation of certain mycotoxins in food : fifty-sixth report of the Joint FAO/WHO
1499 Expert Committee on Food Additives. Geneva: World Health Organization.
- 1500 Fridman JS & Lowe SW 2003. Control of apoptosis by p53. *Oncogene*, 22, 9030-9040.
- 1501 Fu Y, Jia G, Pang X, Wang RN, Wang X, Li CJ, Smemo S, Dai Q, Bailey KA, Nobrega MA, et al.
1502 2013. FTO-mediated formation of N6-hydroxymethyladenosine and N6-formyladenosine in
1503 mammalian RNA. *Nat Commun*, 4, 1798-1798.
- 1504 Futerman AH & Riezman H 2005. The ins and outs of sphingolipid synthesis. *Trends Cell Biol*, 15,
1505 312-318.
- 1506 Gardner NM, Riley RT, Showker JL, Voss KA, Sachs AJ, Maddox JR & Gelineau-van Waes JB 2016.
1507 Elevated nuclear sphingoid base-1-phosphates and decreased histone deacetylase activity after
1508 fumonisin B1 treatment in mouse embryonic fibroblasts. *Toxicology and applied pharmacology*, 298,
1509 56-65.
- 1510 Geiman TM, Sankpal UT, Robertson AK, Chen Y, Mazumdar M, Heale JT, Schmiesing JA, Kim W,
1511 Yokomori K & Zhao Y 2004. Isolation and characterization of a novel DNA methyltransferase complex
1512 linking DNMT3B with components of the mitotic chromosome condensation machinery. *Nucleic Acids*
1513 *Res*, 32, 2716-2729.

- 1514 Ghazi T, Arumugam T, Foolchand A & Chuturgoon AA 2020a. The Impact of Natural Dietary
1515 Compounds and Food-Borne Mycotoxins on DNA Methylation and Cancer. *Cells*, 9.
- 1516 Ghazi T, Nagiah S & Chuturgoon AA 2020b. Fusaric acid decreases p53 expression by altering
1517 promoter methylation and m6A RNA methylation in human hepatocellular carcinoma (HepG2) cells.
1518 *Epigenetics*, 1-13.
- 1519 Giglia-Mari G, Zotter A & Vermeulen W 2011. DNA damage response. *Cold Spring Harbor*
1520 *perspectives in biology*, 3, a000745-a000745.
- 1521 Glowacki S, Synowiec E & Blasiak J 2013. The Role of Mitochondrial DNA Damage and Repair in the
1522 Resistance of BCR/ABL-Expressing Cells to Tyrosine Kinase Inhibitors. *Int J Mol Sci*, 14, 16348-
1523 16364.
- 1524 Grandy RA, Whitfield TW, Wu H, Fitzgerald MP, VanOudenhove JJ, Zaidi SK, Montecino MA, Lian
1525 JB, van Wijnen AJ & Stein JL 2016. Genome-wide studies reveal that H3K4me3 modification in
1526 bivalent genes is dynamically regulated during the pluripotent cell cycle and stabilized upon
1527 differentiation. *Mol Cell Biol*, 36, 615-627.
- 1528 Greenblatt MS, Bennett WP, Hollstein M & Harris CC 1994. Mutations in the p53 tumor suppressor
1529 gene: clues to cancer etiology and molecular pathogenesis. *Cancer Res*, 54, 4855-4878.
- 1530 Grenier B & Oswald I 2011. Mycotoxin co-contamination of food and feed: Meta-Analysis of
1531 publications describing toxicological interactions. *World Mycotoxin Journal*, 4, 285-313.
- 1532 Guccione E & Richard S 2019. The regulation, functions and clinical relevance of arginine methylation.
1533 *Nature Reviews Molecular Cell Biology*, 20, 642-657.
- 1534 Guo D, Wu B, Yan J, Li X, Sun H & Zhou D 2012. A possible gene silencing mechanism:
1535 Hypermethylation of the Keap1 promoter abrogates binding of the transcription factor Sp1 in lung
1536 cancer cells. *Biochemical and Biophysical Research Communications*, 428, 80-85.
- 1537 Guo JU, Su Y, Zhong C, Ming G-l & Song H 2011. Hydroxylation of 5-methylcytosine by TET1
1538 promotes active DNA demethylation in the adult brain. *Cell*, 145, 423-434.
- 1539 Guo P, Qiao F, Huang D, Wu Q, Chen T, Badawy S, Cheng G, Hao H, Xie S & Wang X 2020. MiR-
1540 155-5p plays as a “janus” in the expression of inflammatory cytokines induced by T-2 toxin. *Food and*
1541 *Chemical Toxicology*, 140, 111258.
- 1542 Han J, Wang T, Fu L, Shi L-Y, Zhu C-C, Liu J, Zhang Y, Cui X-S, Kim N-H & Sun S-C 2015. Altered
1543 oxidative stress, apoptosis/autophagy, and epigenetic modifications in Zearalenone-treated porcine
1544 oocytes. *Toxicology Research*, 4, 1184-1194.
- 1545 Haschek WM, Gumprecht LA, Smith G, Tumbleson ME & Constable PD 2001. Fumonisin toxicosis in
1546 swine: an overview of porcine pulmonary edema and current perspectives. *Environ Health Perspect*,
1547 109, 251-257.
- 1548 Hata K, Okano M, Lei H & Li E 2002. Dnmt3L cooperates with the Dnmt3 family of de novo DNA
1549 methyltransferases to establish maternal imprints in mice. *Development*, 129, 1983-1993.
- 1550 He J, Zhang J, Wang Y, Liu W, Gou K, Liu Z & Cui S 2018. MiR-7 Mediates the Zearalenone Signaling
1551 Pathway Regulating FSH Synthesis and Secretion by Targeting FOS in Female Pigs. *Endocrinology*,
1552 159, 2993-3006.
- 1553 He YF, Li BZ, Li Z, Liu P, Wang Y, Tang Q, Ding J, Jia Y, Chen Z, Li L, et al. 2011. Tet-mediated
1554 formation of 5-carboxylcytosine and its excision by TDG in mammalian DNA. *Science (New York,*
1555 *N.Y.)*, 333, 1303-1307.
- 1556 Hellman A & Chess A 2007. Gene body-specific methylation on the active X chromosome. *Science*
1557 *(New York, N.Y.)*, 315, 1141-1143.
- 1558 Hendrich B, Hardeland U, Ng HH, Jiricny J & Bird A 1999. The thymine glycosylase MBD4 can bind
1559 to the product of deamination at methylated CpG sites. *Nature*, 401, 301-304.

- 1560 Hengartner MO 2000. The biochemistry of apoptosis. *Nature*, 407, 770-776.
- 1561 Hermann A, Goyal R & Jeltsch A 2004. The Dnmt1 DNA-(cytosine-C5)-methyltransferase methylates
1562 DNA processively with high preference for hemimethylated target sites. *J Biol Chem*, 279, 48350-
1563 48359.
- 1564 Holliday R 2006. Epigenetics: A Historical Overview. *Epigenetics*, 1, 76-80.
- 1565 Hon GC, Hawkins RD, Caballero OL, Lo C, Lister R, Pelizzola M, Valsesia A, Ye Z, Kuan S & Edsall
1566 LE 2012. Global DNA hypomethylation coupled to repressive chromatin domain formation and gene
1567 silencing in breast cancer. *Genome research*, 22, 246-258.
- 1568 Huang D, Cui L, Sajid A, Zainab F, Wu Q, Wang X & Yuan Z 2019a. The epigenetic mechanisms in
1569 Fusarium mycotoxins induced toxicities. *Food and Chemical Toxicology*, 123, 595-601.
- 1570 Huang X, Gao X, Li W, Jiang S, Li R, Hong H, Zhao C, Zhou P, Chen H & Bo X 2019b. Stable
1571 H3K4me3 is associated with transcription initiation during early embryo development. *Bioinformatics*,
1572 35, 3931-3936.
- 1573 Huarte M, Guttman M, Feldser D, Garber M, Koziol MJ, Kenzelmann-Broz D, Khalil AM, Zuk O,
1574 Amit I, Rabani M, et al. 2010. A large intergenic noncoding RNA induced by p53 mediates global gene
1575 repression in the p53 response. *Cell*, 142, 409-419.
- 1576 Hung T, Wang Y, Lin MF, Koegel AK, Kotake Y, Grant GD, Horlings HM, Shah N, Umbricht C, Wang
1577 P, et al. 2011. Extensive and coordinated transcription of noncoding RNAs within cell-cycle promoters.
1578 *Nature genetics*, 43, 621-629.
- 1579 Hyun K, Jeon J, Park K & Kim J 2017. Writing, erasing and reading histone lysine methylations.
1580 *Experimental & Molecular Medicine*, 49, e324-e324.
- 1581 IARC 2002. Some traditional herbal medicines, some mycotoxins, naphthalene and styrene. *IARC*
1582 *monographs on the evaluation of carcinogenic risks to humans*, 82, 1-556.
- 1583 Ito S, Shen L, Dai Q, Wu SC, Collins LB, Swenberg JA, He C & Zhang Y 2011. Tet proteins can
1584 convert 5-methylcytosine to 5-formylcytosine and 5-carboxylcytosine. *Science (New York, N.Y.)*, 333,
1585 1300-1303.
- 1586 Jambhekar A, Dhall A & Shi Y 2019. Roles and regulation of histone methylation in animal
1587 development. *Nature reviews. Molecular cell biology*, 20, 625-641.
- 1588 Jarroux J, Morillon A & Pinskaya M 2017. History, Discovery, and Classification of lncRNAs. *Adv*
1589 *Exp Med Biol*, 1008, 1-46.
- 1590 Jenuwein T & Allis CD 2001. Translating the histone code. *Science (New York, N.Y.)*, 293, 1074-1080.
- 1591 Jia G, Fu Y, Zhao X, Dai Q, Zheng G, Yang Y, Yi C, Lindahl T, Pan T, Yang Y-G, et al. 2011. N6-
1592 Methyladenosine in nuclear RNA is a major substrate of the obesity-associated FTO. *Nature Chemical*
1593 *Biology*, 7, 885-887.
- 1594 Jin Z & Liu Y 2018. DNA methylation in human diseases. *Genes & diseases*, 5, 1-8.
- 1595 Jjingo D, Conley AB, Yi SV, Lunyak VV & Jordan IK 2012. On the presence and role of human gene-
1596 body DNA methylation. *Oncotarget*, 3, 462-474.
- 1597 Jo MH, Shin S, Jung SR, Kim E, Song JJ & Hohng S 2015. Human Argonaute 2 Has Diverse Reaction
1598 Pathways on Target RNAs. *Molecular cell*, 59, 117-124.
- 1599 Jones PA 1996. DNA methylation errors and cancer. *Cancer Res*, 56, 2463-2467.
- 1600 Kader F, Ghai M & Maharaj L 2018. The effects of DNA methylation on human psychology.
1601 *Behavioural Brain Research*, 346, 47-65.
- 1602 Kang KA, Piao MJ, Kim KC, Kang HK, Chang WY, Park IC, Keum YS, Surh YJ & Hyun JW 2014.
1603 Epigenetic modification of Nrf2 in 5-fluorouracil-resistant colon cancer cells: involvement of TET-
1604 dependent DNA demethylation. *Cell Death Dis*, 5, e1183-e1183.

- 1605 Kanherkar RR, Bhatia-Dey N & Csoka AB 2014. Epigenetics across the human lifespan. *Frontiers in*
1606 *Cell and Developmental Biology*, 2.
- 1607 Kansanen E, Kuosmanen SM, Leinonen H & Levonen A-L 2013. The Keap1-Nrf2 pathway:
1608 Mechanisms of activation and dysregulation in cancer. *Redox Biology*, 1, 45-49.
- 1609 Kapranov P, Cawley SE, Drenkow J, Bekiranov S, Strausberg RL, Fodor SP & Gingeras TR 2002.
1610 Large-scale transcriptional activity in chromosomes 21 and 22. *Science (New York, N.Y.)*, 296, 916-
1611 919.
- 1612 Kapranov P, Willingham AT & Gingeras TR 2007. Genome-wide transcription and the implications for
1613 genomic organization. *Nature Reviews Genetics*, 8, 413-423.
- 1614 Karachentsev D, Sarma K, Reinberg D & Steward R 2005. PR-Set7-dependent methylation of histone
1615 H4 Lys 20 functions in repression of gene expression and is essential for mitosis. *Genes & development*,
1616 19, 431-435.
- 1617 Kareta MS, Botello ZM, Ennis JJ, Chou C & Chédin F 2006. Reconstitution and mechanism of the
1618 stimulation of de novo methylation by human DNMT3L. *J Biol Chem*, 281, 25893-25902.
- 1619 Ke S, Alemu EA, Mertens C, Gantman EC, Fak JJ, Mele A, Haripal B, Zucker-Scharff I, Moore MJ,
1620 Park CY, et al. 2015. A majority of m6A residues are in the last exons, allowing the potential for 3'
1621 UTR regulation. *Genes & development*, 29, 2037-2053.
- 1622 Kelly TK, De Carvalho DD & Jones PA 2010. Epigenetic modifications as therapeutic targets. *Nature*
1623 *biotechnology*, 28, 1069-1078.
- 1624 Khaldi N & Wolfe KH 2011. Evolutionary Origins of the Fumonisin Secondary Metabolite Gene
1625 Cluster in *Fusarium verticillioides* and *Aspergillus niger*. *International Journal of Evolutionary*
1626 *Biology*, 2011, 423821.
- 1627 Khandelwal A, Bacolla A, Vasquez K & Jain A 2015. Long non-coding RNA: A new paradigm for
1628 lung cancer. *Molecular carcinogenesis*, 54.
- 1629 Khor TO, Fuentes F, Shu L, Paredes-Gonzalez X, Yang AY, Liu Y, Smiraglia DJ, Yegnasubramanian
1630 S, Nelson WG & Kong A-NT 2014. Epigenetic DNA Methylation of Antioxidative Stress Regulator
1631 NRF2 in Human Prostate Cancer. *Cancer Prevention Research*, 7, 1186-1197.
- 1632 Kimura H & Shiota K 2003. Methyl-CpG-binding protein, MeCP2, is a target molecule for maintenance
1633 DNA methyltransferase, Dnmt1. *J Biol Chem*, 278, 4806-4812.
- 1634 King FW, Skeen J, Hay N & Shtivelman E 2004. Inhibition of Chk1 by activated PKB/Akt. *Cell Cycle*,
1635 3, 634-637.
- 1636 Klarić M & Pepeljnjak S 2001. Fumonisin and their effects on animal health - A brief review.
1637 *Veterinarski Arhiv*, 71, 299-323.
- 1638 Kohli RM & Zhang Y 2013. TET enzymes, TDG and the dynamics of DNA demethylation. *Nature*,
1639 502, 472-479.
- 1640 Kong YW, Cannell IG, de Moor CH, Hill K, Garside PG, Hamilton TL, Meijer HA, Dobbyn HC,
1641 Stoneley M, Spriggs KA, et al. 2008. The mechanism of micro-RNA-mediated translation repression is
1642 determined by the promoter of the target gene. *Proceedings of the National Academy of Sciences of the*
1643 *United States of America*, 105, 8866-8871.
- 1644 Kopp F & Mendell JT 2018. Functional Classification and Experimental Dissection of Long Noncoding
1645 RNAs. *Cell*, 172, 393-407.
- 1646 Kouadio JH, Dano SD, Moukha S, Mobio TA & Creppy EE 2007. Effects of combinations of *Fusarium*
1647 mycotoxins on the inhibition of macromolecular synthesis, malondialdehyde levels, DNA methylation
1648 and fragmentation, and viability in Caco-2 cells. *Toxicol*, 49, 306-317.
- 1649 Krug RM, Morgan MA & Shatkin AJ 1976. Influenza viral mRNA contains internal N6-
1650 methyladenosine and 5'-terminal 7-methylguanosine in cap structures. *J Virol*, 20, 45-53.

- 1651 Lagos-Quintana M, Rauhut R, Lendeckel W & Tuschl T 2001. Identification of novel genes coding for
1652 small expressed RNAs. *Science (New York, N.Y.)*, 294, 853-858.
- 1653 Laird PW & Jaenisch R 1996. The role of DNA methylation in cancer genetics and epigenetics. *Annual*
1654 *review of genetics*, 30, 441-464.
- 1655 Larizza L & Finelli P 2019. Developmental disorders with intellectual disability driven by chromatin
1656 dysregulation: Clinical overlaps and molecular mechanisms. *Clinical genetics*, 95, 231-240.
- 1657 Lasda E & Parker R 2014. Circular RNAs: diversity of form and function. *RNA*, 20, 1829-1842.
- 1658 Lee HJ & Ryu D 2017. Worldwide Occurrence of Mycotoxins in Cereals and Cereal-Derived Food
1659 Products: Public Health Perspectives of Their Co-occurrence. *Journal of Agricultural and Food*
1660 *Chemistry*, 65, 7034-7051.
- 1661 Lee RC, Feinbaum RL & Ambros V 1993. The *C. elegans* heterochronic gene *lin-4* encodes small RNAs
1662 with antisense complementarity to *lin-14*. *cell*, 75, 843-854.
- 1663 Leonhardt H, Page AW, Weier HU & Bestor TH 1992. A targeting sequence directs DNA
1664 methyltransferase to sites of DNA replication in mammalian nuclei. *Cell*, 71, 865-873.
- 1665 Li E, Bestor TH & Jaenisch R 1992. Targeted mutation of the DNA methyltransferase gene results in
1666 embryonic lethality. *Cell*, 69, 915-926.
- 1667 Li E, Beard C & Jaenisch R 1993. Role for DNA methylation in genomic imprinting. *Nature*, 366, 362-
1668 365.
- 1669 Li G & Zhu P 2015. Structure and organization of chromatin fiber in the nucleus. *FEBS Letters*, 589,
1670 2893-2904.
- 1671 Li J & Yuan J 2008. Caspases in apoptosis and beyond. *Oncogene*, 27, 6194-6206.
- 1672 Li Z, Xu L, Tang N, Xu Y, Ye X, Shen S, Niu X, Lu S & Chen Z 2014. The polycomb group protein
1673 EZH2 inhibits lung cancer cell growth by repressing the transcription factor Nrf2. *FEBS Letters*, 588,
1674 3000-3007.
- 1675 Liao S, Sun H & Xu C 2018. YTH Domain: A Family of N6-methyladenosine (m6A) Readers.
1676 *Genomics, Proteomics & Bioinformatics*, 16, 99-107.
- 1677 Lin CH, Hsieh SY, Sheen IS, Lee WC, Chen TC, Shyu WC & Liaw YF 2001. Genome-wide
1678 hypomethylation in hepatocellular carcinogenesis. *Cancer Res*, 61, 4238-4243.
- 1679 Liu A, Sun Y, Wang X, Ihsan A, Tao Y, Chen D, Peng D, Wu Q, Wang X & Yuan Z 2019. DNA
1680 methylation is involved in pro-inflammatory cytokines expression in T-2 toxin-induced liver injury.
1681 *Food and Chemical Toxicology*, 132, 110661.
- 1682 Liu H, Shang X & Zhu H 2017. LncRNA/DNA binding analysis reveals losses and gains and lineage
1683 specificity of genomic imprinting in mammals. *Bioinformatics*, 33, 1431-1436.
- 1684 Liu J, Yue Y, Han D, Wang X, Fu Y, Zhang L, Jia G, Yu M, Lu Z, Deng X, et al. 2014. A METTL3-
1685 METTL14 complex mediates mammalian nuclear RNA N6-adenosine methylation. *Nat Chem Biol*, 10,
1686 93-95.
- 1687 Loughery JEP, Dunne PD, O'Neill KM, Meehan RR, McDaid JR & Walsh CP 2011. DNMT1 deficiency
1688 triggers mismatch repair defects in human cells through depletion of repair protein levels in a process
1689 involving the DNA damage response. *Human Molecular Genetics*, 20, 3241-3255.
- 1690 Luger K, Mäder AW, Richmond RK, Sargent DF & Richmond TJ 1997. Crystal structure of the
1691 nucleosome core particle at 2.8 Å resolution. *Nature*, 389, 251-260.
- 1692 Lumsangkul C, Chiang H-I, Lo N-W, Fan Y-K & Ju J-C 2019. Developmental Toxicity of Mycotoxin
1693 Fumonisin B₁ in Animal Embryogenesis: An Overview. *Toxins (Basel)*, 11, 114.
- 1694 Lyko F 2018. The DNA methyltransferase family: a versatile toolkit for epigenetic regulation. *Nature*
1695 *Reviews Genetics*, 19, 81-92.

- 1696 Ma S, Chen C, Ji X, Liu J, Zhou Q, Wang G, Yuan W, Kan Q & Sun Z 2019. The interplay between
1697 m6A RNA methylation and noncoding RNA in cancer. *Journal of Hematology & Oncology*, 12, 121.
- 1698 Machnicka MA, Milanowska K, Osman Oglou O, Purta E, Kurkowska M, Olchowik A, Januszewski
1699 W, Kalinowski S, Dunin-Horkawicz S, Rother KM, et al. 2013. MODOMICS: a database of RNA
1700 modification pathways--2013 update. *Nucleic Acids Res*, 41, D262-D267.
- 1701 Macleod D, Charlton J, Mullins J & Bird AP 1994. Sp1 sites in the mouse aprt gene promoter are
1702 required to prevent methylation of the CpG island. *Genes Dev*, 8, 2282-2292.
- 1703 Marasas WF 2001. Discovery and occurrence of the fumonisins: a historical perspective. *Environ*
1704 *Health Perspect*, 109 Suppl 2, 239-243.
- 1705 Marasas WF, Riley RT, Hendricks KA, Stevens VL, Sadler TW, Gelineau-van Waes J, Missmer SA,
1706 Cabrera J, Torres O & Gelderblom WC 2004. Fumonisins disrupt sphingolipid metabolism, folate
1707 transport, and neural tube development in embryo culture and in vivo: a potential risk factor for human
1708 neural tube defects among populations consuming fumonisin-contaminated maize. *The Journal of*
1709 *nutrition*, 134, 711-716.
- 1710 Marczylo EL, Jacobs MN & Gant TW 2016. Environmentally induced epigenetic toxicity: potential
1711 public health concerns. *Crit Rev Toxicol*, 46, 676-700.
- 1712 McIlwain DR, Berger T & Mak TW 2013. Caspase Functions in Cell Death and Disease. *Cold Spring*
1713 *Harbor Perspectives in Biology*, 5.
- 1714 Medina A, Schmidt-Heydt M, Cárdenas-Chávez DL, Parra R, Geisen R & Magan N 2013. Integrating
1715 toxin gene expression, growth and fumonisin B1 and B2 production by a strain of *Fusarium*
1716 *verticillioides* under different environmental factors. *Journal of The Royal Society Interface*, 10,
1717 20130320.
- 1718 Meyer KD, Saletore Y, Zumbo P, Elemento O, Mason CE & Jaffrey SR 2012. Comprehensive analysis
1719 of mRNA methylation reveals enrichment in 3' UTRs and near stop codons. *Cell*, 149, 1635-1646.
- 1720 Mishra M, Zhong Q & Kowluru RA 2014. Epigenetic Modifications of Keap1 Regulate Its Interaction
1721 With the Protective Factor Nrf2 in the Development of Diabetic Retinopathy. *Investigative*
1722 *Ophthalmology & Visual Science*, 55, 7256-7265.
- 1723 Missmer SA, Suarez L, Felkner M, Wang E, Merrill AH, Jr., Rothman KJ & Hendricks KA 2006.
1724 Exposure to fumonisins and the occurrence of neural tube defects along the Texas-Mexico border.
1725 *Environ Health Perspect*, 114, 237-241.
- 1726 Mizuguchi G, Tsukiyama T, Wisniewski J & Wu C 1997. Role of Nucleosome Remodeling Factor
1727 NURF in Transcriptional Activation of Chromatin. *Molecular cell*, 1, 141-150.
- 1728 Mobio TA, Anane R, Baudrimont I, Carratú MR, Shier TW, Dano SD, Ueno Y & Creppy EE 2000.
1729 Epigenetic properties of fumonisin B(1): cell cycle arrest and DNA base modification in C6 glioma
1730 cells. *Toxicology and applied pharmacology*, 164, 91-96.
- 1731 Mohn F, Weber M, Rebhan M, Roloff TC, Richter J, Stadler MB, Bibel M & Schübeler D 2008.
1732 Lineage-specific polycomb targets and de novo DNA methylation define restriction and potential of
1733 neuronal progenitors. *Molecular cell*, 30, 755-766.
- 1734 Moore LD, Le T & Fan G 2013. DNA Methylation and Its Basic Function. *Neuropsychopharmacology*,
1735 38, 23-38.
- 1736 Morey C & Avner P 2004. Employment opportunities for non-coding RNAs. *FEBS letters*, 567, 27-34.
- 1737 Morgan HD, Dean W, Coker HA, Reik W & Petersen-Mahrt SK 2004. Activation-induced cytidine
1738 deaminase deaminates 5-methylcytosine in DNA and is expressed in pluripotent tissues: implications
1739 for epigenetic reprogramming. *J Biol Chem*, 279, 52353-52360.
- 1740 Morris KV, Chan SW, Jacobsen SE & Looney DJ 2004. Small interfering RNA-induced transcriptional
1741 gene silencing in human cells. *Science (New York, N.Y.)*, 305, 1289-1292.

- 1742 Mortusewicz O, Schermelleh L, Walter J, Cardoso MC & Leonhardt H 2005. Recruitment of DNA
1743 methyltransferase I to DNA repair sites. *Proc Natl Acad Sci U S A*, 102, 8905-8909.
- 1744 Müller MM & Muir TW 2015. Histones: at the crossroads of peptide and protein chemistry. *Chem Rev*,
1745 115, 2296-2349.
- 1746 Nagano T, Mitchell JA, Sanz LA, Pauler FM, Ferguson-Smith AC, Feil R & Fraser P 2008. The Air
1747 Noncoding RNA Epigenetically Silences Transcription by Targeting G9a to Chromatin. *Science (New*
1748 *York, N.Y.)*, 322, 1717-1720.
- 1749 Nakajima YI & Kuranaga E 2017. Caspase-dependent non-apoptotic processes in development. *Cell*
1750 *Death Differ*, 24, 1422-1430.
- 1751 Nan X, Ng H-H, Johnson CA, Laherty CD, Turner BM, Eisenman RN & Bird A 1998. Transcriptional
1752 repression by the methyl-CpG-binding protein MeCP2 involves a histone deacetylase complex. *Nature*,
1753 393, 386-389.
- 1754 Nesic K, Ivanovic S & Nesic V 2014. Fusarial toxins: secondary metabolites of *Fusarium* fungi. *Rev*
1755 *Environ Contam Toxicol*, 228, 101-120.
- 1756 Ng HH, Zhang Y, Hendrich B, Johnson CA, Turner BM, Erdjument-Bromage H, Tempst P, Reinberg
1757 D & Bird A 1999. MBD2 is a transcriptional repressor belonging to the MeCP1 histone deacetylase
1758 complex. *Nat Genet*, 23, 58-61.
- 1759 Ninova M, Fejes Tóth K & Aravin AA 2019. The control of gene expression and cell identity by H3K9
1760 trimethylation. *Development*, 146, dev181180.
- 1761 O'Brien J, Hayder H, Zayed Y & Peng C 2018. Overview of MicroRNA Biogenesis, Mechanisms of
1762 Actions, and Circulation. *Frontiers in Endocrinology*, 9.
- 1763 Okano M, Xie S & Li E 1998. Cloning and characterization of a family of novel mammalian DNA
1764 (cytosine-5) methyltransferases. *Nature Genetics*, 19, 219-220.
- 1765 Oliva-Rico D & Herrera LA 2017. Regulated expression of the lncRNA TERRA and its impact on
1766 telomere biology. *Mechanisms of ageing and development*, 167, 16-23.
- 1767 Ouyang J, Hu J & Chen JL 2016. lncRNAs regulate the innate immune response to viral infection. *Wiley*
1768 *Interdisciplinary Reviews: RNA*, 7, 129-143.
- 1769 Palsamy P, Ayaki M, Elanchezhian R & Shinohara T 2012. Promoter demethylation of Keap1 gene in
1770 human diabetic cataractous lenses. *Biochemical and Biophysical Research Communications*, 423, 542-
1771 548.
- 1772 Panzeri I, Rossetti G & Pagani M 2016. Chapter 4 - Basic Principles of Noncoding RNAs in
1773 Epigenetics. In: TOLLEFSBOL, T. O. (ed.) *Medical Epigenetics*. Boston: Academic Press.
- 1774 Patil DP, Chen CK, Pickering BF, Chow A, Jackson C, Guttman M & Jaffrey SR 2016. m(6)A RNA
1775 methylation promotes XIST-mediated transcriptional repression. *Nature*, 537, 369-373.
- 1776 Patil M, Pabla N & Dong Z 2013. Checkpoint kinase 1 in DNA damage response and cell cycle
1777 regulation. *Cellular and molecular life sciences : CMLS*, 70, 4009-4021.
- 1778 Paul P, Chakraborty A, Sarkar D, Langthasa M, Rahman M, Bari M, Singha RS, Malakar AK &
1779 Chakraborty S 2018. Interplay between miRNAs and human diseases. *Journal of cellular physiology*,
1780 233, 2007-2018.
- 1781 Payer B & Lee JT 2008. X Chromosome Dosage Compensation: How Mammals Keep the Balance.
1782 *Annual Review of Genetics*, 42, 733-772.
- 1783 Pellanda H, Forges T, Bressenot A, Chango A, Bronowicki JP, Guéant JL & Namour F 2012. Fumonisin
1784 FB1 treatment acts synergistically with methyl donor deficiency during rat pregnancy to produce
1785 alterations of H3- and H4-histone methylation patterns in fetuses. *Molecular nutrition & food research*,
1786 56, 976-985.

- 1787 Pena P, Hom R, Hung T, Lin H, Kuo A, Wong R, Subach O, Champagne K, Zhao R & Verkhusha V
 1788 2008. Histone H3K4me3 binding is required for the DNA repair and apoptotic activities of ING1 tumor
 1789 suppressor. *Journal of molecular biology*, 380, 303-312.
- 1790 Perry RP & Kelley DE 1974. Existence of methylated messenger RNA in mouse L cells. *Cell*, 1, 37-
 1791 42.
- 1792 Pfeffer S, Zavolan M, Grässer FA, Chien M, Russo JJ, Ju J, John B, Enright AJ, Marks D, Sander C, et
 1793 al. 2004. Identification of Virus-Encoded MicroRNAs. *Science (New York, N.Y.)*, 304, 734-736.
- 1794 Pfeifer GP 2018. Defining Driver DNA Methylation Changes in Human Cancer. *Int J Mol Sci*, 19, 1166.
- 1795 Ping XL, Sun BF, Wang L, Xiao W, Yang X, Wang WJ, Adhikari S, Shi Y, Lv Y, Chen YS, et al. 2014.
 1796 Mammalian WTAP is a regulatory subunit of the RNA N6-methyladenosine methyltransferase. *Cell*
 1797 *Res*, 24, 177-189.
- 1798 Place RF, Li L-C, Pookot D, Noonan EJ & Dahiya R 2008. MicroRNA-373 induces expression of genes
 1799 with complementary promoter sequences. *Proceedings of the National Academy of Sciences*, 105, 1608-
 1800 1613.
- 1801 Prokhortchouk A, Hendrich B, Jørgensen H, Ruzov A, Wilm M, Georgiev G, Bird A & Prokhortchouk
 1802 E 2001. The p120 catenin partner Kaiso is a DNA methylation-dependent transcriptional repressor.
 1803 *Genes & development*, 15, 1613-1618.
- 1804 Puc J, Keniry M, Li HS, Pandita TK, Choudhury AD, Memeo L, Mansukhani M, Murty VVVS,
 1805 Gaciong Z, Meek SEM, et al. 2005. Lack of PTEN sequesters CHK1 and initiates genetic instability.
 1806 *Cancer Cell*, 7, 193-204.
- 1807 Quinn JJ & Chang HY 2016. Unique features of long non-coding RNA biogenesis and function. *Nature*
 1808 *Reviews Genetics*, 17, 47-62.
- 1809 Rao RC & Dou Y 2015. Hijacked in cancer: the KMT2 (MLL) family of methyltransferases. *Nature*
 1810 *Reviews Cancer*, 15, 334-346.
- 1811 Ray PD, Huang B-W & Tsuji Y 2012. Reactive oxygen species (ROS) homeostasis and redox regulation
 1812 in cellular signaling. *Cell Signal*, 24, 981-990.
- 1813 Reddy B & Raghavender C 2008. Outbreaks of fusarial-toxicoses in India. *Cereal Research*
 1814 *Communications*, 36, 321-325.
- 1815 Rheeder JP, Marasas WFO & Vismer HF 2002. Production of Fumonisin Analogs by FusariumSpecies.
 1816 *Applied and Environmental Microbiology*, 68, 2101-2105.
- 1817 Rideout WM, 3rd, Coetzee GA, Olumi AF & Jones PA 1990. 5-Methylcytosine as an endogenous
 1818 mutagen in the human LDL receptor and p53 genes. *Science (New York, N.Y.)*, 249, 1288-1290.
- 1819 Riley RT & Merrill AH, Jr. 2019. Ceramide synthase inhibition by fumonisins: a perfect storm of
 1820 perturbed sphingolipid metabolism, signaling, and disease. *Journal of lipid research*, 60, 1183-1189.
- 1821 Robertson KD 2005. DNA methylation and human disease. *Nature Reviews Genetics*, 6, 597-610.
- 1822 Saito K, Kawakami K, Matsumoto I, Oda M, Watanabe G & Minamoto T 2010. Long interspersed
 1823 nuclear element 1 hypomethylation is a marker of poor prognosis in stage IA non-small cell lung cancer.
 1824 *Clinical cancer research*, 16, 2418-2426.
- 1825 Saldaña-Meyer R & Recillas-Targa F 2011. Transcriptional and epigenetic regulation of the p53 tumor
 1826 suppressor gene. *Epigenetics*, 6, 1068-1077.
- 1827 Sancak D & Ozden S 2015. Global histone modifications in Fumonisin B1 exposure in rat kidney
 1828 epithelial cells. *Toxicology in vitro : an international journal published in association with BIBRA*, 29,
 1829 1809-1815.
- 1830 Saraste A & Pulkki K 2000. Morphologic and biochemical hallmarks of apoptosis. *Cardiovascular*
 1831 *Research*, 45, 528-537.

- 1832 Saxonov S, Berg P & Brutlag DL 2006. A genome-wide analysis of CpG dinucleotides in the human
1833 genome distinguishes two distinct classes of promoters. *Proceedings of the National Academy of*
1834 *Sciences of the United States of America*, 103, 1412-1417.
- 1835 Schulz WA, Steinhoff C & Florl AR 2006. Methylation of endogenous human retroelements in health
1836 and disease. *Curr Top Microbiol Immunol*, 310, 211-250.
- 1837 Shamsi MB, Firoz AS, Imam SN, Alzaman N & Samman MA 2017. Epigenetics of human diseases
1838 and scope in future therapeutics. *Journal of Taibah University Medical Sciences*, 12, 205-211.
- 1839 Shen Y & White E 2001. p53-dependent apoptosis pathways. *Adv Cancer Res*, 82, 55-84.
- 1840 Shephard GS, Burger H-M, Rheeder JP, Alberts JF & Gelderblom WCA 2019. The effectiveness of
1841 regulatory maximum levels for fumonisin mycotoxins in commercial and subsistence maize crops in
1842 South Africa. *Food Control*, 97, 77-80.
- 1843 Shirima CP, Kimanya ME, Kinabo JL, Routledge MN, Srey C, Wild CP & Gong YY 2013. Dietary
1844 exposure to aflatoxin and fumonisin among Tanzanian children as determined using biomarkers of
1845 exposure. *Molecular nutrition & food research*, 57, 1874-1881.
- 1846 Singh T, Kurki MI, Curtis D, Purcell SM, Crooks L, McRae J, Suvisaari J, Chheda H, Blackwood D &
1847 Breen G 2016. Rare loss-of-function variants in SETD1A are associated with schizophrenia and
1848 developmental disorders. *Nature neuroscience*, 19, 571-577.
- 1849 Song M-J, Kim M, Choi Y, Yi M-h, Kim J, Park S-J, Yong T-S & Kim H-P 2017. Epigenome mapping
1850 highlights chromatin-mediated gene regulation in the protozoan parasite *Trichomonas vaginalis*.
1851 *Scientific Reports*, 7, 45365.
- 1852 Soriano JM, González L & Catalá AI 2005. Mechanism of action of sphingolipids and their metabolites
1853 in the toxicity of fumonisin B1. *Progress in lipid research*, 44, 345-356.
- 1854 Steger DJ, Lefterova MI, Ying L, Stonestrom AJ, Schupp M, Zhuo D, Vakoc AL, Kim J-E, Chen J &
1855 Lazar MA 2008. DOT1L/KMT4 recruitment and H3K79 methylation are ubiquitously coupled with
1856 gene transcription in mammalian cells. *Mol Cell Biol*, 28, 2825-2839.
- 1857 Strahl BD & Allis CD 2000. The language of covalent histone modifications. *Nature*, 403, 41-45.
- 1858 Straussman R, Nejman D, Roberts D, Steinfeld I, Blum B, Benvenisty N, Simon I, Yakhini Z & Cedar
1859 H 2009. Developmental programming of CpG island methylation profiles in the human genome. *Nat*
1860 *Struct Mol Biol*, 16, 564-571.
- 1861 Sun G, Wang S, Hu X, Su J, Huang T, Yu J, Tang L, Gao W & Wang J-S 2007. Fumonisin B1
1862 contamination of home-grown corn in high-risk areas for esophageal and liver cancer in China. *Food*
1863 *Additives & Contaminants*, 24, 181-185.
- 1864 Sydenham EW, Thiel PG, Marasas WF, Shephard GS, Van Schalkwyk DJ & Koch KR 1990. Natural
1865 occurrence of some *Fusarium* mycotoxins in corn from low and high esophageal cancer prevalence
1866 areas of the Transkei, Southern Africa. *Journal of Agricultural and Food Chemistry*, 38, 1900-1903.
- 1867 Tahiliani M, Koh KP, Shen Y, Pastor WA, Bandukwala H, Brudno Y, Agarwal S, Iyer LM, Liu DR,
1868 Aravind L, et al. 2009. Conversion of 5-methylcytosine to 5-hydroxymethylcytosine in mammalian
1869 DNA by MLL partner TET1. *Science (New York, N.Y.)*, 324, 930-935.
- 1870 Tay Y, Rinn J & Pandolfi PP 2014. The multilayered complexity of ceRNA crosstalk and competition.
1871 *Nature*, 505, 344-352.
- 1872 Thannickal VJ & Fanburg BL 2000. Reactive oxygen species in cell signaling. *American Journal of*
1873 *Physiology-Lung Cellular and Molecular Physiology*, 279, L1005-L1028.
- 1874 Torres OA, Palencia E, de Pratdesaba LL, Grajeda R, Fuentes M, Speer MC, Merrill Jr AH, O'Donnell
1875 K, Bacon CW & Glenn AE 2007. Estimated fumonisin exposure in Guatemala is greatest in consumers
1876 of lowland maize. *The Journal of nutrition*, 137, 2723-2729.

- 1877 Treiber T, Treiber N & Meister G 2019. Regulation of microRNA biogenesis and its crosstalk with
1878 other cellular pathways. *Nature Reviews Molecular Cell Biology*, 20, 5-20.
- 1879 Tsai M-C, Manor O, Wan Y, Mosammamarast N, Wang JK, Lan F, Shi Y, Segal E & Chang HY 2010.
1880 Long noncoding RNA as modular scaffold of histone modification complexes. *Science (New York,*
1881 *N.Y.)*, 329, 689-693.
- 1882 Ueda M & Seki M 2020. Histone Modifications Form Epigenetic Regulatory Networks to Regulate
1883 Abiotic Stress Response. *Plant Physiology*, 182, 15-26.
- 1884 Verdone L, Agricola E, Caserta M & Di Mauro E 2006. Histone acetylation in gene regulation. *Briefings*
1885 *in Functional Genomics*, 5, 209-221.
- 1886 Vidigal JA & Ventura A 2015. The biological functions of miRNAs: lessons from in vivo studies.
1887 *Trends Cell Biol*, 25, 137-147.
- 1888 Villa R, Morey L, Raker VA, Buschbeck M, Gutierrez A, De Santis F, Corsaro M, Varas F, Bossi D,
1889 Minucci S, et al. 2006. The methyl-CpG binding protein MBD1 is required for PML-RAR α function.
1890 *Proceedings of the National Academy of Sciences*, 103, 1400-1405.
- 1891 von Meyenn F, Iurlaro M, Habibi E, Liu NQ, Salehzadeh-Yazdi A, Santos F, Petrini E, Milagre I, Yu
1892 M, Xie Z, et al. 2016. Impairment of DNA Methylation Maintenance Is the Main Cause of Global
1893 Demethylation in Naive Embryonic Stem Cells. *Molecular cell*, 62, 848-861.
- 1894 Voss KA, Smith GW & Haschek WM 2007. Fumonisin: Toxicokinetics, mechanism of action and
1895 toxicity. *Animal Feed Science and Technology*, 137, 299-325.
- 1896 Voss TC & Hager GL 2014. Dynamic regulation of transcriptional states by chromatin and transcription
1897 factors. *Nat Rev Genet*, 15, 69-81.
- 1898 Waddington CH 1956. Embryology, Epigenetics and Biogenetics. *Nature*, 177, 1241-1241. Wahid F,
1899 Shehzad A, Khan T & Kim YY 2010. MicroRNAs: Synthesis, mechanism, function, and recent clinical
1900 trials. *Biochimica et Biophysica Acta (BBA) - Molecular Cell Research*, 1803, 1231-1243.
- 1901 Wang E, Norred WP, Bacon CW, Riley RT & Merrill AH, Jr. 1991. Inhibition of sphingolipid
1902 biosynthesis by fumonisins. Implications for diseases associated with *Fusarium moniliforme*. *J Biol*
1903 *Chem*, 266, 14486-14490.
- 1904 Wang J, Samuels DC, Zhao S, Xiang Y, Zhao YY & Guo Y 2017a. Current Research on Non-Coding
1905 Ribonucleic Acid (RNA). *Genes (Basel)*, 8.
- 1906 Wang J, Ishfaq M, Xu L, Xia C, Chen C & Li J 2019. METTL3/m(6)A/miRNA-873-5p Attenuated
1907 Oxidative Stress and Apoptosis in Colistin-Induced Kidney Injury by Modulating Keap1/Nrf2 Pathway.
1908 *Front Pharmacol*, 10, 517-517.
- 1909 Wang KC & Chang HY 2011. Molecular mechanisms of long noncoding RNAs. *Molecular cell*, 43,
1910 904-914.
- 1911 Wang X-N, Zhang L-H, Cui X-D, Wang M, Zhang G-Y & P.-L. Y. HOXA 11-AS is involved in fracture
1912 healing through regulating mir-1243 p. 2017b.
- 1913 Wang X, Lu Z, Gomez A, Hon GC, Yue Y, Han D, Fu Y, Parisien M, Dai Q, Jia G, et al. 2014a. N6-
1914 methyladenosine-dependent regulation of messenger RNA stability. *Nature*, 505, 117-120.
- 1915 Wang X, Feng J, Xue Y, Guan Z, Zhang D, Liu Z, Gong Z, Wang Q, Huang J, Tang C, et al. 2016.
1916 Structural basis of N(6)-adenosine methylation by the METTL3-METTL14 complex. *Nature*, 534, 575-
1917 578.
- 1918 Wang Y, Li Y, Toth JI, Petroski MD, Zhang Z & Zhao JC 2014b. N6-methyladenosine modification
1919 destabilizes developmental regulators in embryonic stem cells. *Nat Cell Biol*, 16, 191-198.
- 1920 Wei C, Zhao L, Liang H, Zhen Y & Han L 2020. Recent advances in unraveling the molecular
1921 mechanisms and functions of HOXA11-AS in human cancers and other diseases (Review). *Oncology*
1922 *reports*, 43, 1737-1754.

- 1923 Wei J-W, Huang K, Yang C & Kang C-S 2017. Non-coding RNAs as regulators in epigenetics
1924 (Review). *Oncol Rep*, 37, 3-9.
- 1925 Wen J, Lv R, Ma H, Shen H, He C, Wang J, Jiao F, Liu H, Yang P, Tan L, et al. 2018. Zc3h13 Regulates
1926 Nuclear RNA m(6)A Methylation and Mouse Embryonic Stem Cell Self-Renewal. *Molecular cell*, 69,
1927 1028-1038.e1026.
- 1928 Wightman B, Ha I & Ruvkun G 1993. Posttranscriptional regulation of the heterochronic gene lin-14
1929 by lin-4 mediates temporal pattern formation in *C. elegans*. *cell*, 75, 855-862.
- 1930 Woo YH & Li W-H 2012. Evolutionary conservation of histone modifications in mammals. *Mol Biol*
1931 *Evol*, 29, 1757-1767.
- 1932 Wu CS, Lu YJ, Li HP, Hsueh C, Lu CY, Leu YW, Liu HP, Lin KH, Hui-Ming Huang T & Chang YS
1933 2010. Glutamate receptor, ionotropic, kainate 2 silencing by DNA hypermethylation possesses tumor
1934 suppressor function in gastric cancer. *International journal of cancer*, 126, 2542-2552.
- 1935 Wu S, Lu H & Bai Y 2019. Nrf2 in cancers: A double-edged sword. *Cancer Med*, 8, 2252-2267.
- 1936 Xiao W, Adhikari S, Dahal U, Chen YS, Hao YJ, Sun BF, Sun HY, Li A, Ping XL, Lai WY, et al. 2016.
1937 Nuclear m(6)A Reader YTHDC1 Regulates mRNA Splicing. *Molecular cell*, 61, 507-519.
- 1938 Xie S, Wang Z, Okano M, Nogami M, Li Y, He WW, Okumura K & Li E 1999. Cloning, expression
1939 and chromosome locations of the human DNMT3 gene family. *Gene*, 236, 87-95.
- 1940 Yang B, Guo M, Herman JG & Clark DP 2003. Aberrant promoter methylation profiles of tumor
1941 suppressor genes in hepatocellular carcinoma. *The American journal of pathology*, 163, 1101-1107.
- 1942 Yang X, Liu M, Li M, Zhang S, Hiju H, Sun J, Mao Z, Zheng M & Feng B 2020. Epigenetic modulations
1943 of noncoding RNA: a novel dimension of Cancer biology. *Molecular Cancer*, 19, 64.
- 1944 Yu W, Peng W, Jiang H, Sha H & Li J 2017. LncRNA HOXA11-AS promotes proliferation and
1945 invasion by targeting miR-124 in human non-small cell lung cancer cells. *Tumour Biol*, 39,
1946 1010428317721440.
- 1947 Yue Y, Liu J & He C 2015. RNA N6-methyladenosine methylation in post-transcriptional gene
1948 expression regulation. *Genes Dev*, 29, 1343-1355.
- 1949 Zaccara S, Ries RJ & Jaffrey SR 2019. Reading, writing and erasing mRNA methylation. *Nat Rev Mol*
1950 *Cell Biol*, 20, 608-624.
- 1951 Zamudio NM, Scott HS, Wolski K, Lo C-Y, Law C, Leong D, Kinkel SA, Chong S, Jolley D, Smyth
1952 GK, et al. 2011. DNMT3L Is a Regulator of X Chromosome Compaction and Post-Meiotic Gene
1953 Transcription. *PLOS ONE*, 6, e18276.
- 1954 Zamurrad S, Hatch HA, Drelon C, Belalcazar HM & Secombe J 2018. A *Drosophila* model of
1955 intellectual disability caused by mutations in the histone demethylase KDM5. *Cell reports*, 22, 2359-
1956 2369.
- 1957 Zhang B, Zheng H, Huang B, Li W, Xiang Y, Peng X, Ming J, Wu X, Zhang Y & Xu Q 2016. Allelic
1958 reprogramming of the histone modification H3K4me3 in early mammalian development. *Nature*, 537,
1959 553-557.
- 1960 Zhang C, Fu J & Zhou Y 2019. A Review in Research Progress Concerning m6A Methylation and
1961 Immunoregulation. *Front Immunol*, 10, 922.
- 1962 Zhang G-L, Sun X-F, Feng Y-Z, Li B, Li Y-P, Yang F, Nyachoti CM, Shen W, Sun S-D & Li L 2017.
1963 Zearalenone exposure impairs ovarian primordial follicle formation via down-regulation of Lhx8
1964 expression in vitro. *Toxicol Appl Pharmacol*, 317, 33-40.
- 1965 Zhao T, Wang J, Shen L-J, Long C-L, Liu B, Wei Y, Han L-D, Wei Y-X & Wei G-H 2020. Increased
1966 m6A RNA modification is related to the inhibition of the Nrf2-mediated antioxidant response in di-(2-
1967 ethylhexyl) phthalate-induced prepubertal testicular injury. *Environmental Pollution*, 259, 113911.

1968 Zhao X, Li X, Zhou L, Ni J, Yan W, Ma R, Wu J, Feng J & Chen P 2018. LncRNA HOXA11-AS drives
1969 cisplatin resistance of human LUAD cells via modulating miR-454-3p/Stat3. *Cancer Sci*, 109, 3068-
1970 3079.

1971 Zhao Z & Shilatifard A 2019. Epigenetic modifications of histones in cancer. *Genome Biology*, 20, 245.

1972 Zheng G, Dahl JA, Niu Y, Fedorcsak P, Huang C-M, Li CJ, Vågbø CB, Shi Y, Wang W-L, Song S-H,
1973 et al. 2013. ALKBH5 is a mammalian RNA demethylase that impacts RNA metabolism and mouse
1974 fertility. *Molecular cell*, 49, 18-29.

1975 Zhengchang W, Chao X, Haifei W, Song G, Shenglong W & Wenbin B 2020. Transcriptome-wide
1976 assessment of the m6A methylome of intestinal porcine epithelial cells treated with deoxynivalenol.
1977 *Research Square*.

1978 Zhou B-BS & Elledge SJ 2000. The DNA damage response: putting checkpoints in perspective. *Nature*,
1979 408, 433-439.

1980 Zhou Y, He F, Pu W, Gu X, Wang J & Su Z 2020. The Impact of DNA Methylation Dynamics on the
1981 Mutation Rate During Human Germline Development. *G3: Genes/Genomes/Genetics*, 10, 3337-3346.

1982 Zhu C-C, Zhang Y, Duan X, Han J & Sun S-C 2016. Toxic effects of HT-2 toxin on mouse oocytes and
1983 its possible mechanisms. *Archives of toxicology*, 90, 1495-1505.

1984

1985

1986

1987

1988

1989

1990

1991

1992

1993

1994

1995

1996

1997

1998

1999

2000

2001

2002

2003

2004

2005 **CHAPTER 3**

2006 **Molecular and Epigenetic Modes of FB₁ Mediated Toxicity and Carcinogenesis and**
2007 **Detoxification Strategies**

2008 Thilona Arumugam, Terisha Ghazi, Anil A Chuturgoon*

2009 Discipline of Medical Biochemistry, School of Laboratory Medicine and Medical Sciences, University
2010 of KwaZulu-Natal, Durban, KwaZulu-Natal, South Africa

2011 Corresponding author:

2012 Professor Anil A. Chuturgoon,

2013 Discipline of Medical Biochemistry and Chemical Pathology,

2014 School of Laboratory Medicine and Medical Sciences

2015 College of Health Sciences

2016 George Campbell Building, Howard College, University of KwaZulu-Natal, Durban, 4041, South
2017 Africa. Telephone: +27312604404. Email: chutur@ukzn.ac.za

2018

2019 ORCIDs:

2020 TA: <https://orcid.org/0000-0002-1791-8219>

2021 TG: <https://orcid.org/0000-0002-0179-213X>

2022 AAC: <https://orcid.org/0000-0003-4649-4133>

2023

2024 **Critical Reviews in Toxicology (*In Review*).**

2025 Manuscript ID: BTXC-2020-0101.

2026

2027

2028

2029

2030

2031

2032

2033

2034 **Abstract**

2035 Fumonisin B₁ (FB₁) is a natural contaminant of agricultural commodities that has displayed a myriad
2036 of toxicities in animals and humans. Moreover, it is known to be a hepatorenal carcinogen in rodents
2037 and may be associated with oesophageal and hepatocellular carcinomas in humans. The most well
2038 elucidated mode of FB₁-mediated toxicity is its disruption of sphingolipid metabolism; however,
2039 enhanced oxidative stress, endoplasmic reticulum stress, autophagy and alterations in immune response
2040 may also play a role in its toxicity and carcinogenicity. Alterations to the host epigenome may impact
2041 on the toxic and carcinogenic response to FB₁. Seeing that the contamination of FB₁ in food poses a
2042 considerable risk to human and animal health, a great deal of research has focused on new methods to
2043 prevent and attenuate FB₁-induced toxic consequences. The focus of the present review is on the
2044 molecular and epigenetic interactions of FB₁ as well as recent research involving FB₁ detoxification.

2045 **Key Words**

2046 Fusarium, Mycotoxins, Fumonisin B₁, Toxicity, Oxidative Stress, ER Stress, Immunotoxicity,
2047 Epigenetics, Mycotoxin Detoxification

2048 **Introduction**

2049 Fumonisin are a ubiquitous group of secondary fungal metabolites (mycotoxins) which are produced
2050 by the *Fusarium* genus, particularly *F. verticillioides* and *F. Proliferatum* (Rheeder et al., 2002). The
2051 discovery of fumonisins were prompted by a field outbreak of equine leukoencephalomalacia (ELEM)
2052 in 1970, South Africa. After extensive research it was concluded that the causative agent of this neurotic
2053 disease was associated with mouldy maize that was predominately contaminated with *F. verticillioides*
2054 (formally, *F. moniliforme*) (Kellerman et al., 1972). Almost a decade later, *F. verticillioides*
2055 contaminated maize was found to be linked with the high incidence of oesophageal cancer in South
2056 Africa's former Transkei region, where maize is a dietary staple (Marasas et al., 1981). Experimental
2057 studies also showed that *F. verticillioides* induced ELEM in horses as well as pulmonary oedema in
2058 swine (Kriek et al., 1981a). In rats, the fungi were found to be hepatotoxic, cardiotoxic and induced
2059 primary hepatocellular carcinomas and cholangiocarcinoma (Kriek et al., 1981b, Marasas, 2001).
2060 Several mycotoxins were identified to be metabolites of *F. verticillioides*, but the causative agent of
2061 these incidents remained elusive until fumonisins were finally isolated and characterized in 1988
2062 (Gelderblom et al., 1988b).

2063 Since then, at least 28 fumonisins have been identified and grouped into one of four classes (A, B, C
2064 and P) of which fumonisin B₁ (FB₁) is regarded as the most abundant and toxicologically relevant
2065 homologue (Rheeder et al., 2002). FB₁ persistently contaminates the food supply of both animals and
2066 humans across the world. Maize and maize-based products are one of the most common foods infected
2067 by FB₁ (Lee and Ryu, 2017). It is also found in abundance in other cereals such as wheat, rice, oats,
2068 barley, and millet (Lee and Ryu, 2017), and has been reported to contaminate numerous food products

2069 including vine fruit (Varga et al., 2010), asparagus (Waskiewicz et al., 2010), beers (Piacentini et al.,
2070 2017), and milk (Gazzotti et al., 2009). FB₁ contamination of crops can occur pre- and/or post-harvest,
2071 making it difficult to control contamination. Factors favouring *Fusarium* growth and FB₁ production
2072 include heat stress, insect damage, and high humidity (Ferrigo et al., 2016). Furthermore, improper
2073 storage conditions that are not moisture and temperature-controlled account for a large amount of FB₁
2074 contamination (Phokane et al., 2019). Due to regional climatic variations, the Americas have the highest
2075 incidence of FB₁ contamination (96%), followed by Africa and Asia (62%) (Lee and Ryu, 2017).
2076 Moreover, the rise in average temperatures and humidity due to climate change may potentially give
2077 rise to increased levels of FB₁ in agricultural products. It is expected that additional regions may begin
2078 to experience issues with FB₁ contamination while countries with existing FB₁ contamination may
2079 expect higher levels in their crops (Magan et al., 2011).

2080 Developed countries have set federal regulations to limit FB₁ contamination of foods and feeds. For
2081 example, the United States Food and Drug Administration set the maximum tolerable limit for FB₁ in
2082 maize products at 2 ppm while the European Union regulation of FB₁ levels in maize is 1 ppm (Wild
2083 and Gong, 2010). In 2000, the Scientific Committee on Food established a maximum daily intake of
2084 0.2 mg/kg body weight (bw) based on no observed adverse effects in the liver and kidneys of rodents.
2085 Later, the limit was expanded to include FB₂ and FB₃. The Joint FAO-WHO Expert Committee
2086 (JECFA) has also declared that the provisional maximum tolerable intake of FB₁ alone or in
2087 combination with FB₂ and FB₃ should be 2 µg/kg bw/day (FOA/WHO, 2002), however, in developing
2088 countries where maize is a dietary staple, intake far exceeds the recommended maximum daily limits.
2089 FB₁ intake can range from 2.87–8.14 µg/kg bw/day in Eastern Cape, South Africa (van der Westhuizen
2090 et al., 2011); 3.5-15.6 µg/kg bw/day in Guatemala (Torres et al., 2007); 0.1-26 µg/kg bw/day in
2091 Tanzanian children (Kimanya et al., 2009); and can reach as high as 10,541.6 µg/kg bw/day in Fusui,
2092 China (Sun et al., 2011).

2093 FB₁ contamination is especially prominent in rural areas where subsistence farming is common
2094 (Shephard et al., 2019). Most subsistence farmers do not have the resources to implement the same
2095 agronomic practices seen in commercial settings. Lack of pest control and crop rotation, use of untreated
2096 seeds from previous seasons, maize monoculture, poor sorting and inadequate storage conditions, and
2097 general lack of mycotoxin awareness can exacerbate the incidence of fungal infection and FB₁
2098 production in crops (Mboya and Kolanisi, 2014, Alberts et al., 2019, Phokane et al., 2019). FB₁-related
2099 adverse health conditions are especially common in rural areas that depend on “homegrown” crops.
2100 Areas along the Mexican-American borders have reported that maternal consumption of maize and
2101 maize products contaminated with FB₁ during gestation was related to an increased risk of their
2102 offspring developing neural tube defects (NTD) such as spinal bifida and anencephaly with extremely
2103 high exposure leading to foetal death (Hendricks, 1999, Missmer et al., 2006). In rural Tanzania,
2104 infantile exposure to FB₁ contributes to the high growth impairment and developmental issues (Shirima

2105 et al., 2015, Chen et al., 2018). Outbreaks of acute toxicosis presenting with transient abdominal pain,
 2106 borborygmus, and diarrhoea were reported in South India after the consumption of bread made from
 2107 FB₁-contaminated sorghum and corn (Reddy and Raghavender, 2008). In addition to the 1981 cohort,
 2108 several other epidemiological studies have demonstrated a close link between the high incidence of
 2109 oesophageal carcinomas and FB₁ (Sydenham et al., 1990, Yoshizawa et al., 1994, Wang et al., 2000,
 2110 Qiu et al., 2001, Sun et al., 2007, Alizadeh et al., 2012). A Chinese cohort also found that FB₁ may be
 2111 linked with a high incidence of hepatocellular carcinomas (Sun et al., 2007). While FB₁ exposure is a
 2112 suspected contributing factor for carcinogenesis in humans; FB₁ has both cancer initiating and
 2113 promoting effects in animal models (Table 3.1). The type of tumour present in these models are both
 2114 sex and species dependent. After evaluating published epidemiological studies and experimental models
 2115 that demonstrated a link between FB₁ consumption and cancer occurrence, the International Agency for
 2116 Research on Cancer (IARC) concluded that there was enough evidence to classify FB₁ as a class 2B
 2117 carcinogen (IARC, 2002).

2118 The carcinogenic character of fumonisins is not fully understood; however, it has been hypothesized
 2119 that tumour development could be a result of FB₁ mimicking genotoxic carcinogens by inducing toxicity
 2120 resulting in compensatory proliferation and survival (Ramljak et al., 2000). The primary mode in which
 2121 FB₁ induces toxicity is through the disruption of sphingolipid metabolism which can trigger or
 2122 potentiate a host of toxic responses such as oxidative stress, endoplasmic reticulum (ER) stress,
 2123 autophagy, and alterations in immune responses. Furthermore, FB₁ can mediate changes in the
 2124 epigenome, altering the expression of cancer-related genes (Chuturgoon et al., 2014b, Demirel et al.,
 2125 2015). Therefore, this review focuses on the molecular and epigenetic modes of action involved in FB₁
 2126 toxicity and carcinogenicity with emphasis on recent findings. Furthermore, we discuss new strategies
 2127 related to the detoxification of this harmful mycotoxin.

2128 **Table 3.1: Studies evaluating the development of neoplastic lesions in *in vivo* models exposed to**
 2129 ***F. verticillioides* and/or FB₁**

Model	Target organ	Summary and Findings	Reference
Male BDIX Rats	Liver	In a life-long feeding experiment, BDIX rats were fed diets containing 4% culture of <i>F. moniliforme</i> . 80% of rats fed diets containing culture material developed hepatocellular carcinomas; while 63% developed ductular carcinomas. The incidence of both carcinomas increased with increased exposure time and the two distinctive tumours often developed concurrently in the same liver.	(Marasas et al., 1984)

Male F344 Rats	Liver	F344 rats were fed maize naturally contaminated with <i>F. moniliforme</i> (MRC 826) for 123 to 176 days. Three distinct lesions: neoplastic nodules, adenofibrosis and cholangiocarcinomas were observed in the liver of all rats in the treatment group.	(Wilson et al., 1985)
Male BD IX Rats	Liver	The cancer-promoting activity of FB ₁ isolated from <i>F. moniliforme</i> (MRC 826) was evaluated. FB ₁ (0.1%) was incorporated into the diet of male rats where cancer was initiated with DEN or not for 4-weeks. There was a marked increase in the formation of GGT ⁺ foci in both DEN-initiated and non-initiated groups. After 33 days, proliferation and fibrosis of bile ducts were also observed.	(Gelderblom et al., 1988a)
Male BD IX Rats	Liver	Progression of lesions were assessed at 6, 12 and 24 months in male BD IX rats fed a corn-based diet containing 50 mg/kg of purified FB ₁ isolated from <i>F. moniliforme</i> (MRC 826). All FB ₁ -fed rats developed regenerative nodules which manifested characteristics of preneoplastic nodules with 93.3% developing cholangiofibrosis. All rats that survived to the terminal end of the study developed cirrhosis and hepatocellular carcinomas. Neoplasms metastasized in the heart and lung in 2 of the rats and in the kidney for one of them.	(Gelderblom et al., 1991)
Male Fischer Rats	Liver	Varying concentrations of FB ₁ -containing diets (0-500 mg FB ₁ /kg) were fed to DEN-initiated rats for 21 days. The number of GGT ⁺ foci were increased in livers of rats fed 100 mg/kg FB ₁ and greater. Marked increases in number and size of GSTP ⁺ foci were present in livers fed 50 mg/kg and higher. The cancer-promoting activity of FB ₁ was associated with an inhibitory effect on PH-induced regenerative hepatocyte proliferation.	(Gelderblom et al., 1996)
B6C3F ₁ Mice and F344 Rats	Liver and Kidney	Doses of FB ₁ were administered to male (0-150 mg/kg diet) and female (0-80 mg/kg diet) mice as well as male (0-150 mg/kg diet) and female (0-100 mg/kg diet) rats for 104 weeks.	(Howard et al., 1999)

		<p>Mice: Significant tumour incidence was only detected in female mice. At 50 ppm FB₁, 40.4% of the mice had either adenomas or carcinomas, while at 80 ppm FB₁, 86.7% of the mice had either adenomas or carcinomas.</p> <p>Rats: There was no significant FB₁ tumour development in female F344 rats. 4.2% and 14.6% of male F344 fed 50 ppm and 150 ppm developed renal tubule adenomas while 10.4% and 20.8% fed 50 ppm and 150 ppm developed renal tubule carcinomas. Increased renal tubule apoptosis and hyperplasia occurred in livers with lesions.</p>	
B6C3F ₁ Mice and F344 Rats	Liver and Kidney	<p>Doses of FB₁ were administered to male (0-150 ppm) and female (0-80 ppm) mice and male (0-150 ppm) and female (0-100 ppm) rats for 104 weeks.</p> <p>Mice: Hepatocellular adenomas were present in 36.3% (50 ppm FB₁) and 73.7% (80 ppm FB₁) of female B6C3F₁ mice. Hepatocellular carcinomas were also present in 22.5% (50 ppm FB₁) and 23% (80 ppm FB₁) of female mice. Adenomas and carcinomas were also evident in the lower concentration but were not statistically significant. FB₁ did not affect the incidence of neoplasia in male mice.</p> <p>Rats: There was no significant FB₁ tumour development in female F344 rats, while their male counterparts groups dosed with higher concentrations of FB₁ developed renal tubule carcinomas, with 38.1% of rats dosed with 150 ppm developing either adenomas or carcinomas.</p>	(Howard et al., 2001)
B6C3F ₁ Mice and F344 Rats	Liver and Kidneys	<p>Male and female F344 rats and B6C3F₁ mice were fed diets containing 0–150 ppm FB₁ for 104 weeks.</p> <p>Mice: FB₁ increased the incidence of hepatocellular adenomas and carcinomas with 88% of female mice fed 80 ppm FB₁ developing either lesion. Carcinomas were locally invasive and metastatic.</p> <p>Rats: Tumour incidence in female rats was unaffected by FB₁; however, there was a dose-dependent rise in the incidence of renal tumours in males. Renal tubule adenomas</p>	(Voss et al., 2002)

		or carcinomas were present in 26% and 38% of male rats fed 50 ppm and 150 ppm, respectively.	
F344 Rats	Kidney	A 2-year carcinogenicity bioassay was conducted on male and female F344 rats fed 0-150 ppm and 0-100 ppm FB ₁ , respectively. Nephrotoxicity manifested in a dose-dependent manner. FB ₁ induced proximal tubule loss and sustained regeneration which is a risk factor for tumour development. In males, renal tubule tumours were observed at 100 (21%) and 150 (33%) ppm. Atypical tubule hyperplasia, a preneoplastic lesion were found in 8% and 19% of these 2 groups. Tumour development in female rats was statistically insignificant. Furthermore, there was a correlation between proliferative lesions and nephrotoxicity.	(Hard et al., 2001)
Male F344 Rats	Liver	The separate and combined effects of FB ₁ and AFB ₁ on the cancer initiation and promotion in hepatocarcinogenesis were evaluated in rats. There was a significant increase in the number of large GSTP ⁺ lesions in AFB ₁ and FB ₁ -treated rats subjected to PH promoting treatment. The induction of GSTP ⁺ lesions was also significantly enhanced in rats treated either with AFB ₁ or FB ₁ without the 2-AAF/PH promoting stimuli. The underlying mechanism that resulted in the significant increase in the size of GSTP ⁺ foci and nodules during the successive AFB ₁ /FB ₁ treatment regimen could be ascribed to the potent cancer promoting potential of FB ₁ .	(Gelderblom et al., 2002)
F344 Rats	Liver	Male F344 mice were fed diets of AFB ₁ (150 µg/kg), FB ₁ (250 mg/kg) or AFB ₁ and FB ₁ sequentially. GSTP ⁺ preneoplastic hepatic foci were evaluated after 8 weeks. The number and mean size of GSTP ⁺ foci were higher in the AFB ₁ -only group than that of the FB ₁ -only treated group. Sequential treatment markedly and significantly increased the number and size of GSTP ⁺ foci by approximately 7-fold and 12-fold as compared to the AFB ₁ or FB ₁ only treatment groups, respectively. This indicates that there is a synergistic	(Qian et al., 2016)

		effect by sequential treatment on preneoplastic foci induction.	
--	--	---	--

2130 *DEN: Diethylnitrosamine; GGT⁺: gamma-glutamyl-transpeptidase-positive; GSTP⁺: glutathione-S-transferase-*
 2131 *positive; PH: partial hepatectomy; AFB₁: aflatoxin B₁; 2-AAF/PH: 2-acetylaminofluorene/partial hepatectomy*

2132 **Overview of literature search**

2133 We performed a systematic search of published research studies pertaining to the molecular and
 2134 epigenetic modes of FB₁-induced toxicity and carcinogenicity. We further identified recent studies that
 2135 assessed strategies to reduce and detoxify FB₁ contaminated foods and feeds. To identify eligible studies
 2136 for this review, the following academic databases and search engines were used: Pubmed, Google
 2137 scholar and Europe PMC. Keywords searched included a combination of fumonisin b₁, toxicity, cancer,
 2138 sphingolipid metabolism, oxidative stress, endoplasmic reticulum stress, autophagy, immunotoxicity,
 2139 epigenetics, DNA methylation, histone modifications, microRNA, and detoxification. Moreover, we
 2140 used the bibliography of papers obtained using the above-mentioned database to identify additional
 2141 studies. Articles eligible for inclusion in this review included original research studies and review
 2142 papers that reported an association between FB₁ exposure and negative health outcomes in animal
 2143 models as well as negative effects on cultures cells of human and animal origin. Additionally, we
 2144 included papers that assessed, developed or improved on methods (physical, chemical or biological)
 2145 that may possibly reduce FB₁ contamination of food and feeds or attenuate the effects of FB₁ exposure.
 2146 Only full text articles published in English in scientific journals with high peer-reviewing standards
 2147 were included. Following sourcing suitable literature, we assessed the quality of research based on the
 2148 scientific approach. This included assessing details of methods, validity and reliability of results and
 2149 accuracy of statistical analysis. The results from the relevant studies are included under the appropriate
 2150 sections which summarizes and analyses findings on the molecular and epigenetic aspects of FB₁
 2151 toxicity and as well as recent methods used to detoxify FB₁ contaminated foods and feed.

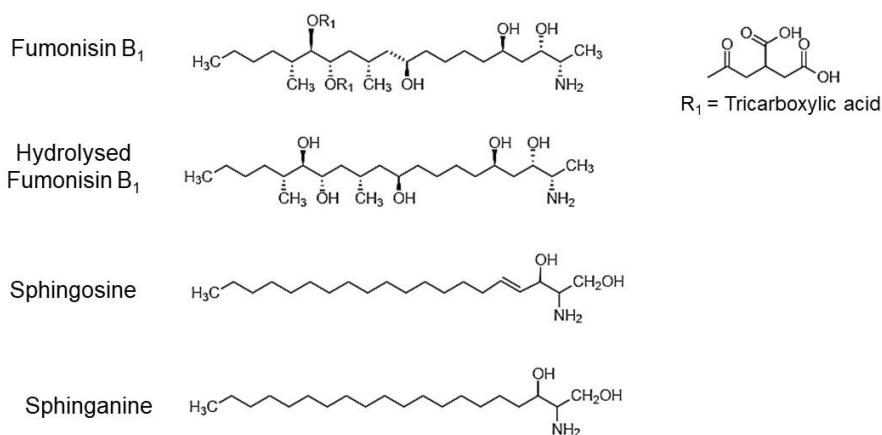
2152 **Disruption of Sphingolipid Metabolism**

2153 The disruption of sphingolipid metabolism has been identified as a key molecular mode of FB₁ toxicity.
 2154 Sphingolipids are abundant in all eukaryotic cells as they form major components of membranes,
 2155 lipoproteins, and other lipid-rich structures. They are critical in maintaining the fluidity and structure
 2156 of membranes and modulating the activity of receptors (Merrill, Schmelz et al. 1997). Bio-active
 2157 sphingolipids [ceramide, sphinganine (Sa), sphingosine (So) and their phosphorylated counterparts]
 2158 also mediate vital signalling pathways such as differentiation, cell cycle progression, proliferation, and
 2159 apoptosis (Merrill, Sullards et al. 2001). Thus, disruptions in sphingolipid metabolism can trigger a
 2160 chain of events leading to FB₁-altered cell growth, differentiation, and cell injury.

2161 The initiation of *de novo* sphingolipid synthesis occurs in the ER where, serine palmitoyltransferase
 2162 (SPT) catalyses the condensation of serine and palmitoyl Coenzyme A (palmitoyl CoA) to form 3-

2163 ketosphinganine; which is subsequently reduced to Sa (Futerman and Riezman, 2005). Sa is either
 2164 phosphorylated by sphingosine kinase to form sphinganine-1-phosphate (Sa1p) or acylated to form
 2165 dihydroceramide by ceramide synthase (CS). Dihydroceramide is desaturated to ceramide, which can
 2166 then be converted to complex sphingolipids such as glycosphingolipids and sphingomyelin (Futerman
 2167 and Riezman, 2005). CS is also responsible for reacylation of So to ceramide via the sphingolipid
 2168 salvage pathway (Kitatani et al., 2008).

2169 FB₁ and its hydrolysed form (HFB₁) bare close structural resemblance to the aminopentol backbone of
 2170 sphingoid bases (Figure 3.1). Due to this similarity, CS recognizes the amino group of FB₁ and HFB₁
 2171 as a substrate and allows it to compete with sphingoid bases for the same binding site (Wang et al.,
 2172 1991). CS is also able to recognize the tricarboxylic acid side chain of FB₁ as an analogue of fatty acyl
 2173 CoA and can thus obstruct the fatty acyl-CoA binding site of CS (Wang et al., 1991). *In vitro* assessment
 2174 showed that FB₁ blocks the incorporation of serine into the So backbone, completely inhibits the
 2175 formation of sphingolipids and depletes the total mass of cellular sphingolipids (Wang et al., 1991, Yoo
 2176 et al., 1992, Merrill et al., 1993). Accumulation of free sphingoid bases and their phosphorylated
 2177 counterparts are evident in affected tissues, serum, and urine of animals exposed to contaminated feed
 2178 [summarised by Riley et al. (2001)].



2179
 2180 **Figure 3.1.** The molecular structure of FB₁, HFB₁ and the sphingoid bases, Sa and So. The aminopentol
 2181 backbone of FB₁ and HFB₁ bare close structural resemblance to that of Sa and So.

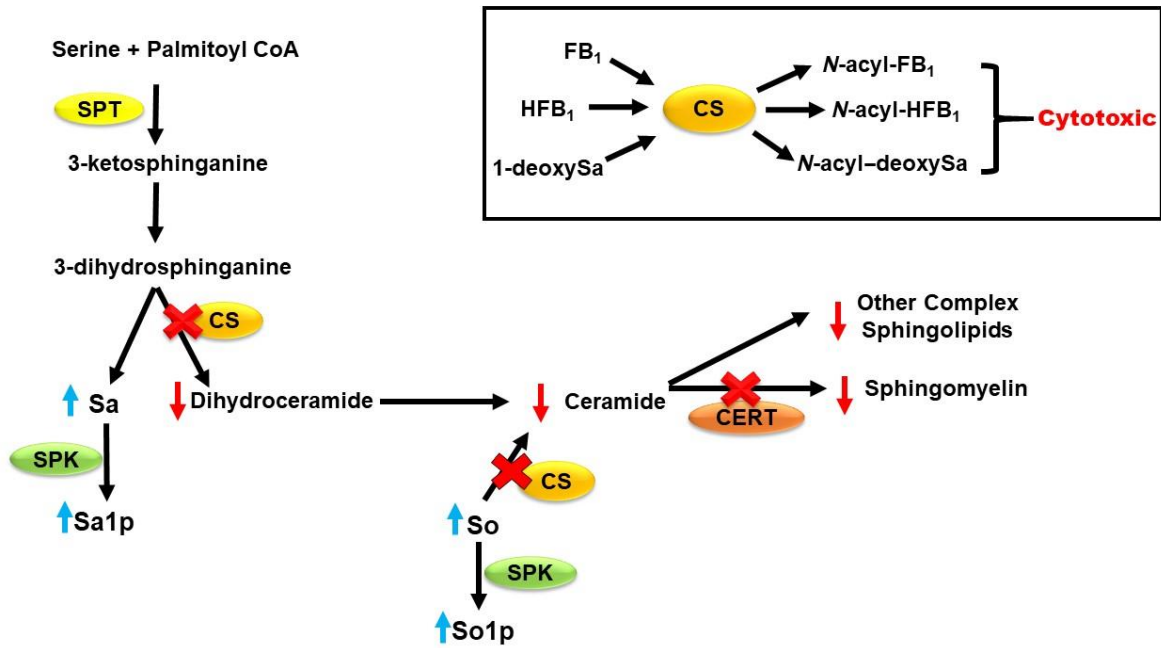
2182 HFB₁ is considered a weak disruptor of sphingolipid metabolism and is not as toxic in comparison to
 2183 FB₁. The lack of tricarboxylic acid side chains reduces the potency of HFB₁ as a ceramide synthase
 2184 inhibitor by almost 10-fold (Howard et al., 2002, Collins et al., 2006, Hahn et al., 2015, Harrer et al.,
 2185 2015). Rats fed hydrolysed *Fusarium* culture material containing hydrolysed fumonisins but not FB₁
 2186 presented with liver and kidney lesions and demonstrated hepatic tumour promoting activity (Hendrich

2187 et al., 1993, Voss et al., 1996). In contrast, studies on pregnant rats have found no evidence of tissue
2188 lesions or changes in sphingoid bases (Collins et al., 2006); while studies in female mice fed HFB₁
2189 found no signs of hepatic lesions but altered sphingolipid metabolism was observed (Howard et al.,
2190 2002). A recent study found that exposure to HFB₁ or partially hydrolysed FB₁ (PHFB₁) did not affect
2191 Sa/So ratios and slightly increased the number of lesions observed in the kidney of exposed rats; while
2192 a significant increase in Sa/So ratios and number of lesions were observed in FB₁ exposed rats (Hahn
2193 et al., 2015). Regardless, HFB₁ can undergo acylation by CS to form cytotoxic *N*-acylated HFB₁
2194 metabolites (C_n-HFB₁). The type of metabolite produced is dependent on the isoform of CS and the acyl
2195 CoA chain used (Seiferlein et al., 2007). Humpf et al. (1998) found that the *N*-acyl derivative, *N*-
2196 palmitoyl-HFB₁ (C16-HFB₁) was only half as effective as FB₁ in inhibiting CS but caused significantly
2197 greater accumulation of Sa and toxicity in human colonic (HT-29) cells. Seiferlein et al. (2007) also
2198 investigated the impact *N*-acyl-HFB₁ derivatives; incubation of rat liver microsomes with HFB₁ and
2199 either nervonoyl-CoA or palmitoyl-CoA resulted in the formation of *N*-nervonoyl-HFB₁ (C24:1-HFB₁)
2200 and *N*-palmitoyl-HFB₁ (C16-HFB₁), respectively. *In vivo* assessment of these derivatives in HT-29 cells
2201 were undertaken to determine toxicity and its ability to inhibit CS. There was a 50% reduction in cell
2202 viability after a 24-hour treatment with 25 µM of C24:1-HFB₁ and C16-HFB₁. These results suggest
2203 that the *N*-acylated metabolites are more potent than FB₁ and HFB₁ in HT-29 cells (Schmelz et al.,
2204 1998, Seiferlein et al., 2007). Furthermore, just 1 µM of C24:1-HFB₁ and C16-HFB₁ inhibited CS
2205 activity by 30%, while up to 80% inhibition was observed at 10 µM (Seiferlein et al., 2007). An *in vitro*
2206 assessment showed that the most prevalent metabolites were the HFB₁-acyl compounds containing
2207 long-chain fatty acids (C24, C24:1, C22 and C20) in rats dosed with HFB₁ (52, 115 and 230 µg/day for
2208 5 days); however, gross and microscopic examinations of the liver and kidneys of these animals found
2209 no treatment-related alterations (Seiferlein et al., 2007). It has long been regarded that FB₁ is unable to
2210 undergo *N*-acylation due to its tricarboxylic acid side chains; however, *N*-acyl-FB₁ metabolites were
2211 recently discovered. Human fibroblasts, hepatoma (Hep3B), and embryonic kidney (HEK293) cells
2212 were treated with 20 µM of either FB₁ or HFB₁ for 24 hours; subsequently FB₁ metabolites were then
2213 quantified by HPLC-ESI-MS/MS. Similar to HFB₁, the *N*-acylation of FB₁ corresponded to the acyl
2214 chain specificity of each of the CS isoforms and the *N*-acyl-FB₁ metabolites were significantly more
2215 cytotoxic than FB₁ in cell culture (Harrer et al., 2013). The *in vivo* formation of *N*-acyl-FB₁ were tissue
2216 specific and depended on the dominant CS isoform. C₁₆ derivatives were dominant in the kidney and
2217 C₂₄ derivatives were more prevalent in the liver (Harrer et al., 2015). However, further investigation on
2218 *N*-acyl-FB₁ toxicity *in vivo* should be undertaken.

2219 Computational modelling has revealed that FB₁ disruption of sphingolipids goes beyond inhibition of
2220 CS. While ceramide synthesis occurs in the ER, the formation of the complex sphingolipid -
2221 sphingomyelin occurs in the Golgi apparatus (Futerman and Riezman, 2005). Ceramide transport
2222 protein (CERT) mediates the non-vesicular transport of ceramide from the ER to the Golgi via the

2223 steroidogenic acute regulatory protein-related lipid transfer (START) domain (Hanada et al., 2003).
2224 Through docking simulations, Dellafiora et al. (2018) demonstrated that *N*-acyl derivatives of HFB₁
2225 might fit the START binding site depending on the fatty acid chain length. *N*-capryl- and *N*-palmitoyl-
2226 HFB₁ might compete with ceramides for CERT-dependent ER-to-Golgi transport, although
2227 polar/hydrophobic mismatch may limit binding into the START pocket. Nevertheless, disruptions to
2228 CERT mediated ceramide transport may be a contributing factor in reduced sphingomyelin synthesis
2229 that is observed post FB₁ exposure (He et al., 2006). Dellafiora et al. (2018) also demonstrated that
2230 HFB₁ was able to fit the enzyme pocket of sphingosine kinase 1 (SPK1), the enzyme responsible for
2231 the conversion of So to sphingosine-1-phosphate (So1P) (Maceyka et al., 2002). The calculated fit of
2232 HFB₁ was similar to that calculated for known SPK1 inhibitors. This stimulation contradicted work
2233 done by He et al. (2006) and collaborators who observed an increase in SPK1 activity, and several other
2234 studies have demonstrated the accumulation of So1p and Sa1p during FB₁ exposure (Gelineau-van
2235 Waes et al., 2012, Riley et al., 2015a, Riley et al., 2015b, Gardner et al., 2016).

2236 FB₁ not only induces the accumulation of Sa, So and its phosphorylated counterparts, but also results
2237 in the accumulation of 1-deoxysphinganine (1-deoxySa). 1-deoxySa is formed when SPT utilizes
2238 alanine instead of serine in the initial steps of sphingolipid synthesis. *In vivo* and *in vitro* exposure to
2239 FB₁ results in the accumulation of this atypical sphingoid base. *In vitro* experimentation also revealed
2240 that the cytotoxicity of 1-deoxySa was greater than or equal to Sa (Zitomer et al., 2009). 1-DeoxySa
2241 can also undergo acylation by CS; however, these acylated derivatives are unable to produce complex
2242 sphingolipids and function as membrane disruptors (Jiménez-Rojo et al., 2014). In summary, the
2243 inhibition of CS by FB₁ and HFB₁ results in: 1. reduced levels of dihydroceramide, ceramide, and
2244 complex sphingolipids; 2. accumulation of sphingoid bases and phosphorylated sphingoid bases; 3.
2245 elevation in 1-deoxySa bases; and 4. the accumulation of cytotoxic *N*-acylated HFB₁/FB₁ metabolites
2246 (Figure 3.2). These changes result in several toxicologically relevant perturbations such as ER stress,
2247 accumulation of ROS, altered mitochondrial and immune functioning, and disruption to developmental
2248 regulation (Riley and Merrill, 2019). Furthermore, FB₁-induced alterations in sphingolipid signalling
2249 pathways will lead to altered rates of cell death and regeneration, which may play a major role in FB₁-
2250 mediated tumorigenesis via continuous compensatory regeneration of cells as a response to the
2251 apoptosis induced by FB₁ (Riley et al., 2001, Soriano et al., 2005).



2252

2253 **Figure 3.2.** An overview of the effect of FB₁ and its metabolites on sphingolipid metabolism. A)
 2254 Sphingolipid biosynthesis begins in the ER, where serine and palmitoyl-CoA are incorporated into 3-
 2255 ketosphinganine before sphinganine (Sa), followed by acylation to dihydroceramides by ceramide
 2256 synthase (CS). Likewise, 1-deoxysphinganine (1-deoxy-Sa) is made from alanine (not shown).
 2257 Dihydroceramide is desaturated to ceramide and subsequently incorporated into complex sphingolipids.
 2258 The formation of some complex sphingolipids such as sphingomyelin occurs in the golgi apparatus and
 2259 requires ceramide transport protein (CERT) mediated trafficking of ceramide. Sphingolipid degradation
 2260 occurs to release Sphingosine (So) and is recycled via CS phosphorylated by sphingosine kinase (SPK1)
 2261 to sphingosine-1-phosphate (So1p). SPK1 can also phosphorylate Sa to sphinganine-1-phosphate
 2262 (Sa1p). FB₁ and/or its metabolites disrupts sphingolipid metabolism by inhibiting CS and CERT,
 2263 altering levels of sphingolipid metabolites. The metabolites with the blue arrow are generally elevated
 2264 when CS is inhibited by FB₁ while the metabolites with the red arrow are reduced. B) FB₁, HFB₁ and
 2265 deoxy-1Sa act as substrates for CS, releasing cytotoxic N-acylated metabolites.

2266 **Oxidative Stress**

2267 Reactive oxygen species (ROS) are radical and nonradical derivatives of oxygen; formed predominantly
 2268 during normal aerobic respiration (Andreyev et al., 2005). Low basal levels of ROS mediate several
 2269 biological processes such as cell proliferation, apoptosis, cell cycle, phosphorylation of proteins,
 2270 activation of transcription factors and immune regulation (Pizzino et al., 2017). Contrarily, excessive
 2271 ROS levels and a diminished capacity of cells to detoxify excess ROS results in oxidative stress
 2272 (Phaniendra et al., 2015). This disturbance in redox homeostasis inflicts damage to macromolecules and
 2273 can trigger the onset or progression of diseases such as cancer, diabetes, metabolic disorders,
 2274 atherosclerosis, and cardiovascular diseases (Phaniendra et al., 2015, Pizzino et al., 2017).

2275 Mitochondria metabolize carbohydrates and fatty acids via the electron transport chain (ETC) to
2276 produce ATP. During this process, unpaired electrons leak into the mitochondrial matrix, where it
2277 reduces oxygen to form ROS (Ma, 2013). Unwarranted production of ROS from the ETC can be
2278 stimulated by several factors, such as the inhibition of complexes of the ETC (Bratic and Larsson,
2279 2013). Domijan and Abramov (2011) have reported that FB₁ inhibits complex I of the ETC. FB₁
2280 inhibited state 4 respiration in the presence of substrates for complex I. This resulted in the enhanced
2281 generation of mitochondrial ROS and subsequent mitochondrial depolarization. The activation of
2282 cytochrome P450 (CYP450) enzymes by FB₁ may also be a driving force in ROS production as seen in
2283 spleen mononuclear cells of Wistar rats and colonic tissue of ICR mice (Mary et al., 2012, Kim et al.,
2284 2018). Several other studies reported elevated levels of ROS after FB₁ exposure in rodent GT1-7
2285 hypothalamic cells, C6 glioblastoma, and spleen mononuclear cells as well as in human fibroblast, U-
2286 118MG glioblastoma, and HepG2 hepatocellular carcinoma cells (Galvano et al., 2002, Stockmann-
2287 Juvala et al., 2004a, Mary et al., 2012, Arumugam et al., 2019); with only one study showing that low
2288 doses of FB₁ had the opposite effect on ROS levels in human oesophageal carcinoma cells (SNO) (Khan
2289 et al., 2018).

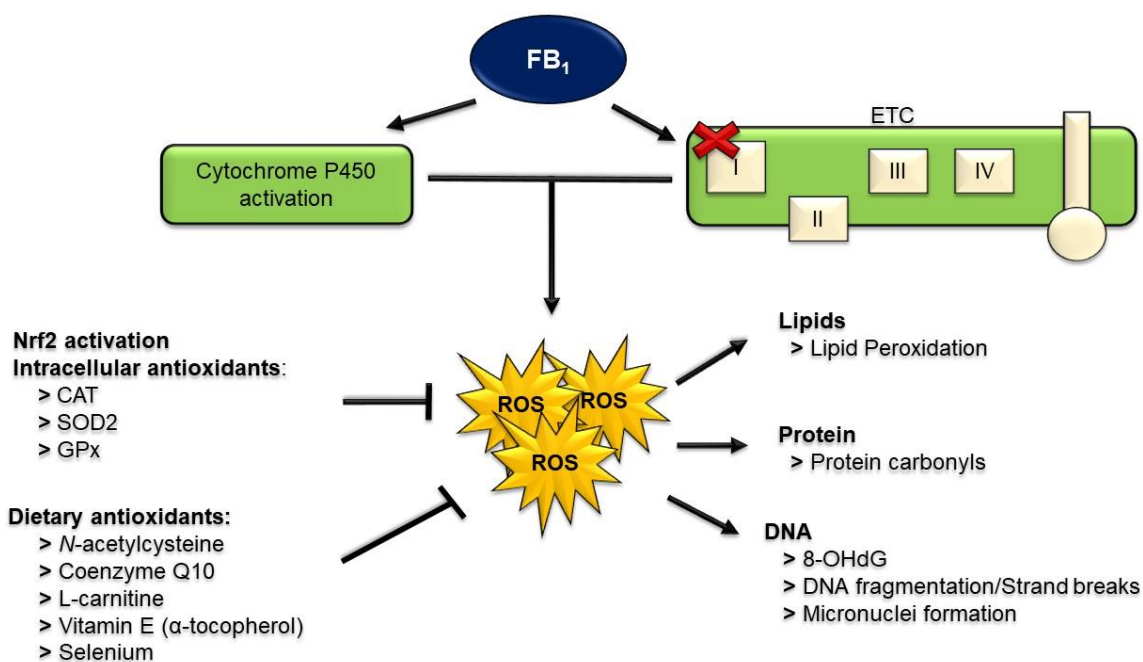
2290 A major consequence of ROS overproduction is oxidative injury to macromolecules and organelles
2291 (Phaniendra et al., 2015). Besides disrupting sphingolipid metabolism, FB₁ can indirectly disrupt lipid
2292 homeostasis through the oxidative degradation of lipids. Lipid peroxidation results in the formation of
2293 lipid peroxyl radicals that can accelerate the peroxidation of other unsaturated fatty acid moieties,
2294 disrupt membrane receptor signalling as well as membrane permeability (Ayala et al., 2014).
2295 Malondialdehyde (MDA), is a cytotoxic and tumorigenic by-product of lipid peroxidation that is often
2296 used as a biomarker in determining oxidative stress (Ayala et al., 2014). Varying concentrations and
2297 treatment periods showed that FB₁ is a potent inducer of lipid peroxidation and elevates MDA levels
2298 (Abado-Becognee et al., 1998, Mobio et al., 2003, Stockmann-Juvala et al., 2004b, Stockmann-Juvala
2299 et al., 2004a, Kouadio et al., 2005, Domijan et al., 2007a, Domijan et al., 2008, Theumer et al., 2010,
2300 Domijan and Abramov, 2011, Mary et al., 2012, Minervini et al., 2014, Hassan et al., 2015, Arumugam
2301 et al., 2019). Interestingly, SNO cells were more resistant to lipid peroxidation when exposed to low
2302 doses of FB₁ (Khan et al., 2018).

2303 A strong correlation between elevated ROS levels and structural damage to proteins in the form of
2304 protein carbonyls have also been made in the presence of FB₁ (Domijan et al., 2007a, Domijan et al.,
2305 2007b, Mary et al., 2012, Arumugam et al., 2019). HepG2 cells were extremely sensitive to FB₁ as
2306 indicated by the 11.9-fold increase in protein carbonyls (Arumugam et al., 2019). The carbonylation of
2307 proteins alters polypeptide confirmation which can impair protein functioning. This may have various
2308 downstream consequences such as disrupting signalling pathways, modifying enzyme activity, and
2309 impairing other protein functions including binding of transcription factors to DNA (Gonos et al., 2018).
2310 Moreover, protein carbonyls can inhibit proteasomal activity which is necessary for the degradation of

2311 carbonylated proteins. Thus, protein carbonylation can result in cellular dysfunction and eventually
2312 contribute to the aetiology and progression of disease states (Dalle-Donne et al., 2006).

2313 The threat of oxidative damage is particularly significant to nucleic acids. Elevated levels of ROS can
2314 induce strand breaks, protein-DNA crosslinking and has mutagenic potential (Loft et al., 2008). Several
2315 studies have demonstrated the genotoxic potential of FB₁ in humans and animals. With the use of the
2316 micronuclei test, Ehrlich et al. (2002), Theumer et al. (2010) and Karuna and Rao (2013) assessed
2317 genotoxic potential of FB₁. Micronuclei are formed when there are breakages in chromosomes or when
2318 spindle assembly is disturbed. A dose-dependent formation of micronuclei occurred in FB₁-exposed
2319 HepG2 cells (Ehrlich et al., 2002) and Wistar rats (Theumer et al., 2010). Conversely, FB₁ failed to
2320 induce micronuclei in BALB/C mice (Karuna and Rao, 2013). DNA strand breaks and fragmentation
2321 were studied *in vivo* and *in vitro*. These studies found that DNA fragmentation and strand breaks
2322 occurred as a consequence of FB₁-induced oxidative stress (Atroshi et al., 1999, Mobio et al., 2003,
2323 Stockmann-Juvala et al., 2004b, Theumer et al., 2010, Hassan et al., 2015). 8-hydroxy-deoxyguanosine
2324 (8-OHdG) is a predominant oxidative DNA lesion, and thus widely used as a critical biomarker for
2325 oxidative stress and carcinogenesis (Valavanidis et al., 2009). FB₁-mediated the oxidation of guanine
2326 in both *in vivo* and *in vitro* studies (Mobio et al., 2003, Mary et al., 2012, Arumugam et al., 2020). Only
2327 one study found that DNA damage occurred independent of ROS levels (Galvano et al., 2002)

2328 The detoxification capacity of cells is also affected by FB₁-induced ROS. Kelch-like ECH-associated
2329 protein 1 (Keap1)/Nuclear factor erythroid 2-related factor 2 (Nrf2) signalling pathway is activated in
2330 response to excess ROS production. Antioxidant defence depends on the disassociation of the
2331 antioxidant transcription factor, Nrf2, from Keap1 degradation. Surplus ROS alters Keap1 conformation
2332 and activates phosphorylation pathways which in turn phosphorylate Nrf2. These changes trigger the
2333 dissociation of Nrf2 from Keap1 degradation and promotes anti-oxidant transcription (Huang et al.,
2334 2002, Nguyen et al., 2009). In response to FB₁-induced ROS, HepG2 cells significantly upregulate
2335 phosphorylation of Nrf2 leading to the transcription of major antioxidants: superoxide dismutase 2
2336 (SOD2), catalase (CAT), and glutathione peroxidase (GPx) (Arumugam et al., 2019). Nrf2 was also
2337 activated in SNO cells but antioxidant expression did not correspond (Khan et al., 2018). Furthermore,
2338 FB₁ reduced antioxidant status in BALB/C mice, Wistar rats and bovine peripheral blood mononuclear
2339 cells (PBMC) exposed to FB₁ (Domijan et al., 2007a, Bernabucci et al., 2011, Abbès et al., 2016).
2340 However, subchronic exposure of Wistar rats with FB₁ boosted SOD2 and CAT activity (Theumer et
2341 al., 2010). The use of antioxidants is being investigated as a method to reduce FB₁ toxicity. Antioxidants
2342 such as *N*-acetylcysteine, coenzyme Q10, L-carnitine, vitamin E (α -tocopherol) and selenium were
2343 shown to attenuate FB₁-mediated oxidative stress and toxicity (Abel and Gelderblom, 1998, Atroshi et
2344 al., 1999, Zhang et al., 2018). In summary, FB₁ promotes ROS generation and alters antioxidant status,
2345 which results in oxidative injury to cells (Figure 3.3). The use of antioxidants may be a promising
2346 approach to minimize the effects of FB₁ on cellular redox status and subsequently cytotoxicity.



2347

2348 **Figure 3.3.** FB₁ disrupts redox homeostasis. High levels of ROS are generated through the activation
 2349 of cytochrome P450 enzymes and inhibition of the electron transport chain (ETC) by FB₁. Reduced
 2350 capacity of intracellular antioxidants to detoxify ROS leads to oxidative injury to lipids, protein and
 2351 DNA. The use of dietary antioxidants may normalize ROS levels.

2352 Endoplasmic Reticulum Stress and Autophagy

2353 The role of the ER is not exclusive to sphingolipid synthesis. It is a highly dynamic organelle
 2354 responsible for protein folding, free calcium storage, carbohydrate metabolism, synthesis of other lipids
 2355 and assembly of lipid bilayers (Koch, 1990, Stevens and Argon, 1999, Hebert and Molinari, 2007, Bravo
 2356 et al., 2013, Schwarz and Blower, 2016, Jacquemyn et al., 2017). The ER also has tissue-specific
 2357 functioning; liver ER contain cytochrome P450 enzymes that can metabolize and detoxify hydrophobic
 2358 drugs and carcinogens (Kwon et al., 2020); whereas in the muscle, specialized ER (sarcoplasmic
 2359 reticulum) regulate calcium flux to execute muscle contraction and relaxation (Guerrero-Hernandez et
 2360 al., 2010). Despite its dynamic role, the ER is sensitive to a multitude of intracellular and
 2361 microenvironmental changes. Cellular stressors such as imbalances in redox and calcium homeostasis
 2362 or defects in lipid metabolism or protein folding can cause unfolded or misfolded proteins to accumulate
 2363 in the ER. This phenomenon is known as ER stress (Senft and Ronai, 2015). The accumulation of
 2364 damaged proteins in the ER can lead to irreversible damage to cellular functioning and pose a threat to
 2365 cell survival. Fortunately, eukaryotes have developed several signalling mechanisms to sense and
 2366 ameliorate the effects of ER stress and restore ER homeostasis and functioning (Bravo et al., 2013).
 2367 Principal pathways involved in this response include the unfolded protein response (UPR), ER-
 2368 associated degradation (ERAD), autophagy, hypoxia signalling and mitochondrial biogenesis. These

2369 pathways work in concert to determine whether cells re-establish ER homeostasis or activate cell death
2370 mechanisms (Senft and Ronai, 2015).

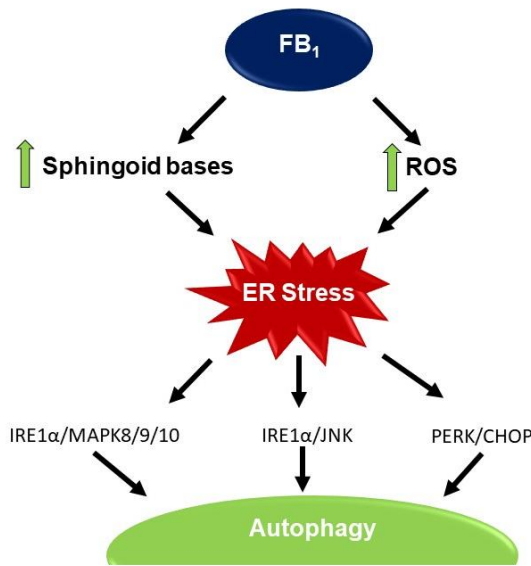
2371 In unstressed conditions, the master regulator – binding immunoglobulin protein (GRP78) sequesters and
2372 maintains UPR sensors in an inactive state. During UPR, the ER lumen binds to GRP78, releasing UPR
2373 sensors. Together, these sensors [protein kinase RNA-like endoplasmic reticulum kinase (PERK),
2374 activating transcription factor 6 (ATF6) and inositol-requiring protein 1 (IRE1 α)] and their respective
2375 transducers [activating transcription factor 4 (ATF4), cleaved ATF6, and X-Box Binding Protein 1
2376 (XBP1)] suppress protein translation and folding, facilitate ERAD to degrade misfolded proteins and
2377 mediate cell death and survival (Chakrabarti et al., 2011, Senft and Ronai, 2015). ER stress is also a
2378 potent trigger for autophagy, a self-degradative process that has both pro-survival and pro-apoptotic
2379 functioning (Yorimitsu et al., 2006, Glick et al., 2010). Both UPR signalling and autophagy are
2380 interconnected with the 3 canonical arms of UPR regulating autophagy during ER stress (Kouroku et
2381 al., 2007, Margariti et al., 2013, Li et al., 2014, Kabir et al., 2018).

2382 Several *in vivo* and *in vitro* investigations have revealed that FB₁ induces ER stress through the
2383 disruption of sphingolipid metabolism and subsequent accumulation of sphingoid bases and
2384 intracellular ROS (Yin et al., 2016, Singh and Chul, 2017, Kim et al., 2018, Liu et al., 2020, Yu et al.,
2385 2020). Autophagy was also observed in these studies; however, the activation and role of autophagy
2386 differed. FB₁-induced autophagy was first observed in MARC145 green monkey kidney cells. Yin et
2387 al. (2016) showed a dose-dependent increase in the phosphorylation and activation of ER stress markers
2388 [IRE1 α , eIF2AK2 and eIF2S1] after exposure to FB₁ for 48 hours. IRE1 α mediated mitogen-activated
2389 protein kinase 8/9/10 (MAPK8/9/10) autophagy in response to ER stress as numerous autophagic
2390 vacuoles and increased LC3 I/LC3 II conversion was observed. Inhibition of IRE1 α via RNA
2391 interference or chemical inhibition attenuated MAPK activity, LC3 conversion as well as autophagy
2392 confirming the role of IRE1 α /MAPK8/9/10 in FB₁-mediated autophagy (Yin et al., 2016).

2393 In colon tissue of male mice, both IRE1 α and PERK levels were upregulated after exposure to 2.5 mg/kg
2394 bw FB₁ for 24 to 96 hours. Rather than MAPK8//9/10 activation, IRE1 α activated JNK, which led to
2395 the subsequent elevation in autophagy markers (beclin, ATG5, ATG7) and LC3 I conversion in all FB₁
2396 treated mice (Kim et al., 2018). Most recently, Yu et al. (2020) found that human gastro-intestinal
2397 epithelial (GES-1) cells were also sensitive to FB₁-mediated ER stress autophagy via the PERK/CHOP
2398 pathway. All 3 of these studies reported that pro-death mediated autophagy and apoptosis occurred in
2399 response to FB₁ (Yin et al., 2016, Kim et al., 2018, Yu et al., 2020). With the use of the SPT inhibitor,
2400 myriocin in the presence of FB₁, levels of free sphingoid bases diminished which in turn reduced ER
2401 stress biomarkers and abolished FB₁-mediated autophagy apoptosis (Yin et al., 2016, Yu et al., 2020).
2402 This data strongly suggests that disruptions in sphingolipid metabolism is an essential event for FB₁ to
2403 trigger autophagic cell death.

2404 However, *in vitro* and *in vivo* assessment by Singh and Chul (2017) and Liu et al. (2020) proved that
2405 FB₁ mediated autophagy is a pro-survival mechanism in the liver. ER stress activated PKC, PERK and
2406 JNK, which lead to the activation of autophagy related gene 5 (ATG5), ATG7, and LC3 conversion.
2407 Mammalian target of rapamycin (mTOR) signalling was suppressed resulting in the dissociation of pro-
2408 autophagic Beclin from B-cell lymphoma 2 (Bcl2). Both research groups found that FB₁ mediated ER
2409 stress activated PERK and IRE1 α but concluded the main mechanism of autophagy was facilitated via
2410 the IRE1 α /JNK pathway. The pre-treatment of HepG2 cells with the autophagy inhibitor 3-
2411 methyladenine (3-MA) followed by FB₁ significantly reduced cell viability with respect to the control
2412 and individual treatment with 3-MA and FB₁. Only 20% loss in viability was observed after 24 hours,
2413 with proliferation occurring after 12 hours. The inhibition of autophagy using RNA interference led to
2414 increased cell death in mouse liver cells, while the autophagy inducer rapamycin protected the liver
2415 cells from FB₁-induced cell death. (Liu et al., 2020) Taken together, these results suggest that FB₁-
2416 mediated autophagy protects cells from hepatic injury (Singh and Chul, 2017, Liu et al., 2020).

2417 The difference in the role of autophagy can be explained by the type of cell (cancerous versus non-
2418 cancerous), duration of FB₁ exposure (acute versus prolonged), and the duration and extent of
2419 autophagy (Sun et al., 2013, Linder and Kögel, 2019). The extent and duration of autophagy may have
2420 been greater in kidney, gastric, and colon tissue. This could be due to the prolonged exposure to FB₁ in
2421 these cells in comparison to the acute exposure received by the liver. Furthermore, the HepG2 cell line
2422 is cancerous and FB₁ is known to induce cancer in hepatic tissues in mice. Autophagy is used as a pro-
2423 survival mechanism in the latter stages of tumorigenesis to cope with metabolic stress, hypoxia, nutrient
2424 deprivation, and ER stress (Sun et al., 2013, Linder and Kögel, 2019). As previously mentioned, FB₁
2425 has been shown to upregulate sphingosine kinase activity. Recently, sphingosine kinases were shown
2426 to play a role in ER stress mediated through the inhibition of mTOR signalling via Sa1P. This is a pro-
2427 survival phenomenon used by cancer cells and should be further investigated in relation to FB₁ (Lépine
2428 et al., 2011). But what we do know is that FB₁-induced ER stress mediates autophagy through either
2429 the IRE1 α /MAPK8/9/10, IRE1 α /JNK or PERK/CHOP pathway (Figure 3.4). The outcome of
2430 autophagy depends on several factors.



2431

2432 **Figure 3.4.** FB1-induced ER stress mediates autophagy. The accumulation of sphingolipids and ROS
 2433 in the ER after exposure to FB1 triggers ER stress. Cells cope with stress by activating UPR signalling
 2434 and autophagy via IRE1 α /MAPK8/9/10, IRE1 α /JNK, or PERK/CHOP pathways. FB1-induced
 2435 autophagy can be either pro-death or pro-survival depending on several factors.

2436 **Immunotoxicity**

2437 The immune system is a major defence mechanism in animals and humans, protecting them from
 2438 invading micro-organisms and foreign chemicals and its' effectiveness is an important determinant of
 2439 animal and human health (Surai and Mezes, 2005). Mycotoxins are major immuno-suppressive agents
 2440 and FB₁-induced immunotoxicity is an area of active research (Surai and Mezes, 2005). Current studies
 2441 have observed diverse immunomodulatory effects of FB₁, which include altered inflammatory, cellular,
 2442 and humoral responses (Oswald et al., 2005).

2443 Inflammation is a non-specific response that acts by removing harmful stimuli and initiating repair
 2444 through the activation of phagocytes. The activated phagocytes secrete cytokines that act as chemical
 2445 messengers between other immune cells (Oswald et al., 2005). They stimulate or inhibit the growth and
 2446 activity of various immune cells, which mediate and regulate immunity and inflammation.
 2447 Proinflammatory cytokines mediate inflammation via receptor activation, which can trigger
 2448 intracellular signalling pathways such as MAPK, nuclear factor kappa B (NF κ B), and Janus
 2449 kinase/Signal transducer and activator of transcription (JAK/STAT). While inflammation plays an
 2450 important role in immune response, excessive production of inflammatory cytokines can lead to
 2451 cytotoxicity and tissue damage (Chen et al., 2017).

2452 Alterations in proinflammatory cytokine profiles have been shown to be one of the factors that influence
 2453 toxicity. Localized network of key proinflammatory cytokines: tumour necrosis factor alpha (TNF- α),

2454 interferon gamma (INF- γ) and interleukin-12 (IL-12) are involved in FB₁-induced hepatotoxicity in
2455 mice (Bhandari et al., 2002). Knockout of TNF α and IFN- γ or their receptors greatly reduced toxicity
2456 in the liver of mice (Sharma et al., 2000, Sharma et al., 2001, Sharma et al., 2003). The differential
2457 hepatotoxic response to FB₁ in male and female mice can also be attributed to the difference in
2458 proinflammatory cytokine profiles (Bhandari et al., 2001). Several studies have investigated the
2459 immunomodulatory effect of FB₁ in porcine intestinal systems as the intestine is the first physical barrier
2460 to protect against ingested FB₁. Furthermore, the results obtained from these studies may be valid for
2461 humans due to the similarities between the porcine and human intestinal system. In porcine intestinal
2462 epithelial (IPEC-J2) cells, both non-cytotoxic (20 μ M) and cytotoxic (40 μ M) concentrations of FB₁
2463 significantly increased the expression of inflammatory cytokines [monocyte chemoattractant protein
2464 (MCP-1), TNF- α , IL-1 β , IL-6, and IL-8]; however, 40 μ M had no significant effect on IL-1 α (Wan et
2465 al., 2013). Gu et al. (2019) investigated the effects of FB₁ and HFB₁ in a co-culture of IPEC-J2 and
2466 porcine PBMCs that had been stimulated with lipopolysaccharide (LPS) and Deoxynivalenol (DON).
2467 FB₁ significantly increased intestinal permeability and reduced barrier integrity. This may be due to
2468 disruptions in sphingolipid metabolism and depletion of glycosphingolipids which act as a structural
2469 component of tight junctions. FB₁ exacerbated proinflammatory responses through the upregulation of
2470 IL-8, MCP-1 and C-C Motif Chemokine Ligand 20 (CCL20) in the presence of LPS/DON compared to
2471 only LPS/DON treatments. The use of HFB₁ leads to decreased cytokine expression; however, the effect
2472 of HFB₁ on IPEC-J2 cell viability and barrier integrity was comparable to that of FB₁. Thus, FB₁
2473 degradation could be an effective strategy to reduce intestinal inflammation. Moreover, FB₁ but not
2474 HFB₁ provoked PBMC cell death in the presence of LPS/DON. In another study, FB₁ reduced IL-2
2475 expression and inhibited porcine PBMC proliferation via blockage of G0/G1 transition of CD2⁺, CD4⁺,
2476 CD8⁺ and immunoglobulin⁺ (Ig⁺) lymphocyte subsets (Marin et al., 2007).

2477 In humans, cytokine profiles were investigated in lymphocytes, gastric adenocarcinoma (AGS) and
2478 colon cancer (SW742) cells. FB₁ stimulated the synthesis of TNF- α , IL-1 β , inhibited IL-8 expression,
2479 and reduced cell viability in a dose-dependent manner in all 3 cell lines. The changes in cytokine profiles
2480 were more evident in SW742 cells than AGS cells; this higher sensitivity of colon cells might be due to
2481 FB₁ having a greater inhibitory effect on CS in the colon compared to the stomach (Mahmoodi et al.,
2482 2012). FB₁ was found to be immunosuppressive in human cancer patients. Lymphocytes and
2483 neutrophils, harvested from the circulation of healthy subjects and patients with breast or oesophageal
2484 cancer, were dosed with 20 μ g/ml to 100 μ g/ml for 0 to 24 hours. Ultrastructure visualization of exposed
2485 lymphocytes and neutrophils showed cell membrane disruption, damage to cytoplasmic organelles and
2486 loss of nuclear integrity. The extensive cellular damage observed in all 3 populations correlated with
2487 enhanced apoptosis in exposed cells (Odhav and Bhoola, 2008). In some cancer therapies, cytokines
2488 are used to activate the immune system of cancer patients (Conlon et al., 2019). FB₁ downregulated
2489 TNF- α and GCSF receptors on lymphocytes and neutrophils, inhibiting cytokine signalling.

2490 Furthermore, FB₁ increased expression of IL-1 and decreased IL-10 in lymphocytes of breast cancer
2491 patients and decreased IL-6 in oesophageal cancer patients (Odhav and Bhoola, 2008). Taken together,
2492 this data suggests FB₁ suppresses immune functioning in a population that is already
2493 immunocompromised. Not only does FB₁ diminish immune response to cancer but also raises
2494 susceptibility to infectious diseases. Pig weanlings were given 0.5 mg/kg bw FB₁ for 6 weeks before
2495 being orally inoculated with a septicaemic *Escherichia coli* (*E. coli*) strain. FB₁ facilitated intestinal
2496 colonization of septicaemic *E. coli* and its translocation. Bacterial translocation was prominent in
2497 mesenteric lymph nodes and lungs and to a lesser extent in the liver and spleen (Oswald et al., 2003).
2498 FB₁ also prolonged intestinal infection of enterotoxigenic *E. coli* in pigs. This was achieved through the
2499 impairment of antigen-presenting cells maturation by downregulating IL-12p40 and major
2500 histocompatibility complex class II molecules (MHC-II) (Devriendt et al., 2009). Antigen processing
2501 and presentation was also affected in human gastric epithelium (GES-1) cells. FB₁ reduced expression
2502 of antigen processing complexes: transporter associated with antigen processing 1 (TAP1) and low
2503 molecular weight peptide (LMP2), which contributed to reduced expression of human leukocyte antigen
2504 (HLA)-class I expression. This may also lead to CD8⁺ T cells resistance (Yao et al., 2010).

2505 Finally, FB₁ can affect humoral immune response by diminishing the specific antibody response built
2506 during vaccination. IL-4 plays a key role in the development of the humoral immune response and
2507 antibody production (Yang et al., 2017). Prolonged exposure (8 mg FB₁/kg; 28 days) to FB₁
2508 significantly decreased the expression of IL-4 in porcine lymphocytes, which in turn diminished
2509 antibody response after vaccination against *Mycoplasma agalactiae* (Taranu et al., 2005). A decrease
2510 in the specific antibody production was also observed in rodents immunized with sheep red blood cells
2511 (Martinova and Merrill, 1995, Tryphonas et al., 1997). However, exposure of piglets for up to 4 months
2512 to FB₁-contaminated feed had no significant effect on antibody production against Aujeszky's disease
2513 (Tornyos et al., 2003). In summary, exposure to FB₁ activates proinflammatory networks, impairs
2514 maturation of antigen-presenting cells and affects immune cell viability and responses. These
2515 immunosuppressive effects increase susceptibility to infectious diseases, affects the treatment of
2516 diseases such as cancer, and diminishes vaccine efficacy.

2517 **FB₁-mediated changes to the epigenome**

2518 Exogenous stimuli such as mycotoxins are prominent disrupters to the epigenome (Huang et al., 2019).
2519 They can induce phenotypic changes by differentially regulating gene expression rather than altering
2520 DNA sequences. Epigenetic modifications are essential for the normal cellular processes and
2521 maintenance of gene expression patterns. In contrast, aberrant alterations to the epigenome can affect
2522 genome stability and may activate transcription of various genes, such as oncogenes, or silence the
2523 expression of tumour suppressor genes (Sharma et al., 2010, Ho et al., 2012, Peschansky and
2524 Wahlestedt, 2014). Epigenetic mechanisms include DNA methylation, histone modifications and the
2525 production of non-coding RNA transcripts such as microRNA (miRNA) and long non-coding (lncRNA)

2526 (Lennartsson and Ekwall, 2009, Smith and Meissner, 2013, Peschansky and Wahlestedt, 2014). These
2527 modifications play an important role in the toxicity and sometimes carcinogenicity of mycotoxins.
2528 Epigenetic alterations in response to FB₁ have been investigated *in vivo* and *in vitro* (Mobio et al., 2000,
2529 Kouadio et al., 2007, Pellanda et al., 2012, Chuturgoon et al., 2014a, Chuturgoon et al., 2014b, Demirel
2530 et al., 2015, Sancak and Ozden, 2015, Arumugam et al., 2020).

2531 *DNA methylation*

2532 DNA methylation is the most widely studied epigenetic modification. It is facilitated by DNA
2533 methyltransferases (DNMTs), which catalyses the transfer of methyl groups to selective cytosine and
2534 to a lesser extent adenine of mammalian DNA (Lyko, 2018). DNA methylation usually occurs in CpG
2535 islands of gene promoters although non-CpG methylation can also occur. Hypermethylation of CpG
2536 islands in gene promoter regions inhibit the binding of transcription factors and suppress gene
2537 transcription (Moore et al., 2013). FB₁ (9 and 18 μ M) induced significant DNA hypermethylation in rat
2538 C6 glioma cells after 24 hours; however, failed to induce hypermethylation at higher concentrations (27
2539 and 54 μ M). It was suggested that the lack of DNA methylation in higher concentrations could be due
2540 to higher toxicity and DNA damage inflicted by FB₁ (Mobio et al., 2000). Hypermethylation is known
2541 to play a role in the regulation of DNA replication and gene expression in cell division and
2542 differentiation processes (Moore et al., 2013). Hypermethylation observed at 9-18 μ M may have
2543 resulted in the hypermethylation of gene promoters involved in protein synthesis, DNA synthesis and
2544 cell cycle regulation which may explain the impairment of G₀/G₁ transition, DNA and protein synthesis
2545 and the low percentage of cells observed in the S phase of the cell cycle (Mobio et al., 2000). In human
2546 intestinal Caco-2 cells, FB₁ (10, 20, 40 μ M for 24 hours) was also shown to significantly increase DNA
2547 methylation from 4.5% in control cells to 9%, 9.5% and 8% at concentrations of 10, 20 and 40 μ M of
2548 FB₁, respectively (Kouadio et al., 2007). Moreover, Demirel et al. (2015) evaluated the effect of FB₁
2549 on both global DNA methylation and candidate gene methylation. While no significant changes to
2550 global DNA methylation occurred in rat liver (Clone 9 cells) and kidney epithelial cells (NRK-52E);
2551 CpG promoter methylation occurred in selective tumour suppressor genes. CpG islands of VHL and e-
2552 cadherin promoters were methylated in both cell lines. In addition, c-Myc was found methylated
2553 exclusively in Clone 9 cells and methylation of p16 gene occurred in NRK-52E cells (Demirel et al.,
2554 2015). Hypermethylation of tumour suppressor genes inhibits the transcription of these genes aiding
2555 carcinogenesis (Sharma et al., 2010). Global DNA hypomethylation is also characteristic of cancer cells
2556 and is found in early carcinogenesis and during tumour progression (Sheaffer et al., 2016). In HepG2
2557 cells, FB₁ (200 μ M; 24 hours) induced significant global DNA hypomethylation which was
2558 accompanied by decreased expression of DNA methyltransferases (DNMT1, DNMT3a, and DNMT3b)
2559 and increased expression of DNA demethylase, MBD2 (Chuturgoon et al., 2014a). A major
2560 consequence of global DNA hypomethylation is the lack of sufficient ability to maintain genomic
2561 stability and activate appropriate DNA damage responses (Sheaffer et al., 2016). Global

2562 hypomethylation by FB₁ leads to the loss of genomic integrity which was observed by the increased
2563 comet tail lengths induced by FB₁ (Chuturgoon et al., 2014a). The inconsistencies in global methylation
2564 across these 4 studies maybe due to a number of factors: i) heterogeneity of the cells used – DNA
2565 methylation regulates gene expression in a cell and tissue specific manner; ii) doses of FB₁ used – low
2566 doses seemed to favour hypermethylation; whereas high dose favoured hypomethylation.
2567 Hypermethylation of tumour suppressor genes observed by Demirel et al. (2015) in combination with
2568 a gross loss of global DNA methylation witnessed by Chuturgoon et al. (2014a) may be one of the
2569 mechanisms responsible for FB₁-related carcinogenesis.

2570 *Histone Modifications*

2571 Modifications to histones are another means in which FB₁ can affect chromatin architecture and gene
2572 expression. Histone modifications are covalent post-translational modifications that can influence
2573 chromatin structure and subsequently the transcriptional status of genes. Histone modifications include
2574 the methylation, acetylation, phosphorylation, sumoylation and ubiquitination of specific amino acid
2575 residues (Cosgrove et al., 2004). In FB₁-treated NRK-52E cells (25, 50 and 100 µM), a global increase
2576 in di- and tri- methylation of lysine 9 on histone 3 (H3K9me_{2/3}) was accompanied by an increase in
2577 H3K9 histone methyltransferase (HMT). However, high doses (50 and 100 µM, 24 hours) and
2578 prolonged exposure (25 µM, 27 and 96 hours) to FB₁ significantly reduced methylation of lysine 20 of
2579 histone 4 (H4K20) (Sancak and Ozden, 2015). Similar results in H3K9me₃ and H4K20me₃ were
2580 observed in the foetus of methyl deficient dams exposed to FB₁ (Pellanda et al., 2012). Both H3K9me₃
2581 and H4K20me₃ establishes a condensed and transcriptionally inert chromatin conformation that
2582 contributes to the maintenance of genome stability (Saksouk et al., 2015). Loss of H4K20me₃ provokes
2583 genome instability and is considered a hallmark of cancer (Van Den Broeck et al., 2008); The rise in
2584 H3K9me₃ might be the defence mechanism promoting the cell to resist heterochromatin disorganization
2585 by FB₁ (Pellanda et al., 2012). These changes in H3K9 methylation are associated with closed chromatin
2586 and inhibition of transcription, further pointing to the probability that FB₁ silences genes especially,
2587 tumour suppresser genes (Sharma et al., 2010). However, the study by Chuturgoon et al. (2014a)
2588 indicated that FB₁ significantly increased the expression of two histone demethylase genes *KDM5B* and
2589 *KDM5C*, which may promote H3K4me₃/me₂ demethylation. But this was not the case in NRK-52E
2590 cells and in a recent study which used HepG2 cells (Sancak and Ozden, 2015, Arumugam et al., 2020).
2591 Regarding histone acetylation, FB₁ had little effect on H4K16 and H3K18 acetylation (Pellanda et al.,
2592 2012, Gardner et al., 2016). A dose and time-dependent decrease was observed in the H3K9ac levels in
2593 response to FB₁, while histone acetyl transferase activity was only inhibited as a consequence of
2594 prolonged exposure (96 hours) (Sancak and Ozden, 2015). In LM/Bc embryonic fibroblasts, the
2595 elevation in Sa1P after FB₁-mediated inhibition of CS, inhibited histone deacetylase activity, promoting
2596 histone acetylation of H2NK12, H3K9 and H3K23 (Gardner et al., 2016) The results of this study along
2597 with Pellanda et al. (2012), provides a potential mechanism for the failure of neural tube closure

2598 observed in mice and humans following FB₁ exposure. However, further *in vitro* studies should be
2599 undertaken to confirm this hypothesis. Histone phosphorylation also contributes to the toxicity of FB₁.
2600 Downregulation in the phosphorylation of γ -H2AX was observed upon FB₁ (200 μ M, 24 hours)
2601 exposure in HepG2 cells (Chaturgoon et al., 2015). Poor phosphorylation of γ -H2AX provokes genome
2602 instability and prevents appropriate responses to DNA damage leading to gene mutations and
2603 tumorigenesis (Podhorecka et al., 2010).

2604 *MicroRNA profiles*

2605 Only two studies has investigated the effect of FB₁ on miRNA profiles (Chaturgoon et al., 2014b,
2606 Arumugam et al., 2020). MiRNAs are a class on small non-coding RNAs that target mRNAs to induce
2607 mRNA degradation and translational repression (O'Brien et al., 2018). Quantitative polymerase chain
2608 reaction array-based profiling of miRNA and hierarchical cluster analysis by Chaturgoon et al. (2014b)
2609 found that miR-135b, miR-181d, miR-27a, miR-27b, and miR-30c were significantly downregulated.
2610 They further investigated miR-27b and found a 10-fold decrease that correlated with increased
2611 expression of cytochrome 1B1, which mediates the bioactivation of procarcinogens (Chaturgoon et al.,
2612 2014b). A recent study found that FB₁ induced miR-30c expression which altered H3K4me as well as
2613 inhibited the translation of the tumour suppressor, phosphatase and tensin homolog (PTEN) leading to
2614 diminished response and repair of FB₁-induced oxidative DNA lesions (Arumugam et al., 2020). By
2615 evaluating all the previous data, it is evident that epigenetic modifications are involved in FB₁ toxicity
2616 and possibly the aetiology of diseases such as neural tube defects and cancer. Nevertheless, further
2617 research should be undertaken to fully explore the effect of FB₁ on the epigenome as a whole and to
2618 elucidate the impact of gene-specific epigenetic modifications in relation to a particular toxicological
2619 phenotype.

2620 **Current strategies in minimizing FB₁ toxicity**

2621 Considering that FB₁ contamination of agricultural staples is unavoidable and the negative impact it has
2622 on human health, a great deal of research has focused on strategies to mitigate FB₁ contamination and
2623 toxicity. The implementation of good agricultural, storage and processing practices can reduce FB₁
2624 contamination and subsequent exposure to humans and animals (Okabe et al., 2015). Several new
2625 approaches are being investigated to detoxify FB₁ contaminated foods and feeds. These strategies
2626 include the use of physical, chemical or biological means to remove FB₁ or attenuate its effects. Below
2627 we review some recent research investigating FB₁ detoxification.

2628 *Physical methods*

2629 Although FB₁ is relatively heat stable, the use of extrusion cooking (high temperature/high pressure)
2630 has been shown to be an effective method of reducing FB₁ levels in maize [reviewed by Jackson et al.
2631 (2012)]. At the right temperature and pressure, extrusion cooking can reduce FB₁ concentration by 64%
2632 in grits; however, cooking grits with the addition of glucose along with extrusion can eliminate 99% of

2633 FB₁ from this maize-based porridge. Furthermore, this cooking technique prevented the disruption of
2634 sphingolipid metabolism and development of kidney lesions in male rats fed diets consisting of FB₁
2635 contaminated grits that have undergone extrusion and glucose supplementation (Voss et al., 2011).
2636 Nixtamalization is an alternative cooking method of corn and other grains. This ancient cooking process
2637 involves cooking and steeping grains in an alkaline solution (calcium hydroxide) to improve nutritional
2638 value and possibly reduce toxin contamination (Voss et al., 2017). However, the fate of FB₁ during
2639 nixtamalization is not fully understood and potentially toxic reaction products, including matrix-
2640 associated “masked” FB₁ might remain in nixtamalized corn (Voss et al., 2013). Nixtamalization
2641 involves the removal of one or both tricarboxylic acid groups from FB₁ yielding pHFB₁ or HFB₁,
2642 respectively (Voss et al., 2017). De Girolamo et al. (2016) found that while cooking without an alkaline
2643 solution did reduce the levels of FB₁ and pHFB₁; HFB₁ levels remained the same. However, the use of
2644 an alkaline solution reduced FB₁ and pHFB₁ by converting it to HFB₁. This confirms the role of alkaline
2645 in releasing matrix associated FB₁. No evidence of “masked” FB₁ was found in another study that
2646 investigated the role of nixtamalization on FB₁ detoxification. Moreover, nixtamalization not only
2647 reduced FB₁ levels in the feed of Sprague Dawley rats but also lowered Sa and So levels and reduced
2648 the number of renal lesions in comparison to rats fed uncooked corn (Voss et al., 2013).

2649 *Chemical methods*

2650 Organic and inorganic compounds can be used to bind or adsorb mycotoxins from the gastrointestinal
2651 tract preventing their entry into circulation. Calcium montmorillonite (NovaSil), a dioctahedral smectite
2652 clay, is an effective aflatoxin binder and is considered safe in humans. Robinson et al. (2012) evaluated
2653 the effectiveness of NovaSil with regards to FB₁ in male F344 rats and humans. NovaSil reduced rat
2654 urinary FB₁ levels by 20% in the first 24 hours and 50% after 48 hours. In a clinical trial, 3 g/day
2655 NovaSil eliminated 90% of FB₁. The protonation of the amino group of FB₁ in acidic conditions like
2656 that of the stomach allows for its binding to the negatively charged surfaces of the clay. Nanosilicate
2657 platelets exfoliated from montmorillonite have a large surface area and high density which may allow
2658 for effective FB₁ binding. Nanosilicate platelets lowered FB₁ levels in circulation, reversed sphingolipid
2659 perturbations and prevented abnormalities in mice dams fed FB₁ contaminated diets. It also lowered the
2660 incidence of neural tube defects in their offspring (Liao et al., 2014). Two studies independently
2661 evaluated the effects of novel nanocellulose compounds on FB₁. Jebali et al. (2015) modified
2662 nanocellulose with polylysine (NMPL); which has a high affinity to the carboxyl groups of FB₁; while
2663 Zadeh and Shahdadi (2015) coated nanocellulose with free fatty acids which bind to the hydrophobic
2664 tail of FB₁. Both studies found that the nanocellulose compounds effectively adsorbed FB₁ and reduced
2665 toxicity in mouse liver cells (Jebali et al., 2015, Zadeh and Shahdadi, 2015). However, NMPL is
2666 sensitive to changes in pH (Jebali et al., 2015), and both compounds should be tested *in vivo*. Lastly, 2-
2667 5 g/kg of relatively new mycotoxin inactivator, AdidetoxTM moderately reduced FB₁ toxicity in Sprague

2668 Dawley rats; however, it did not fully avoid a significant accumulation of sphingolipids (Denli et al.,
2669 2015).

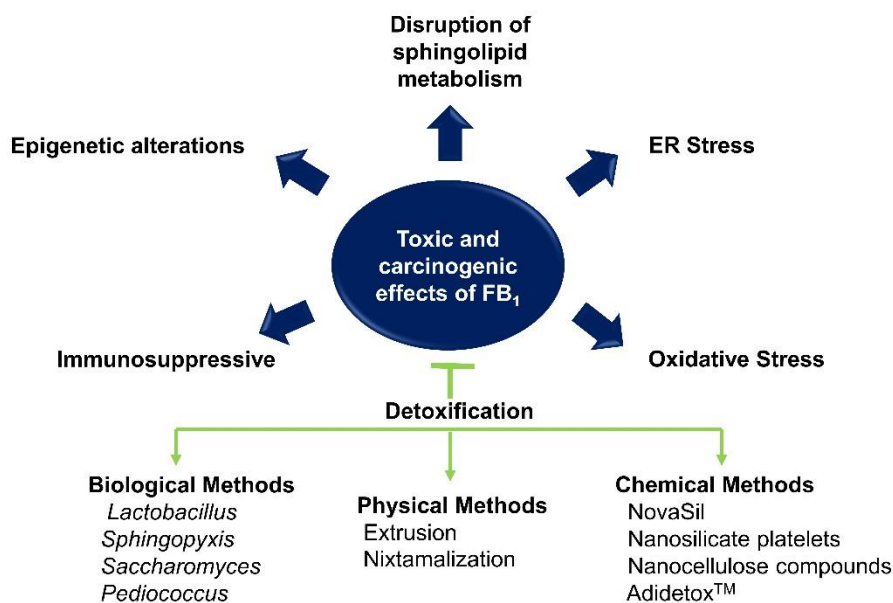
2670 *Biological Methods*

2671 Certain micro-organism form part of normal gut flora and its consumption is associated with a range of
2672 health benefits, including improved immune function, antioxidant capacity and prevention of cancer
2673 (Hullar et al., 2014). Consequently, the role of these micro-organisms as mycotoxin detoxification
2674 agents are being investigated and inclusion of such microbes in the diet may decrease availability and
2675 absorption of FB₁ in the gastrointestinal tract. 12 *Lactobacillus* bacterial strains and 6 *Saccharomyces*
2676 *cerevisiae* yeast strains significantly reduced FB₁ levels by 62-77% and 67-74%, respectively (Chlebicz
2677 and Śliżewska, 2020). FB₁ binds to the micro-organism's cell wall through weak noncovalent
2678 interactions. The interactions need as little time as a minute, suggesting that neither FB₁ cell entry nor
2679 metabolism may occur. Further, they can absorb FB₁ and aflatoxin simultaneously without changes in
2680 their efficiency (Pizzolitto et al., 2012). The use of *Lactobacillus delbrueckii* and *Pediococcus*
2681 *acidilactici* as probiotics ameliorated FB₁-induced hepatorenal toxicity and genotoxicity in rats by
2682 normalizing kidney function, restoring redox homeostasis and reducing DNA fragmentation (Khalil et
2683 al., 2015, Abdellatef and Khalil, 2016). Antioxidant capabilities of probiotics against FB₁ were also
2684 demonstrated by *Lactobacillus paracaeseu* which upregulated antioxidant capacity, inhibited lipid
2685 peroxidation, increased free radical scavenging and reduced DNA fragmentations. It also had protective
2686 effects against immunotoxicity induced by FB₁ (Abbès et al., 2016). The use of recombinant
2687 carboxylesterase, *FUMD*, from yeast (*Pichia pastoris*) has been shown to degrade FB₁ in the
2688 gastrointestinal tract of pigs. *FUMD* is responsible for the removal of the tricarboxylic acid side chains
2689 of FB₁, forming HFB₁ (Masching et al., 2016). As shown previously, HFB₁ can undergo *N*-acylation
2690 forming toxic derivatives, thus deamination is necessary for effective detoxification. *FUMD* along with
2691 *FUMI* were shown to be the genes responsible for the degradation of FB₁ by the bacterium
2692 *Sphingopyxis* sp. MTA144. *FUMD*, was responsible for the desulfuration; while *FUMI*, an
2693 aminotransferase, deaminated FB₁ and HFB₁. HFB₁ only has 1 amino group therefore, the product of
2694 these reactions can no longer inhibit CS activity. The authors believe the product to be 2-keto-HFB₁;
2695 however, the products need to undergo characterization (Heinl et al., 2010).

2696 **Conclusion**

2697 Fumonisin contamination of global agricultural produce is unavoidable and unpredictable. This poses
2698 a unique challenge to food quality and safety. The most potent and abundant class of fumonisins is FB₁,
2699 which is the cause of several species-specific toxicities and is involved in carcinogenesis. Therefore, it
2700 is necessary to investigate the mode of action of FB₁ as well as interventions that aide in detoxification.
2701 As discussed above, the main mode of FB₁ toxicity is via the disruption of sphingolipid metabolism.
2702 This results in the accumulation of sphingoid bases in the ER, which disrupts signalling pathways and
2703 results in ER stress and autophagy. FB₁ also enhances ROS production leading to oxidative damage to

2704 cells and alters immune responses. Furthermore, FB₁ induces epigenetic changes that affect cell cycle
 2705 regulation, DNA and protein synthesis as well as promotes cancer via the inhibition of tumour
 2706 suppressor genes and activation of procarcinogens. Considering only a handful of studies have
 2707 investigated the impact of FB₁ on the epigenome, it is necessary that more accurate epigenetic
 2708 mechanisms of FB₁-induced toxicity are explored. Through proper crop management and storage, FB₁
 2709 levels in crops can be minimized. Dietary interventions that eliminate or detoxify FB₁ in the gut, such
 2710 as the use of chemical adsorbents or probiotics may also be crucial in mitigating the unpleasant
 2711 consequences of FB₁ (Figure 3.5).



2712
 2713 **Figure 3.5.** An overview of the toxic and carcinogenic modes of action by FB₁ as well as strategies
 2714 involved in its detoxification

2715 **Disclosure Statement**

2716 The authors declare to have no conflict of interest. The authors acknowledge the National Research
 2717 Foundation (NRF) of South Africa for funding this review. The review was conceptualized by the
 2718 authors and represents an unbiased professional assessment of available literature. The conclusions
 2719 drawn are exclusively those of the authors. None of the authors have appeared during the last 10 years
 2720 in any regulatory or legal proceedings related to the contents of this paper.

2721
 2722
 2723
 2724
 2725

2726 **References**

- 2727 Abado-Becognee K, Mobio TA, Ennamany R, Fleurat-Lessard F, Shier WT, Badria F & Creppy EE
2728 1998. Cytotoxicity of fumonisin B1: implication of lipid peroxidation and inhibition of protein and
2729 DNA syntheses. *Arch Toxicol*, 72, 233-236.
- 2730 Abbès S, Ben Salah-Abbès J, Jebali R, Younes RB & Oueslati R 2016. Interaction of aflatoxin B1 and
2731 fumonisin B1 in mice causes immunotoxicity and oxidative stress: Possible protective role using lactic
2732 acid bacteria. *Journal of immunotoxicology*, 13, 46-54.
- 2733 Abdellatef AA & Khalil AA 2016. Ameliorated effects of *Lactobacillus delbrueckii* subsp. *lactis* DSM
2734 20076 and *Pediococcus acidilactici* NNRL B-5627 on Fumonisin B1-induced Hepatotoxicity and
2735 Nephrotoxicity in rats. *Asian Journal of Pharmaceutical Sciences*, 11, 326-336.
- 2736 Abel S & Gelderblom WCA 1998. Oxidative damage and fumonisin B1-induced toxicity in primary rat
2737 hepatocytes and rat liver in vivo. *Toxicology*, 131, 121-131.
- 2738 Alberts J, Rheeder J, Gelderblom W, Shephard G & Burger H-M 2019. Rural Subsistence Maize
2739 Farming in South Africa: Risk Assessment and Intervention models for Reduction of Exposure to
2740 Fumonisin Mycotoxins. *Toxins*, 11, 334.
- 2741 Alizadeh AM, Roshandel G, Roudbarmohammadi S, Roudbary M, Sohanaki H, Ghiasian SA,
2742 Taherkhani A, Semnani S & Aghasi M 2012. Fumonisin B1 contamination of cereals and risk of
2743 esophageal cancer in a high risk area in northeastern Iran. *Asian Pacific journal of cancer prevention*,
2744 13, 2625-2628.
- 2745 Andreyev AY, Kushnareva YE & Starkov A 2005. Mitochondrial metabolism of reactive oxygen
2746 species. *Biochemistry (Moscow)*, 70, 200-214.
- 2747 Arumugam T, Pillay Y, Ghazi T, Nagiah S, Abdul NS & Chuturgoon AA 2019. Fumonisin B1-induced
2748 oxidative stress triggers Nrf2-mediated antioxidant response in human hepatocellular carcinoma
2749 (HepG2) cells. *Mycotoxin research*, 35, 99-109.
- 2750 Arumugam T, Ghazi T & Chuturgoon A 2020. Fumonisin B1 Epigenetically Regulates PTEN
2751 Expression and Modulates DNA Damage Checkpoint Regulation in HepG2 Liver Cells. *Toxins*, 12,
2752 625.
- 2753 Atroshi F, Rizzo A, Biese I, Veijalainen P, Saloniemi H, Sankari S & Andersson K 1999. Fumonisin
2754 B1-induced DNA damage in rat liver and spleen: effects of pretreatment with coenzyme Q10, L-
2755 carnitine, α -tocopherol and selenium. *Pharmacological Research*, 40, 459-467.
- 2756 Ayala A, Munoz MF & Arguelles S 2014. Lipid peroxidation: production, metabolism, and signaling
2757 mechanisms of malondialdehyde and 4-hydroxy-2-nonenal. *Oxid Med Cell Longev*, 2014, 360438.

2758 Bernabucci U, Colavecchia L, Danieli PP, Basiricò L, Lacetera N, Nardone A & Ronchi B 2011.
2759 Aflatoxin B1 and fumonisin B1 affect the oxidative status of bovine peripheral blood mononuclear
2760 cells. *Toxicology in vitro*, 25, 684-691.

2761 Bhandari N, He Q & Sharma RP 2001. Gender-related differences in subacute fumonisin B1
2762 hepatotoxicity in BALB/c mice. *Toxicology*, 165, 195-204.

2763 Bhandari N, Brown CC & Sharma RP 2002. Fumonisin B1-induced localized activation of cytokine
2764 network in mouse liver. *Food and chemical toxicology : an international journal published for the*
2765 *British Industrial Biological Research Association*, 40, 1483-1491.

2766 Bratic A & Larsson N-G 2013. The role of mitochondria in aging. *The Journal of clinical investigation*,
2767 123, 951-957. Bravo R, Parra V, Gatica D, Rodriguez AE, Torrealba N, Paredes F, Wang ZV, Zorzano
2768 A, Hill JA, Jaimovich E, et al. 2013. Endoplasmic reticulum and the unfolded protein response:
2769 dynamics and metabolic integration. *Int Rev Cell Mol Biol*, 301, 215-290.

2770 Chakrabarti A, Chen AW & Varner JD 2011. A review of the mammalian unfolded protein response.
2771 *Biotechnol Bioeng*, 108, 2777-2793.

2772 Chen C, Mitchell NJ, Gratz J, Houpt ER, Gong Y, Egner PA, Groopman JD, Riley RT, Showker JL,
2773 Svensen E, et al. 2018. Exposure to aflatoxin and fumonisin in children at risk for growth impairment
2774 in rural Tanzania. *Environ Int*, 115, 29-37.

2775 Chen L, Deng H, Cui H, Fang J, Zuo Z, Deng J, Li Y, Wang X & Zhao L 2017. Inflammatory responses
2776 and inflammation-associated diseases in organs. *Oncotarget*, 9, 7204-7218.

2777 Chlebicz A & Śliżewska K 2020. In Vitro Detoxification of Aflatoxin B1, Deoxynivalenol, Fumonisin,
2778 T-2 Toxin and Zearalenone by Probiotic Bacteria from Genus *Lactobacillus* and *Saccharomyces*
2779 *cerevisiae* Yeast. *Probiotics and Antimicrobial Proteins*, 12, 289-301.

2780 Chuturgoon A, Phulukdaree A & Moodley D 2014a. Fumonisin B1 induces global DNA
2781 hypomethylation in HepG2 cells - An alternative mechanism of action. *Toxicology*, 315, 65-69.

2782 Chuturgoon AA, Phulukdaree A & Moodley D 2014b. Fumonisin B₁ modulates expression of human
2783 cytochrome P450 1b1 in human hepatoma (Hepg2) cells by repressing Mir-27b. *Toxicology letters*, 227,
2784 50-55.

2785 Chuturgoon AA, Phulukdaree A & Moodley D 2015. Fumonisin B₁ inhibits apoptosis in HepG2 cells
2786 by inducing Birc-8/ILP-2. *Toxicology letters*, 235, 67-74.

2787 Collins TFX, Sprando RL, Black TN, Olejnik N, Eppley RM, Shackelford ME, Howard PC, Rorie JI,
2788 Bryant M & Ruggles DI 2006. Effects of aminopentol on in utero development in rats. *Food and*
2789 *Chemical Toxicology*, 44, 161-169.

- 2790 Conlon KC, Miljkovic MD & Waldmann TA 2019. Cytokines in the Treatment of Cancer. *Journal of*
2791 *interferon & cytokine research : the official journal of the International Society for Interferon and*
2792 *Cytokine Research*, 39, 6-21.
- 2793 Cosgrove MS, Boeke JD & Wolberger C 2004. Regulated nucleosome mobility and the histone code.
2794 *Nature structural & molecular biology*, 11, 1037-1043.
- 2795 Dalle-Donne I, Aldini G, Carini M, Colombo R, Rossi R & Milzani A 2006. Protein carbonylation,
2796 cellular dysfunction, and disease progression. *Journal of cellular and molecular medicine*, 10, 389-406.
- 2797 De Girolamo A, Lattanzio VMT, Schena R, Visconti A & Pascale M 2016. Effect of alkaline cooking
2798 of maize on the content of fumonisins B1 and B2 and their hydrolysed forms. *Food chemistry*, 192,
2799 1083-1089.
- 2800 Dellafiora L, Galaverna G & Dall'Asta C 2018. Mechanisms of Fumonisin B1 Toxicity: A
2801 Computational Perspective beyond the Ceramide Synthases Inhibition. *Chemical research in*
2802 *toxicology*, 31, 1203-1212.
- 2803 Demirel G, Alpertunga B & Ozden S 2015. Role of fumonisin B1 on DNA methylation changes in rat
2804 kidney and liver cells. *Pharmaceutical Biology*, 53, 1302-1310.
- 2805 Denli M, Blandon JC, Salado S, Guynot ME, Casas J & Pérez JF 2015. Efficacy of AdiDetox™ in
2806 reducing the toxicity of fumonisin B1 in rats. *Food and Chemical Toxicology*, 78, 60-63.
- 2807 Devriendt B, Gallois MI, Verdonck F, Wache Y, Bimczok D, Oswald I, P., Goddeeris B, M. & Cox E
2808 2009. The food contaminant fumonisin B1 reduces the maturation of porcine CD11R1(+) intestinal
2809 antigen presenting cells and antigen-specific immune responses, leading to a prolonged intestinal ETEC
2810 infection. *Vet. Res.*, 40, 40.
- 2811 Domijan A-M, Peraica M, Vrdoljak AL, Radić B, Žlender V & Fuchs R 2007a. The involvement of
2812 oxidative stress in ochratoxin A and fumonisin B1 toxicity in rats. *Molecular nutrition & food research*,
2813 51, 1147-1151.
- 2814 Domijan A, Zeljezic D, Peraica M, Kovacevic G, Gregorovic G, Krstanac Z, Horvatin K & Kalafatic
2815 M 2008. Early toxic effects of fumonisin B1 in rat liver. *Human & experimental toxicology*, 27, 895-
2816 900.
- 2817 Domijan AM, Peraica M, Vrdoljak AL, Radić B, Zlender V & Fuchs R 2007b. The involvement of
2818 oxidative stress in ochratoxin A and fumonisin B1 toxicity in rats. *Molecular nutrition & food research*,
2819 51, 1147-1151.
- 2820 Domijan AM & Abramov AY 2011. Fumonisin B1 inhibits mitochondrial respiration and deregulates
2821 calcium homeostasis--implication to mechanism of cell toxicity. *The international journal of*
2822 *biochemistry & cell biology*, 43, 897-904.

2823 Ehrlich V, Darroudi F, Uhl M, Steinkellner H, Zsivkovits M & Knasmueller S 2002. Fumonisin B1 is
2824 genotoxic in human derived hepatoma (HepG2) cells. *Mutagenesis*, 17, 257-260.

2825 Ferrigo D, Raiola A & Causin R 2016. Fusarium Toxins in Cereals: Occurrence, Legislation, Factors
2826 Promoting the Appearance and Their Management. *Molecules*, 21, 627.

2827 FOA/WHO 2002. Evaluation of certain mycotoxins in food : fifty-sixth report of the Joint FAO/WHO
2828 Expert Committee on Food Additives. Geneva: World Health Organization.

2829 Futerman AH & Riezman H 2005. The ins and outs of sphingolipid synthesis. *Trends in cell biology*,
2830 15, 312-318.

2831 Galvano F, Russo A, Cardile V, Galvano G, Vanella A & Renis M 2002. DNA damage in human
2832 fibroblasts exposed to fumonisin B(1). *Food and chemical toxicology : an international journal*
2833 *published for the British Industrial Biological Research Association*, 40, 25-31.

2834 Gardner NM, Riley RT, Showker JL, Voss KA, Sachs AJ, Maddox JR & Gelineau-van Waes JB 2016.
2835 Elevated nuclear sphingoid base-1-phosphates and decreased histone deacetylase activity after
2836 fumonisin B1 treatment in mouse embryonic fibroblasts. *Toxicology and applied pharmacology*, 298,
2837 56-65.

2838 Gazzotti T, Lugoboni B, Zironi E, Barbarossa A, Serraino A & Pagliuca G 2009. Determination of
2839 fumonisin B1 in bovine milk by LC–MS/MS. *Food Control*, 20, 1171-1174.

2840 Gelderblom W, Jaskiewicz K, Marasas W, Thiel P, Horak R, Vleggaar R & Kriek N 1988a. Fumonisin-
2841 novel mycotoxins with cancer-promoting activity produced by *Fusarium moniliforme*. *Applied and*
2842 *environmental microbiology*, 54, 1806-1811.

2843 Gelderblom W, Snyman S, Abel S, Lebepe-Mazur S, Smuts C, Van der Westhuizen L, Marasas W,
2844 Victor T, Knasmüller S & Huber W 1996. Hepatotoxicity and-carcinogenicity of the fumonisins in rats.
2845 *Fumonisin in food*. Springer.

2846 Gelderblom WC, Jaskiewicz K, Marasas WF, Thiel PG, Horak RM, Vleggaar R & Kriek NP 1988b.
2847 Fumonisin--novel mycotoxins with cancer-promoting activity produced by *Fusarium moniliforme*.
2848 *Applied and environmental microbiology*, 54, 1806-1811.

2849 Gelderblom WC, Marasas WF, Lebepe-Mazur S, Swanevelder S, Vessey CJ & Hall Pde L 2002.
2850 Interaction of fumonisin B(1) and aflatoxin B(1) in a short-term carcinogenesis model in rat liver.
2851 *Toxicology*, 171, 161-173.

2852 Gelderblom WCA, Kriek NPJ, Marasas WFO & Thiel PG 1991. Toxicity and carcinogenicity of the
2853 *Fusarium moniliforme* metabolite, fumonisin B1, in rats. *Carcinogenesis*, 12, 1247-1251.

2854 Gelineau-van Waes J, Rainey MA, Maddox JR, Voss KA, Sachs AJ, Gardner NM, Wilberding JD &
2855 Riley RT 2012. Increased sphingoid base-1-phosphates and failure of neural tube closure after exposure

2856 to fumonisin or FTY720. *Birth defects research. Part A, Clinical and molecular teratology*, 94, 790-
2857 803.

2858 Glick D, Barth S & Macleod KF 2010. Autophagy: cellular and molecular mechanisms. *J Pathol*, 221,
2859 3-12.

2860 Gonos ES, Kapetanou M, Sereikaite J, Bartosz G, Naparło K, Grzesik M & Sadowska-Bartosz I 2018.
2861 Origin and pathophysiology of protein carbonylation, nitration and chlorination in age-related brain
2862 diseases and aging. *Aging (Albany NY)*, 10, 868-901.

2863 Gu MJ, Han SE, Hwang K, Mayer E, Reisinger N, Schatzmayr D, Park B-C, Han SH & Yun C-H 2019.
2864 Hydrolyzed fumonisin B1 induces less inflammatory responses than fumonisin B1 in the co-culture
2865 model of porcine intestinal epithelial and immune cells. *Toxicology letters*, 305, 110-116.

2866 Guerrero-Hernandez A, Dagnino-Acosta A & Verkhatsky A 2010. An intelligent sarco-endoplasmic
2867 reticulum Ca²⁺ store: release and leak channels have differential access to a concealed Ca²⁺ pool. *Cell*
2868 *calcium*, 48, 143-149.

2869 Hahn I, Nagl V, Schwartz-Zimmermann HE, Varga E, Schwarz C, Slavik V, Reisinger N, Malachová
2870 A, Cirlini M, Generotti S, et al. 2015. Effects of orally administered fumonisin B1 (FB1), partially
2871 hydrolysed FB1, hydrolysed FB1 and N-(1-deoxy-D-fructos-1-yl) FB1 on the sphingolipid metabolism
2872 in rats. *Food and Chemical Toxicology*, 76, 11-18.

2873 Hanada K, Kumagai K, Yasuda S, Miura Y, Kawano M, Fukasawa M & Nishijima M 2003. Molecular
2874 machinery for non-vesicular trafficking of ceramide. *Nature*, 426, 803-809.

2875 Hard GC, Howard PC, Kovatch RM & Bucci TJ 2001. Rat Kidney Pathology Induced by Chronic
2876 Exposure to Fumonisin B1 Includes Rare Variants of Renal Tubule Tumor. *Toxicologic Pathology*, 29,
2877 379-386.

2878 Harrer H, Laviad EL, Humpf HU & Futerman AH 2013. Identification of N-acyl-fumonisin B1 as new
2879 cytotoxic metabolites of fumonisin mycotoxins. *Molecular nutrition & food research*, 57, 516-522.

2880 Harrer H, Humpf HU & Voss KA 2015. In vivo formation of N-acyl-fumonisin B1. *Mycotoxin research*,
2881 31, 33-40.

2882 Hassan AM, Abdel-Aziem SH, El-Nekeety AA & Abdel-Wahhab MA 2015. Panaxginseng extract
2883 modulates oxidative stress, DNA fragmentation and up-regulate gene expression in rats sub chronically
2884 treated with aflatoxin B 1 and fumonisin B 1. *Cytotechnology*, 67, 861-871.

2885 He Q, Suzuki H, Sharma N & Sharma RP 2006. Ceramide synthase inhibition by fumonisin B1
2886 treatment activates sphingolipid-metabolizing systems in mouse liver. *Toxicological sciences : an*
2887 *official journal of the Society of Toxicology*, 94, 388-397.

2888 Hebert DN & Molinari M 2007. In and Out of the ER: Protein Folding, Quality Control, Degradation,
2889 and Related Human Diseases. *Physiological Reviews*, 87, 1377-1408.

2890 Heinel S, Hartinger D, Thamhesl M, Vekiru E, Krska R, Schatzmayr G, Moll W-D & Grabherr R 2010.
2891 Degradation of fumonisin B1 by the consecutive action of two bacterial enzymes. *Journal of*
2892 *Biotechnology*, 145, 120-129.

2893 Hendrich S, Miller KA, Wilson TM & Murphy PA 1993. Toxicity of Fusarium proliferatum-fermented
2894 nixtamalized corn-based diets fed to rats: effect of nutritional status. *J Agric Food Chem*, 41, 1649-
2895 1654.

2896 Hendricks K 1999. Fumonisin and neural tube defects in south Texas. *Epidemiology*, 198-200.

2897 Ho SM, Johnson A, Tarapore P, Janakiram V, Zhang X & Leung YK 2012. Environmental epigenetics
2898 and its implication on disease risk and health outcomes. *ILAR journal*, 53, 289-305.

2899 Howard P, Eppley R, Stack M, Warbritton A, Voss K, Lorentzen R, Kovach R & Bucci T 1999.
2900 Carcinogenicity of Fumonisin B1 in a Two-year Bioassay with Fischer 344 Rats and B6C3F1 Mice.
2901 *Mycotoxins*, 1999, 45-54.

2902 Howard PC, Warbritton A, Voss KA, Lorentzen RJ, Thurman JD, Kovach RM & Bucci TJ 2001.
2903 Compensatory regeneration as a mechanism for renal tubule carcinogenesis of fumonisin B1 in the
2904 F344/N/Nctr BR rat. *Environ Health Perspect*, 109 Suppl 2, 309-314.

2905 Howard PC, Couch LH, Patton RE, Eppley RM, Doerge DR, Churchwell MI, Marques MM & Okerberg
2906 CV 2002. Comparison of the toxicity of several fumonisin derivatives in a 28-day feeding study with
2907 female B6C3F(1) mice. *Toxicology and applied pharmacology*, 185, 153-165.

2908 Huang D, Cui L, Sajid A, Zainab F, Wu Q, Wang X & Yuan Z 2019. The epigenetic mechanisms in
2909 Fusarium mycotoxins induced toxicities. *Food and Chemical Toxicology*, 123, 595-601.

2910 Huang HC, Nguyen T & Pickett CB 2002. Phosphorylation of Nrf2 at Ser-40 by protein kinase C
2911 regulates antioxidant response element-mediated transcription. *J Biol Chem*, 277, 42769-42774.

2912 Hullar MAJ, Burnett-Hartman AN & Lampe JW 2014. Gut microbes, diet, and cancer. *Cancer Treat*
2913 *Res*, 159, 377-399.

2914 Humpf H-U, Schmelz E-M, Meredith FI, Vesper H, Vales TR, Wang E, Menaldino DS, Liotta DC &
2915 Merrill AH 1998. Acylation of Naturally Occurring and Synthetic 1-Deoxysphinganine by Ceramide
2916 Synthase: Formation of N-palmitoyl-aminopentol produces a toxic metabolite of hydrolyzed fumonisin,
2917 AP1, and a new category of ceramide synthase inhibitor. *Journal of Biological Chemistry*, 273, 19060-
2918 19064.

2919 IARC 2002. Some traditional herbal medicines, some mycotoxins, naphthalene and styrene. *IARC*
2920 *monographs on the evaluation of carcinogenic risks to humans*, 82, 1-556.

- 2921 Jackson L, Voss K & Ryu D 2012. Effects of different extrusion conditions on the chemical and
2922 toxicological fate of fumonisin B1 in maize: a short review. *World Mycotoxin Journal*, 5, 251-260.
- 2923 Jacquemyn J, Cascalho A & Goodchild RE 2017. The ins and outs of endoplasmic reticulum-controlled
2924 lipid biosynthesis. *EMBO Rep*, 18, 1905-1921.
- 2925 Jebali A, Ardakani SAY, Shahdadi H, Zadeh MHB & Hekmatimoghaddam S 2015. Modification of
2926 nanocellulose by poly-lysine can inhibit the effect of fumonisin B1 on mouse liver cells. *Colloids and*
2927 *Surfaces B: Biointerfaces*, 126, 437-443.
- 2928 Jiménez-Rojo N, Sot J, Busto JV, Shaw WA, Duan J, Merrill AH, Jr., Alonso A & Goñi FM 2014.
2929 Biophysical properties of novel 1-deoxy-(dihydro)ceramides occurring in mammalian cells. *Biophys J*,
2930 107, 2850-2859.
- 2931 Kabir M, Kim HR & Chae H-J 2018. Endoplasmic Reticulum Stress and Autophagy.
- 2932 Karuna R & Rao BS 2013. Lack of micronuclei induction by fumonisin B(1) mycotoxin in BALB/c
2933 mice. *Mycotoxin research*, 29, 9-15.
- 2934 Kellerman TS, Marasas WFO, Pienaar J & Naudé T 1972. A mycotoxicosis of equidae caused by
2935 *Fusarium moniliforme sheldoni*. A preliminary communication.
- 2936 Khalil AA, Abou-Gabal AE, Abdellatef AA & Khalid AE 2015. Protective role of probiotic lactic acid
2937 bacteria against dietary fumonisin B1-induced toxicity and DNA-fragmentation in sprague-dawley rats.
2938 *Preparative Biochemistry and Biotechnology*, 45, 530-550.
- 2939 Khan RB, Phulukdaree A & Chuturgoon AA 2018. Fumonisin B1 induces oxidative stress in
2940 oesophageal (SNO) cancer cells. *Toxicon : official journal of the International Society on Toxinology*,
2941 141, 104-111.
- 2942 Kim SH, Singh MP, Sharma C & Kang SC 2018. Fumonisin B1 actuates oxidative stress-associated
2943 colonic damage via apoptosis and autophagy activation in murine model. *Journal of Biochemical and*
2944 *Molecular Toxicology*, 32, e22161.
- 2945 Kimanya ME, Meulenaer BD, Baert K, Tiisekwa B, Van Camp J, Samapundo S, Lachat C & Kolsteren
2946 P 2009. Exposure of infants to fumonisins in maize-based complementary foods in rural Tanzania.
2947 *Molecular nutrition & food research*, 53, 667-674.
- 2948 Kitatani K, Idkowiak-Baldys J & Hannun YA 2008. The sphingolipid salvage pathway in ceramide
2949 metabolism and signaling. *Cell Signal*, 20, 1010-1018.
- 2950 Koch GL 1990. The endoplasmic reticulum and calcium storage. *Bioessays*, 12, 527-531.
- 2951 Kouadio JH, Mobio TA, Baudrimont I, Moukha S, Dano SD & Creppy EE 2005. Comparative study of
2952 cytotoxicity and oxidative stress induced by deoxynivalenol, zearalenone or fumonisin B1 in human
2953 intestinal cell line Caco-2. *Toxicology*, 213, 56-65.

- 2954 Kouadio JH, Dano SD, Moukha S, Mobio TA & Creppy EE 2007. Effects of combinations of Fusarium
2955 mycotoxins on the inhibition of macromolecular synthesis, malondialdehyde levels, DNA methylation
2956 and fragmentation, and viability in Caco-2 cells. *Toxicon : official journal of the International Society*
2957 *on Toxinology*, 49, 306-317.
- 2958 Kouroku Y, Fujita E, Tanida I, Ueno T, Isoai A, Kumagai H, Ogawa S, Kaufman RJ, Kominami E &
2959 Momoi T 2007. ER stress (PERK/eIF2alpha phosphorylation) mediates the polyglutamine-induced LC3
2960 conversion, an essential step for autophagy formation. *Cell Death Differ*, 14, 230-239.
- 2961 Kriek NP, Kellerman TS & Marasas WF 1981a. A comparative study of the toxicity of Fusarium
2962 verticillioides (= F. moniliforme) to horses, primates, pigs, sheep and rats. *The Onderstepoort journal*
2963 *of veterinary research*, 48, 129-131.
- 2964 Kriek NPJ, Marasas WFO & Thiel PG 1981b. Hepato- and cardiotoxicity of Fusarium verticillioides
2965 (F. moniliforme) isolates from Southern African maize. *Food and Cosmetics Toxicology*, 19, 447-456.
- 2966 Kwon D, Kim S-M & Correia MA 2020. Cytochrome P450 endoplasmic reticulum-associated
2967 degradation (ERAD): therapeutic and pathophysiological implications. *Acta Pharmaceutica Sinica B*,
2968 10, 42-60.
- 2969 Lee HJ & Ryu D 2017. Worldwide Occurrence of Mycotoxins in Cereals and Cereal-Derived Food
2970 Products: Public Health Perspectives of Their Co-occurrence. *J Agric Food Chem*, 65, 7034-7051.
- 2971 Lennartsson A & Ekwall K 2009. Histone modification patterns and epigenetic codes. *Biochimica et*
2972 *Biophysica Acta* 1790, 863-868.
- 2973 Lépine S, Allegood J, Park M, Dent P, Milstien S & Spiegel S 2011. Sphingosine-1-phosphate
2974 phosphohydrolase-1 regulates ER stress-induced autophagy. *Cell death and differentiation*, 18, 350-
2975 361.
- 2976 Li Y, Guo Y, Tang J, Jiang J & Chen Z 2014. New insights into the roles of CHOP-induced apoptosis
2977 in ER stress. *Acta biochimica et biophysica Sinica*, 46, 629-640.
- 2978 Liao Y-J, Yang J-R, Chen S-E, Wu S-J, Huang S-Y, Lin J-J, Chen L-R & Tang P-C 2014. Inhibition of
2979 fumonisin B1 cytotoxicity by nanosilicate platelets during mouse embryo development. *PLoS one*, 9,
2980 e112290.
- 2981 Linder B & Kögel D 2019. Autophagy in Cancer Cell Death. *Biology (Basel)*, 8, 82.
- 2982 Liu X, Zhang E, Yin S, Zhao C, Fan L & Hu H 2020. Activation of the IRE1 α Arm, but not the PERK
2983 Arm, of the Unfolded Protein Response Contributes to Fumonisin B1-Induced Hepatotoxicity. *Toxins*,
2984 12, 55.
- 2985 Loft S, Høgh Danielsen P, Mikkelsen L, Risom L, Forchhammer L & Møller P 2008. Biomarkers of
2986 oxidative damage to DNA and repair. *Biochemical Society transactions*, 36, 1071-1076.

- 2987 Lyko F 2018. The DNA methyltransferase family: a versatile toolkit for epigenetic regulation. *Nature*
2988 *Reviews Genetics*, 19, 81-92.
- 2989 Ma Q 2013. Role of nrf2 in oxidative stress and toxicity. *Annual review of pharmacology and*
2990 *toxicology*, 53, 401-426.
- 2991 Maceyka M, Payne SG, Milstien S & Spiegel S 2002. Sphingosine kinase, sphingosine-1-phosphate,
2992 and apoptosis. *Biochimica et Biophysica Acta* 1585, 193-201.
- 2993 Magan N, Medina A & Aldred D 2011. Possible climate-change effects on mycotoxin contamination
2994 of food crops pre- and postharvest. *Plant Pathology*, 60, 150-163.
- 2995 Mahmoodi M, Alizadeh AM, Sohanaki H, Rezaei N, Amini-Najafi F, Khosravi AR, Hosseini SK, Safari
2996 Z, Hydarnasab D & Khor V 2012. Impact of fumonisin B1 on the production of inflammatory cytokines
2997 by gastric and colon cell lines. *Iranian journal of allergy, asthma, and immunology*, 11, 165-173.
- 2998 Marasas W, Wehner F, Van Rensburg S & Van Schalkwyk D 1981. Mycoflora of corn produced in
2999 human esophageal cancer areas in Transkei, southern Africa. *Phytopathology*, 71, 792-796.
- 3000 Marasas W 2001. Discovery and occurrence of the fumonisins: a historical perspective. *Environ Health*
3001 *Perspect*, 109, 239-243.
- 3002 Marasas WF, Kriek NP, Fincham JE & Van Rensburg SJ 1984. Primary liver cancer and oesophageal
3003 basal cell hyperplasia in rats caused by *Fusarium moniliforme*. *International Journal of Cancer*, 34,
3004 383-387.
- 3005 Margariti A, Li H, Chen T, Martin D, Vizcay-Barrena G, Alam S, Karamariti E, Xiao Q, Zampetaki A,
3006 Zhang Z, et al. 2013. XBP1 mRNA splicing triggers an autophagic response in endothelial cells through
3007 BECLIN-1 transcriptional activation. *J Biol Chem*, 288, 859-872.
- 3008 Marin DE, Gouze M-E, Taranu I & Oswald IP 2007. Fumonisin B1 alters cell cycle progression and
3009 interleukin-2 synthesis in swine peripheral blood mononuclear cells. *Molecular nutrition & food*
3010 *research*, 51, 1406-1412.
- 3011 Martinova EA & Merrill AH 1995. Fumonisin B 1 alters sphingolipid metabolism and immune function
3012 in BALB/c mice: Immunological responses to fumonisin B 1. *Mycopathologia*, 130, 163-170.
- 3013 Mary VS, Theumer MG, Arias SL & Rubinstein HR 2012. Reactive oxygen species sources and
3014 biomolecular oxidative damage induced by aflatoxin B1 and fumonisin B1 in rat spleen mononuclear
3015 cells. *Toxicology*, 302, 299-307.
- 3016 Masching S, Naehrer K, Schwartz-Zimmermann H-E, Sărăndan M, Schaumberger S, Dohnal I, Nagl V
3017 & Schatzmayr D 2016. Gastrointestinal Degradation of Fumonisin B₁ by Carboxylesterase FumD
3018 Prevents Fumonisin Induced Alteration of Sphingolipid Metabolism in Turkey and Swine. *Toxins*, 8,
3019 84.

3020 Mboya R & Kolanisi U 2014. Subsistence Farmers' Mycotoxin Contamination Awareness in the SADC
3021 Region: Implications on Millennium Development Goal 1, 4 and 6. *Journal of Human Ecology*, 46, 21-
3022 31.

3023 Merrill AH, Jr., van Echten G, Wang E & Sandhoff K 1993. Fumonisin B1 inhibits sphingosine
3024 (sphinganine) N-acyltransferase and de novo sphingolipid biosynthesis in cultured neurons in situ. *J*
3025 *Biol Chem*, 268, 27299-27306.

3026 Minervini F, Garbetta A, D'Antuono I, Cardinali A, Martino NA, Debellis L & Visconti A 2014. Toxic
3027 mechanisms induced by fumonisin b1 mycotoxin on human intestinal cell line. *Archives of*
3028 *environmental contamination and toxicology*, 67, 115-123.

3029 Missmer SA, Suarez L, Felkner M, Wang E, Merrill AH, Rothman KJ & Hendricks KA 2006. Exposure
3030 to Fumonisin and the Occurrence of Neural Tube Defects along the Texas–Mexico Border.
3031 *Environ Health Perspect*, 114, 237-241.

3032 Mobio TA, Anane R, Baudrimont I, Carratú MR, Shier TW, Dano SD, Ueno Y & Creppy EE 2000.
3033 Epigenetic properties of fumonisin B(1): cell cycle arrest and DNA base modification in C6 glioma
3034 cells. *Toxicology and applied pharmacology*, 164, 91-96.

3035 Mobio TA, Tavan E, Baudrimont I, Anane R, Carratú M-R, Sanni A, Gbeassor MF, Shier TW,
3036 Narbonne J-F & Creppy EE 2003. Comparative study of the toxic effects of fumonisin B1 in rat C6
3037 glioma cells and p53-null mouse embryo fibroblasts. *Toxicology*, 183, 65-75.

3038 Moore LD, Le T & Fan G 2013. DNA methylation and its basic function. *Neuropsychopharmacology*,
3039 38, 23-38.

3040 Nguyen T, Nioi P & Pickett CB 2009. The Nrf2-antioxidant response element signaling pathway and
3041 its activation by oxidative stress. *J Biol Chem*, 284, 13291-13295.

3042 O'Brien J, Hayder H, Zayed Y & Peng C 2018. Overview of MicroRNA Biogenesis, Mechanisms of
3043 Actions, and Circulation. *Frontiers in Endocrinology*, 9.

3044 Odhav B & Bhoola K 2008. Modulating effects of fumonisin B1 and ochratoxin A on leukocytes and
3045 messenger cytokines of the human immune system. *International immunopharmacology*, 8, 799-809.

3046 Okabe I, Hiraoka H & Miki K 2015. Influence of harvest time on fumonisin contamination of forage
3047 maize for whole-crop silage. *Mycoscience*, 56, 470-475.

3048 Oswald IP, Desautels C, Laffitte J, Fournout S, Peres SY, Odin M, Le Bars P, Le Bars J & Fairbrother
3049 JM 2003. Mycotoxin Fumonisin B1 Increases Intestinal Colonization by Pathogenic Escherichia coli in
3050 Pigs. *Applied and Environmental Microbiology*, 69, 5870-5874.

3051 Oswald IP, Marin DE, Bouhet S, Pinton P, Taranu I & Accensi F 2005. Immunotoxicological risk of
3052 mycotoxins for domestic animals. *Food Additives & Contaminants*, 22, 354-360.

3053 Pellanda H, Forges T, Bressenot A, Chango A, Bronowicki JP, Guéant JL & Namour F 2012. Fumonisin
3054 FB1 treatment acts synergistically with methyl donor deficiency during rat pregnancy to produce
3055 alterations of H3- and H4-histone methylation patterns in fetuses. *Molecular nutrition & food research*,
3056 56, 976-985.

3057 Peschansky VJ & Wahlestedt C 2014. Non-coding RNAs as direct and indirect modulators of epigenetic
3058 regulation. *Epigenetics*, 9, 3-12.

3059 Phaniendra A, Jestadi DB & Periyasamy L 2015. Free radicals: properties, sources, targets, and their
3060 implication in various diseases. *Indian J Clin Biochem*, 30, 11-26.

3061 Phokane S, Flett BC, Ncube E, Rheeder JP & Rose LJ 2019. Agricultural practices and their potential
3062 role in mycotoxin contamination of maize and groundnut subsistence farming. *South African Journal*
3063 *of Science*, 115, 1-6.

3064 Piacentini KC, Rocha LO, Fontes LC, Carnielli L, Reis TA & Corrêa B 2017. Mycotoxin analysis of
3065 industrial beers from Brazil: The influence of fumonisin B1 and deoxynivalenol in beer quality. *Food*
3066 *chemistry*, 218, 64-69.

3067 Pizzino G, Irrera N, Cucinotta M, Pallio G, Mannino F, Arcoraci V, Squadrito F, Altavilla D & Bitto A
3068 2017. Oxidative Stress: Harms and Benefits for Human Health. *Oxid Med Cell Longev*, 2017, 8416763-
3069 8416763.

3070 Pizzolitto RP, Salvano MA & Dalcerro AM 2012. Analysis of fumonisin B1 removal by microorganisms
3071 in co-occurrence with aflatoxin B1 and the nature of the binding process. *International Journal of Food*
3072 *Microbiology*, 156, 214-221.

3073 Podhorecka M, Skladanowski A & Bozko P 2010. H2AX Phosphorylation: Its Role in DNA Damage
3074 Response and Cancer Therapy. *J Nucleic Acids*, 2010, 920161.

3075 Qian G, Tang L, Lin S, Xue KS, Mitchell NJ, Su J, Gelderblom WC, Riley RT, Phillips TD & Wang J-
3076 S 2016. Sequential dietary exposure to aflatoxin B1 and fumonisin B1 in F344 rats increases liver
3077 preneoplastic changes indicative of a synergistic interaction. *Food and chemical toxicology* 95, 188-
3078 195.

3079 Qiu M, Liu X, Wang Y & Zhang C 2001. [Survey on the fumonisins intake and the urinary Sa/So ratio
3080 of people suffered from a high incidence of esophageal cancer]. *Wei Sheng Yan Jiu*, 30, 365-367.

3081 Ramljak D, Calvert RJ, Wiesenfeld PW, Diwan BA, Catipovic B, Marasas WFO, Victor TC, Anderson
3082 LM & Gelderblom WCA 2000. A potential mechanism for fumonisin B1-mediated
3083 hepatocarcinogenesis: cyclin D1 stabilization associated with activation of Akt and inhibition of GSK-
3084 β activity. *Carcinogenesis*, 21, 1537-1546

3085 Reddy B & Raghavender C 2008. Outbreaks of fusarial-toxicoses in India. *Cereal Research*
3086 *Communications*, 36, 321-325.

3087 Rheeder JP, Marasas WFO & Vismer HF 2002. Production of Fumonisin Analogs by *Fusarium* Species.
3088 *Applied and Environmental Microbiology*, 68, 2101-2105.

3089 Riley RT, Enongene E, Voss KA, Norred WP, Meredith FI, Sharma RP, Spitsbergen J, Williams DE,
3090 Carlson DB & Merrill AH, Jr. 2001. Sphingolipid perturbations as mechanisms for fumonisin
3091 carcinogenesis. *Environ Health Perspect*, 109 Suppl 2, 301-308.

3092 Riley RT, Showker JL, Lee CM, Zipperer CE, Mitchell TR, Voss KA, Zitomer NC, Torres O, Matute
3093 J, Gregory SG, et al. 2015a. A blood spot method for detecting fumonisin-induced changes in putative
3094 sphingolipid biomarkers in LM/Bc mice and humans. *Food additives & contaminants. Part A,*
3095 *Chemistry, analysis, control, exposure & risk assessment*, 32, 934-949.

3096 Riley RT, Torres O, Matute J, Gregory SG, Ashley-Koch AE, Showker JL, Mitchell T, Voss KA,
3097 Maddox JR & Gelineau-van Waes JB 2015b. Evidence for fumonisin inhibition of ceramide synthase
3098 in humans consuming maize-based foods and living in high exposure communities in Guatemala.
3099 *Molecular nutrition & food research*, 59, 2209-2224.

3100 Riley RT & Merrill AH, Jr. 2019. Ceramide synthase inhibition by fumonisins: a perfect storm of
3101 perturbed sphingolipid metabolism, signaling, and disease. *Journal of lipid research*, 60, 1183-1189.

3102 Robinson A, Johnson NM, Strey A, Taylor JF, Marroquin-Cardona A, Mitchell NJ, Afriyie-Gyawu E,
3103 Ankrah NA, Williams JH, Wang JS, et al. 2012. Calcium montmorillonite clay reduces urinary
3104 biomarkers of fumonisin B1 exposure in rats and humans. *Food Additives & Contaminants: Part A*, 29,
3105 809-818.

3106 Saksouk N, Simboeck E & Déjardin J 2015. Constitutive heterochromatin formation and transcription
3107 in mammals. *Epigenetics Chromatin*, 8, 3-3.

3108 Sancak D & Ozden S 2015. Global histone modifications in Fumonisin B1 exposure in rat kidney
3109 epithelial cells. *Toxicology in vitro : an international journal published in association with BIBRA*, 29,
3110 1809-1815.

3111 Schmelz EM, Dombrink-Kurtzman MA, Roberts PC, Kozutsumi Y, Kawasaki T & Merrill AH 1998.
3112 Induction of apoptosis by fumonisin B1 in HT29 cells is mediated by the accumulation of endogenous
3113 free sphingoid bases. *Toxicology and applied pharmacology*, 148, 252-260.

3114 Schwarz DS & Blower MD 2016. The endoplasmic reticulum: structure, function and response to
3115 cellular signaling. *Cell Mol Life Sci*, 73, 79-94.

3116 Seiferlein M, Humpf H-U, Voss KA, Sullards MC, Allegood JC, Wang E & Merrill Jr. AH 2007.
3117 Hydrolyzed fumonisins HFB1 and HFB2 are acylated in vitro and in vivo by ceramide synthase to form
3118 cytotoxic N-acyl-metabolites. *Molecular nutrition & food research*, 51, 1120-1130.

3119 Senft D & Ronai ZeA 2015. UPR, autophagy, and mitochondria crosstalk underlies the ER stress
3120 response. *Trends Biochem Sci*, 40, 141-148.

3121 Sharma RP, Bhandari N, Riley RT, Voss KA & Meredith FI 2000. Tolerance to fumonisin toxicity in a
3122 mouse strain lacking the P75 tumor necrosis factor receptor. *Toxicology*, 143, 183-194.

3123 Sharma RP, Bhandari N, He Q, Riley RT & Voss KA 2001. Decreased fumonisin hepatotoxicity in
3124 mice with a targeted deletion of tumor necrosis factor receptor 1. *Toxicology*, 159, 69-79.

3125 Sharma RP, He Q & Johnson VJ 2003. Deletion of IFN-gamma reduces fumonisin-induced
3126 hepatotoxicity in mice via alterations in inflammatory cytokines and apoptotic factors. *Journal of*
3127 *interferon & cytokine research : the official journal of the International Society for Interferon and*
3128 *Cytokine Research*, 23, 13-23.

3129 Sharma S, Kelly TK & Jones PA 2010. Epigenetics in cancer. *Carcinogenesis*, 31, 27-36.

3130 Sheaffer KL, Elliott EN & Kaestner KH 2016. DNA Hypomethylation Contributes to Genomic
3131 Instability and Intestinal Cancer Initiation. *Cancer Prev Res (Phila)*, 9, 534-546

3132 Shephard GS, Burger H-M, Rheeder JP, Alberts JF & Gelderblom WCA 2019. The effectiveness of
3133 regulatory maximum levels for fumonisin mycotoxins in commercial and subsistence maize crops in
3134 South Africa. *Food Control*, 97, 77-80.

3135 Shirima CP, Kimanya ME, Routledge MN, Srey C, Kinabo JL, Humpf H-U, Wild CP, Tu Y-K & Gong
3136 YY 2015. A prospective study of growth and biomarkers of exposure to aflatoxin and fumonisin during
3137 early childhood in Tanzania. *Environ Health Perspect*, 123, 173-178.

3138 Singh MP & Chul S 2017. Endoplasmic reticulum stress-mediated autophagy activation attenuates
3139 fumonisin B1 induced hepatotoxicity in vitro and in vivo. *Food and Chemical Toxicology*, 110, 371–
3140 382.

3141 Smith ZD & Meissner A 2013. DNA methylation: roles in mammalian development. *Nature Reviews*
3142 *Genetics*, 14, 204-220.

3143 Soriano JM, González L & Catalá AI 2005. Mechanism of action of sphingolipids and their metabolites
3144 in the toxicity of fumonisin B1. *Progress in lipid research*, 44, 345-356.

3145 Stevens FJ & Argon Y 1999. Protein folding in the ER. *Seminars in Cell & Developmental Biology*, 10,
3146 443-454.

3147 Stockmann-Juvala H, Mikkola J, Naarala J, Loikkanen J, Elovaara E & Savolainen K 2004a. Oxidative
3148 stress induced by fumonisin B1 in continuous human and rodent neural cell cultures. *Free radical*
3149 *research*, 38, 933-942.

3150 Stockmann-Juvala H, Mikkola J, Naarala J, Loikkanen J, Elovaara E & Savolainen K 2004b. Fumonisin
3151 B1-induced toxicity and oxidative damage in U-118MG glioblastoma cells. *Toxicology*, 202, 173-183.

3152 Sun G, Wang S, Hu X, Su J, Huang T, Yu J, Tang L, Gao W & Wang J-S 2007. Fumonisin B1
3153 contamination of home-grown corn in high-risk areas for esophageal and liver cancer in China. *Food*
3154 *Additives & Contaminants*, 24, 181-185.

3155 Sun G, Wang S, Hu X, Su J, Zhang Y, Xie Y, Zhang H, Tang L & Wang JS 2011. Co-contamination
3156 of aflatoxin B1 and fumonisin B1 in food and human dietary exposure in three areas of China. *Food*
3157 *Additives & Contaminants: Part A*, 28, 461-470.

3158 Sun K, Deng W, Zhang S, Cai N, Jiao S, Song J & Wei L 2013. Paradoxical roles of autophagy in
3159 different stages of tumorigenesis: protector for normal or cancer cells. *Cell Biosci*, 3, 35-35.

3160 Surai P & Mezes M 2005. Mycotoxins and immunity: theoretical consideration and practical
3161 applications. *Praxis veterinaria*, 53, 71-88.

3162 Sydenham EW, Thiel PG, Marasas WF, Shephard GS, Van Schalkwyk DJ & Koch KR 1990. Natural
3163 occurrence of some Fusarium mycotoxins in corn from low and high esophageal cancer prevalence
3164 areas of the Transkei, Southern Africa. *J Agric Food Chem*, 38, 1900-1903.

3165 Taranu I, Marin DE, Bouhet S, Pascale F, Bailly J-D, Miller JD, Pinton P & Oswald IP 2005. Mycotoxin
3166 Fumonisin B1 Alters the Cytokine Profile and Decreases the Vaccinal Antibody Titer in Pigs.
3167 *Toxicological Sciences*, 84, 301-307.

3168 Theumer MG, Cánepa MC, López AG, Mary VS, Dambolena JS & Rubinstein HR 2010. Subchronic
3169 mycotoxicoses in Wistar rats: assessment of the in vivo and in vitro genotoxicity induced by fumonisins
3170 and aflatoxin B(1), and oxidative stress biomarkers status. *Toxicology*, 268, 104-110.

3171 Tornyos G, Kovács M, Rusvai M, Horn P, Fodor J & Kovacs F 2003. Effect of dietary fumonisin B1
3172 on certain immune parameters of weaned pigs. *Acta Veterinaria Hungarica*, 51, 171-179.

3173 Torres OA, Palencia E, de Pratdesaba LL, Grajeda R, Fuentes M, Speer MC, Merrill Jr AH, O'Donnell
3174 K, Bacon CW & Glenn AE 2007. Estimated fumonisin exposure in Guatemala is greatest in consumers
3175 of lowland maize. *The Journal of nutrition*, 137, 2723-2729.

3176 Tryphonas H, Bondy G, Miller J, Lacroix F, Hodgen M, Mcguire P, Fernie S, Miller D & Hayward S
3177 1997. Effects of fumonisin B1 on the immune system of Sprague-Dawley rats following a 14-day oral
3178 (gavage) exposure. *Toxicological Sciences*, 39, 53-59.

3179 Valavanidis A, Vlachogianni T & Fiotakis C 2009. 8-hydroxy-2'-deoxyguanosine (8-OHdG): A critical
3180 biomarker of oxidative stress and carcinogenesis. *J Environ Sci Health C*, 27, 120-139.

3181 Van Den Broeck A, Brambilla E, Moro-Sibilot D, Lantuejoul S, Brambilla C, Eymin B, Khochbin S &
3182 Gazzeri S 2008. Loss of Histone H4K20 Trimethylation Occurs in Preneoplasia and Influences
3183 Prognosis of Non-Small Cell Lung Cancer. *Clinical Cancer Research*, 14, 7237-7245.

3184 van der Westhuizen L, Shephard GS, Burger HM, Rheeder JP, Gelderblom WCA, Wild CP & Gong
3185 YY 2011. Fumonisin B1 as a Urinary Biomarker of Exposure in a Maize Intervention Study Among
3186 South African Subsistence Farmers. *Cancer Epidemiology Biomarkers & Prevention*, 20, 483-489.

3187 Varga J, Kocsubé S, Suri K, Szigeti G, Szekeres A, Varga M, Tóth B & Bartók T 2010. Fumonisin
3188 contamination and fumonisin producing black Aspergilli in dried vine fruits of different origin.
3189 *International Journal of Food Microbiology*, 143, 143-149.

3190 Voss K, Ryu D, Jackson L, Riley R & Waes J 2017. Reduction of Fumonisin Toxicity by Extrusion and
3191 Nixtamalization (Alkaline Cooking). *J Agric Food Chem*, 65.

3192 Voss KA, Bacon CW, Meredith FI & Norred WP 1996. Comparative subchronic toxicity studies of
3193 nixtamalized and water-extracted *Fusarium moniliforme* culture material. *Food and Chemical*
3194 *Toxicology*, 34, 623-632.

3195 Voss KA, Howard PC, Riley RT, Sharma RP, Bucci TJ & Lorentzen RJ 2002. Carcinogenicity and
3196 mechanism of action of fumonisin B1: a mycotoxin produced by *Fusarium moniliforme* (= *F.*
3197 *verticillioides*). *Cancer detection and prevention*, 26, 1-9.

3198 Voss KA, Riley RT, Jackson LS, Jablonski JE, Bianchini A, Bullerman LB, Hanna MA & Ryu D 2011.
3199 Extrusion cooking with glucose supplementation of fumonisin-contaminated corn grits protects against
3200 nephrotoxicity and disrupted sphingolipid metabolism in rats. *Molecular nutrition & food research*, 55,
3201 S312-S320.

3202 Voss KA, Riley RT, Moore ND & Burns TD 2013. Alkaline cooking (nixtamalisation) and the reduction
3203 in the in vivo toxicity of fumonisin-contaminated corn in a rat feeding bioassay. *Food Additives &*
3204 *Contaminants: Part A*, 30, 1415-1421.

3205 Wan L-YM, Woo C-SJ, Turner PC, Wan JM-F & El-Nezami H 2013. Individual and combined effects
3206 of *Fusarium* toxins on the mRNA expression of pro-inflammatory cytokines in swine jejunal epithelial
3207 cells. *Toxicology letters*, 220, 238-246.

3208 Wang E, Norred WP, Bacon CW, Riley RT & Merrill AH, Jr. 1991. Inhibition of sphingolipid
3209 biosynthesis by fumonisins. Implications for diseases associated with *Fusarium moniliforme*. *J Biol*
3210 *Chem*, 266, 14486-14490.

- 3211 Wang H, Wei H, Ma J & Luo X 2000. The fumonisin B1 content in corn from North China, a high-risk
3212 area of esophageal cancer. *J Environ Pathol Toxicol Oncol*, 19, 139-141.
- 3213 Waskiewicz A, Irzykowska L, Bocianowski J, Karolewski Z, Kostecki M, Weber Z & Golinski P 2010.
3214 Occurrence of Fusarium Fungi and Mycotoxins in Marketable Asparagus Spears. *Polish Journal of*
3215 *Environmental Studies*, 19, 219-225.
- 3216 Wild CP & Gong YY 2010. Mycotoxins and human disease: a largely ignored global health issue.
3217 *Carcinogenesis*, 31, 71-82.
- 3218 Wilson TM, Nelson PE & Knepp C 1985. Hepatic neoplastic nodules, adenofibrosis, and
3219 cholangiocarcinomas in male Fisher 344 rats fed corn naturally contaminated with Fusarium
3220 moniliforme. *Carcinogenesis*, 6, 1155-1160.
- 3221 Yang W-C, Hwang Y-S, Chen Y-Y, Liu C-L, Shen C-N, Hong W-H, Lo S-M & Shen C-R 2017.
3222 Interleukin-4 Supports the Suppressive Immune Responses Elicited by Regulatory T Cells. *Front*
3223 *Immunol*, 8, 1508-1508.
- 3224 Yao ZG, Zhang XH, Hua F, Wang J, Xing X, Wang JL, Yan X & Xing LX 2010. Effects of fumonisin
3225 B1 on HLA class I antigen presentation and processing pathway in GES-1 cells in vitro. *Human &*
3226 *experimental toxicology*, 30, 379-390.
- 3227 Yin S, Guo X, Li J, Fan L & Hu H 2016. Fumonisin B1 induces autophagic cell death via activation of
3228 ERN1-MAPK8/9/10 pathway in monkey kidney MARC-145 cells. *Archives of Toxicology*, 90, 985-
3229 996.
- 3230 Yoo HS, Norred WP, Wang E, Merrill AH, Jr. & Riley RT 1992. Fumonisin inhibition of de novo
3231 sphingolipid biosynthesis and cytotoxicity are correlated in LLC-PK1 cells. *Toxicology and applied*
3232 *pharmacology*, 114, 9-15.
- 3233 Yorimitsu T, Nair U, Yang Z & Klionsky DJ 2006. Endoplasmic reticulum stress triggers autophagy.
3234 *Journal of Biological Chemistry*, 281, 30299-30304.
- 3235 Yoshizawa T, Yamashita A & Luo Y 1994. Fumonisin occurrence in corn from high- and low-risk areas
3236 for human esophageal cancer in China. *Applied and Environmental Microbiology*, 60, 1626-1629.
- 3237 Yu S, Jia B, Yang Y, Liu N & Wu A 2020. Involvement of PERK-CHOP pathway in fumonisin B1-
3238 induced cytotoxicity in human gastric epithelial cells. *Food and Chemical Toxicology*, 136, 111080.
- 3239 Zadeh MHB & Shahdadi H 2015. Nanocellulose coated with various free fatty acids can adsorb
3240 fumonisin B1, and decrease its toxicity. *Colloids and Surfaces B: Biointerfaces*, 134, 26-30.
- 3241 Zhang W, Zhang S, Zhang M, Yang L, Cheng B, Li J & Shan A 2018. Individual and combined effects
3242 of Fusarium toxins on apoptosis in PK15 cells and the protective role of N-acetylcysteine. *Food and*

3243 *chemical toxicology : an international journal published for the British Industrial Biological Research*
3244 *Association*, 111, 27-43.

3245 Zitomer NC, Mitchell T, Voss KA, Bondy GS, Pruett ST, Garnier-Amblard EC, Liebeskind LS, Park
3246 H, Wang E, Sullards MC, et al. 2009. Ceramide synthase inhibition by fumonisin B1 causes
3247 accumulation of 1-deoxysphinganine: a novel category of bioactive 1-deoxysphingoid bases and 1-
3248 deoxydihydroceramides biosynthesized by mammalian cell lines and animals. *J Biol Chem*, 284, 4786-
3249 4795.

3250

3251

3252

3253

3254

3255

3256

3257

3258

3259

3260

3261

3262

3263

3264

3265

3266

3267

3268

3269

3270

3271

3272 **CHAPTER 4**

3273 **Fumonisin B₁ Epigenetically Regulates PTEN Expression and Modulates DNA Damage**
3274 **Checkpoint Regulation in HepG2 Liver Cells**

3275 **Thilona Arumugam, Terisha Ghazi ¹, and Anil Chuturgoon ***

3276 Discipline of Medical Biochemistry and Chemical Pathology, School of Laboratory Medicine and
3277 Medical Sciences, College of Health Sciences, George Campbell Building, Howard College, University
3278 of KwaZulu-Natal, Durban 4041, South Africa.

3279 *Corresponding author: Professor Anil A. Chuturgoon, Discipline of Medical Biochemistry and
3280 Chemical Pathology, School of Laboratory Medicine and Medical Science, College of Health Sciences,
3281 Howard College Campus, University of Kwa-Zulu Natal, Durban 4041, South Africa. Telephone: +27
3282 31 260 4404; Fax: +27 31 260 4785; Email: CHUTUR@ukzn.ac.za

3283 Author Email Addresses:

3284 Thilona Arumugam: cyborglona@gmail.com

3285 Terisha Ghazi: terishaghazi@gmail.com

3286 Anil A. Chuturgoon: CHUTUR@ukzn.ac.za

3287

3288

3289 **Toxins** 12(10): 625 (2020)

3290 **DOI:** 10.3390/toxins12100625

3291

3292

3293

3294

3295

3296

3297

3298

3299

3300

3301 **Abstract**

3302 Fumonisin B₁ (FB₁), a *Fusarium*-produced mycotoxin, is found in various foods and feeds. It is a well-
3303 known liver carcinogen in experimental animals; however, its role in genotoxicity is controversial. The
3304 current study investigated FB₁-triggered changes in the epigenetic regulation of PTEN and determined
3305 its effect on DNA damage checkpoint regulation in human liver hepatoma G2 (HepG2) cells. Following
3306 treatment with FB₁ (IC₅₀: 200 μM; 24 h), the expression of miR-30c, KDM5B, PTEN, H3K4me3, PI3K,
3307 AKT, p-ser473-AKT, CHK1, and p-ser280-CHK1 was measured using qPCR and/or Western blot.
3308 H3K4me3 enrichment at the PTEN promoter region was assayed via a ChIP assay and DNA damage
3309 was determined using an ELISA. FB₁ induced oxidative DNA damage. Total KDM5B expression was
3310 reduced, which subsequently increased the total H3K4me3 and the enrichment of H3K4me3 at PTEN
3311 promoters. Increased H3K4me3 induced an increase in PTEN transcript levels. However, miR-30c
3312 inhibited PTEN translation. Thus, PI3K/AKT signaling was activated, inhibiting CHK1 activity via
3313 phosphorylation of its serine 280 residue preventing the repair of damaged DNA. In conclusion, FB₁
3314 epigenetically modulates the PTEN/PI3K/AKT signaling cascade, preventing DNA damage checkpoint
3315 regulation, and induces significant DNA damage.

3316 **Keywords:** Fumonisin B₁; DNA damage; epigenetics; PTEN; H3K4me3; Checkpoint Kinase 1

3317 **Key Contributions**

3318 Fumonisin B₁ (FB₁) induces oxidative damage to DNA and alters the epigenetic status of cells. This
3319 study confirms the genotoxic potential of FB₁ and provides novel insight into the impairment of DNA
3320 damage responses by FB₁ via the epigenetic downregulation of PTEN; which in turns inhibits DNA
3321 damage checkpoint regulation via the PI3K/AKT/CHK1 axis. The diminished repair of FB₁-induced
3322 oxidative DNA lesions may contribute to the cytotoxic effects of FB₁.

3323 **Introduction**

3324 Fumonisin B₁ (FB₁) is a major food-borne mycotoxin produced by fungi belonging to the *Fusarium* genus [1,2].
3325 Presently, 28 fumonisin homologues have been characterized into the following groups: fumonisins A,
3326 B, C, and P [2]. Over 70% of fumonisins produced are fumonisin B₁ (FB₁), making it the most prevalent
3327 and toxicologically relevant homologue [3]. FB₁ contamination is common in maize and cereal-related
3328 products in several countries throughout the world, with concentrations reaching as high as 30,000
3329 μg/kg [4]. Poor food processing, handling, and storage conditions aide FB₁ contamination, thereby
3330 increasing the risk of exposure for both animals and humans [5]. The effect of FB₁ in animals is sex-
3331 dependent and has species-specific toxicity, with the liver, kidney, and nervous system being the most
3332 common targets [6–11]. The International Agency for Research on Cancer (IARC) has classified FB₁
3333 as a class 2B carcinogen [12]. Studies on rodents have demonstrated that FB₁ can initiate and promote
3334 cancer [1,13], while the consumption of FB₁-contaminated commodities has been associated with
3335 increased incidence of hepatocellular and/or esophageal carcinomas [14,15]. Earlier studies have

3336 dismissed FB₁ as a mutagen and reported that FB₁ is a weak genotoxin [16] or that it showed no signs
3337 of genotoxicity [17,18]. Irrespective of these earlier studies, numerous studies have since observed that
3338 a consequence of FB₁ exposure is extensive DNA damage through strand breaks, micronuclei induction,
3339 and fragmentation [19–21].

3340 Cells are equipped with a complex network of DNA damage responses (DDRs) that coordinate DNA
3341 repair and consequently cell fate [22]. The tumor suppressor phosphatase and tensin homolog (PTEN)
3342 controls multiple cellular processes including growth and differentiation by opposing the
3343 phosphoinositide 3-kinases (PI3K)/protein kinase B (AKT) signaling cascade [23,24]. Emerging
3344 evidence has demonstrated the unique role PTEN plays in maintaining genomic stability and DNA
3345 repair [25,26]. PTEN responds to DNA damage by inhibiting the PI3K/AKT cascade and preventing
3346 the inhibitory phosphorylation of checkpoint kinase 1 (CHK1). This activates checkpoint regulation
3347 and induces cell cycle arrest, which allows for the repair of DNA [27,28]. Underlining the important
3348 role of PTEN, poor expression of PTEN is a common risk factor in the occurrence of liver pathologies
3349 [29,30]. Studies have elucidated that poor expression of PTEN may be due to epigenetic alterations
3350 [31]. Small non-coding RNAs, known as microRNAs (miRNA), such as miR-19a and miR-21, reduce
3351 PTEN gene expression by binding to the 3' untranslated region (3'UTR) of *PTEN* mRNA and inhibits
3352 its translation [32,33], while the trimethylation of lysine 4 residues of histone 3 (H3K4me3) on the
3353 promoter region of *PTEN* is associated with active transcription [34].

3354 While the role of PTEN in cellular functioning has been well established, further research should be
3355 undertaken to determine the epigenetic mechanisms in which PTEN is regulated. Moreover, the
3356 epigenetic effects of FB₁ in humans have only recently begun to be uncovered and no study to date has
3357 determined the effects FB₁ has on PTEN [21,35]. Previously, Chuturgoon et al. [35] conducted miRNA
3358 profile arrays in human hepatoma G2 (HepG2) cells following FB₁ exposure and found miR-30c to be
3359 one of the major miRNAs affected. Through computational prediction analysis, we found a possible
3360 link between miR30c, PTEN, and the histone lysine demethylase 5B (KDM5B). KDM5B catalyzes the
3361 removal of methyl groups from histone 3 lysine 4 (H3K4) [36]. H3K4me3 is predominantly found at
3362 transcriptional start sites, where it promotes gene transcription [37]. Therefore, we proposed that
3363 together miR-30c and KDM5B mediate the epigenetic regulation of PTEN. The current study
3364 determined the consequences of FB₁ exposure on DNA damage and DNA damage checkpoint
3365 regulation via the PTEN/PI3K/AKT network. Further, we determined FB₁ epigenetic regulation of
3366 PTEN via miR-30c and H3K4me3 in human liver (HepG2) cells.

3367 **Method and Materials**

3368 ***Materials***

3369 FB₁ (*Fusarium moniliforme*, 62580) was purchased from Cayman Chemicals (Michigan, MI, USA).
3370 The HepG2 cell line (HB-8065) was procured from the American Type Culture Collection (ATCC).

3371 Cell culture consumables were purchased from Whitehead Scientific (Johannesburg, South Africa).
3372 Western blot reagents were obtained from Bio-Rad (California, CA, USA). All other reagents were
3373 purchased from Merck (Massachusetts, MA, USA), unless otherwise stated.

3374 ***Cell Culture and Treatments***

3375 HepG2 cells (passage 3; 1.5×10^6) were cultured in complete culture media [CCM: Eagle's Minimum
3376 Essentials Medium (EMEM) supplemented with 10% fetal calf serum, 1% penicillin–streptomycin–
3377 fungizone, and 1% L-glutamine] at 37°C in a 5% CO₂ humidified incubator until 80% confluent.
3378 Thereafter, cells were treated with varying concentrations of FB₁ (5, 100, and 200 μM) for 24 h. These
3379 FB₁ concentrations were obtained from the crystal violet assay (Supplementary Figure S4.1) and
3380 represented 90%, 70%, and 50% cell viabilities, respectively. An untreated control was prepared along
3381 with the FB₁ treatments. Data obtained using 200 μM FB₁ (IC₅₀) are shown in the main text. The results
3382 for all assays conducted using 5 and 100 μM FB₁ are available in the Supplementary material
3383 (Supplementary Figure S4.2–S4.7). Results were verified by performing two independent experiments
3384 in triplicate.

3385 ***DNA Damage***

3386 DNA was isolated using the FlexiGene DNA isolation kit (Qiagen, Hilden, Germany, 512608).
3387 Extracted DNA was used to determine 8-OHdG levels using the DNA damage ELISA kit (Enzo Life
3388 Sciences, New York, USA, ADI-EKS-350), as per the manufacturer's instructions.

3389 ***RNA Isolation and Quantitative Polymerase Chain Reaction (qPCR)***

3390 RNA was isolated according to the method described by Ghazi et al. (2019) [38]. For miRNA
3391 expression, cDNA was synthesized using the miScript II RT Kit (Qiagen, Hilden, Germany, 218161),
3392 as per the manufacturer's instructions. The expression of miR-30c was analyzed using the miScript
3393 SYBR Green PCR Kit (Qiagen, Hilden, Germany, 218073) and the miR-30c primer assay (Qiagen,
3394 Hilden, Germany, MS00009366), as per the manufacturer's instructions. Samples were amplified using
3395 the CFX96 Touch™ Real-Time PCR Detection System (Bio-Rad, Hercules, CA, USA) with the
3396 following cycling conditions: initial denaturation (95 °C, 15 min), followed by 40 cycles of denaturation
3397 (94°C, 15 sec), annealing (55°C, 30 sec), and extension (70°C, 30 sec).

3398 For mRNA expression, cDNA was prepared using the Maxima H Minus First Strand cDNA Synthesis
3399 Kit (Thermo-Fisher Scientific, Waltham, MA, USA, K1652), as per the manufacturer's instructions.
3400 The expression of *KDM5B*, *PTEN*, *AKT*, and *CHK1* was determined using the Powerup SYBR Green
3401 Master Mix (Thermo-Fisher Scientific, Waltham, MA, USA, A25742), as per the manufacturer's
3402 instructions. Samples were amplified using the CFX96 Touch™ Real-Time PCR Detection System
3403 (Bio-Rad, Hercules, CA, USA) with the following cycling conditions: initial denaturation (95°C, 8

3404 min), followed by 40 cycles of denaturation (95°C, 15 sec), annealing (Temperatures: Table 4.1, 15
 3405 sec), and extension (72°C, 30 sec).

3406 **Table 4.1. The annealing temperatures (°C) and primer sequences for the genes of interest.**

Gene	Annealing Temperature (°C)	Primer	Sequence
<i>KDM5B</i>	55	Sense	5'-CGA CAA AGC CAA GAG TCT CC-3'
		Anti-sense	5'-CTG CCG TAG CAA GGC TATTC-3'
<i>PTEN</i>	56.6	Sense	5'-TTT GAA GAC CAT AAC CCA CCA C-3'
		Anti-sense	5'-ATT ACA CCA GTT CGT CCC TTT C-3'
<i>AKT1</i>	55	Sense	5'-GCC TGG GTC AAA GAA GTC AA-3'
		Anti-sense	5'-CAT CCC TCC AAG CTA TCG TC-3'
<i>CHK1</i>	59.1	Sense	5'-CCA GAT GCT CAG AGA TTC TTC CA-3'
		Anti-sense	5'-TGT TCAACA AAC GCT CAC GAT TA-3'
<i>GAPDH</i>	Same as gene of interest	Sense	5'-TCCACCACCCTGTTGCTGTA-3'
		Anti-sense	5'-ACCACAGTCCATGCCATCAC-3'

3407

3408 Relative gene expression was determined using the method described by Livak and Schmittgen [39]. $2^{-\Delta\Delta Ct}$
 3409 $\Delta\Delta Ct$ represents the fold change relative to the untreated control. miRNA and mRNA of interest were
 3410 normalized against the house-keeping genes, *RNU6* (Qiagen, Hilden, Germany, Ms000033740) and
 3411 *GAPDH*, respectively.

3412 **Chromatin Immunoprecipitation Assay**

3413 H3K4me3 at the *PTEN* promoter region was determined using the chromatin immunoprecipitation
 3414 (ChIP) assay. Histones were crosslinked to DNA by incubating (37°C, 10 min) the cells in 37%
 3415 formaldehyde. Cells were washed in cold 0.1 M PBS (containing protease inhibitors), mechanically
 3416 lysed and centrifuged (2000 rpm, 4°C, 4 min). The DNA pellet was re-suspended in sodium dodecyl

3417 sulphate (SDS)–lysis buffer (200 µl; 1% SDS, 10 mM ethylenediaminetetraacetic acid (EDTA), and 50
3418 mM Tris; pH 8.1) and sheared by homogenization. Samples were centrifuged (13,000 rpm, 4°C, 10
3419 min) and supernatants were diluted with CHIP dilution buffer [0.01% SDS, 1.1% Tritonx-100, 1.2 mM
3420 EDTA, 16.7 mM Tris-HCl (pH 8.1), and 167 mM NaCl]. The diluted supernatants were split into equal
3421 fractions. Anti-H3K4me3 (Abcam, Cambridge, UK, ab12209) was added to one fraction, while no
3422 antibody was added to its counterpart. Both fractions were incubated overnight at 4°C. A 50% slurry of
3423 Protein A agarose and salmon sperm DNA (Merck, Kenilworth, NJ, USA, 16-157) was added to all
3424 samples and incubated (4°C, 1 h) with gentle rotation. Thereafter, samples were centrifuged (1000 rpm,
3425 4 °C, 1 min), and pellets were washed once with the following buffers: low salt immune complex wash
3426 buffer (0.1% SDS, 1% Tritonx-100, 2 mM EDTA, 20 mM Tris-HCl (pH 8.1), and 150 Mm NaCl), high
3427 salt immune complex wash buffer [0.1% SDS, 1% Tritonx-100, 2 mM EDTA, 20 mM Tris-HCl (pH
3428 8.1), and 500 mM NaCl], Lithium chloride immune complex wash buffer (0.25 M LiCl, 1% IGEPAL,
3429 1% deoxycholic acid, 1 mM EDTA, and 10 mM Tris; pH 8.1), and twice with TE buffer (10 mM Tris-
3430 HCl, 1 mM EDTA; pH 8.0). DNA was eluted using elution buffer (1% SDS, 0.1 M NaCHO₃) for 15
3431 min (gentle rotation, RT). Samples were centrifuged (1000 rpm, 4°C, 1 min) and elution was repeated
3432 on the protein A agarose/ssDNA pellet. Eluates were combined and incubated in 5 M NaCl (65°C, 4 h)
3433 to reverse crosslinks. DNA was further purified using a DNA Clean & Concentrator-5 kit, as per the
3434 manufacturer’s instructions (Zymo research, Irvine, CA, USA, D4003).

3435 H3K4me3 immunoprecipitated chromatin was used in a RT-qPCR reaction (as previously described)
3436 to determine H3K4me3 at the *PTEN* promoter (Sense: 5'- CGC CCA GCT CCT TTT CCC-3'; Anti-
3437 sense: 5'- CTG CCG CCG ATT CTT AC-3'). The fold enrichment method was used to normalize data
3438 obtained from the CHIP-qPCR.

3439 ***Protein Isolation and Western Blotting***

3440 Protein was isolated using Cytobuster reagent (Merck, Kenilworth, NJ, USA, 71009-3) supplemented
3441 with protease and phosphatase inhibitors (Roche, Basel, Switzerland, 05892791001 and 04906837001,
3442 respectively). Cells were mechanically lysed, and centrifuged (13,000 rpm, 4°C, 10 min). Supernatants
3443 were used to quantify protein concentration via the bicinchoninic acid assay (BCA). Proteins were
3444 standardized to 1 mg/mL. The expression of KDM5B (Abcam, Cambridge, UK, ab19884), H3K4me3
3445 (Abcam, Cambridge, UK, ab12209), PTEN (Cell Signalling Technologies, Danvers, MA, USA,
3446 9552S), p-ser473-AKT (Cell Signaling Technologies, Danvers, MA, USA, 9271S), AKT (Cell
3447 Signaling Technologies, Danvers, MA, USA 9272S), PI3K (Cell Signaling Technologies, Danvers,
3448 MA, USA, 4249S), p-ser280-CBK1 (Cell Signaling Technologies, Danvers, MA, USA, 23475), and
3449 CBK1 (Cell Signaling Technologies, Danvers, MA, USA, 2360S) were determined using Western
3450 blotting as previously described [43]. The Image Lab Software version 5.0 (Bio-Rad, Hercules, CA,
3451 USA) was used to measure band densities of expressed proteins. Protein expression is represented as

3452 relative band density and calculated by normalizing the protein of interest against the housekeeping
3453 protein, β -actin.

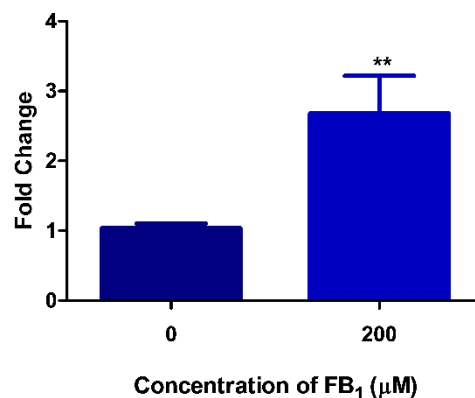
3454 *Statistical Analysis*

3455 All statistical analysis was performed using GraphPad Prism version 5.0 (GraphPad Software Inc., San
3456 Diego CA, USA). The unpaired t test was used for all assays. One-way ANOVA with Dunnet's post-
3457 test was used to evaluate the significant effect of FB₁ in all Supplementary Figures. All results are
3458 presented as the mean \pm standard deviation, unless otherwise stated. A value of $p < 0.05$ was considered
3459 to be statistically significant.

3460 **Results**

3461 *FB₁ Induces DNA Damage in HepG2 Cells*

3462 FB₁ negatively impacts redox homeostasis, which results in oxidative damage to cellular structures. We
3463 assessed FB₁-mediated DNA damage by evaluating levels of the oxidative DNA damage biomarker—
3464 8-hydroxy-2'-deoxyguanosine (8-OHdG). FB₁ significantly increased the level of 8-OHdG (2.68-fold)
3465 compared with the control ($p = 0.0061$; Control: 1.04 ± 0.0641 vs. FB₁: 2.68 ± 0.534 ; Figure 4.1.).



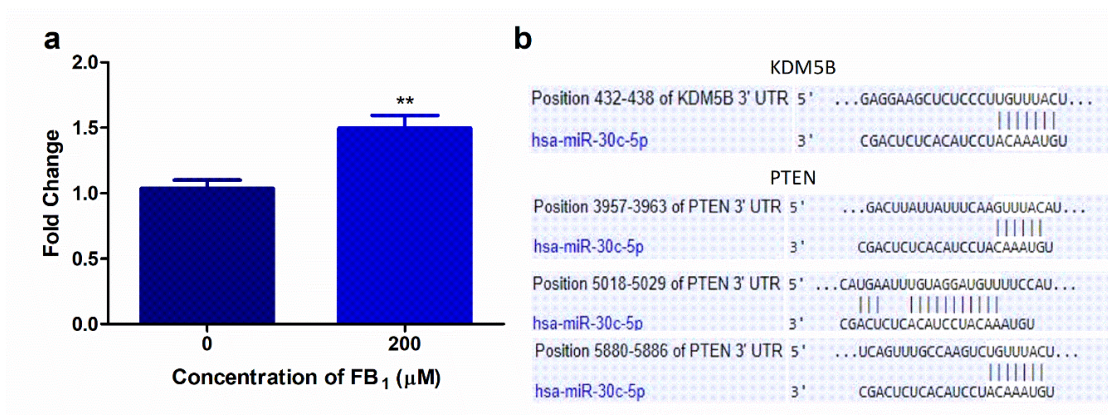
3466

3467 **Figure 4.1.** Fumonisin B₁ (FB₁) significantly increased the oxidative DNA damage biomarker, 8-
3468 OHdG, in human hepatoma G2 (HepG2) cells (** $p < 0.01$).

3469 *FB₁ Increases miR-30c Expression in HepG2 Cells*

3470 Since PTEN initiates DNA damage responses and miR-30c has been shown to disrupt DNA damage
3471 responses, we investigated the epigenetic regulation of PTEN [26,40]. miR-30c is involved in regulating
3472 cell cycle transition, proliferation, and lipid metabolism. FB₁ (IC₅₀; 200 μM) significantly upregulated
3473 miR-30c by 1.47-fold ($p = 0.0023$; Control: 1.04 ± 0.0642 vs. FB₁ 1.47 ± 0.149 ; Figure 4.2a).

3474 Target Scan version 7.2 (http://www.targetscan.org/vert_72/) was used to identify putative mRNA
 3475 targets of miR-30c. miR-30c has complimentary base pairs with *PTEN* (at positions 3957–3963, 5018–
 3476 5029, and 5880–5886 in the 3'UTR) and *KDM5B* (at positions 432–438 in the 3'UTR) (Figure 4.2b)



3477
 3478 **Figure 4.2.** The effect of FB₁ on miR-30c levels in HepG2 cells and potential miR-30c targets. **(a)**
 3479 FB₁ significantly elevated miR-30c expression (** $p \leq 0.01$). **(b)** Target Scan analysis of miR-30c
 3480 with the 3' untranslated region (3'UTR) of *KDM5B* and *PTEN*.

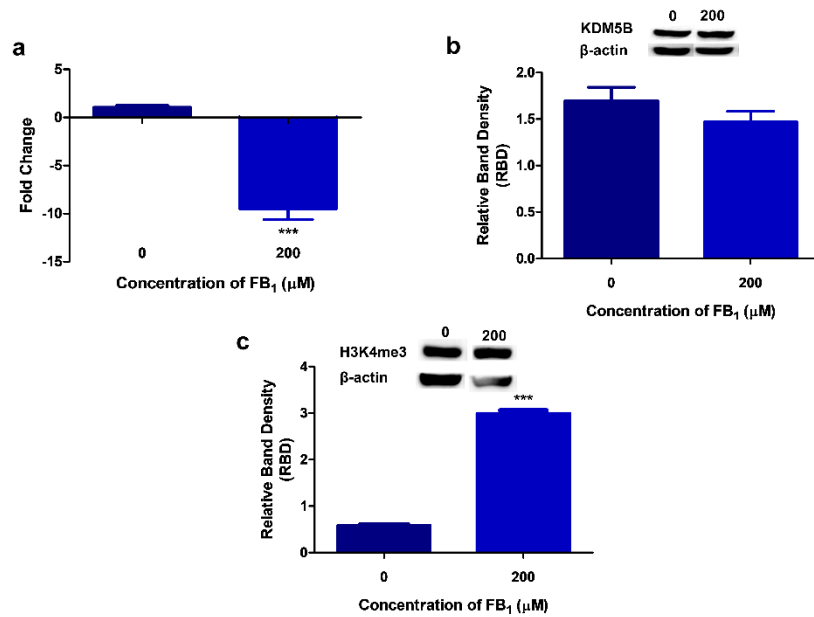
3481 ***FB₁ Induces H3K4me3 by Downregulating KDM5B in HepG2 Cells***

3482 Since FB₁ altered the expression of miR-30c (which has a complimentary sequence to KDM5B 3' UTR),
 3483 we evaluated the gene and protein expression of KDM5B. FB₁ decreased *KDM5B* transcript levels by
 3484 9.86-fold ($p < 0.0001$; Control: 1.04 ± 0.0642 vs. FB₁: 9.86 ± 1.15 ; Figure 4.3a). *KDM5B* protein
 3485 expression (Figure 4.3b) was reduced slightly ($p = 0.2966$) by FB₁ (1.47 ± 0.117 RBD) in comparison
 3486 with the control (1.70 ± 0.142 RBD).

3487 *KDM5B* is a negative regulator of H3K4me₃; hence, we determined the effect of FB₁ on H3K4me₃.
 3488 FB₁ (3.00 ± 0.0589 RBD) induced a considerable increase ($p < 0.0001$) in total H3K4me₃ compared
 3489 with the control (0.585 ± 0.00423 RBD; Figure 4.3c).

3490

3491



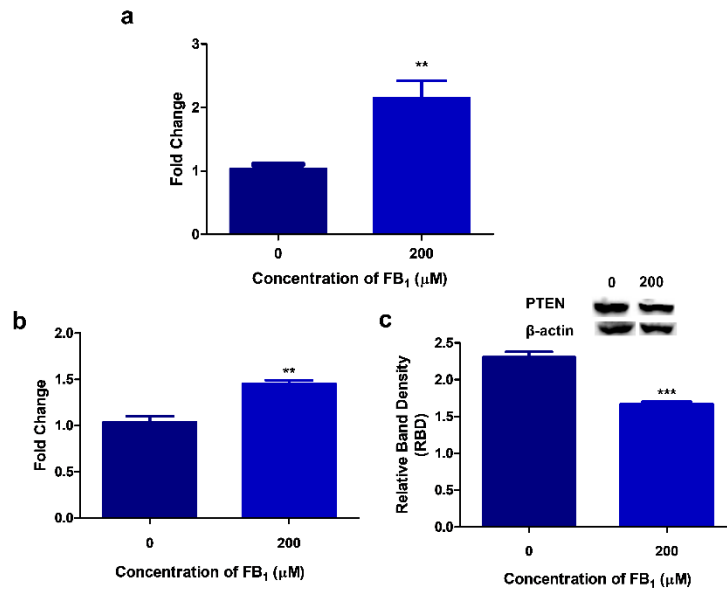
3492

3493 **Figure 4.3.** The effect of FB₁ on KDM5B and H3K4me3 levels in HepG2 cells. FB₁ reduced both
 3494 the transcript (**a**; *** $p \leq 0.0001$) and protein (**b**; $p > 0.05$) expression of KDM5B. This may have
 3495 led to the subsequent increase in total H3K4me3 (**c**; *** $p \leq 0.0001$).

3496 ***FB₁ Alters PTEN Expression in HepG2 Cells***

3497 PTEN expression may be influenced by KDM5B and miR-30c. In addition to the total H3K4me3 levels,
 3498 FB₁ also induced a significant 2.5-fold upregulation of H3K4me3 at *PTEN* promoter regions ($p =$
 3499 0.0052 ; Control: 1.04 ± 0.0641 vs. FB₁: 2.15 ± 0.273 ; Figure 4.4a).

3500 H3K4me3 at promoter regions is associated with active transcription. The FB₁-induced increase in
 3501 H3K4me3 corresponded with active transcription of the *PTEN* gene with a 1.46-fold increase ($p =$
 3502 0.0039 ; Control: 1.04 ± 0.0641 vs. FB₁: 1.46 ± 0.0354 ; Figure 4.4b). However, PTEN protein expression
 3503 was significantly downregulated ($p = 0.0001$) by FB₁ (1.67 ± 0.0110 RBD) compared with the control
 3504 (2.31 ± 0.0749 RBD; Figure 4.4c).



3505

3506 **Figure 4.4.** FB₁-induced KDM5B and miR-30c modulates PTEN expression. PTEN expression is
 3507 influenced by both KDM5B and miR-30c. FB₁ increased H3K4me3 at *PTEN* promoter regions (a; **
 3508 $p < 0.01$), which resulted in significantly higher levels of PTEN transcripts (b; ** $p < 0.01$). However,
 3509 miR-30c negatively influenced PTEN translation/protein expression (c; *** $p < 0.0001$).

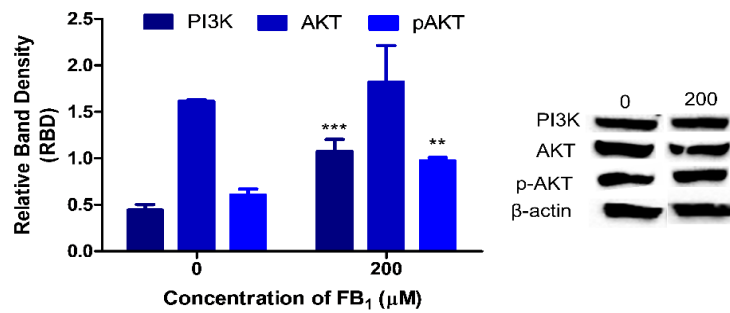
3510 *FB₁ Affects PI3K/AKT Signaling in HepG2 Cells*

3511 Numerous biological processes are regulated by the PTEN/PI3K/AKT signaling network. PI3K protein
 3512 expression ($p = 0.0014$; Figure 4.5) was 2.44-fold greater in FB₁-exposed cells (1.08 ± 0.126 RBD)
 3513 compared with the control (0.443 ± 0.0600 RBD).

3514 Total AKT protein expression was slightly increased ($p = 0.4200$; Figure 4.5) by FB₁ (Control $1.61 \pm$
 3515 0.0148 RBD vs. FB₁ 1.82 ± 0.396 RBD). AKT is activated by the phosphorylation of serine 473 within
 3516 the carboxy terminus. FB₁ significantly increased the phosphorylation of AKT ($p = 0.001$, $0.973 \pm$
 3517 0.0350 RBD; Figure 4.5) compared with the control (0.604 ± 0.0661 RBD).

3518

3519



3520

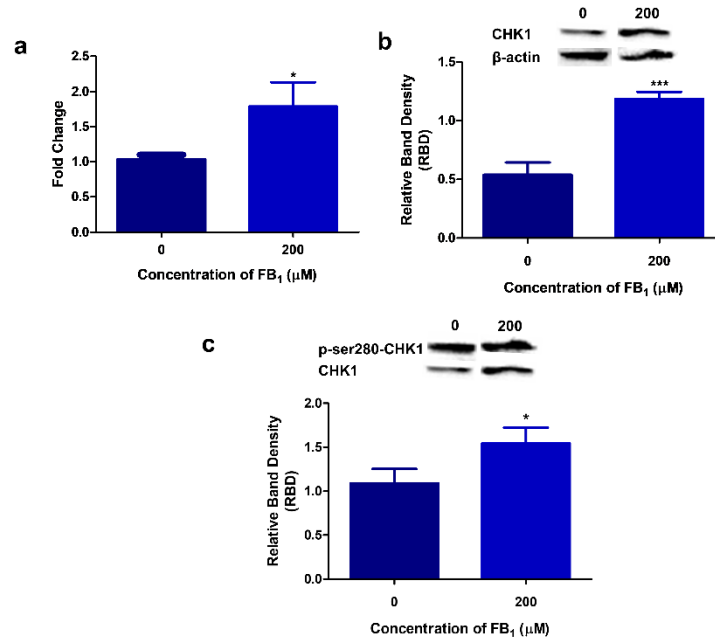
3521 **Figure 4.5.** The effect of FB₁ on the PI3K/AKT signaling cascade. The protein expression of PI3K,
 3522 AKT, and pAKT in HepG2 cells was evaluated using western blotting. FB₁ increased PI3K (***) $p <$
 3523 0.0001), AKT ($p > 0.05$), and p-ser473-AKT (** $p < 0.01$) protein expression. PI3K and AKT
 3524 expression was normalized against β-actin, and p-ser473-AKT was normalized against AKT.

3525 ***FB₁ Modulates CHK1 Expression and Activity in HepG2 Cells***

3526 CHK1 is critical in coordinating DDR and cell cycle checkpoints. FB₁ elevated *CHK1* transcript levels
 3527 by 1.79-fold ($p = 0.0209$; Figure 4.6a). Western blotting revealed an increase in total CHK1 protein
 3528 expression ($p = 0.0008$; Control 0.540 ± 0.105 RBD vs. FB₁ 1.18 ± 0.0614 RBD; Figure 4.6b). Active
 3529 PI3K/AKT signaling phosphorylates serine 280 of CHK1 and inactivates it. FB₁ significantly elevated
 3530 ($p = 0.0314$; 1.54 ± 0.179 RBD) p-ser280-CHK1 expression in comparison with the control ($1.09 \pm$
 3531 0.162 RBD; Figure 4.6c). This suggests that FB₁ inactivates CHK1 via the PI3K/AKT signaling
 3532 pathway.

3533

3534



3535

3536 **Figure 4.6.** The effect of FB₁ on CHK1 expression. FB₁ significantly increased *CHK1* transcript
 3537 levels (**a**; * $p < 0.05$), CHK1 protein expression (**b**; *** $p < 0.0001$), and p-ser280-CHK1 (**c**; * $p <$
 3538 0.05). CHK1 expression was normalized against β -actin and p-ser280-CHK1 was normalized
 3539 against CHK1.

3540 Discussion

3541 Considering that FB₁ contamination of agricultural products is common throughout the world, it is
 3542 necessary to evaluate the health hazards FB₁ poses to humans and animals. Several studies have
 3543 attributed oxidative stress as one of the mechanisms in which FB₁ exerts its toxicity [41–45]. Excessive
 3544 production of reactive oxygen species (ROS) results in oxidative damage to cells and macromolecules
 3545 including DNA [44]. While some studies have disputed the genotoxic potential of FB₁ [17,18], others
 3546 have reported chromosomal aberrations and oxidative DNA damage triggered by FB₁ exposure
 3547 [16,41,47,48]. Apart from inducing DNA damage, FB₁ may disrupt DDR network and repair processes.
 3548 One potential mechanism could be through the PTEN/PI3K/AKT/CHK1 axis.

3549 To better understand the genotoxic potential of FB₁, we set out to determine if FB₁ induces DNA
 3550 damage and if it alters DNA damage checkpoint regulation via the PTEN/PI3K/AKT/CHK1 network.
 3551 Seeing that poor PTEN expression is common in toxicity, we further determined the effects of FB₁ on
 3552 the epigenetic regulation of PTEN via miR-30c and H3K4me3 in human hepatoma G2 (HepG2) cells.
 3553 The liver is one of the primary organs in which FB₁ is thought to accumulate, and is usually the initial
 3554 site for the metabolism and detoxification of food and food contaminants [49,50]. Due to the limitations
 3555 of primary hepatocytes such as poor availability, short life span, inter-donor variability, loss of hepatic
 3556 function, and early phenotypic changes, we opted to use the HepG2 cell line for this study [51,52]. The
 3557 DNA of HepG2 cells is less sensitive to damage caused by xenobiotics than intact hepatocytes [53,54].

3558 Moreover, no mutations have been found in the PTEN gene of the HepG2 cell line, making it an apt
3559 model for testing genotoxicity and epigenetic changes that may occur as a result of FB₁ exposure [55].
3560 The effect of FB₁ on HepG2 cell viability was conducted using a crystal violet assay in accordance with
3561 Feoktistova et al. [56] (Supplementary Figure S4.1). FB₁ reduced HepG2 cell viability in a dose-
3562 dependent manner (5, 50, 100, 200 μM). For subsequent assays, HepG2 cells were exposed to 5, 100,
3563 and 200 μM FB₁ as they represented 90%, 70%, and 50% cell viabilities, respectively. Results obtained
3564 for 5 and 100 μM can be found in the supplementary materials (Supplementary Figures S4.2–S4.7).

3565 We evaluated the genotoxic potential of FB₁ by determining if FB₁ inflicted damage on DNA.
3566 Previously, we showed that at 200 μM FB₁ enhanced ROS production, resulting in oxidative stress [45].
3567 Thus, in the present study we measured 8-OHdG levels as a marker of oxidative DNA damage. The low
3568 redox potential of guanine makes it the most vulnerable base and its product (8-OHdG) the best
3569 characterized oxidative lesion [57]. We found a significant 2.63-fold increase in 8-OHdG levels in the
3570 DNA of FB₁-exposed cells (Figure 4.1). The incorporation of 8-OHdG into DNA can generate double
3571 strand breaks, making this a harmful lesion [58]. Several other *in vivo* and *in vitro* studies observed
3572 DNA fragmentation as a consequence of FB₁ exposure, proving that FB₁ is genotoxic [19–21,42].

3573 While the impact FB₁ has on DNA damage has been thoroughly researched, little is known on the impact
3574 it may have on DNA damage responses. Hence, we investigated the effect of FB₁ on the
3575 PTEN/PI3K/AKT/CHK1 axis and further determined if FB₁ effects the epigenetic regulation of PTEN.
3576 Currently, only a few studies have demonstrated the effects of FB₁ on epigenetic modifications in
3577 humans. Previously, Chuturgoon et al. (2014) screened for alterations in the miRNA expression profile
3578 of HepG2 cells exposed to 200 μM FB₁. miR-30c was one of the miRNAs shown to be dysregulated
3579 [35]. MiR-30c is an important regulator of hepatic liver metabolism, apoptosis, cell cycle transition,
3580 proliferation, and differentiation [59–61]. We found that the expression of miR-30c was significantly
3581 increased after exposure to 200 μM FB₁ (Figure 4.2a). Using an online computational prediction
3582 algorithm (TargetScan version 7.2), miR-30c was found to possibly target PTEN and KDM5B (Figure
3583 4.2b). miRNAs silence their mRNA targets through mRNA cleavage or translational repression [62–
3584 64]. FB₁ reduced KDM5B transcript and protein levels in HepG2 cells (Figure 4.3a, b). While FB₁
3585 reduced KDM5B mRNA levels by 9.86-fold, only a slight decrease in protein expression was observed.
3586 A previous study did find a minor increase in *KDM5B* transcript levels at 200 μM FB₁; however, these
3587 results were not statistically significant [35]. Further studies using miR-30c inhibitors and mimics need
3588 to be conducted to validate miR-30c regulation of KDM5B expression.

3589 FB₁ can also induce epigenetic changes through the post-translational modifications of histones, but no
3590 study to date has investigated these changes in humans [65–67]. Here, we identified changes to H3K4
3591 methylation. Although there was a slight decrease in KDM5B, we found a significant increase in global
3592 H3K4me3 (Figure 4.3c). H3K4me3 is predominantly found at transcriptional start sites, where it
3593 regulates the binding of transcription factors and activates gene transcription [68,69]. Thus, we

3594 determined H3K4me3 levels at the *PTEN* promoter region using the ChIP assay; FB₁ significantly
3595 increased H3K4me3 at the *PTEN* promoter region (Figure 4.4a). These results correspond to the
3596 substantial elevation in *PTEN* transcript levels; however, the protein expression of PTEN was decreased
3597 (Figure 4.4b, c). PTEN may be post-transcriptionally regulated by miR-30c, as the decrease in PTEN
3598 protein expression corresponded to the increased miR-30c levels. Hence, miR-30c may act as a possible
3599 inhibitor of PTEN translation.

3600 PTEN functions in regulating several cellular processes by antagonizing the PI3K/AKT signaling
3601 cascade [70]. Emerging evidence has revealed that PTEN is central in maintaining the DNA integrity
3602 by regulating DDR pathways via its interaction with CHK1 [27,28]. Additionally, PTEN regulates the
3603 activity of CHK1 via the PI3K/AKT axis [71–74]. Briefly, PTEN dephosphorylates the primary product
3604 of PI3K, phosphatidylinositol-3,4,5-triphosphate (PIP3). PIP3 activates AKT via its phosphorylation at
3605 serine residue 473 [71]. Downregulation of PTEN permitted PI3K/AKT signaling to proceed
3606 undisturbed as PI3K and p-ser473-AKT expression was upregulated (Figure 4.5). FB₁ inhibits ceramide
3607 formation and promotes the formation of sphingoid bases [75]. This may explain the activation of AKT
3608 by FB₁, as ceramide inhibits PI3K and promotes the dephosphorylation of AKT on serine 473 [76,77].
3609 Furthermore, sphingosine-1-phosphate activates PI3K/AKT signaling by binding to G_i-coupled
3610 receptors [78].

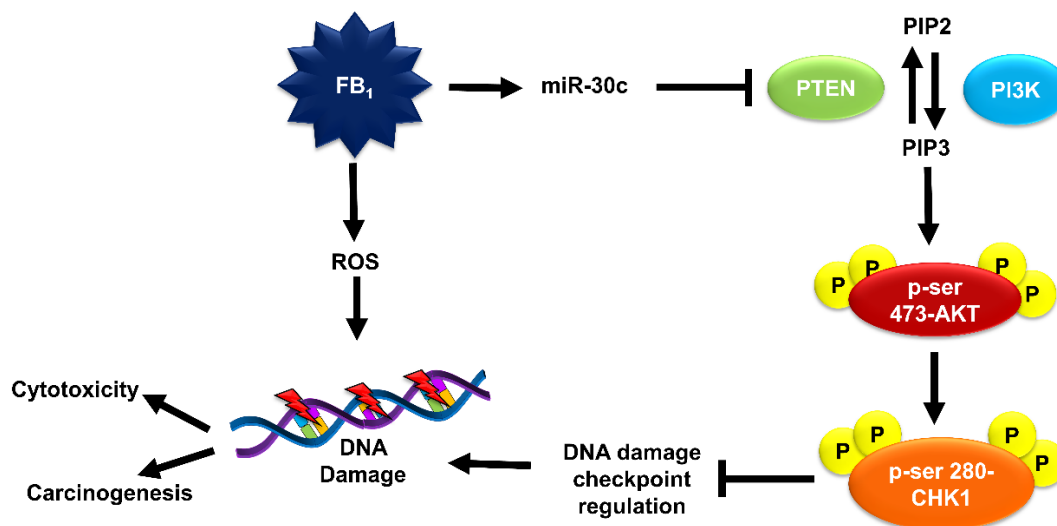
3611 AKT, in its activated form, inhibits CHK1 functioning by phosphorylating serine 280 of CHK1
3612 [71,73,74]. Activated PI3K/AKT signaling impaired CHK1 function via increased p-ser-280-CHK1
3613 after FB₁ exposure (Figure 4.6). During DDR, CHK1 arrests cells at the G1/S, S, and G2/M phases by
3614 phosphorylating the cdc25 family of phosphatases [79,80]. This allows for DNA repair to occur prior
3615 to determining cell fate. Although we did not analyze changes in cell cycle, previous studies have shown
3616 that FB₁ disrupts G1/S blockade; however, increased G2/M arrest was observed [81–83]. Nonetheless,
3617 the inhibitory phosphorylation of CHK1 coincided with DNA damage after FB₁ exposure in HepG2
3618 cells, as cell cycle checkpoints were disrupted, inhibiting repair.

3619 In addition to 200 μM FB₁, the effects of 5 and 100 μM FB₁ were investigated (Supplementary Figures
3620 S4.2–S4.7). While cells exposed to 5 and 200 μM FB₁ responded in a similar manner, the effect at 200
3621 μM FB₁ was exacerbated. Additionally, we observed that 100 μM FB₁ generally had the opposite effect
3622 on 8-OHdG levels, H3K4 trimethylation on the *PTEN* promoter, and the expression of miR-30c,
3623 KDM5B, *PTEN*, PI3K, p-ser423-AKT, CHK1, and p-ser-280-CHK1 in HepG2 cells in comparison
3624 with the 5 and 200 μM FB₁. As with many toxins, this suggests that FB₁ is associated with a biphasic
3625 dose response [84].

3626 **Conclusions**

3627 This study further confirms the genotoxic potential of FB₁, and that the inhibition of DNA damage
3628 checkpoint regulation may allow cells to evade DNA repair. FB₁ epigenetically downregulates the

3629 expression of PTEN via miR-30c. The downregulation of PTEN inhibits DNA damage checkpoint
 3630 regulation via the PI3K/AKT signaling network, preventing the repair of oxidative DNA lesions
 3631 induced by FB₁ (Figure 4.7). Needless to say, further investigation should be conducted using miRNA
 3632 inhibitors and mimics, and on whether the outcome of FB₁-induced DNA damage and impaired DNA
 3633 damage checkpoint regulation contributes to its cytotoxicity or carcinogenicity.



3634
 3635 **Figure 4.7.** FB₁ induces oxidative DNA damage. It further impairs DNA damage checkpoint
 3636 regulation pathways via the PTEN/PI3K/AKT/CHK1 axis by epigenetically regulating PTEN. FB₁
 3637 upregulates miR-30c, which inhibits PTEN translation, allowing for the phosphorylation of PIP2
 3638 to PIP3 by PI3K. This triggers the phosphorylation of AKT and subsequent phosphorylation of
 3639 ser-280-CHK1, inhibiting CHK1 activity. Inhibition of CHK1 inhibits DNA damage checkpoint
 3640 regulation. The resulted DNA damage may either contribute to FB₁-mediated cytotoxicity or
 3641 carcinogenicity.

3642 **Ethics Approval:** Approval was received from the University of Kwa-Zulu Natal’s Biomedical
 3643 Research Ethics Committee. Ethics number: BE322/19.

3644 **Author Contributions:** T.A., T.G., and A.C. conceptualized and designed the study. T.A.
 3645 conducted all laboratory experiments, analyzed the data, and wrote the manuscript. T.G. and A.C.
 3646 revised the manuscript. All authors have read and agreed to the published version of the
 3647 manuscript.

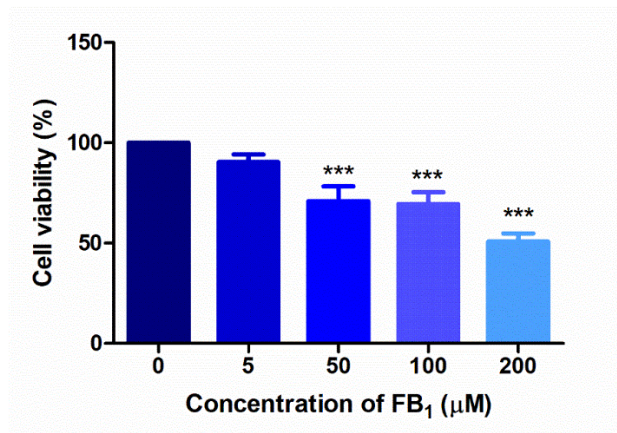
3648 **Funding:** The authors acknowledge the National Research Foundation (NRF) of South Africa and the
 3649 College of Health Science (University of Kwa-Zulu Natal) for funding this study.

3650 **Conflicts of Interest:** The authors declare no conflicts of interest.

3651

Supplementary Information

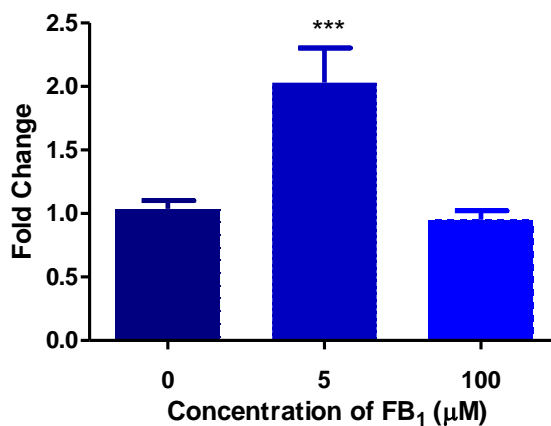
3652



3653

3654 **Supplementary Figure S4.1. The cytotoxic effects of FB₁ on HepG2 cells.** HepG2 cells were treated
3655 with 0, 5, 50, 100 and 200 µM FB₁ for 24h. Cell viability was determined using the crystal violet assay
3656 and expressed as a percentage of the untreated control. Control viability was taken as 100%. FB₁
3657 significantly altered the cell viability of HepG2 cells. Data is represented as mean percentage cell
3658 viability ± SD (n=3) (***) $p \leq 0.001$; one-way ANOVA with the Dunnet: compare all columns to control
3659 post-test).

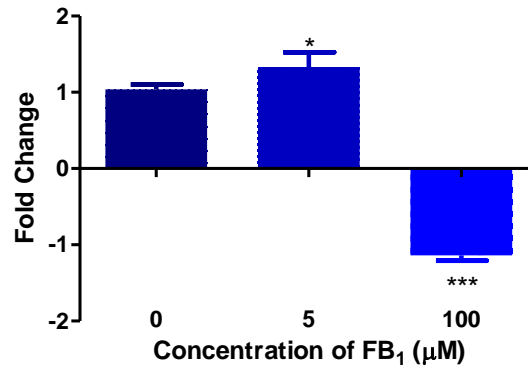
3660



3661

3662 **Supplementary Figure 4.2. FB₁ induced 8-OHdG levels in HepG2 cells.** 8-OHdG levels were
3663 measured as a marker of oxidative DNA damage. FB₁ significantly altered 8-OHdG levels in HepG2
3664 cells (***) $p = 0.0007$). Data is represented as mean fold change ± SD (n=3) (***) $p \leq 0.001$; one-way
3665 ANOVA with the Dunnet: compare all columns to control post-test).

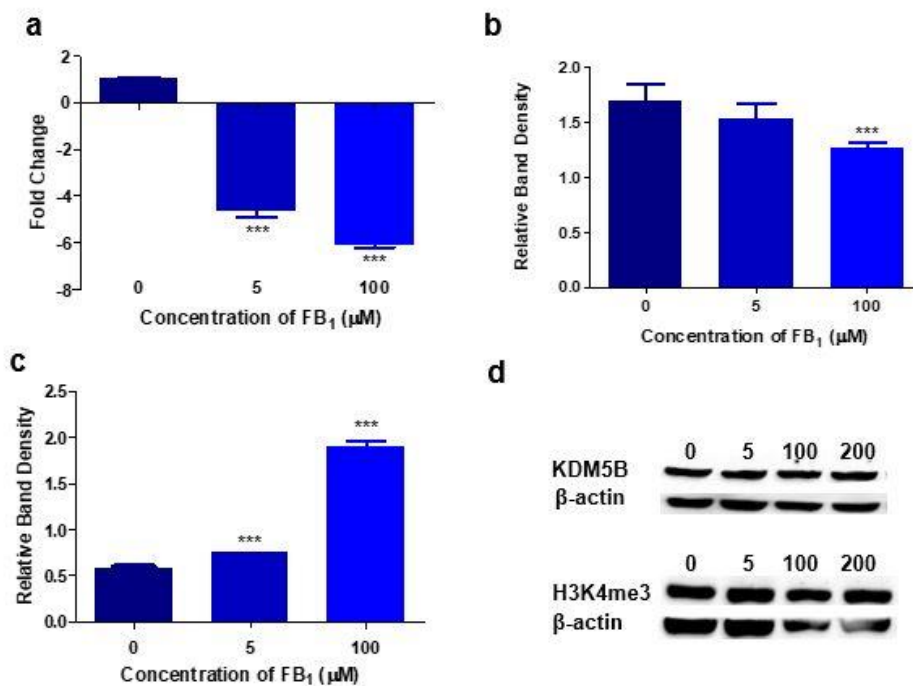
3666



3667

3668 **Supplementary Figure S4.3: FB₁ altered miR-30c expression in HepG2 cells.** qPCR analysis of
 3669 miR-30c showed that FB₁ significantly altered miR-30c expression (***p* < 0.0001). Results are
 3670 represented as mean fold-change ± SD (n=3) (**p* < 0.05, ***p* < 0.0001; one-way ANOVA with the
 3671 Dunnet: compare all columns to control post-test).

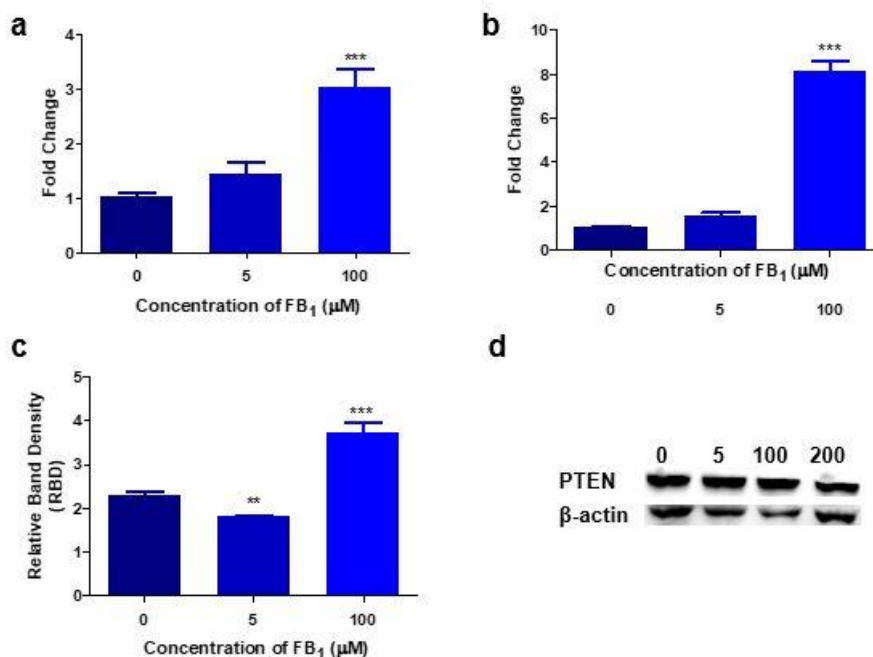
3672



3673

3674 **Supplementary Figure S4.4: The effect of FB₁ on KDM5B and H3K4me3 expression in HepG2**
 3675 **cells.** FB₁ reduced both the transcript (a; ***p* < 0.0001) and protein (b; **p* = 0.0106) expression of
 3676 KDM5B. There was a dose-dependent increase in total H3K4me3 (c; ***p* < 0.0001). Western blot
 3677 images of KDM5B and H3K4me3 (d). KDM5B and H3K4me3 expression was normalized against β-
 3678 actin. Results are represented as mean fold-change ± SD (n=3) for gene expression and mean relative
 3679 band density ± SD (n=3) for protein expression (***p* < 0.0001; one-way ANOVA with the Dunnet:
 3680 compare all columns to control post-test).

3681



3682

3683 **Supplementary Figure 4.5: FB₁ induced KDM5B and miR-30c modulates PTEN expression.**

3684 PTEN expression is under the influence of both KDM5B and miR-30c. (a) Low levels of KDM5B
3685 allowed for the increased H3K4me3 at *PTEN* promoter regions (***p* < 0.0001). (b) This resulted in
3686 significantly higher levels of *PTEN* transcripts (***p* < 0.0001). (c) However, miR-30c inhibited PTEN
3687 translation/protein expression at 5 μM FB₁ but increased PTEN translation at 100 μM FB₁ (***p* <
3688 0.0001). (d) Western blot images of PTEN. PTEN expression was normalized against β-actin. Results
3689 are represented as mean fold-change ± SD (n=3) for gene expression and mean relative band density ±
3690 SD (n=3) for protein expression (**p* < 0.05, ***p* < 0.0001; one-way ANOVA with the Dunnett: compare
3691 all columns to control post-test).

3692

3693

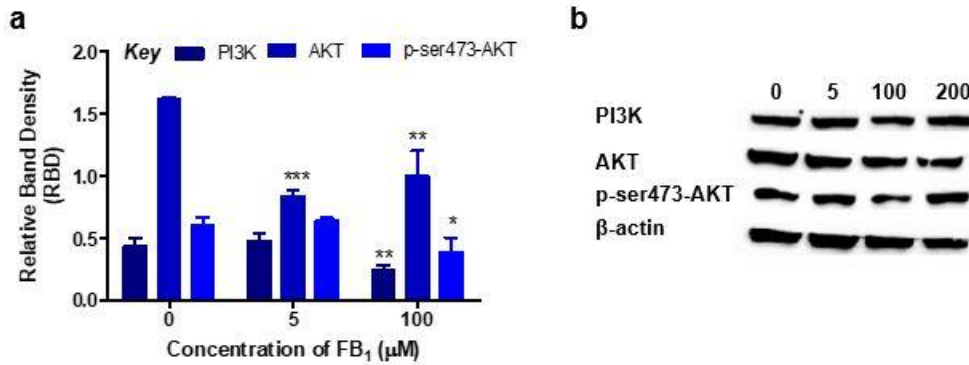
3694

3695

3696

3697

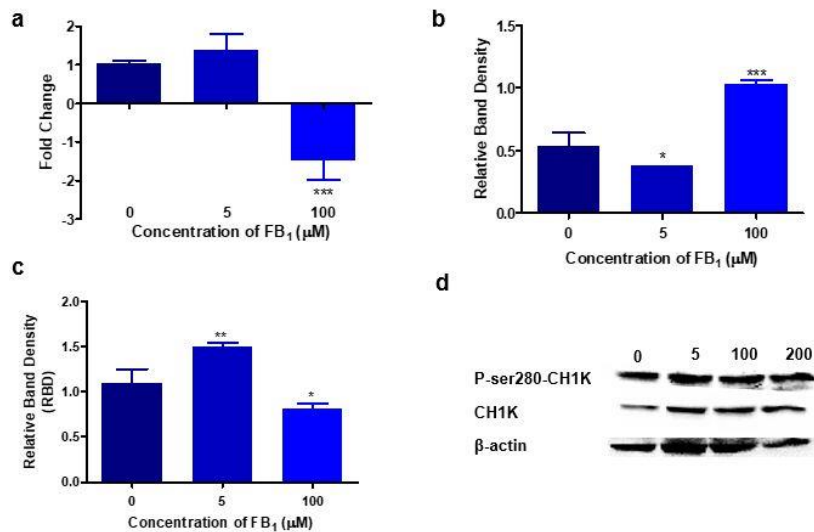
3698



3699

3700 **Supplementary Figure 4.6: The effect of FB₁ on the PI3K/AKT signalling cascade.** (a) Western
 3701 blotting was used to determine the effect of FB₁ on the PTEN/PI3K/AKT signalling network. FB₁
 3702 significantly altered PI3K (***p* < 0.0001), AKT (***p* = 0.0004) and p-ser473-AKT (**p* < 0.0174)
 3703 protein expression. (b) Western blot images of PI3K, AKT and pAKT. p-ser473-AKT expression was
 3704 normalized against AKT and PI3K and AKT expression was normalized against β-actin. Data is
 3705 represented as mean RBD ± SD (n=3), (**p* ≤ 0.05, ***p* ≤ 0.01 and ****p* ≤ 0.001; one-way ANOVA with
 3706 the Dunnett: compare all columns to control post-test).

3707



3708

3709 **Supplementary Figure 4.7: The influence of FB₁ on CHK1 expression in HepG2 cells.** FB₁
 3710 significantly altered *CHK1* gene expression (a; ****p* = 0.0001), CHK1 protein expression (b; ****p*
 3711 < 0.0001) and p-ser280-CHK1 (c; ****p* = 0.0006). (d) Western blot images of CHK1 and p-ser280-
 3712 CHK1. CHK1 expression was normalized against β-actin and p-ser280-CHK1 was normalized against
 3713 CHK1. Gene expression is represented as fold changes ± SD relative to the control and protein
 3714 expression is represented as mean RBD ± SD (**p* ≤ 0.05, ***p* ≤ 0.01 and ****p* ≤ 0.001; one-way ANOVA
 3715 with the Dunnett: compare all columns to control post-test).

3716 **References**

- 3717 1. Gelderblom, W.C.; Jaskiewicz, K.; Marasas, W.F.; Thiel, P.G.; Horak, R.M.; Vleggaar, R.; Kriek,
 3718 N.P. Fumonisin—Novel mycotoxins with cancer-promoting activity produced by *Fusarium*
 3719 *moniliforme*. *Appl. Environ. Microbiol.* **1988**, *54*, 1806–1811.
- 3720 2. Rheeder, J.P.; Marasas, W.F.; Vismer, H.F. Production of fumonisin analogs by *Fusarium* species.
 3721 *Appl. Environ. Microbiol.* **2002**, *68*, 2101–2105.
- 3722 3. Martins, F.A.; Ferreira, F.M.D.; Ferreira, F.D.; Bando, É.; Nerilo, S.B.; Hirooka, E.Y.; Machinski
 3723 Jr, M. Daily intake estimates of fumonisins in corn-based food products in the population of Parana,
 3724 Brazil. *Food Control* **2012**, *26*, 614–618.
- 3725 4. Kamle, M.; Mahato, D.K.; Devi, S.; Lee, K.E.; Kang, S.G.; Kumar, P. Fumonisin: Impact on
 3726 Agriculture, Food, and Human Health and their Management Strategies. *Toxins* **2019**, *11*, 328.
- 3727 5. Marin, S.; Ramos, A.J.; Cano-Sancho, G.; Sanchis, V. Mycotoxins: Occurrence, toxicology, and
 3728 exposure assessment. *Food Chem. Toxicol.* **2013**, *60*, 218–237.
- 3729 6. Bhandari, N.; He, Q.; Sharma, R.P. Gender-related differences in subacute fumonisin B1
 3730 hepatotoxicity in BALB/c mice. *Toxicology* **2001**, *165*, 195–204.
- 3731 7. Marin, D.E.; Taranu, L.; Pascale, F.; Lionide, A.; Burlacu, R.; Bailly, J.D.; Oswalt, I.P. Sex-related
 3732 differences in the immune response of weanling piglets exposed to low doses of fumonisin extract.
 3733 *Br. J. Nutr.* **2006**, *95*, 1185–1192.
- 3734 8. Domijan, A.-M. Fumonisin B1: A neurotoxic mycotoxin. *Arch. Ind. Hyg. Toxicol.* **2012**, *63*, 531–
 3735 544.
- 3736 9. Mathur, S.; Constable, P.D.; Eppley, R.M.; Waggoner, A.L.; Tumbleson, M.E.; Haschek, W.M.
 3737 Fumonisin B1 is hepatotoxic and nephrotoxic in milk-fed calves. *Toxicol. Sci.* **2001**, *60*, 385–396.
- 3738 10. Müller, S.; Dekant, W.; Mally, A. Fumonisin B1 and the kidney: Modes of action for renal tumor
 3739 formation by fumonisin B1 in rodents. *Food Chem. Toxicol.* **2012**, *50*, 3833–3846.
- 3740 11. da Rocha, M.E.B.; Freire, F.C.O.; Maia, F.E.F.; Guedes, M.I.F.; Rondina, D. Mycotoxins and their
 3741 effects on human and animal health. *Food Control* **2014**, *36*, 159–165.
- 3742 12. IARC. Some traditional herbal medicines, some mycotoxins, naphthalene and styrene. *IARC*
 3743 *Monogr. Eval. Carcinog. Risks Hum.* **2002**, *82*, 1–556.
- 3744 13. Gelderblom, W.; Abel, S.; Smuts, C.M.; Marnewick, J.; Marasas, W.F.; Lemmer, E.R.; Ramljak,
 3745 D. Fumonisin-induced hepatocarcinogenesis: Mechanisms related to cancer initiation and
 3746 promotion. *Environ. Health Perspect.* **2001**, *109* (Suppl. 2), 291–300.
- 3747 14. Sun, G.; Wang, S.; Hu, X.; Su, J.; Huang, T.; Yu, J.; Tang, L.; Gao, W.; Wang, J.S. Fumonisin B1
 3748 contamination of home-grown corn in high-risk areas for esophageal and liver cancer in China.
 3749 *Food Addit. Contam.* **2007**, *24*, 181–185.
- 3750 15. Alizadeh, A.M.; Roshandel, G.; Roudbarmohammadi, S.; Roudbary, M.; Sohanaki, H.; Ghiasian,
 3751 S.A.; Taherkhani, A.; Semenani, S.; Aghasi, M. Fumonisin B1 contamination of cereals and risk of

- 3752 esophageal cancer in a high-risk area in northeastern Iran. *Asian Pac. J. Cancer Prev.* **2012**, *13*,
3753 2625–2628.
- 3754 16. Knasmüller, S.; Bresgen, N.; Kassie, F.; Volker, M.S.; Gelderblom, W.; Zöhrer, E.; Eckl, P.M.
3755 Genotoxic effects of three Fusarium mycotoxins, fumonisin B1, moniliformin and vomitoxin in
3756 bacteria and in primary cultures of rat hepatocytes. *Mutat. Res. Genet. Toxicol. Environ.*
3757 *Mutagenesis* **1997**, *391*, 39–48.
- 3758 17. Norred, W.P.; Plattner, W.P.; Vesonder, R.F.; Bacon, C.W.; Voss, K.A. Effects of selected
3759 secondary metabolites of Fusarium moniliforme on unscheduled synthesis of DNA by rat primary
3760 hepatocytes. *Food Chem. Toxicol.* **1992**, *30*, 233–237.
- 3761 18. Gelderblom, W.C.A.; Semple, E.; Marasas, W.F.O.; Farber, E. The cancer-initiating potential of the
3762 fumonisin B mycotoxins. *Carcinogenesis* **1992**, *13*, 433–437.
- 3763 19. Theumer, M.G.; Cánepa, M.C.; López, A.G.; Mary, V.S.; Dambolena, J. S.; Rubinstein, H.R.
3764 Subchronic mycotoxicoses in Wistar rats: Assessment of the in vivo and in vitro genotoxicity
3765 induced by fumonisins and aflatoxin B, and oxidative stress biomarkers status. *Toxicology* **2010**,
3766 *268*, 104–110.
- 3767 20. Hassan, A.M.; Abdel-Aziem, S.H.; El-Nekeety, A.A.; Abdel-Wahhab, M.A. Panaxginseng extract
3768 modulates oxidative stress, DNA fragmentation and up-regulate gene expression in rats sub
3769 chronically treated with aflatoxin B 1 and fumonisin B 1. *Cytotechnology* **2015**, *67*, 861–871.
- 3770 21. Chaturgoon, A.; Phulukdaree, A.; Moodley, D. Fumonisin B1 induces global DNA
3771 hypomethylation in HepG2 cells—An alternative mechanism of action. *Toxicology* **2014**, *315*, 65–
3772 69.
- 3773 22. Jackson, S.P.; Bartek, J. The DNA-damage response in human biology and disease. *Nature* **2009**,
3774 *461*, 1071–1078.
- 3775 23. Lu, X.X.; Cao, L.L.; Chen, X.; Xiao, J.; Zou, Y.; Chen, Q. PTEN Inhibits Cell Proliferation,
3776 Promotes Cell Apoptosis, and Induces Cell Cycle Arrest via Downregulating the
3777 PI3K/AKT/hTERT Pathway in Lung Adenocarcinoma A549 Cells. *Biomed. Res. Int.* **2016**, *2016*,
3778 2476842.
- 3779 24. Otaegi, G.; Yusta-Boyo, M.J.; Vergaño-Vera, E.; Méndez-Gómez, H.R.; Carrera, A.C.; Abad, J.L.;
3780 González, M.; Enrique, J.; Vicario-Abejón, C.; de Pablo, F. Modulation of the PI 3-kinase—Akt
3781 signalling pathway by IGF-I and PTEN regulates the differentiation of neural stem/precursor cells.
3782 *J. Cell Sci.* **2006**, *119*, 2739–2748.
- 3783 25. Bassi, C.; Ho, J.; Srikumar, T.; Dowling, R.J.O.; Gorrini, C.; Miller, S.J.; Mak, T.W.; Neel, B.G.;
3784 Raught, B.; Stambolic, V. Nuclear PTEN controls DNA repair and sensitivity to genotoxic stress.
3785 *Science* **2013**, *341*, 395–399.
- 3786 26. Ming, M.; He, Y.-Y. PTEN in DNA damage repair. *Cancer Lett.* **2012**, *319*, 125–129.
- 3787 27. Puc, J.; Parsons, R. PTEN loss inhibits CHK1 to cause double stranded-DNA breaks in cells. *Cell*
3788 *Cycle* **2005**, *4*, 927–929.

- 3789 28. Puc, J Keniry, M.; Li, H.S.; Pandita, T.J.; Choudhury, A.D.; Memeo, L.; Mansukhani, M.; Murty,
3790 V.V.V.S; Gaciong, Z.; Meek, S.E.M. Lack of PTEN sequesters CHK1 and initiates genetic
3791 instability. *Cancer Cell* **2005**, *7*, 193–204.
- 3792 29. Peyrou, M.; Bourgoin, L.; Foti, M. PTEN in liver diseases and cancer. *World J. Gastroenterol.*
3793 **2010**, *16*, 4627–4633.
- 3794 30. Vinciguerra, M.; Foti, M. PTEN at the crossroad of metabolic diseases and cancer in the liver. *Ann.*
3795 *Hepatol.* **2008**, *7*, 192–199.
- 3796 31. Wang, L.; Wang, W.L.; Zhang, Y.; Guo, S.P.; Zhang, J.; Li, Q.L. Epigenetic and genetic alterations
3797 of PTEN in hepatocellular carcinoma. *Hepatol. Res.* **2007**, *37*, 389–396.
- 3798 32. Jiang, X.M.; Yu, X.N.; Liu, T.T.; Zhu, H.R.; Shi, X.; Bilegsaikhan, E.; Guo, H.Y.; Song, G.Q.;
3799 Weng, S.Q.; Huang, X.X.; et al. microRNA-19a-3p promotes tumor metastasis and
3800 chemoresistance through the PTEN/Akt pathway in hepatocellular carcinoma. *Biomed. Pharm.*
3801 **2018**, *105*, 1147–1154.
- 3802 33. Meng, F.; Henson, R.; Wehbe-Janek, H.; Ghoshal, K.; Jacob, S.T.; Patel, T. MicroRNA-21 regulates
3803 expression of the PTEN tumor suppressor gene in human hepatocellular cancer. *Gastroenterology*
3804 **2007**, *133*, 647–658.
- 3805 34. Shen, X; Cheng, G.; Xu, L.; Wu, W.; Chen, Z.; Du, P. Jumonji AT-rich interactive domain 1B
3806 promotes the growth of pancreatic tumors via the phosphatase and tensin homolog/protein kinase
3807 B signaling pathway. *Oncol. Lett.* **2018**, *16*, 267–275.
- 3808 35. Chuturgoon, A.A.; Phulukdaree, A.; Moodley, D. Fumonisin B1 modulates expression of human
3809 cytochrome P450 1b1 in human hepatoma (Hepg2) cells by repressing Mir-27b. *Toxicol. Lett.* **2014**,
3810 *227*, 50–55.
- 3811 36. Klose, R.J.; Kallin, E.M.; Zhang, Y. JmjC-domain-containing proteins and histone demethylation.
3812 *Nat. Rev. Genet.* **2006**, *7*, 715.
- 3813 37. Kidder, B.L.; Hu, G.; Zhao, K. KDM5B focuses H3K4 methylation near promoters and enhancers
3814 during embryonic stem cell self-renewal and differentiation. *Genome Biol.* **2014**, *15*, R32.
- 3815 38. Ghazi, T.; Nagiah, S.; Naidoo, P.; Chuturgoon, A.A. Fusaric acid-induced promoter methylation of
3816 DNA methyltransferases triggers DNA hypomethylation in human hepatocellular carcinoma
3817 (HepG2) cells. *Epigenetics* **2019**, *14*, 804–817.
- 3818 39. Livak, K.J.; Schmittgen, T.D. Analysis of relative gene expression data using real-time quantitative
3819 PCR and the $2^{-\Delta\Delta CT}$ method. *Methods* **2001**, *25*, 402–408.
- 3820 40. Su, W.; Hong, L.; Xu, X.; Huang, S.; Herpai, D.; Li, L.; Xu, Y.; Truong, L.; Hu, W.Y.; Wu, X.; et
3821 al. miR-30 disrupts senescence and promotes cancer by targeting both p16 (INK4A) and DNA
3822 damage pathways. *Oncogene* **2018**, *37*, 5618–5632.
- 3823 41. Galvano, F.; Russo, A.; Cardile, V.; Galvano, G.; Vanella, A.; Renis, M. DNA damage in human
3824 fibroblasts exposed to fumonisin B1. *Food Chem. Toxicol.* **2002**, *40*, 25–31.

- 3825 42. Stockmann-Juvala, H.; Mikkola, J.; Naarala, J.; Loikkanen, J.; Elovaara, E.; Saolainen, K.
3826 Fumonisin B1-induced toxicity and oxidative damage in U-118MG glioblastoma cells. *Toxicology*
3827 **2004**, *202*, 173–183.
- 3828 43. Domijan, A.M.; Abramov, A.Y. Fumonisin B1 inhibits mitochondrial respiration and deregulates
3829 calcium homeostasis--implication to mechanism of cell toxicity. *Int. J. Biochem. Cell Biol.* **2011**,
3830 *43*, 897–904.
- 3831 44. Mary, V.S.; Theumer, M.G.; Arias, S.L.; Rubinstein, H.R. Reactive oxygen species sources and
3832 biomolecular oxidative damage induced by aflatoxin B1 and fumonisin B1 in rat spleen
3833 mononuclear cells. *Toxicology* **2012**, *302*, 299–307.
- 3834 45. Arumugam, T.; Pillay, Y.; Ghazi, T.; Nagiah, S.; Abdul, N.S.; Chuturgoon, A.A. Fumonisin B 1-
3835 induced oxidative stress triggers Nrf2-mediated antioxidant response in human hepatocellular
3836 carcinoma (HepG2) cells. *Mycotoxin Res.* **2019**, *35*, 99–109.
- 3837 46. Patel, R.; Rinker, L.; Peng, J.; Chilian, W. Reactive Oxygen Species: The Good and the Bad. *React.*
3838 *Oxyg. Species Living Cells* **2018**, doi:10.5772/intechopen.71547.
- 3839 47. Ehrlich, V.; Darroudi, F.; Uhl, M.; Steinkellner, H.; Zsivkovits, M.; Knasmueller, S. Fumonisin B1
3840 is genotoxic in human derived hepatoma (HepG2) cells. *Mutagenesis* **2002**, *17*, 257–260.
- 3841 48. Domijan, A.-M.; Želježić, D.; Milić, M.; Peraica, M. Fumonisin B1: Oxidative status and DNA
3842 damage in rats. *Toxicology* **2007**, *232*, 163–169.
- 3843 49. Martinez-Larranaga, M.R.; Anadon, A.; Anadon, A.; Diaz, M.J.; Fernandez-Cruz, M.L.; Martinez,
3844 M.A.; Frejo, M.T.; Martinez, M.; Fernandez, R.; Anton, R.M.; et al. Toxicokinetics and oral
3845 bioavailability of fumonisin B1. *Vet. Hum. Toxicol.* **1999**, *41*, 357–362.
- 3846 50. Kammerer, S.; Küpper, J.-H. Human hepatocyte systems for in vitro toxicology analysis. *J. Cell*
3847 *Biotechnol.* **2018**, *3*, 85–93.
- 3848 51. den Braver-Sewradj, S.P.; den Braver, M.W.; Vermeulen, N.P.; Commandeur, J.N.; Richert, L.;
3849 Vos, J.C. Inter-donor variability of phase I/phase II metabolism of three reference drugs in
3850 cryopreserved primary human hepatocytes in suspension and monolayer. *Toxicol. Vitro.* **2016**, *33*,
3851 71–79.
- 3852 52. Guo, X.; Seo, J.E.; Li, X.; Mei, N. Genetic toxicity assessment using liver cell models: Past, present,
3853 and future. *J. Toxicol. Environ. Health Part B* **2020**, *23*, 27–50.
- 3854 53. Dearfield, K.L.; Jacobson-Kram, D.; Brown, N.A.; Williams, J.R. Evaluation of a human hepatoma
3855 cell line as a target cell in genetic toxicology. *Mutat. Res.* **1983**, *108*, 437–449.
- 3856 54. Knasmüller, S.; Mersch-Sundermann, V.; Kevekordes, S.; Darroudi, F.; Huber, W.W.; Hoelzl, C.;
3857 Bichler, J.; Majer, B.J. Use of human-derived liver cell lines for the detection of environmental and
3858 dietary genotoxicants; current state of knowledge. *Toxicology* **2004**, *198*, 315–328.
- 3859 55. Ma, D.-Z.; Xu, Z.; Liang, Y.L.; Su, J.M.; Li, Z.X.; Zhang, W.; Wang, L.Y.; Zha, X.L. Down-
3860 regulation of PTEN expression due to loss of promoter activity in human hepatocellular carcinoma
3861 cell lines. *World J. Gastroenterol.* **2005**, *11*, 4472.

- 3862 56. Feoktistova, M.; Geserick, P.; Leverkus, M. Crystal violet assay for determining viability of
3863 cultured cells. *Cold Spring Harb. Protoc.* **2016**, 2016, pdb-prot087379.
- 3864 57. van Loon, B.; Markkanen, E.; Hubscher, U. Oxygen as a friend and enemy: How to combat the
3865 mutational potential of 8-oxo-guanine. *DNA Repair* **2010**, 9, 604–616.
- 3866 58. Cheng, K.C.; Cahill, D.S.; Kasai, H.; Nishimura, S.; Loeb, L.A. 8-Hydroxyguanine, an abundant
3867 form of oxidative DNA damage, causes G---T and A---C substitutions. *J. Biol. Chem.* **1992**, 267,
3868 166–172.
- 3869 59. Irani, S.; Hussain, M.M. Role of microRNA-30c in lipid metabolism, adipogenesis, cardiac
3870 remodeling and cancer. *Curr. Opin. Lipidol.* **2015**, 26, 139–146.
- 3871 60. Shukla, K.; Sharma, A.K.; Ward, A.; Will, R.; Hielscher, T.; Balwierz, A.; Breuing, C.;
3872 Munstermann, E.; Konig, R.; Keklikoglou, L. et al. MicroRNA-30c-2-3p negatively regulates NF-
3873 kappaB signaling and cell cycle progression through downregulation of TRADD and CCNE1 in
3874 breast cancer. *Mol. Oncol.* **2015**, 9, 1106–1119.
- 3875 61. Liu, X.; Li, M.; Peng, Y.; Hu, X.; Xu, J.; Zhu, S.; Yu, Z.; Han, S. miR-30c regulates proliferation,
3876 apoptosis and differentiation via the Shh signaling pathway in P19 cells. *Exp. Mol. Med.* **2016**, 48,
3877 e248.
- 3878 62. Yekta, S.; Shih, I.-h.; Bartel, D.P. MicroRNA-Directed Cleavage of *HOXB8* mRNA.
3879 *Science* **2004**, 304, 594–596.
- 3880 63. Mathonnet, G.; Fabian, M.R.; Svitkin, Y.V.; Parsyan, A.; Huck, L.; Murata, T.; Biffo, S.; Merrick,
3881 W.C.; Darzynkiewicz, E.; Pillai, R.S. MicroRNA Inhibition of Translation Initiation in Vitro by
3882 Targeting the Cap-Binding Complex eIF4F. *Science* **2007**, 317, 1764–1767.
- 3883 64. Valencia-Sanchez, M.A.; et al. Control of translation and mRNA degradation by miRNAs and
3884 siRNAs. *Genes Dev.* **2006**, 20, 515–524.
- 3885 65. Pellanda, H.; Forges, T.; Bressenot, A.; Chango, A.; Bronowicki, J.P.; Guéant, J.L.; Namour, F.
3886 Fumonisin FB 1 treatment acts synergistically with methyl donor deficiency during rat pregnancy
3887 to produce alterations of H 3- and H 4-histone methylation patterns in fetuses. *Mol. Nutr. Food Res.*
3888 **2012**, 56, 976–985.
- 3889 66. Sancak, D.; Ozden, S. Global histone modifications in fumonisin B1 exposure in rat kidney
3890 epithelial cells. *Toxicol. Vitro.* **2015**, 29, 1809–1815.
- 3891 67. Gardner, N.M.; Riley, R.T.; Showker, J.L.; Voss, K.A.; Sachs, A.J.; Maddox, J.R.; Gelineau-van
3892 Waes, J.B. Elevated nuclear sphingoid base-1-phosphates and decreased histone deacetylase
3893 activity after fumonisin B1 treatment in mouse embryonic fibroblasts. *Toxicol. Appl. Pharm.* **2016**,
3894 298, 56–65.
- 3895 68. Guenther, M.G.; Levine, S.S.; Boyer, L.A.; Jaenisch R.; Young, R.A. A chromatin landmark and
3896 transcription initiation at most promoters in human cells. *Cell* **2007**, 130, 77–88.
- 3897 69. Barski, A.; et al. High-resolution profiling of histone methylations in the human genome. *Cell* **2007**,
3898 129, 823–837.

- 3899 70. Cantley, L.C.; Neel, B.G. New insights into tumor suppression: PTEN suppresses tumor formation
3900 by restraining the phosphoinositide 3-kinase/AKT pathway. *Proc. Natl. Acad. Sci. USA* **1999**, *96*,
3901 4240–4245.
- 3902 71. King, F.W.; et al. Inhibition of Chk1 by activated PKB/Akt. *Cell Cycle* **2004**, *3*, 632–635.
- 3903 72. Kandel, E.S.; Skeen, J.; Majewski, N.; Di Cristofano, A.; Pandolfi, P.P.; Feliciano, C.S.; Gartel, A.;
3904 Hay, N. Activation of Akt/protein kinase B overcomes a G2/M cell cycle checkpoint induced by
3905 DNA damage. *Mol. Cell Bio.* **2002**, *22*, 7831–7841.
- 3906 73. Tonic, I.; Yu, W.N.; Park, Y.; Chen, C.C.; Hay, N. Akt activation emulates Chk1 inhibition and
3907 Bcl2 overexpression and abrogates G2 cell cycle checkpoint by inhibiting BRCA1 foci. *J. Biol.*
3908 *Chem.* **2010**, *285*, 23790–23798.
- 3909 74. Shtivelman, E.; Sussman, J.; Stokoe, D. A role for PI3K and PKB activity in the G2/M phase of the
3910 cell cycle. *Curr. Biol.* **2002**, *12*, 919–924.
- 3911 75. Wang, E.; Norred; W.P.; Bacon, C.W.; Riley, R.T.; Merrill, A.H. Inhibition of sphingolipid
3912 biosynthesis by fumonisins. Implications for diseases associated with *Fusarium moniliforme*. *J.*
3913 *Biol. Chem.* **1991**, *266*, 14486–14490.
- 3914 76. Schubert, K.M.; Scheid, M.P.; Duronio, V. Ceramide Inhibits Protein Kinase B/Akt by Promoting
3915 Dephosphorylation of Serine 473. *J. Biol. Chem.* **2000**, *275*, 13330–13335.
- 3916 77. Zundel, W.; Giaccia, A. Inhibition of the anti-apoptotic PI K/Akt/Bad pathway by stress. *Genes*
3917 *Devel.* **1998**, *12*, 1941–1946.
- 3918 78. Morales-Ruiz, M.; Lee, M.J. Zöllner, S.; Gratton, J.P.; Scotland, R.; Shiojima, I.; Walsh, K.; Hla,
3919 T.; Sessa, W.C. Sphingosine 1-Phosphate Activates Akt, Nitric Oxide Production, and Chemotaxis
3920 through a GiProtein/Phosphoinositide 3-Kinase Pathway in Endothelial Cells. *J. Biol. Chem.* **2001**,
3921 *276*, 19672–19677.
- 3922 79. Xiao, Z.; Chen, Z.; Gunasekera, A.H.; Sowin, T.J.; Rosenberg, S.H.; Fesik, S.; Zhang, H. Chk1
3923 mediates S and G2 arrests through Cdc25A degradation in response to DNA-damaging agents. *J.*
3924 *Biol. Chem.* **2003**, *278*, 21767–21773.
- 3925 80. Uto, K.; Inoue, D.; Shimauta, K.; Nakajo, N.; Sagata, N. Chk1, but not Chk2, inhibits Cdc25
3926 phosphatases by a novel common mechanism. *EMBO J.* **2004**, *23*, 3386–3396.
- 3927 81. Mobio, T.A.; Anane, R.; Baudrimont, I.; Carratú, M.R.; Shier, T.W.; Dano, S.D.; Ueno, Y.; Creppy,
3928 E.E. Epigenetic properties of fumonisin B1: Cell cycle arrest and DNA base modification in C6
3929 glioma cells. *Toxicol. App. Pharmacol.* **2000**, *164*, 91–96.
- 3930 82. Ramljak, D.; Calvert, R.; Wiesenfeld, P.; Diwan, B.; Catipovic, B.; Marasas, W.; Victor, T.;
3931 Anderson, L.; Gelderblom, W. A potential mechanism for fumonisin B1-mediated
3932 hepatocarcinogenesis: Cyclin D1 stabilization associated with activation of Akt and inhibition of
3933 GSK-3 β activity. *Carcinogenesis* **2000**, *21*, 1537–1546.
- 3934 83. Wang, S.-K.; Liu, S.; Yang, L.G.; Shi, R.F.; Sun, G.J Effect of fumonisin B1 on the cell cycle of
3935 normal human liver cells. *Mol. Med. Rep.* **2013**, *7*, 1970–1976.

3936 84. Mattson, M.P. Hormesis defined. *Ageing Res. Rev.* **2008**, 7, 1–7.

3937

3938

3939

3940

3941

3942

3943

3944

3945

3946

3947

3948

3949

3950

3951

3952

3953

3954

3955

3956

3957

3958

3959

3960

3961 **CHAPTER 5**

3962 **Fumonisin B₁ Alters Global m⁶A RNA Methylation and Epigenetically Regulates Keap1/Nrf2**
3963 **Signaling in Human Hepatoma (HepG2) Cells**

3964 Thilona Arumugam, Terisha Ghazi, Anil A Chuturgoon

3965 Discipline of Medical Biochemistry, School of Laboratory Medicine and Medical Sciences, University
3966 of KwaZulu-Natal, Durban, KwaZulu-Natal, South Africa

3967 **Corresponding author:**

3968 Professor Anil A. Chuturgoon,

3969 Discipline of Medical Biochemistry and Chemical Pathology,

3970 School of Laboratory Medicine and Medical Sciences

3971 College of Health Sciences

3972 George Campbell Building, Howard College, University of KwaZulu-Natal, Durban, 4041, South
3973 Africa. Telephone: +27312604404. Email: chatur@ukzn.ac.za

3974 **EMAILS:**

3975 TA: cyborglona@gmail.com

3976 TG: terishaghazi@gmail.com

3977 **Archives of Toxicology (In Review).**

3978 Manuscript ID: ATOX-D-20-00996.

3979

3980

3981

3982

3983

3984

3985

3986

3987

3988

3989

3990 **Abstract**

3991 Fumonisin B₁ (FB₁) is a common contaminant of cereal grains that affects human and animal health. It
3992 has become increasingly evident that epigenetic changes are implicated in FB₁ toxicity. N6-
3993 methyladenosine (m6A) is the most abundant post-transcriptional RNA modification that is influenced
3994 by fluctuations in redox status. Since oxidative stress is a characteristic of FB₁ exposure, we determined
3995 if there is cross talk between oxidative stress and m6A in FB₁ exposed HepG2 cells. Briefly, HepG2
3996 cells were treated with FB₁ (0, 5, 50, 100, 200 μM; 24h) and ROS, LDH and m6A levels were quantified.
3997 qPCR was used to determine expression of m6A modulators, *Nrf2*, *Keap1* and miR-27b while western
3998 blotting was used to quantify Keap1 and Nrf2 protein expression. Methylation status of *Keap1* and *Nrf2*
3999 promoters was assessed and RNA immunoprecipitation quantified m6A-*Keap1* and m6A-*Nrf2* levels.
4000 FB₁ induced an accumulation of intracellular ROS (p≤0.001) and LDH leakage (p≤0.001). Elevated
4001 m6A levels (p≤0.05) were accompanied by an increase in m6A “writers” [METLL3 (p≤0.01) and
4002 METLL14 (p≤0.01)], and “readers” [YTHDF1 (p≤0.01), YTHDF2 (p≤0.01), YTHDF3 (p≤0.001) and
4003 YTHDC2 (p≤0.01)] and a decrease in m6A “erasers” [ALKBH5 (p≤0.001) and FTO (p≤0.001)].
4004 Hypermethylation and hypomethylation occurred at *Keap1* (p≤0.001) and *Nrf2* (p≤0.001) promoters,
4005 respectively. MiR-27b was reduced (p≤0.001); however, m6A-*Keap1* (p≤0.05) and m6A-*Nrf2* (p≤0.01)
4006 levels were upregulated. This resulted in the ultimate decrease in Keap1 (p≤0.001) and increase in Nrf2
4007 (p≤0.001) expression. Our findings reveal that m6A RNA methylation can be modified by exposure to
4008 FB₁, and a cross talk between m6A and redox regulators does occur.

4009 **Keywords**

4010 Fumonisin B₁, epigenetics, m6A RNA Methylation, Oxidative Stress, Keap1, Nrf2

4011 **Introduction**

4012 As one of the most toxic mycotoxins produced by the *Fusarium* fungal species, fumonisin B₁ (FB₁,
4013 C₃₄H₅₉NO₁₅) is a highly problematic agricultural contaminant in developing countries (Idahor, 2010,
4014 Kamle et al., 2019). Not only does it affect food quality in regions that have already inadequate food
4015 supplies but it also impinges on human and animal health. FB₁ has been conjectured to be a major factor
4016 is hepato-, nephro- and neuro-toxicity (Domijan, 2012, Müller et al., 2012, Singh and Kang, 2017,
4017 Szabó et al., 2018). It has been implicated in carcinogenesis of the liver and kidney in animals and may
4018 play a role in esophageal carcinogenesis in humans (Gelderblom et al., 2001, Alizadeh et al., 2012,
4019 Müller et al., 2012). While it is universally acknowledged that inhibition of sphingolipid metabolism is
4020 the major mechanism of FB₁ toxicity (Riley and Merrill, 2019), mounting evidence suggests that
4021 changes to the epigenetic landscape may also be critically involved in its toxicity. Although changes in
4022 DNA methylation, microRNA (miRNA) profiles and histone modifications have already been linked to
4023 FB₁-induced toxicity (Mobio et al., 2000, Kouadio et al., 2007, Chaturgoon et al., 2014a, Chaturgoon

4024 et al., 2014b, Demirel et al., 2015, Arumugam et al., 2020); the link between RNA methylation and
4025 FB₁-induced hepatotoxicity remains uncharted territory.

4026 RNA methylation accounts for over 60% of all RNA modifications and has been identified on all four
4027 ribonucleic acid bases (Cantara et al., 2010, Roundtree et al., 2017). However, methylation to the sixth
4028 nitrogen of adenosine, known as N⁶-methyladenosine (m⁶A), is the most prevalent modification that
4029 occurs on mammalian messenger RNA (mRNA) and long non-coding RNA (lncRNA) (Desrosiers et
4030 al., 1974, Pan, 2013). It functions in various biological processes by controlling the fate of m⁶A
4031 modified-RNA through splicing, export, translation, and degradation (Zaccara et al., 2019).
4032 Transcriptome-wide analysis revealed that m⁶A sites are preferentially distributed within long exons,
4033 in 3' untranslated regions (3'UTR) and adjacent to stop codons of mRNA and non-coding RNAs in
4034 various eukaryotes and some nuclear replicating viruses (Dominissini et al., 2012, Meyer et al., 2012,
4035 Yue et al., 2015, Kennedy et al., 2016).

4036 M⁶A “writers”, “erasers” and “readers” are responsible for this dynamic and reversible modification
4037 (Zaccara et al., 2019). M⁶A sites are methylated by “writers” [which include methyltransferase-like 3
4038 (METTL3), methyltransferase-like 14 (METTL14) and Wilms’s tumour 1-associated protein (WTAP)]
4039 (Schwartz et al., 2014, Wang et al., 2016) whereas “erasers” [such as ALKB homolog 5 (ALKBH5)
4040 and fat mass and obesity-associated protein (FTO)] are responsible for its demethylation (Jia et al.,
4041 2011, Zheng et al., 2013). Furthermore, m⁶A-modified transcripts are specifically recognized by
4042 “readers” namely, the YT521-B homology domain containing proteins 1 and 2 (YTHDC1 and
4043 YTHDC2) and the YT521-B homology domain family proteins 1, 2, and 3 (YTHDF1, YTHDF2, and
4044 YTHDF3) which bind to m⁶A within the consensus DRACH (where D = A/G/U, R = A/G, H = A/C/U)
4045 sequence to regulate the expression and function of specific mRNAs and proteins (Dominissini et al.,
4046 2012, Zaccara et al., 2019).

4047 Aberrant m⁶A patterns contribute to defective physiological processes, unusual immune responses,
4048 abnormal metabolism, neurodegeneration and have been implicated in hepatic diseases, rheumatoid
4049 arthritis, osteoporosis, type 2 diabetes mellitus, obesity, neurodegenerative complications, infectious
4050 diseases and various cancers (Shen et al., 2015, Lan et al., 2019, Xu et al., 2019, Han et al., 2020,
4051 Paramasivam et al., 2020). Of particular interest, studies have suggested that oxidative stress may be
4052 prevalent in altering m⁶A methylation levels and that m⁶A modifications may in turn affect oxidative
4053 stress through changes in the expression of redox regulating mRNA (Li et al., 2017, Zhao et al., 2019,
4054 Wu et al., 2020, Zhao et al., 2020a).

4055 We previously found that FB₁ enhanced ROS production which led to liver cell injury. We further
4056 observed activation of Kelch-like ECH associated protein 1 (Keap1)/ nuclear factor erythroid 2 (NF-
4057 E2)-related factor 2 (Nrf2) antioxidant signalling to counter the oxidative effects of FB₁ (Arumugam et
4058 al., 2019). Under physiological conditions, Keap1 maintains Nrf2 in an inhibitory state through

4059 ubiquitination, tagging it for proteasomal degradation. Changes in redox status triggers Nrf2 release
4060 allowing it to translocate to the nucleus where it promotes the transcription of anti-oxidants and other
4061 detoxifying enzymes (Kobayashi et al., 2006). However, whether FB₁-mediated oxidative stress affects
4062 m6A levels and if m6A modifications are a potential factor contributing to FB₁-mediated oxidative
4063 stress is unknown. Thus, the aim of this study was to investigate the effects of FB₁ on m6A RNA
4064 methylation and its crosstalk with oxidative stress responses in human hepatoma (HepG2) cells. We
4065 further examined FB₁-mediated alterations in the epigenetic regulation of Keap1/Nrf2 expression by
4066 evaluating changes in promoter methylation, m6A-*Nrf2*, m6A-*Keap1* and miRNA levels.

4067 **Method and Materials**

4068 *Materials*

4069 The HepG2 cell line (HB-8065) was obtained from the American Type Culture Collection (ATCC) and
4070 cell culture consumables were purchased from Whitehead Scientific (Johannesburg, South Africa).
4071 MiR-27b-3p mimic (MSY0000419), miR-27b-3p inhibitor (MIN0000419), and attractene transfection
4072 reagent (301005) were purchased from Qiagen (Hilden, Germany). Western blot reagents were
4073 purchased from Bio-Rad (Hercules, CA, USA) while primary antibodies: anti-Nrf2 (#12721S), anti-
4074 Keap1 (#8047S); horse-radish peroxidase (HRP)-conjugated secondary antibody: goat anti-rabbit
4075 (#7074S) were obtained from Cell Signalling Technologies (Danvers, MA, USA) and β -actin was
4076 obtained from Sigma-Aldrich (A3854; St. Louis, MO, USA). All other reagents were purchased from
4077 Merck (Boston, MA, USA), unless otherwise stated.

4078 *Cell Culture*

4079 HepG2 cells (1.5×10^6 , passage 3) were seeded in 25 cm^3 polystyrene tissue culture flasks containing
4080 Eagle's Minimum Essentials Medium (EMEM) supplemented with 10% heat-inactivated foetal calf
4081 serum, 1% penicillin-streptomycin-fungizone, and 1% L-glutamine and maintained in a 5% carbon
4082 dioxide (CO₂) atmosphere at 37°C. At 80% confluency, cells were exposed to various concentrations
4083 of FB₁ (5, 50, 100 and 200 μM) for 24 hours (h) (Arumugam et al., 2020). An untreated control
4084 (containing supplemented EMEM) was prepared along with FB₁ treatments. All experiments were
4085 repeated in two independent experiments and triplicate for reproducibility of results.

4086 *Detection of Intracellular Reactive Oxygen Species*

4087 Intracellular ROS was quantified using the 2,7-dichlorodihydrofluorescein-diacetate (H₂DCF-DA)
4088 assay, as previously described (Arumugam et al., 2019).

4089 *Measurement of Lactic Acid Dehydrogenase Leakage*

4090 Membrane damage to HepG2 cells were assessed through the measurement of lactic acid
4091 dehydrogenase (LDH) leakage. Medium collected from control and FB₁ treated cells were centrifuged
4092 (400xg, 24°C, 10 min) and dispensed (100 μl /well) in triplicate into a 96-well microtiter plate. An equal

4093 volume of LDH reagent (11644793001, Sigma Aldrich, St. Louis, MO, USA) was added to each well.
4094 The plate was incubated for 30 min at room temperature (RT) in the dark. Absorbance was read with a
4095 spectrophotometer (Bio-Tek μ Quant, Winooski, VT, USA) at 500 nM. Results are represented as
4096 relative fold change.

4097 ***Transfection of HepG2 cells with MiR-27b Mimic and MiR-27b Inhibitor***

4098 MiR-27b is an oxidative stress responsive miRNA that targets Nrf2. To assess the effects of miR-27b
4099 on Nrf2 mRNA and protein expression, cells were transfected with the mimic (Syn-hsa-miR-27b,
4100 MYS0000419, Qiagen, Hilden, Germany) and inhibitor (Anti-hsa-miR-27b-3p, MIN0000419, Qiagen,
4101 Hilden, Germany) to miR-27b. HepG2 cells were seeded in 25 cm³ polystyrene tissue culture flasks
4102 until 80% confluent. Lyophilised miRNA mimic and inhibitor (5 nmol) was reconstituted to 20 μ M in
4103 nuclease-free water. For the transfection, miR-27b mimic or inhibitor (15 μ l) was added to EMEM (72
4104 μ l) and attractene (3 μ l) in microcentrifuge tubes. Samples were then incubated for 15 min at RT to
4105 allow complex formation. Cells were rinsed with PBS and supplemented EMEM (2,940 μ l) was added
4106 to the flasks. The transfection complex was dispensed in a drop-wise fashion into the appropriate flask
4107 with gentle swirling to ensure uniform distribution. All treatments were then incubated for 24 h (37°C,
4108 5% CO₂) and utilised for RNA and protein isolation.

4109 ***RNA Isolation***

4110 RNA extraction from HepG2 cells was carried out using Qiazol reagent (79306, Qiagen, Hilden,
4111 Germany). Once treatments were removed, HepG2 cells were rinsed thrice with PBS (0.1M) and
4112 incubated with Qiazol and 0.1M PBS for 5 min. Cells were lysed with the cell scraper, and lysates were
4113 incubated (-80°C, overnight). Thereafter, chloroform (100 μ l) was dispensed into thawed samples and
4114 centrifuged (12,000xg, 4°C, 15 min). Supernatants were transferred to sterile microcentrifuge tubes and
4115 incubated with 500 μ l isopropanol (-80°C, overnight). Subsequently, samples were centrifuged
4116 (12,000xg, 4°C, 20 min), supernatants were discarded and residual salts from the RNA-containing
4117 pellets were removed with 75% ice-cold ethanol and thereafter centrifuged (7,400xg, 4°C, 15 min).
4118 RNA pellets were air-dried (30 min, RT) and resuspended in nuclease-free water (10 μ l). RNA
4119 concentration and purity were assessed using the Nanodrop2000 spectrophotometer (Thermo Scientific,
4120 Waltham, USA). RNA with a 260:280 absorbance ratio between 1.8 and 2 was used for subsequent
4121 assays and concentration was adjusted accordingly.

4122 ***Quantification of Global m6A RNA Methylation***

4123 Global m6A RNA methylation was determined using the m6A RNA methylation quantification kit
4124 (ab185912, Abcam, Cambridge, UK). Briefly, total RNA, together with m6A standards (0 – 0.1 ng/ μ l)
4125 were bound to strip wells using a high-affinity RNA binding solution. Thereafter, m6A levels were
4126 detected using an m6A capture and detection antibody. The detected signal was enhanced, and the
4127 absorbance was measured at 450 nM using a spectrophotometer (Bio-Tek μ Quant, Winooski, VT,

4128 USA). The mean absorbance of the standards was used to construct a standard curve from which the
4129 percentage m6A in each sample was determined. Results are presented as relative fold change.

4130 ***Quantitative Polymerase Chain Reaction***

4131 qPCR was used to compare the changes in the expression of *METLL3*, *METLL14*, *FTO*, *WTAP*,
4132 *YTHDF1*, *YTHDF2*, *YTHDF3*, *YTHDC2*, *Nrf2*, *Keap1* and miR-27b. For mRNA expression, cDNA was
4133 prepared from RNA (1000 ng/μl) using the Maxima H Minus First Strand cDNA Synthesis Kit
4134 according to manufacturers' protocol. qPCR was performed using the PowerUp™ SYBR™ Green
4135 Master Mix (A25742, Thermo-Fisher Scientific, Waltham, MA, USA) and CFX96 Touch™ Real-Time
4136 PCR Detection System (Bio-Rad, Hercules, CA, USA) with the following cycling conditions: initial
4137 denaturation (95°C, 8 min), followed by 40 cycles of denaturation (95°C, 15 s), annealing
4138 (Supplementary Table S5.1, 40 s), and extension (72°C, 30 s). Primer sequences and annealing
4139 temperatures are listed in Supplementary Table S5.1.

4140 For miRNA expression, cDNA synthesis was performed with 1000 ng/μl RNA, using the miScript II
4141 RT Kit (218161, Qiagen, Hilden, Germany) according to the manufacturer's instructions. RT-qPCR
4142 was performed on the CFX96 Touch™ Real-Time PCR Detection System (Bio-Rad, Hercules, CA,
4143 USA) using the miScript SYBR Green PCR Kit (218073, Qiagen, Hilden, Germany) and miR-27b
4144 miScript primer assay (MS00009247, Qiagen, Hilden, Germany) according to the manufacturer's
4145 protocol with the following cycling conditions: initial denaturation (95°C, 15 min), followed by 40
4146 cycles of denaturation (94°C, 15 s), annealing (55°C, 30 s), and extension (70°C, 30 s).

4147 *GAPDH* and *RNU6* were used as endogenous controls for mRNA and miRNA expression, respectively
4148 and relative expression was calculated using the comparative threshold cycle ($2^{\Delta\Delta C_t}$) method (Livak and
4149 Schmittgen, 2001).

4150 ***RNA Immunoprecipitation***

4151 Quantification of m6A-*Nrf2* and m6A-*Keap1* levels were determined using RNA immunoprecipitation.
4152 Briefly, RNA (1000 ng/μl) were incubated with m6A-primary antibody (1:100; ab208577, Abcam,
4153 Cambridge, UK) overnight at 4°C. Thereafter, the RNA-antibody complex was precipitated using
4154 protein A beads [20 μl 50% bead slurry (Cell Signalling Technology, #9863), 4°C, 3 h]. Samples were
4155 centrifuged (2,500xg, 4°C, 60s), washed twice in RNA immunoprecipitation buffer (150 mM KCl, 25
4156 mM Tris-Cl (pH 7.4), 5mM EDTA, 0.5mM DTT, 0.5% IGEPAL, 100 U/ml SUPERase IN RNase
4157 Inhibitor (Thermo-Fisher Scientific, AM2694), protease and phosphatase inhibitors (A32961, Thermo-
4158 Fisher Scientific)], washed once in nuclease free water and resuspended in nuclease free water (10 μl).
4159 Immunoprecipitated RNA was standardised to 200 ng/μl, and reverse transcribed into cDNA as
4160 described above. The expression of m6A-*Nrf2* and m6A-*Keap1* was then determined using qPCR as
4161 mentioned above. Primer sequences and annealing temperatures are listed in Supplementary Table S5.1.

4162 ***DNA Isolation and Promoter Methylation Analysis***

4163 Genomic DNA was isolated from HepG2 cells as previously described (Ghazi et al., 2020b). Isolated
4164 DNA was standardized to 4 ng/ μ l and used to determine methylation status at *Nrf2* and *Keap1* promoter
4165 regions. This was done using the OneStep qMethyl Kit (5310, Zymo Research, 5310) as per
4166 manufacturer's instructions. Primer sequences and annealing temperatures are listed in Supplementary
4167 Table 1. Cycling conditions were as follows: digestion by methyl sensitive restriction enzymes (37°C,
4168 2 h), initial denaturation (95°C, 10 min), followed by 45 cycles of denaturation (95°C, 30s), annealing
4169 (Supplementary Table S5.1, 60s), extension (72°C, 60s), final extension (72°C, 60s), and a hold at 4°C.
4170 Results are represented as a fold-change relative to the control.

4171 ***Protein Isolation and Western Blotting***

4172 The western blotting technique was used to determine protein expression of Nrf2 and Keap1. Protein
4173 was isolated and quantified as previously described (Arumugam et al., 2019). The standardized protein
4174 extracts (1 mg/ml) were separated using 10% sodium dodecyl sulphate-polyacrylamide gel
4175 electrophoresis, and transferred to nitrocellulose membranes which were then blocked in 5% non-fat
4176 dry milk (1 h) before incubation with the primary antibodies, anti-Nrf2 (1:1000; #12721S, Cell
4177 Signalling Technologies, Danvers, MA, USA) and anti-Keap1 (1:1000; #8047S, Cell Signalling
4178 Technologies, Danvers, MA, USA) overnight at 4°C. Membranes were washed thrice in Tween 20-Tris
4179 buffer saline (TTBS: 150 mmol/l NaCl, 3 mmol/l KCl, 25 mmol/l Tris, 0.05% Tween 20, dH₂O, pH
4180 7.5) and thereafter incubated with horse-radish peroxidase-conjugated goat anti-rabbit (1:5000; #7074S,
4181 Cell Signalling Technologies, Danvers, MA, USA) secondary antibody for 2 hours. Thereafter,
4182 membranes were washed thrice with TTBS and protein expression was visualised using the Clarity
4183 Western ECL Substrate Kit (1705060, Bio-Rad, Hercules, CA, USA) with the Chemidoc gel
4184 documentation system (Bio-Rad, Hercules, CA, USA). β -actin served as a housekeeping control and
4185 protein expression was determined using the Image Lab Software version 5.0 (Bio-Rad, Hercules, CA,
4186 USA) which measured band densities of expressed proteins. Protein expression is represented as relative
4187 band density and calculated by normalising the protein of interest against β -actin.

4188 ***Statistical Analysis***

4189 Statistical analyses were performed using GraphPad Prism version 5.0 (GraphPad Software Inc., San
4190 Diego, CA, USA). Data were expressed as the mean \pm standard deviation and analysis of variance
4191 (ANOVA) with Dunnet's post-test was used to determine the statistical differences among the groups.
4192 A p value of less than 0.05 was considered statistically significant.

4193

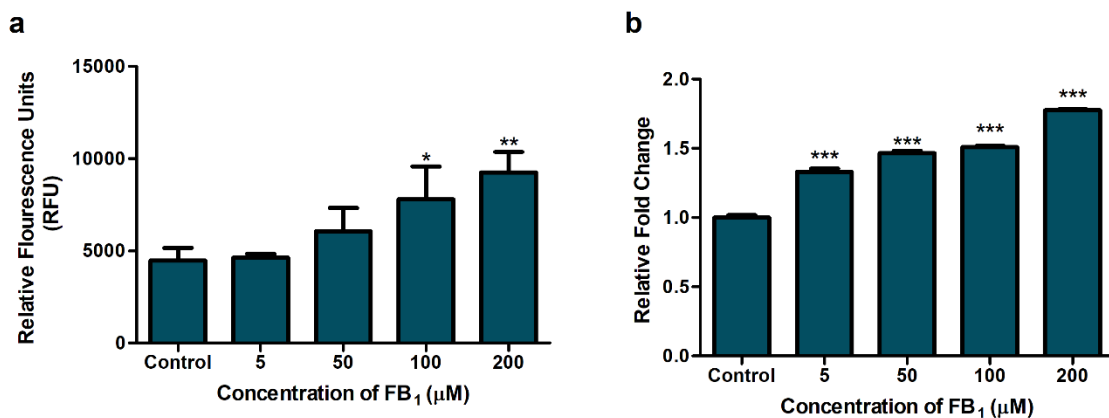
4194

4195

4196 **Results**

4197 ***FB₁ Enhanced ROS Production and Cell Membrane Damage***

4198 The effect of FB₁ on ROS generation was evaluated using the H₂DCF assay. FB₁ altered the redox status
4199 of HepG2 cells by inducing a significant dose-dependent increase in ROS levels (p= 0.0005; Figure.
4200 5.1a). Excessive production of ROS leads to cellular injury and hepatotoxicity. Upon damage to cellular
4201 membranes, cells release the enzyme LDH. As depicted in Figure 5.1b, exposure to FB₁ for 24 h
4202 promoted LDH leakage in a significant dose-dependent manner (p < 0.0001) indicating severe cell
4203 damage occurred.



4204 **Figure 5.1.** FB₁-induced hepatotoxicity in HepG2 cells. HepG2 cells were cultured with varying
4205 concentrations of FB₁ for 24 h. Intracellular ROS generation was examined by an oxidation sensitive
4206 fluorescent probe and ROS generation was significantly accelerated upon FB₁ exposure (a; *** p ≤
4207 0.001). LDH leakage was used as an indicator of hepatic injury and was found to be significantly
4208 increased at all FB₁ concentrations tested (b; *** p ≤ 0.001).

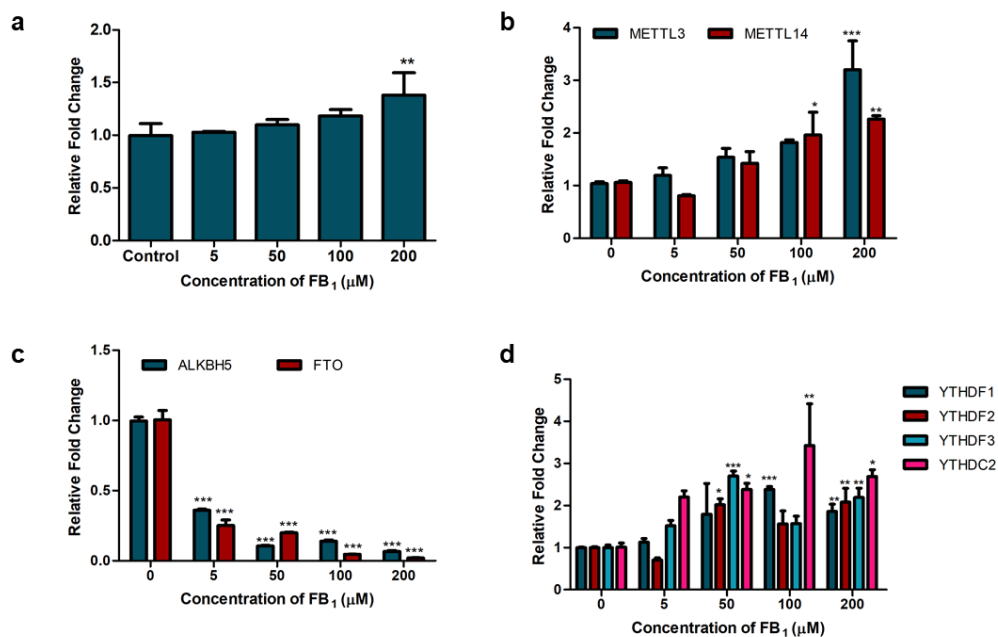
4210 ***FB₁ Altered Global M6A Levels and Expression of M6A Regulatory Elements***

4211 To determine whether FB₁-prompted oxidative stress has the potential to induce aberrant m6A
4212 modifications, levels of total m6A-modified RNA in FB₁-treated HepG2 cells were detected. In Figure
4213 5.2a, the m6A levels of the FB₁-treated groups increased, but only cells treated with 200 μM showed
4214 significant changes in m6A compared to the control (p= 0,0132).

4215 M6A modifications are regulated by methyltransferases and demethylases; therefore, we set out to
4216 determine if changes in the expression of m6A-modifying enzymes were responsible for the changes in
4217 m6A levels observed in FB₁-exposed cells. There was a significant concentration-dependant increase
4218 in the mRNA levels of m6A methyltransferase (Figure 5.2b) *METTL3* (p = 0,0017), while *METTL14*
4219 was reduced at 5 μM FB₁ and upregulated at the higher (50-200 μM) concentration of FB₁ tested (p =
4220 0,0043). Conversely, a significant dose-dependent decrease in the m6A demethylases (Figure 5.2c),
4221 *FTO* (p < 0.0001) and *ALKBH5* (p < 0.0001) were observed in the presence of all FB₁ treatments.

4222 Specific m6A readers recognize m6A-modified RNA and regulate gene expression through various
 4223 mechanisms. Thus, we determined if FB₁ had any effects on the expression of the m6A readers (Figure
 4224 5.2d); and found that FB₁ significantly increased the expression of *YTHDF1* (p = 0,0038), *YTHDF3* (p
 4225 = 0,0005) and *YTHDC2* (p = 0,0064) in HepG2 cells in comparison to the untreated cells. *YTHDF2*
 4226 expression was reduced at 5 μM FB₁ and elevated at the higher (50-200 μM) concentration of FB₁ tested
 4227 (p = 0,0021).

4228 Taken together, the data suggests that FB₁-induced oxidative stress increased m6A methylation,
 4229 possibly, through mediating dysregulation of m6A regulatory genes.



4230

4231 **Figure 5.2.** Aberrant m6A modifications induced by FB₁ in HepG2 cells. FB₁ increased global m6A
 4232 RNA modifications (a; *p ≤ 0.05) and induced changes in m6A writers [b: *METLL3* (** p ≤ 0.01) and
 4233 *METLL14* (** p ≤ 0.01)], erasers [c: *ALKBH5* (***) p ≤ 0.001) and *FTO* (***) p ≤ 0.001] and readers
 4234 [d: *YTHDF1* (** p ≤ 0.01), *YTHDF2* (** p ≤ 0.01), *YTHDF3* (***) p ≤ 0.001) and *YTHDC2* (** p ≤
 4235 0.01)].

4236 *FB₁ Epigenetically Regulates Keap1 Expression*

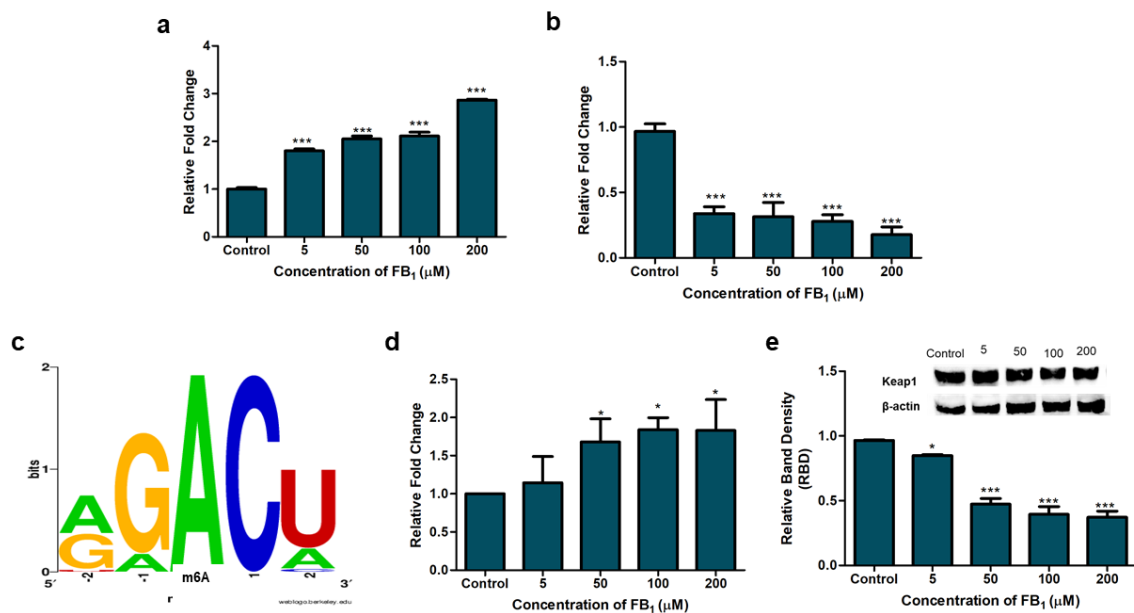
4237 In response to xenobiotic stress, cells activate the Keap1/Nrf2 pathway. Inactivation of Keap1 is
 4238 required for Nrf2-mediated activation of the antioxidant response to oxidative stress (Kobayashi et al.,
 4239 2006). Furthermore, it was recently observed that m6A modifications may also regulate Keap1/Nrf2
 4240 expression (Wang et al., 2019, Zhao et al., 2020a). Thus, we evaluated the epigenetic regulation of
 4241 Keap1 through both post-transcriptional (RNA methylation) and transcriptional (DNA methylation)
 4242 mechanisms.

4243 FB₁ has previously been shown to induce changes in the methylation status of promoter regions in genes
 4244 (Demirel et al., 2015). We observed significant dose-dependent hypermethylation of CpG islands at the
 4245 *Keap1* ($p < 0.0001$; Figure 5.3a), this led to a corresponding significant decrease in *Keap1* mRNA
 4246 expression ($p < 0.0001$; Figure 5.3b).

4247 Since FB₁ altered global m6A RNA levels, we employed the m6A site predictor SRAMP to identify
 4248 m6A sites on *Keap1* mRNA (Zhou et al., 2016). The results showed 29 possible m6A sites including 7
 4249 possible m6A sites with high confidence and 1 with very high confidence. Figure 5.3c represents the
 4250 m6A consensus sequence motif of *Keap1* (AGACU or GGACU) depicted as sequence logo obtained
 4251 by the WebLogo 3 server (weblogo.threeplusone.com/create.cgi). The height of each stack indicates the
 4252 degree of conservation (bits). The height of the letters represents the relative frequency of the base.

4253 Changes in m6A-*Keap1* levels were then evaluated via RNA immunoprecipitation. In Figure 5.3d,
 4254 exposure to varying concentrations of FB₁ lead to a significant dose-dependent increase in m6A-*Keap1*
 4255 levels ($p = 0,0125$). Furthermore, we assessed changes in Keap1 protein expression and found it to be
 4256 dose-dependently reduced by FB₁ ($p < 0.0001$; Figure 5.3e).

4257



4258

4259 **Figure 5.3.** The epigenetic effects of FB₁ on Keap1 expression in HepG2 cells. FB₁ induced hypermethylation at
 4260 *Keap1* promoters (a; *** $p \leq 0.001$) resulting in reduced *Keap1* gene expression (b; *** $p \leq 0.001$). A consensus
 4261 sequence for possible m6A modifications on *Keap1* transcripts was constructed (c). RNA immunoprecipitation
 4262 with m6A antibodies revealed that FB₁ upregulated m6A-*Keap1* (d; * $p \leq 0.05$) while western blotting found
 4263 downregulation in Keap1 protein expression (e; *** $p \leq 0.001$).

4264

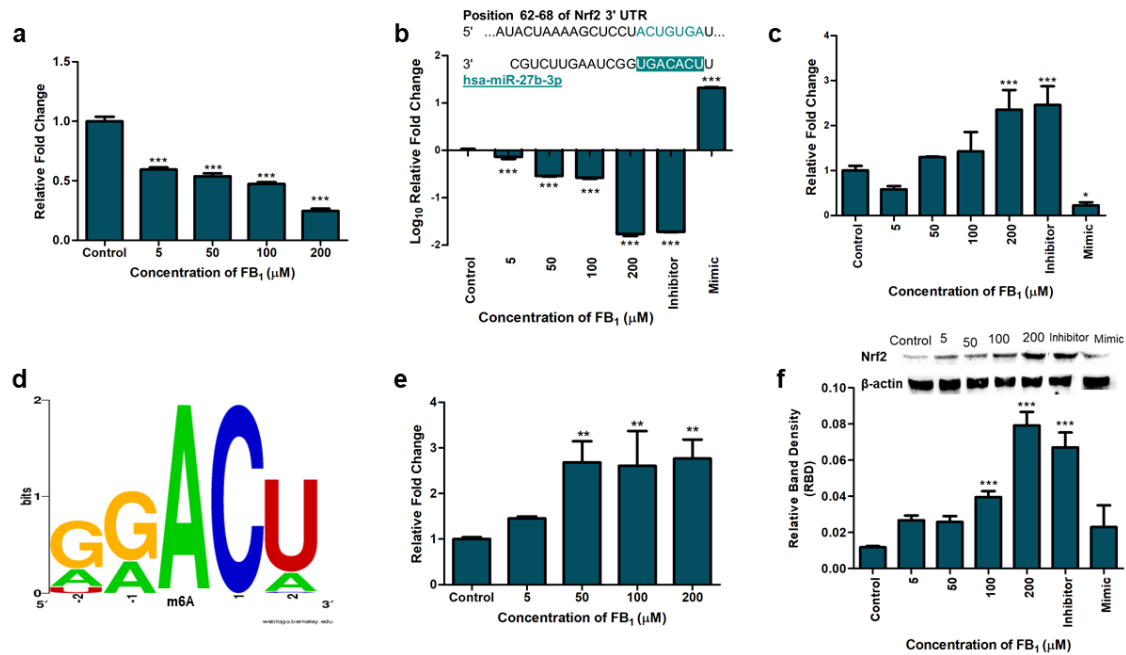
4265 ***FB₁ Promoted Nrf2 Expression Through Epigenetic Modifications***

4266 DNA methylation, miR-27b and m6A-modifications are just a few of the epigenetic factors that play a
4267 role in Nrf2 regulation, thus it was evaluated accordingly (Kang et al., 2014, Xu et al., 2017, Zhao et
4268 al., 2020a).

4269 First, methylation status of *Nrf2* promoters was evaluated in control and FB₁ treated HepG2 cells. FB₁
4270 induced a significant dose-dependent hypomethylation of *Nrf2* promoters (Figure 5.4a; $p < 0.0001$).
4271 Next, posttranscriptional regulation of Nrf2 was determined. MiR-27b was previously shown to directly
4272 target Nrf2 (Xu et al., 2017). This was further confirmed using the bioinformatics prediction algorithm
4273 software, TargetScan (version 7.1), where miR-27b was found to have complementary base pairs with
4274 *Nrf2* at positions 62-68 in humans (Agarwal et al., 2015). Thus, miR-27b expression was determined in
4275 FB₁ treated HepG2 cells using qPCR. The HepG2 cells were also treated with a miR-27b mimic and
4276 inhibitor which acted as a positive and negative control, respectively. Here, miR-27b levels were
4277 diminished at all concentrations of FB₁ tested (Fig. 4b; $p < 0.0001$). The expression of miR-27b in
4278 HepG2 cells treated with the mimic and inhibitor were increased and decreased, respectively (Figure
4279 5.4b; $p < 0.0001$).

4280 *Nrf2* gene expression was also determined by qPCR. FB₁ increased *Nrf2* expression in HepG2 cells.
4281 Treatment of HepG2 cells with the miR-27b mimic and inhibitor resulted in a decrease and increase,
4282 respectively in Nrf2 levels (Figure 5.4c).

4283 SRAMP was also used to predict m6A sites on *Nrf2* transcripts. A total of 54 m6A sites were predicated
4284 with 15 high confidence and 2 very high confidence sites. Figure 5.4d represents the consensus motif
4285 of m6A modification on *Nrf2* which is GGACU. We further tested m6A-*Nrf2* levels and found that like
4286 Keap1, FB₁ significantly upregulated m6A-*Nrf2* levels ($p = 0,0018$; Fig. 4e). Moreover, western blotting
4287 analysis revealed that FB₁ significantly increased Nrf2 protein expression in a dose-dependent manner
4288 ($p < 0.0001$; Figure 5.4f). Treatment of HepG2 cells with the miR-27b mimic and inhibitor resulted in
4289 a decrease and increase, respectively in Nrf2 protein levels (Figure 5.4f); further validating that Nrf2 is
4290 a target of miR-27b.



4291

4292 **Figure 5.4.** FB₁ epigenetically regulates Nrf2 expression in HepG2 cells. FB₁ induced hypomethylation
 4293 at *Nrf2* promoter regions (a; *** $p \leq 0.001$) and reduced miR-27b (b; *** $p \leq 0.001$) expression; which
 4294 led to the subsequent increase in *Nrf2* mRNA levels (c; *** $p \leq 0.001$). A consensus sequence for
 4295 possible m6A modifications on *Nrf2* transcripts was constructed (d). m6A-*Nrf2* (e; $p \leq 0.01$) and Nrf2
 4296 protein expression (f; *** $p \leq 0.001$) were significantly increased.

4297 Discussion

4298 FB₁ is a well-known hepatotoxin and hepatocarcinogen (Gelderblom et al., 2001, Singh and Kang,
 4299 2017). It induces its toxicity via the disruption of sphingolipid metabolism, resulting in oxidative stress,
 4300 endoplasmic reticulum stress and autophagy (Liu et al., 2019). However, epigenetic changes also play
 4301 a critical role in its toxicity and carcinogenicity. For instance, miR-27b is an important regulator of
 4302 cholesterol and lipid metabolism, and prevents the bioactivation of procarcinogens via the suppression
 4303 of cytochrome 1b1 (Tsuchiya et al., 2006, Vickers et al., 2013). However, the downregulation of miR-
 4304 27b by FB₁ and concurrent increase in cytochrome 1b1 facilitates neoplastic transformation observed
 4305 in FB₁ exposed liver cells (Chaturgoon et al., 2014b). Furthermore, FB₁ specifically methylates CpG
 4306 islands found on the promoters of tumour suppressor genes and induces global hypomethylation which
 4307 are both common hallmarks of cancer (Chaturgoon et al., 2014a, Demirel et al., 2015). More recently,
 4308 FB₁ prompted changes in miRNA-30c and histone methylation which led to the loss the tumour
 4309 suppressor, phosphatase and tensin homolog (PTEN) and diminished response and repair of oxidative
 4310 DNA lesions (Arumugam et al., 2020). While alterations in DNA methylation, histone modifications
 4311 and miRNA profiles have been shown to play a part in FB₁-mediated hepatopathologies, little has been
 4312 uncovered about the potential role of RNA methylation in these pathologies.

4313 With more than 100 identified RNA modifications, m6A remains the most prevalent epitranscriptomic
4314 marker (Cantara et al., 2010). Changes in redox homeostasis have been shown to affect m6A levels and
4315 m6A modifications in turn may affect oxidative stress through regulating redox-associated genes (Li et
4316 al., 2017, Zhao et al., 2019, Wu et al., 2020, Zhao et al., 2020a). Therefore, in this study, we explored
4317 the effects of m6A modifications to further analyse the mechanisms by which FB₁ induces its toxicity.
4318 We evaluated changes in ROS, global m6A RNA levels and expression of m6A regulatory genes in
4319 HepG2 cells exposed to varying concentrations of FB₁ for 24 h. We further examined the epigenetic
4320 regulation of Keap1/Nrf2 signalling by assessing changes in promoter methylation, m6A-*Nrf2*, m6A-
4321 *Keap1* and miR-27b levels.

4322 In order to characterize oxidative stress induced by FB₁, intracellular ROS production was quantified
4323 using the fluorometric H₂DCF assay. As presented in Figure 5.1a, exposure to FB₁ for 24 h enhanced
4324 intracellular ROS levels in a dose-dependent manner. Excessive levels of ROS inflict cellular injury.
4325 We previously showed that FB₁ (200µM, 24h) accelerated the production of ROS inducing severe
4326 damage to lipids and proteins, contributing to its toxicity in HepG2 cells (Arumugam et al., 2019). Here,
4327 we found that FB₁-induced ROS inflicted severe cellular damage as LDH leakage was significantly
4328 increased at all FB₁ concentrations tested (Figure 5.1b). Taken together these results confirm that FB₁
4329 induces hepatotoxicity through an accumulation of intracellular ROS.

4330 Environmental stimuli including heat shock and ultra-violet radiation have been shown to alter m6A
4331 patterns in HepG2 cells (Dominissini et al., 2012). To determine whether FB₁ may have an impact on
4332 m6A patterns, we first determined whether FB₁ altered global m6A levels. Analysis of total RNA
4333 revealed that m6A levels were elevated in a dose-dependent manner by FB₁; however, they were only
4334 significantly elevated at the highest concentration of FB₁ tested (200 µM; Figure 5.2a). Previous reports
4335 have indicated that other *Fusarium* toxins that naturally co-occur with FB₁ can alter m6A methylation
4336 patterns. Deoxynivalenol (DON) differentially regulated genes related to the tumour necrosis factor
4337 alpha inflammatory pathway through aberrant m6A patterns (Zhengchang et al., 2020), while fusaric
4338 acid reduced p53 expression through the reduction of m6A-*p53* levels (Ghazi et al., 2020a). Of
4339 particular interest, Wu et al. (2020) demonstrated that ROS-mediated increases in m6A RNA
4340 methylation may be a potential mechanism of aflatoxin B₁-induced hepatotoxicity. Although the
4341 observed trends were different in these studies, the results suggest that m6A modifications are involved
4342 in the toxic effects of these mycotoxins. In addition, m6A modifications promote hepatic growth and
4343 aberrant m6A RNA levels in liver have been associated with liver pathologies such as hepatocellular
4344 carcinogenesis, viral hepatitis and non-alcoholic fatty liver disease. Therefore, we speculate that
4345 increases in m6A modification may be related to the toxic nature of FB₁ in the liver.

4346 Ideally, increased expression of m6A methyltransferases and reduced expression of m6A demethylases
4347 should result in the elevated m6A levels that were observed. Thus, we determined if FB₁ altered the
4348 expression of m6A regulatory genes. M6A marks are installed by the methyltransferase complex

4349 consisting of the catalytic unit METTL3 and structural components METTL14 and WTAP. FB₁ dose-
4350 dependently increased the expression of *METTL3* and *METTL14* (Figure 5.2b); however, like global
4351 m6A levels, results were only significant at the higher FB₁ concentrations tested. M6A marks are
4352 removed by the demethylases: FTO and ALKBH5. Exposure to FB₁ resulted in the drastic decrease in
4353 m6A-demethylases at all concentrations tested (Figure 5.2c). The extremely low levels of FTO may
4354 also contribute to the toxic nature of FB₁ as *FTO* knock down was shown to contribute to chromosomal
4355 instability and cell cycle arrest (Huang et al., 2019). The results suggest that together m6A writers and
4356 erasers are involved in regulating global m6A levels; however, METLL3 may play a more prominent
4357 role as its expression pattern closely matched total m6A levels induced by FB₁. The expression of m6A
4358 readers were also determined as they recognize and govern the fate of m6A modified transcripts. For
4359 instance, YTHDF1, YTHDF3 and YTHDC2 promote the translation of m6A marked transcripts; while
4360 YTHDF2 accelerates the degradation of m6A-modified transcripts. FB₁ increased the mRNA levels of
4361 m6A “readers” in HepG2 cells; however, 200 μM FB₁ was the only concentration to significantly
4362 increase the expression of all m6A “readers” (Figure 5.2d). The differential expression in m6A
4363 regulating enzymes may also contribute to abnormal lipid metabolism and immune profiles in the liver
4364 (Zhao et al., 2020b).

4365 FB₁-induced increases in m6A levels may lead to the altered expression of important genes involved in
4366 its toxicity. Since FB₁ triggered abnormal ROS production, we decided to focus on Keap1 and Nrf2 as
4367 the Keap1/Nrf2 signaling plays a critical role in responding to xenobiotic and electrophilic stress. Not
4368 only did we set out to determine changes in m6A-*Keap1* and m6A-*Nrf2* but we also evaluated other
4369 epigenetic changes that might affect their expression.

4370 The most extensively studied epigenetic modification to eukaryotic genomes is DNA methylation which
4371 occurs primarily at CpG sites. Methylation of CpG islands found in gene promoters prevents the binding
4372 of transcription factors, silencing transcription. As seen in Figure 5.3a, FB₁ induced significant
4373 hypermethylation at the *Keap1* promoter, inhibiting *Keap1* transcription (Figure 5.3b). Before assessing
4374 m6A-*Keap1* levels, a sequence based m6A site predictor (SRAMP) was used to define potential m6A
4375 sites on *Keap1* mRNA (Zhou et al., 2016). 29 possible m6A sites were predicted on *Keap1* transcripts
4376 including 7 possible m6A sites with high confidence and 1 with very high confidence. Furthermore, the
4377 consensus motifs (GGACU and AGACU) matched DRACH motif (Figure 5.3c). The results suggest
4378 that m6A-modified *Keap1* maybe be involved in its translation. Using RNA immunoprecipitation and
4379 western blotting, we determined changes in m6A-*Keap1* and Keap1 protein expression, respectively.
4380 Although m6A modified *Keap1* levels were increased (Figure 5.3d); there was a severe loss in Keap1
4381 protein expression (Figure 5.3e). The m6A-reader YTHDF2 may be responsible for this. The aromatic
4382 cage of YTHDF2 specifically targets m6A modified RNA to cytoplasmic decay sites and accelerates
4383 the degradation of marked transcripts (Wang et al., 2014). The high levels of *YTHDF2* observed post
4384 FB₁ treatments may be involved in *Keap1* degradation. Furthermore, colistin-induced oxidative stress

4385 was attenuated by the overexpression of METTL3 and diminished Keap1 levels. METTL3, enhanced
4386 m6A modifications on pri-miR-873, promoted the generation of mature miR-873-5p which in turn
4387 inhibited Keap1 expression (Wang et al., 2019). Cells may be responding to FB₁-mediated oxidative
4388 stress in a similar manner, however this needs to be further investigated.

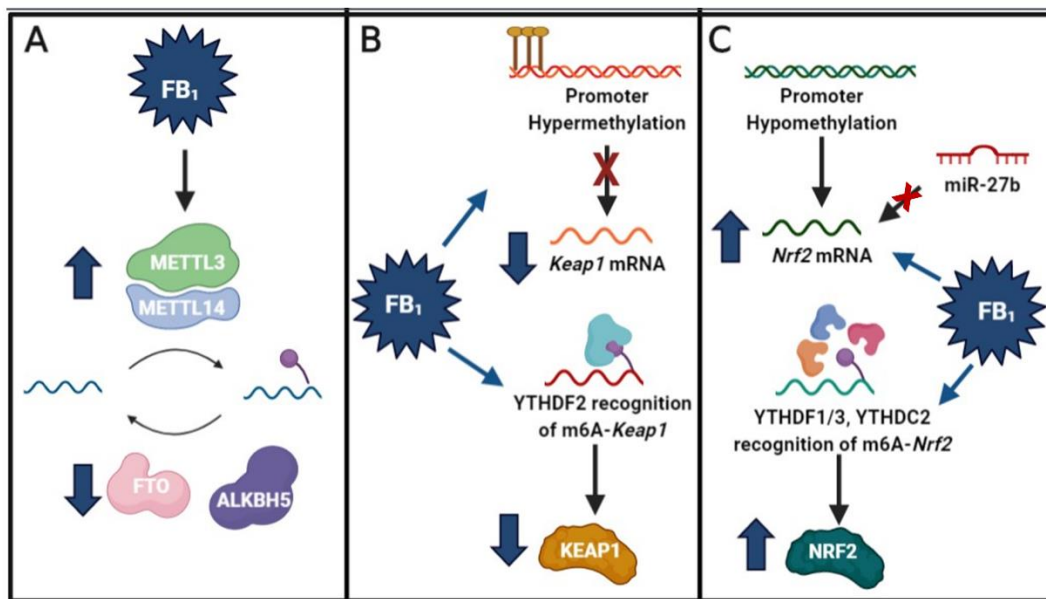
4389 Not only is Nrf2 expression regulated by DNA and RNA methylation but also by miRNA-27b (Kang
4390 et al., 2014, Xu et al., 2017). As mentioned earlier, FB₁ downregulated miR-27b expression
4391 (Chuturgoon et al., 2014b). It was previously shown that miR-27b regulates Nrf2 expression (Xu et al.,
4392 2017) and this was further confirmed using TargetScan version 7.1 (Agarwal et al., 2015).
4393 Hypomethylation of *Nrf2* promoters (Figure 5.4a), coupled with the gross loss of miR-27b (Figure 5.4b)
4394 resulted in elevated *Nrf2* mRNA expression (Figure 5.4c). Moreover, 54 possible m6A sites with 15
4395 high confidence and 2 very high confidence sites were predicted using SRAMP. The consensus motif
4396 (GGACU) also matched the DRACH motif (Figure 5.4d). FB₁ significantly increased m6A-*Nrf2* levels
4397 (Figure 5.4e) and Nrf2 protein expression (Figure 5.4f). It is possible that the increase in YTHDF1,
4398 YTHDF3 and/or YTHDC2 may be responsible for elevated Nrf2 protein expression as these readers
4399 promote the translation of targeted transcripts (Wang et al., 2015). Oxidative stress was also shown to
4400 elevate m6A-*Nrf2* levels in di-(2-ethylhexyl) phthalate (DEHP) exposed rats, however, the fate of m6A-
4401 tagged *Nrf2* transcripts were not further investigated. The authors speculated that Nrf2 protein
4402 expression would be decreased, however, the opposite could be true; like our study YTHDC2 was also
4403 elevated after DEHP exposure.

4404 To our knowledge, this is the first study to identify that FB₁ alters global and transcript-specific m6A
4405 methylation levels. While several studies have noted the accumulation of ROS enhances m6A RNA
4406 levels, we cannot say for certain that the observed changes were due to FB₁ effect on ROS generation
4407 (Li et al., 2017, Zhao et al., 2019, Wu et al., 2020, Zhao et al., 2020a). The use of positive and negative
4408 controls such as hydrogen peroxide and an antioxidant such as *N*-acetylcysteine would have given a
4409 more definitive answer. However, it is evident that FB₁ does significantly alter the expression of m6A
4410 modulator genes especially m6A demethylases. It would be interesting to further explore if the
4411 differential expression of these m6A regulating genes may play a role in FB₁ toxicity aside from m6A
4412 regulation as these genes have been shown to regulate metabolism and immune profiles in the liver (Xu
4413 et al., 2019). Further, FB₁ epigenetically regulates Keap1 and Nrf2 expression, through changes in
4414 promoter methylation, RNA methylation and miR-27b levels. The downregulation of Keap1 and
4415 upregulation of Nrf2 by FB₁ suggests that antioxidant signalling pathways have been activated. An
4416 increase in Nrf2 regulated anti-oxidants were previously observed in response to FB₁-induced oxidative
4417 stress (Arumugam et al., 2019). However, the activation of Nrf2 antioxidant signalling may not be
4418 sufficient to counter the accumulation of ROS induced by FB₁ as severe cellular injury occurred.
4419 Furthermore, prolonged activation of Nrf2 signalling supports a cancerous phenotype through ROS
4420 detoxification and tumorigenesis (Wu et al., 2019). Epigenetic changes such hypermethylation at *Keap1*

4421 promoters, hypomethylation at *Nrf2* promoters and altered miRNA profiles have shown to be involved
 4422 in deregulation of Keap1/Nrf2 in various cancers (Eades et al., 2011, Barbano et al., 2013, Kang et al.,
 4423 2014, Fabrizio et al., 2018). We can only speculate that this may be a possible mechanism by which
 4424 FB₁ promotes hepatocarcinogenesis. However, further studies should be conducted to test this
 4425 hypothesis. The use of longer exposure times and comparing differences in the epigenetic profiles
 4426 linked to Keap1/Nrf2 dysregulation in normal and cancerous cells may be key.

4427 **Conclusion**

4428 The results of this study revealed that FB₁ induces hepatotoxicity as observed by ROS accumulation
 4429 and loss of cell membrane integrity. Global m6A levels were increased in response to changes in the
 4430 expression of m6A-modulating genes (Figure 5.5a). Further, we observed hypermethylation of *Keap1*
 4431 promoters, hypomethylation of *Nrf2* promoters, reduction in miR-27b and increase in m6A-*Keap1* and
 4432 m6A-*Nrf2*, which ultimately led to the activation of Keap1/Nrf2 signalling (Figure 5.5b-c). This study
 4433 provides new evidence that m6A modifications may play a pivotal role in FB₁-induced oxidative stress
 4434 and hepatocarcinogenesis.



4435
 4436 **Figure 5.5.** FB₁ alters global m6A RNA methylation and epigenetically regulates Keap1-Nrf2 signaling. (a) FB₁
 4437 induced changes to global m6A RNA methylation by mediating changes in m6A “writers” (*METLL3* and
 4438 *METLL14*) and m6A demethylases (*FTO* and *ALKBH5*). (b) FB₁ epigenetically downregulates Keap1 through
 4439 hypomethylation of *Keap1* gene promoters and degradation of m6A-*Keap1* transcripts via *YTHDF2*. (c) *Nrf2* is
 4440 epigenetically upregulated by FB₁ via hypomethylation of *Nrf2* promoters, reduced miR-27b and increased
 4441 recognition of m6A-*Nrf2* transcripts by *YTHDF1*, *YTHDF2* and *YTHDC2*.

4442 **Declarations**

4443 *Funding*

4444 The authors acknowledge the National Research Foundation (NRF) of South Africa and College of
 4445 Health Science (University of Kwa-Zulu Natal) for funding this study.

4446 *Conflicts of interest*

4447 The authors declare that they have no conflicts of interest

4448 *Ethics approval*

4449 Ethic was received from the University of Kwa-Zulu Natal's Biomedical Research Ethics Committee.

4450 Ethics number: BE322/19.

4451 *Author Contributions*

4452 TA, TG, and AC conceptualised and designed the study. TA conducted all laboratory experiments,

4453 analysed the data and wrote the manuscript. TG and AC revised the manuscript. All authors have read

4454 the manuscript prior to submission.

4455

4456 **Supplementary Information**

4457 **Supplementary Table S5.1: Primer sequences and annealing temperatures used in qPCRs**

Gene	Sense Primer 5' → 3'	Anti-sense Primer 5' → 3'	Annealing Temperature (°C)
qPCR			
METTL3	TTGTCTCCAACCTTCCGTAGT	CCAGATCAGAGAGGTGGTGTAG	56
METTL14	GAACACAGAGCTTAAATCCCCA	TGTCAGCTAAACCTACATCCCTG	56
FTO	GCTGCTTATTTCTGGGACCTG	AGCCTGGATTACCAATGAGGA	56
ALKBH5	ATCCTCAGGAAGACAAGATTAG	TTCTCTTCCTTGCCATCTC	60
YTHDF1	ATACCTCACCACTACGGACA	GTGCTGATAGATGTTGTTCCCC	56
YTHDF2	CCTTAGGTGGAGCCATGATTG	TCTGTGCTACCCAACCTCAGT	56
YTHDF3	TCAGAGTAACAGCTATCCACCA	GGTTGTCAGATATGGCATAGGCT	56
YTHDC2	CAAAACATGCTGTTAGGAGCCT	CCACTTGTCTTGCTCATTCCC	60
Keap1	CTGGAGGATCATAACCAAGCAGG	GGATACCCTCAATGGACACCAC	57
Nrf2	TCAGCGACGGAAAGAGTATGA	CCACTGGTTTCTGACTGGATGT	58

GAPDH	TCCACCACCCTGTTGCTGTA	ACCACAGTCCATGCCATCAC	Same as gene of interest
Promoter Methylation			
Keap1	TTAGTTATTTAG-GAGGTTGT	AACCCCCCTTCTCACTA	54
Nrf2	TGAGATATTTTGCACATCCGATA	ACTCTCAGGGTTCCTTTACACG	54
RNA Immunoprecipitation			
Keap1	CTGGAGGATCATAACCAAGCAGG	GGATACCCTCAATGGACACCAC	57
Nrf2	TCAGCGACGGAAAGAGTATGA	ACCACAGTCCATGCCATCAC	58

4458

4459

	Predicted consequential pairing of target region (top) and miRNA (bottom)	
Position 62-68 of NFE2L2 3' UTR	5'	...AUACUAAAAGCUCCUACUGUGAU...
hsa-miR-27b-3p	3'	CGUCUUGAAUCGGUGACACUU

4460

4461 **Supplementary Figure S5.1.** TargetScan analyses of miR-27b to the 3' UTR of *NFE2L2* (*Nrf2*) in
4462 humans. MiR-27b has complementary base pairs with the 3' UTR of *Nrf2* at positions 62-68 in humans.

4463 **References**

4464 Agarwal V, Bell GW, Nam J-W & Bartel DP 2015. Predicting effective microRNA target sites in
4465 mammalian mRNAs. *eLife*, 4, e05005.

4466 Alizadeh AM, Roshandel G, Roudbarmohammadi S, Roudbary M, Sohanaki H, Ghiasian SA,
4467 Taherkhani A, Semnani S & Aghasi M 2012. Fumonisin B1 contamination of cereals and risk of
4468 esophageal cancer in a high risk area in northeastern Iran. *Asian Pacific journal of cancer prevention*,
4469 13, 2625-2628.

4470 Arumugam T, Pillay Y, Ghazi T, Nagiah S, Abdul NS & Chuturgoon AA 2019. Fumonisin B(1)-
4471 induced oxidative stress triggers Nrf2-mediated antioxidant response in human hepatocellular
4472 carcinoma (HepG2) cells. *Mycotoxin Res*, 35, 99-109.

4473 Arumugam T, Ghazi T & Chuturgoon A 2020. Fumonisin B 1 Epigenetically Regulates PTEN
4474 Expression and Modulates DNA Damage Checkpoint Regulation in HepG2 Liver Cells. *Toxins*, 12, 2-
4475 15.

4476 Barbano R, Muscarella LA, Pasculli B, Valori VM, Fontana A, Coco M, la Torre A, Balsamo T, Poeta
4477 ML & Marangi GF 2013. Aberrant Keap1 methylation in breast cancer and association with
4478 clinicopathological features. *Epigenetics*, 8, 105-112.

4479 Cantara WA, Crain PF, Rozenski J, McCloskey JA, Harris KA, Zhang X, Vendeix FA, Fabris D &
4480 Agris PF 2010. The RNA modification database, RNAMDB: 2011 update. *Nucleic acids research*, 39,
4481 D195-D201.

4482 Chuturgoon A, Phulukdaree A & Moodley D 2014a. Fumonisin B₁ induces global DNA
4483 hypomethylation in HepG2 cells - An alternative mechanism of action. *Toxicology*, 315, 65-69.

4484 Chuturgoon AA, Phulukdaree A & Moodley D 2014b. Fumonisin B₁ modulates expression of human
4485 cytochrome P450 1b1 in human hepatoma (Hepg2) cells by repressing Mir-27b. *Toxicology letters*, 227,
4486 50-55.

4487 Demirel G, Alpertunga B & Ozden S 2015. Role of fumonisin B1 on DNA methylation changes in rat
4488 kidney and liver cells. *Pharmaceutical Biology*, 53, 1302-1310.

4489 Desrosiers R, Friderici K & Rottman F 1974. Identification of methylated nucleosides in messenger
4490 RNA from Novikoff hepatoma cells. *Proc Natl Acad Sci U S A*, 71, 3971-3975.

4491 Domijan A-M 2012. Fumonisin B1: A neurotoxic mycotoxin/fumonizin B1: Neurotoksični mikotoksin.
4492 *Archives of Industrial Hygiene and Toxicology*, 63, 531-544.

4493 Dominissini D, Moshitch-Moshkovitz S, Schwartz S, Salmon-Divon M, Ungar L, Osenberg S, Cesarkas
4494 K, Jacob-Hirsch J, Amariglio N, Kupiec M, et al. 2012. Topology of the human and mouse m6A RNA
4495 methylomes revealed by m6A-seq. *Nature*, 485, 201-206.

4496 Eades G, Yang M, Yao Y, Zhang Y & Zhou Q 2011. miR-200a regulates Nrf2 activation by targeting
4497 Keap1 mRNA in breast cancer cells. *J Biol Chem*, 286, 40725-40733.

4498 Fabrizio FP, Sparaneo A, Trombetta D & Muscarella LA 2018. Epigenetic versus Genetic Deregulation
4499 of the KEAP1/NRF2 Axis in Solid Tumors: Focus on Methylation and Noncoding RNAs. *Oxidative
4500 Medicine and Cellular Longevity*, 2018, 2492063.

4501 Gelderblom W, Abel S, Smuts CM, Marnewick J, Marasas W, Lemmer ER & Ramljak D 2001.
4502 Fumonisin-induced hepatocarcinogenesis: mechanisms related to cancer initiation and promotion.
4503 *Environmental Health Perspectives*, 109, 291-300.

4504 Ghazi T, Nagiah S & Chuturgoon AA 2020a. Fusaric acid decreases p53 expression by altering
4505 promoter methylation and m6A RNA methylation in human hepatocellular carcinoma (HepG2) cells.
4506 *Epigenetics*, 1-13.

4507 Ghazi T, Nagiah S, Dhani S & Chuturgoon AA 2020b. Fusaric acid-induced epigenetic modulation of
4508 hepatic H3K9me3 triggers apoptosis in vitro and in vivo. *Epigenomics*, 12, 955-972.

4509 Han M, Liu Z, Xu Y, Liu X, Wang D, Li F, Wang Y & Bi J 2020. Abnormality of m6A mRNA
4510 Methylation Is Involved in Alzheimer's Disease. *Front Neurosci*, 14, 98-98.

- 4511 Huang T, Gao Q, Feng T, Zheng Y, Guo J & Zeng W 2019. FTO Knockout Causes Chromosome
4512 Instability and G2/M Arrest in Mouse GC-1 Cells. *Frontiers in Genetics*, 9.
- 4513 Idahor K 2010. Global distribution of Fumonisin B 1 – A review. *acta SATECH*, 3, 25 – 32.
- 4514 Jia G, Fu Y, Zhao X, Dai Q, Zheng G, Yang Y, Yi C, Lindahl T, Pan T, Yang Y-G, et al. 2011. N6-
4515 Methyladenosine in nuclear RNA is a major substrate of the obesity-associated FTO. *Nature Chemical*
4516 *Biology*, 7, 885-887.
- 4517 Kamle M, Mahato D, Devi S, Lee K, Kang SG & Kumar P 2019. Fumonisin: Impact on Agriculture,
4518 Food, and Human Health and their Management Strategies. *Toxins*, 11, 238.
- 4519 Kang KA, Piao MJ, Kim KC, Kang HK, Chang WY, Park IC, Keum YS, Surh YJ & Hyun JW 2014.
4520 Epigenetic modification of Nrf2 in 5-fluorouracil-resistant colon cancer cells: involvement of TET-
4521 dependent DNA demethylation. *Cell Death Dis*, 5, e1183-e1183.
- 4522 Kennedy EM, Bogerd HP, Kornepati AV, Kang D, Ghoshal D, Marshall JB, Poling BC, Tsai K,
4523 Gokhale NS & Horner SM 2016. Posttranscriptional m6A editing of HIV-1 mRNAs enhances viral
4524 gene expression. *Cell host & microbe*, 19, 675-685.
- 4525 Kobayashi A, Kang M-I, Watai Y, Tong KI, Shibata T, Uchida K & Yamamoto M 2006. Oxidative and
4526 electrophilic stresses activate Nrf2 through inhibition of ubiquitination activity of Keap1. *Molecular*
4527 *and cellular biology*, 26, 221-229.
- 4528 Kouadio JH, Dano SD, Moukha S, Mobio TA & Creppy EE 2007. Effects of combinations of Fusarium
4529 mycotoxins on the inhibition of macromolecular synthesis, malondialdehyde levels, DNA methylation
4530 and fragmentation, and viability in Caco-2 cells. *Toxicon*, 49, 306-317.
- 4531 Lan Q, Liu PY, Haase J, Bell JL, Hüttelmaier S & Liu T 2019. The critical role of RNA m6A
4532 methylation in cancer. *Cancer research*, 79, 1285-1292.
- 4533 Li Q, Li X, Tang H, Jiang B, Dou Y, Gorospe M & Wang W 2017. NSUN2-mediated m5C methylation
4534 and METTL3/METTL14-mediated m6A methylation cooperatively enhance p21 translation. *Journal*
4535 *of cellular biochemistry*, 118, 2587-2598.
- 4536 Liu X, Fan L, Yin S, Chen H & Hu H 2019. Molecular mechanisms of fumonisin B1-induced toxicities
4537 and its applications in the mechanism-based interventions. *Toxicon*, 167, 1-5.
- 4538 Livak KJ & Schmittgen TD 2001. Analysis of relative gene expression data using real-time quantitative
4539 PCR and the 2(-Delta Delta C(T)) Method. *Methods*, 25, 402-408.
- 4540 Meyer KD, Saletore Y, Zumbo P, Elemento O, Mason CE & Jaffrey SR 2012. Comprehensive analysis
4541 of mRNA methylation reveals enrichment in 3' UTRs and near stop codons. *Cell*, 149, 1635-1646.

4542 Mobio TA, Anane R, Baudrimont I, Carratú MR, Shier TW, Dano SD, Ueno Y & Creppy EE 2000.
4543 Epigenetic properties of fumonisin B(1): cell cycle arrest and DNA base modification in C6 glioma
4544 cells. *Toxicology and applied pharmacology*, 164, 91-96.

4545 Müller S, Dekant W & Mally A 2012. Fumonisin B1 and the kidney: Modes of action for renal tumor
4546 formation by fumonisin B1 in rodents. *Food and chemical toxicology*, 50, 3833-3846.

4547 Pan T 2013. N6-methyl-adenosine modification in messenger and long non-coding RNA. *Trends in*
4548 *Biochemical Sciences*, 38, 204-209.

4549 Paramasivam A, Priyadharsini JV & Raghunandhakumar S 2020. Implications of m6A modification in
4550 autoimmune disorders. *Cellular & Molecular Immunology*, 17, 550-551.

4551 Riley RT & Merrill AH 2019. Ceramide synthase inhibition by fumonisins: a perfect storm of perturbed
4552 sphingolipid metabolism, signaling, and disease. *Journal of lipid research*, 60, 1183-1189.

4553 Roundtree IA, Evans ME, Pan T & He C 2017. Dynamic RNA Modifications in Gene Expression
4554 Regulation. *Cell*, 169, 1187-1200.

4555 Schwartz S, Mumbach Maxwell R, Jovanovic M, Wang T, Maciag K, Bushkin GG, Mertins P, Ter-
4556 Ovanesyan D, Habib N, Cacchiarelli D, et al. 2014. Perturbation of m6A Writers Reveals Two Distinct
4557 Classes of mRNA Methylation at Internal and 5' Sites. *Cell Reports*, 8, 284-296.

4558 Shen F, Huang W, Huang JT, Xiong J, Yang Y, Wu K, Jia GF, Chen J, Feng YQ, Yuan BF, et al. 2015.
4559 Decreased N(6)-methyladenosine in peripheral blood RNA from diabetic patients is associated with
4560 FTO expression rather than ALKBH5. *J Clin Endocrinol Metab*, 100, E148-154.

4561 Singh MP & Kang SC 2017. Endoplasmic reticulum stress-mediated autophagy activation attenuates
4562 fumonisin B1 induced hepatotoxicity in vitro and in vivo. *Food and chemical toxicology*, 110, 371-382.

4563 Szabó A, Szabó-Fodor J, Kachlek M, Mézes M, Balogh K, Glávits R, Ali O, Zeebone YY & Kovács M
4564 2018. Dose and Exposure Time-Dependent Renal and Hepatic Effects of Intraperitoneally Administered
4565 Fumonisin B1 in Rats. *Toxins*, 10, 465.

4566 Tsuchiya Y, Nakajima M, Takagi S, Taniya T & Yokoi T 2006. MicroRNA regulates the expression of
4567 human cytochrome P450 1B1. *Cancer Res*, 66, 9090-9098.

4568 Vickers KC, Shoucri BM, Levin MG, Wu H, Pearson DS, Osei-Hwedieh D, Collins FS, Remaley AT
4569 & Sethupathy P 2013. MicroRNA-27b is a regulatory hub in lipid metabolism and is altered in
4570 dyslipidemia. *Hepatology*, 57, 533-542.

4571 Wang J, Ishfaq M, Xu L, Xia C, Chen C & Li J 2019. METTL3/m6A/miRNA-873-5p Attenuated
4572 Oxidative Stress and Apoptosis in Colistin-Induced Kidney Injury by Modulating Keap1/Nrf2 Pathway.
4573 *Frontiers in Pharmacology*, 10.

- 4574 Wang X, Lu Z, Gomez A, Hon GC, Yue Y, Han D, Fu Y, Parisien M, Dai Q & Jia G 2014. N 6-
4575 methyladenosine-dependent regulation of messenger RNA stability. *Nature*, 505, 117-120.
- 4576 Wang X, Zhao BS, Roundtree IA, Lu Z, Han D, Ma H, Weng X, Chen K, Shi H & He C 2015. N(6)-
4577 methyladenosine Modulates Messenger RNA Translation Efficiency. *Cell*, 161, 1388-1399.
- 4578 Wang X, Feng J, Xue Y, Guan Z, Zhang D, Liu Z, Gong Z, Wang Q, Huang J, Tang C, et al. 2016.
4579 Structural basis of N6-adenosine methylation by the METTL3–METTL14 complex. *Nature*, 534, 575-
4580 578.
- 4581 Wu J, Gan Z, Zhuo R, Zhang L, Wang T & Zhong X 2020. Resveratrol Attenuates Aflatoxin B(1)-
4582 Induced ROS Formation and Increase of m(6)A RNA Methylation. *Animals (Basel)*, 10, 677.
- 4583 Wu S, Lu H & Bai Y 2019. Nrf2 in cancers: A double-edged sword. *Cancer Med*, 8, 2252-2267.
- 4584 Xu K, Sun Y, Sheng B, Zheng Y, Wu X & Xu K 2019. Role of identified RNA N6-methyladenosine
4585 methylation in liver. *Analytical Biochemistry*, 578, 45-50.
- 4586 Xu W, Li F, Liu Z, Xu Z, Sun B, Cao J & Liu Y 2017. MicroRNA-27b inhibition promotes Nrf2/ARE
4587 pathway activation and alleviates intracerebral hemorrhage-induced brain injury. *Oncotarget*, 8, 70669-
4588 70684.
- 4589 Yue Y, Liu J & He C 2015. RNA N6-methyladenosine methylation in post-transcriptional gene
4590 expression regulation. *Genes Dev*, 29, 1343-1355.
- 4591 Zaccara S, Ries RJ & Jaffrey SR 2019. Reading, writing and erasing mRNA methylation. *Nature*
4592 *Reviews Molecular Cell Biology*, 20, 608-624.
- 4593 Zhao T-X, Wang J-K, Shen L-J, Long C-L, Liu B, Wei Y, Han L-D, Wei Y-X, Wu S-D & Wei G-H
4594 2020a. Increased m6A RNA modification is related to the inhibition of the Nrf2-mediated antioxidant
4595 response in di-(2-ethylhexyl) phthalate-induced prepubertal testicular injury. *Environmental Pollution*,
4596 259, 113911.
- 4597 Zhao T, Li X, Sun D & Zhang Z 2019. Oxidative stress: One potential factor for arsenite-induced
4598 increase of N6-methyladenosine in human keratinocytes. *Environmental toxicology and pharmacology*,
4599 69, 95-103.
- 4600 Zhao Z, Meng J, Su R, Zhang J, Chen J, Ma X & Xia Q 2020b. Epitranscriptomics in liver disease:
4601 Basic concepts and therapeutic potential. *Journal of Hepatology*, 73, 664-679.
- 4602 Zheng G, Dahl John A, Niu Y, Fedorcsak P, Huang C-M, Li Charles J, Vågbø Cathrine B, Shi Y, Wang
4603 W-L, Song S-H, et al. 2013. ALKBH5 Is a Mammalian RNA Demethylase that Impacts RNA
4604 Metabolism and Mouse Fertility. *Molecular Cell*, 49, 18-29.
- 4605 Zhengchang W, Chao X, Haifei W, Song G, Shenglong W & Wenbin B 2020. *Research Square*.

4606 Zhou Y, Zeng P, Li YH, Zhang Z & Cui Q 2016. SRAMP: prediction of mammalian N6-
4607 methyladenosine (m6A) sites based on sequence-derived features. *Nucleic Acids Res*, 44, e91.

4608

4609

4610

4611

4612

4613

4614

4615

4616

4617

4618

4619

4620

4621

4622

4623

4624

4625

4626

4627

4628

4629

4630

4631

4632 **CHAPTER 6**

4633 **Fumonisin B₁ inhibits p53-dependent apoptosis via HOXA11-AS/miR-124/DNMT axis in human**
4634 **hepatoma (HepG2) cells**

4635 Thilona Arumugam, Terisha Ghazi, Anil A Chuturgoon

4636 Discipline of Medical Biochemistry, School of Laboratory Medicine and Medical Sciences, University
4637 of KwaZulu-Natal, Durban, KwaZulu-Natal, South Africa

4638 **Corresponding author:**

4639 Professor Anil A. Chuturgoon,

4640 Discipline of Medical Biochemistry and Chemical Pathology,

4641 School of Laboratory Medicine and Medical Sciences

4642 College of Health Sciences

4643 George Campbell Building, Howard College, University of KwaZulu-Natal, Durban, 4041, South
4644 Africa. Telephone: +27312604404. Email: chatur@ukzn.ac.za

4645 EMAILS:

4646 TA: cyborglona@gmail.com

4647 TG: terishaghazi@gmail.com

4648

4649 **Archives of Toxicology (In Review).**

4650 **Manuscript ID: ATOX-D-20-00999**

4651

4652

4653

4654

4655

4656

4657

4658

4659

4660

4661 **Abstract**

4662 FB₁ is a hazardous mycotoxin that induces toxic and carcinogenic effects in humans and animals. FB₁
4663 induces changes to the epigenome which may provide insight into its toxic and carcinogenic nature.
4664 The lncRNA, HOXA11-AS influences the epigenome by modulating DNA methylation functioning as
4665 a competing endogenous RNA (ceRNA) or molecular scaffold. However, the role of HOXA11-AS in
4666 FB₁-toxicity is unknown. Therefore, we investigated the effect of FB₁ on p53-dependent apoptosis via
4667 the HOXA11-AS/miR-124/DNMT axis. HepG2 cells were treated with various concentrations of FB₁
4668 (0, 5, 50, 100 and 200 µM; 24 h). qPCR and/or western blotting was used to determine expression of
4669 HOXA11-AS, miR-124, SP1, DNMT1, DNMT3A, DNMT3B and p53. Global DNA methylation and
4670 p53 promoter methylation was assessed, whilst luminometry was used to measure caspase activity. FB₁
4671 upregulated HOXA11-AS (p≤0.05) leading to the subsequent decrease in miR-124 (p≤0.01) and
4672 increase in SP1 (p≤0.001), DNMT1 (p≤0.001), DNMT3A (p≤0.001) and DNMT3B (p≤0.001). This
4673 promoted global DNA methylation (p≤0.05) and hypermethylation of p53 promoters (p≤0.001) thereby
4674 reducing p53 expression (p≤0.001) and caspase activity (p≤0.001). Taken together the data suggests
4675 that FB₁ inhibits p53-dependent apoptosis via HOXA11-AS/miR-124/DNMT axis in HepG2 cells.

4676 **Keywords**

4677 Fumonisin B₁, Epigenetics, HOXA11-AS, miR-124, DNA Methylation, p53.

4678 **Introduction**

4679 Our life long development is not only dictated by our genetic code but also a dynamic network
4680 regulating DNA methylation, covalent histone modifications, RNA modifications and non-coding RNA
4681 (Kanherkar et al., 2014). This network is known as the epigenome. Together these modifications
4682 regulate gene expression and bring about phenotypic variations without altering the genetic code
4683 (Marczylo et al., 2016). However, changes to the epigenome brought about by environmental factors
4684 such as mycotoxins can lead to adverse health outcomes (Marczylo et al., 2016, Huang et al., 2019).
4685 Mycotoxins are toxic secondary metabolites produced by various fungi (Bennett, 1987). They
4686 chronically contaminate agricultural foods that are intended for human and animal consumption and
4687 elicit a wide variety of detrimental effects (Bennett and Klich, 2003, Eskola et al., 2020). The
4688 mechanisms by which mycotoxins induce their toxicity vary; however, over the past decade epigenetic
4689 changes have been implicated in various mycotoxin-related diseases and toxicities in humans and
4690 animals (Huang et al., 2019). The most toxicologically relevant mycotoxins include aflatoxins,
4691 ochratoxins, trichothecenes and fumonisins (Fung and Clark, 2004). Fumonisins are naturally produced
4692 by *Fusarium verticillioides* and *Fusarium proliferatum* (Ross et al., 1990, Ross et al., 1992). Due to
4693 poor agricultural practices and storage conditions, fumonisins mainly contaminate cereals and cereal-
4694 based-products thereby, posing a serious threat to human and animal health (Mashinini and Dutton,
4695 2006, Stępień et al., 2011, Ferrigo et al., 2016, Alberts et al., 2019, Phokane et al., 2019). Among the

4696 28 identified fumonisin analogues, fumonisin B₁ (FB₁) is regarded as the most relevant due to its potent
4697 toxicity and widespread distribution (Rheeder et al., 2002).

4698 Epigenetic changes have been linked to FB₁ toxicity. For instance, FB₁-induced changes in miRNA
4699 profiles and covalent histone modifications have been linked to genetic instability, and may be potential
4700 mechanisms for FB₁-related carcinogenesis and neural tube defects (Chuturgoon et al., 2014b, Sancak
4701 and Ozden, 2015, Gardner et al., 2016, Arumugam et al., 2020). Moreover, the effects of FB₁ on global
4702 DNA methylation have been thoroughly investigated by several research groups (Mobio et al., 2000,
4703 Kouadio et al., 2007, Chuturgoon et al., 2014a), with Demirel et al. (2015) demonstrating that FB₁ may
4704 exert its carcinogenic effects by modulating the promoter methylation of specific tumour suppressor
4705 genes. While the effects of FB₁ on DNA methylation, histones modification and miRNA have been
4706 explored, no study has evaluated the impact FB₁ may have on long non-coding RNAs (lncRNAs).
4707 lncRNAs were long considered irrelevant and thought of as merely “transcriptional noise” (Kung et
4708 al., 2013). However, with recent advances in sensitive, high-throughput genomic technologies and next-
4709 generation sequencing, their true potential is finally being recognized (Atkinson et al., 2012, Zhu et al.,
4710 2016). lncRNAs influence chromatin structure and gene expression thereby, regulating several
4711 biological processes such as apoptosis, proliferation differentiation and cell cycle regulation (Hu et al.,
4712 2011, Han and Chang, 2015, Nötzold et al., 2017, Yang et al., 2018c, Li et al., 2019); thus, dysregulation
4713 of lncRNAs have been associated with several pathological states such as, neurodegenerative disorders,
4714 chronic liver diseases, renal failure and numerous cancers (Prensner and Chinnaiyan, 2011, Sun et al.,
4715 2018a, Tang et al., 2019, Kim et al., 2020).

4716 One such lncRNA is homeobox A11 antisense (HOXA11-AS), a highly conserved lncRNA located in
4717 the HOXA gene cluster on chromosome 7p15 (Wei et al., 2020). By acting as a circulating endogenous
4718 RNA (ceRNA) and molecular scaffold, HOXA11-AS contributes to the ever-changing epigenome (Wei
4719 et al., 2020). As a ceRNA, HOXA11-AS sequesters miRNA with complementary binding sites such as
4720 miR-148, miR-200 and miR-124 and blocks the regulatory interaction between the miRNA and its
4721 target mRNA (Chen et al., 2017, Bai et al., 2019). By acting as a molecular scaffold, HOXA11-AS
4722 modulates the transcription of target genes by recruiting proteins including DNA methyltransferases
4723 (DNMTs) and transcription factors to the promoter regions of genes (Sun et al., 2016). Furthermore,
4724 Yu et al. (2017b) demonstrated that HOXA11-AS “sponging” of miR-124 upregulates SP1, a DNMT1
4725 transcription factor (Kishikawa et al., 2002). MiR-124 is also responsible for DNMT3B regulation
4726 (Chen et al., 2015). Thus, it is possible that HOXA11-AS may play a role in FB₁-mediated changes in
4727 both global and gene-specific methylation by regulating DNMT expression. Using bioinformatic
4728 prediction analysis and laboratory-based methods, this study evaluated the potential role of HOXA11-
4729 AS in FB₁ toxicity and DNA methylation. We assessed the relationship between HOXA11-AS and miR-
4730 124 and how it may impact DNMT expression, global DNA methylation and promoter methylation via
4731 DNMT regulation. We looked specifically at *p53* promoter methylation as it is a multifaceted tumour

4732 suppressor and transcription factor that plays a pivotal role in facilitating stress responses (Shieh et al.,
4733 1999, Yin et al., 1999, Vousden and Prives, 2009). Such stresses include oxidative stress, DNA damage
4734 and cell cycle abnormalities (Shieh et al., 1999, Yin et al., 1999). We recently found that FB₁ induced
4735 oxidative DNA damage and inhibited DNA damage checkpoint regulation (Arumugam et al., 2020). It
4736 is possible that p53 may play a role in responding to FB₁-mediated stress. Therefore, the aim of this
4737 study was to determine the effects of FB₁ on HOXA11-AS and the downstream effects it may have on
4738 global and *p53* promoter methylation via HOXA11-AS/miR-124/DNMT axis.

4739 **Method and Materials**

4740 ***Materials***

4741 FB₁ (*Fusarium moniliforme*) was purchased from Cayman Chemicals (62580, Ann Arbor, MI, USA).
4742 Silencing RNA (siRNA) against HOXA11-AS (SI03654588), siRNA negative control (0001027281),
4743 miR-124 mimic (MSY0004591), miR-124 inhibitor (MIN0004591), and attractene transfection reagent
4744 (301005) were purchased from Qiagen (Hilden, Germany). The DNA methylation inhibitor, 5-Aza-2-
4745 deoxycytidine (5-Aza-2-dc; A3653) was purchased from Sigma-Aldrich (A3854, St. Louis, MO, USA)
4746 and the human hepatoma (HepG2) cell line (HB-8065) was procured from the American Type Culture
4747 Collection (ATCC). Cell culture consumables were obtained from Whitehead Scientific (Johannesburg,
4748 South Africa). Western blot reagents were purchased from Bio-Rad (Hercules, CA, USA) while primary
4749 and secondary antibodies were obtained from Cell Signalling Technologies (Danvers, MA, USA) and
4750 β -actin was obtained from Sigma Aldrich (A3854, St. Louis, MO, USA). A detailed list of the antibodies
4751 used in this study is included in Supplementary Table S6.1. All other reagents were purchased from
4752 Merck (Boston, MA, USA), unless otherwise stated.

4753 ***Cell culture***

4754 HepG2 cells were grown in complete culture medium [CCM: Eagle's Minimum Essentials Medium
4755 (EMEM) supplemented with 10% foetal calf serum, 1% penicillin-streptomycin fungizone, and 1% L-
4756 glutamine] under the following conditions: pH 7.4, 37°C, 5% CO₂ and 95% relative humidity. For
4757 experiments, cells (1.5×10^6 , passage 3) were seeded in 25 cm³ sterile tissue culture flasks. When 80%
4758 confluency was achieved, cells were treated with a range of FB₁ concentrations (5, 50, 100 and 200
4759 μ M) (Arumugam et al., 2020). 5-Aza-2-dc, an inhibitor of DNA methylation, was used as a negative
4760 control. To induce DNA hypomethylation, cells were exposed to 10 μ M of 5-Aza-2-dc (Ahn et al.,
4761 2013). An untreated control containing CCM only was also prepared. All treatments occurred for 24
4762 hours (h) and experiments were repeated two independent times and in triplicate for reproducibility of
4763 results.

4764 ***Transfection with siRNA and miRNA mimic and inhibitors***

4765 To assess the effect of HOXA11-AS on miR-124 levels and DNMT1 scaffolding, HepG2 cells were
4766 transfected with the siRNA-against HOXA11-AS (siR-HOXA11-AS) and a negative control siRNA
4767 (siR-NC). HepG2 cells also underwent transfection with miR-124 mimic and miR-124 inhibitor in an
4768 effort to assess the effects of miR-124 on DNMT3B and SP1 expression.

4769 HepG2 cells were grown as described above to 80% confluency in 25 cm³ cell culture flasks. The
4770 lyophilized siRNAs (20 nmol) and miR-124 mimic and inhibitor (1 nmol) were reconstituted in
4771 nuclease-free water to a concentration of 20 µM. The transfection complex consisting of siRNA or
4772 miRNA mimic or inhibitor (15 µl), CCM (72 µl) and attractene (3 µl) was prepared and incubated (15
4773 min, RT). Thereafter, cells were washed with PBS and EMEM (2,910 µl) was added to yield a final
4774 concentration of 100 nM of siRNAs, mimic and inhibitor. The transfection complex was added in a
4775 dropwise manner with gentle swirling to allow even distribution. The cells were then incubated (37°C,
4776 5% CO₂, 24 h).

4777 ***RNA isolation***

4778 Total RNA was isolated from control and treated HepG2 cells. Cells were washed with 0.1M PBS and
4779 incubated (5 min, RT) with Qiazol reagent (79306, Qiagen, Hilden, Germany) and 0.1M PBS (1:1)
4780 before being mechanically lysed. Cell lysates were stored at -80°C overnight. Chloroform (100 µl) was
4781 added to the thawed lysates to promote phase separation, and samples were centrifuged (12,000xg, 4°C,
4782 15 min). RNA in the aqueous phase was precipitated overnight (-80°C) using isopropanol (500 µl).
4783 Once thawed, samples were centrifuged (12,000xg, 4°C, 20 min). The RNA-containing pellets were
4784 washed with 75% ice-cold ethanol and centrifuged (7,400xg, 4°C, 15 min). RNA pellets were air dried
4785 (30 min, RT) and resuspended in nuclease-free water (10 µl). Extracted RNA was quantified using the
4786 Nanodrop2000 spectrophotometer (Thermo Scientific, Waltham, USA) and RNA purity was assessed
4787 using the A260/A280 absorbance ratio. RNA was standardized to 1000 ng/µl in nucleus free water
4788 unless otherwise stated.

4789 ***Quantification of HOXA11-AS levels***

4790 HOXA11-AS expression was determined via real time quantitative polymerase chain reaction (RT-
4791 qPCR). cDNA was prepared from standardized RNA using the RT² First Strand Kit (330404, Qiagen,
4792 Hilden, Germany). Residual genomic DNA was removed from standardized RNA using the Genomic
4793 DNA elimination mix for 5 min at 42°C prior to cDNA synthesis using the reverse transcriptase mix.
4794 Thermocycler conditions for cDNA synthesis were as follows: 25°C for 5 min, 42°C for 30 min, 85°C
4795 for 5 min and a final hold at 4°C. Thereafter, cDNA underwent preamplification using the RT² PreAMP
4796 cDNA Synthesis Kit (330451, Qiagen, Hilden, Germany) and RT² lncRNA PreAMP Primer Mix
4797 (330741, Qiagen, Hilden, Germany) as per manufacturer's protocols. The expression of HOXA11-AS
4798 was determined using the RT² SYBR Green qPCR Master Mix (330503, Qiagen, Hilden, Germany) and
4799 RT² lncRNA qPCR Assay for Human HOXA11-AS (LPH14348A, Qiagen, Hilden, Germany). GAPDH

4800 (LPH31725A-200, Qiagen, Hilden, Germany) was used as housekeeping control and run
4801 simultaneously with HOXA11-AS. Relative changes in gene expression was determined using the
4802 comparative threshold cycle (Ct) method as described by Livak and Schmittgen (2001).

4803 ***Quantification of miR-124 expression***

4804 miR-124 expression was determined using RT-qPCR. The miScript II RT Kit (218161, Qiagen, Hilden,
4805 Germany) was used to reverse transcribe standardized RNA to cDNA. miR-124 expression was
4806 determined using the miScript SYBR Green PCR Kit (218073, Qiagen, Hilden, Germany) and Hs_miR-
4807 124*_1 10X miScript Primer Assay (MS00008547, Qiagen, Hilden, Germany), as per manufacturer's
4808 instructions. Human RNU6 (Qiagen, MS000033740, Qiagen, Hilden, Germany) was used as the
4809 housekeeping gene to normalize miRNA expression. Amplification was conducted using the CFX96
4810 Real Time PCR System (Bio-Rad, Hercules, CA, USA) and analysed using the Bio-Rad CFX Manager
4811 Software version 3.1. Relative changes in gene expression was determined using the method described
4812 by Livak and Schmittgen (2001).

4813 ***Quantification of mRNA levels***

4814 cDNA was synthesized using standardized RNA and the Maxima H Minus First Strand cDNA Synthesis
4815 Kit (K1652, Thermo-Fisher Scientific, Waltham, MA, USA) as per manufacturer's instructions. The
4816 gene expression of *SP1*, *DNMT1*, *DNMT3A*, *DNMT3B* and *p53* was assessed using the PowerUp SYBR
4817 Green Master Mix (A25742, Thermo-Fisher Scientific, Waltham, MA, USA) and the CFX96 Real
4818 Time PCR System (Bio-Rad, Hercules, CA, USA) with the following cycling conditions: initial
4819 denaturation (95°C, 8 min), followed by 40 cycles of denaturation (95°C, 15 s), annealing
4820 (Supplementary Table S6.2, 40 s), and extension (72°C, 30 s). Primer sequences and annealing
4821 temperatures are listed in Supplementary Table S6.2. The housekeeping control, GAPDH was run
4822 alongside the target and mRNA expression was normalized against *GAPDH*. Relative changes in gene
4823 expression was determined using the Ct method as described by Livak and Schmittgen (2001).

4824 ***RNA immunoprecipitation***

4825 RNA immunoprecipitation was performed to assess HOXA11-AS binding to DNMT1. DNMT1
4826 antibody (1:100; 5032S, Cell Signalling Technologies, Danvers, MA, USA) was incubated with
4827 standardized RNA (1000 ng/μl), overnight at 4°C. Protein A beads [20 μl, 50% bead slurry (#9863, Cell
4828 Signalling Technology), 4°C, 3 h] were used to precipitate the RNA-DNMT1 complex. Samples were
4829 centrifuged (2,500xg, 4°C, 60s) and washed twice in RNA immunoprecipitation buffer [150 mM KCl,
4830 25 mM Tris-Cl (pH 7.4), 5mM EDTA, 0.5mM DTT, 0.5% IGEPAL, 100 U/ml SUPERase IN RNase
4831 Inhibitor (AM2694, Thermo-Fisher Scientific), protease and phosphatase inhibitor (A32961, Thermo-
4832 Fisher Scientific)]. Samples were washed once in nuclease free water and resuspended in nuclease free
4833 water (10 μl). Immunoprecipitated RNA was standardised to 200 ng/μl, and reverse transcribed into
4834 cDNA as described above. The expression of DNMT1-HOXA11-AS was then determined using qPCR

4835 as mentioned above. Primer sequences and annealing temperatures are listed in Supplementary Table
4836 S6.2.

4837 ***DNA isolation***

4838 Genomic DNA was isolated from HepG2 cells and used to assess global DNA methylation levels and
4839 methylation status of p53 promoter region. Once treatments were removed, cells were washed thrice
4840 with 0.1M PBS and incubated (RT, 15 min) in cell lysis buffer [0.5 M EDTA (pH 8.0), 1 M Tris-Cl (pH
4841 7.6), and 0.1% SDS] before being mechanically lysed. Potassium acetate (5 M potassium acetate and
4842 glacial acetic acid) was added to samples which were then invert mixed (8 min). Samples were
4843 centrifuged (13,000 x g, 5 min, 24°C) and isopropanol was added to the aqueous phase to precipitate
4844 DNA. Sample were then invert mixed (6 min) before being centrifuged (13,000 x g, 5 min, 24°C).
4845 DNA-containing pellets were washed with 100% cold ethanol to remove residual salts. Samples were
4846 centrifuged (13,000 x g, 5 min, 24°C), ethanol removed and pellets were left to air dry for 30 min. Once
4847 dried, pellets were resuspended in TE buffer [10 mM EDTA (pH 8.0) and 100 mM Tris-Cl (pH 7.4)]
4848 and heated (65°C, 15 min). DNA concentration was quantified using the Nanodrop2000
4849 spectrophotometer and adjusted as required.

4850 ***Quantification of global DNA methylation***

4851 Isolated DNA was standardized to 100 ng/μl and used to quantify global DNA methylation levels
4852 through the Colorimetric Methylated DNA quantification Kit (ab117128, Abcam, Cambridge, UK) as
4853 per manufacturers' protocol.

4854 ***p53 promoter methylation***

4855 Isolated genomic DNA was standardized to 4 ng/μl and used in the OneStep qMethyl Kit (5310, Zymo
4856 Research, Irvine, CA, USA) to asses promoter methylation of p53. Primer sequences used were as
4857 follows; p53 promoter sense: 5'- GTGGATATTACGGAAAGT-3' and p53 promoter anti-sense: 5'-
4858 AAAATATCCCCGAAACC-3'. Cycling conditions were as follows: digestion by methyl sensitive
4859 restriction enzymes (37°C, 2 h), initial denaturation (95°C, 10 min), followed by 45 cycles of
4860 denaturation (95°C, 30s), annealing (54°C, 60s), extension (72°C, 60s), final extension (72°C, 60s), and
4861 a hold at 4°C. Results are represented as a fold-change relative to the control.

4862 ***Protein expression***

4863 HepG2 cells were lysed with Cytobuster reagent (71009-3, Merck, Kenilworth, NJ, USA) which
4864 contained protease and phosphatase inhibitors (A32961, Thermo-Fisher Scientific). The protein
4865 concentration was measured using the bicinchoninic acid assay (Walker, 1994) and standardized to 1
4866 mg/ml. The protein expression of DNMT1, DNMT3A, DNMT3B, and p53 were determined using
4867 western blotting as previously described (Arumugam et al., 2019). Protein expression is represented as
4868 relative band density (RBD) and calculated by normalizing the protein of interest against the

4869 housekeeping protein, β -actin. A list of antibodies and dilutions used can be found in supplementary
4870 table S6.1.

4871 *Caspase activity*

4872 The activity of caspases -3/7, -6, -8, and -9 were assessed using the Caspase-Glo luminometry assays
4873 (G8090, G0970, G8200, and G8210, Promega, Madison, WI, United States). Control and treated cells
4874 (20,000 cells/well) were dispensed into an opaque 96-well microtiter plate in triplicate and incubated
4875 with the respective Caspase-Glo reagent (20 μ l) in the dark for 30 min at RT. Luminescence was
4876 quantified using the Modulus microplate luminometer (Turner Biosystems) and the results were
4877 expressed as relative light units (RLU).

4878 *Statistical analysis*

4879 Statistical analyses were performed using GraphPad Prism version 5.0 (GraphPad Prism Software Inc.).
4880 Data was analysed using the one-way Analysis of Variance (ANOVA) with Dunnet's post-test. The
4881 results were represented as the mean \pm standard deviation (SD) and a p value of less than 0.05 was
4882 considered statistically significant.

4883 **Results**

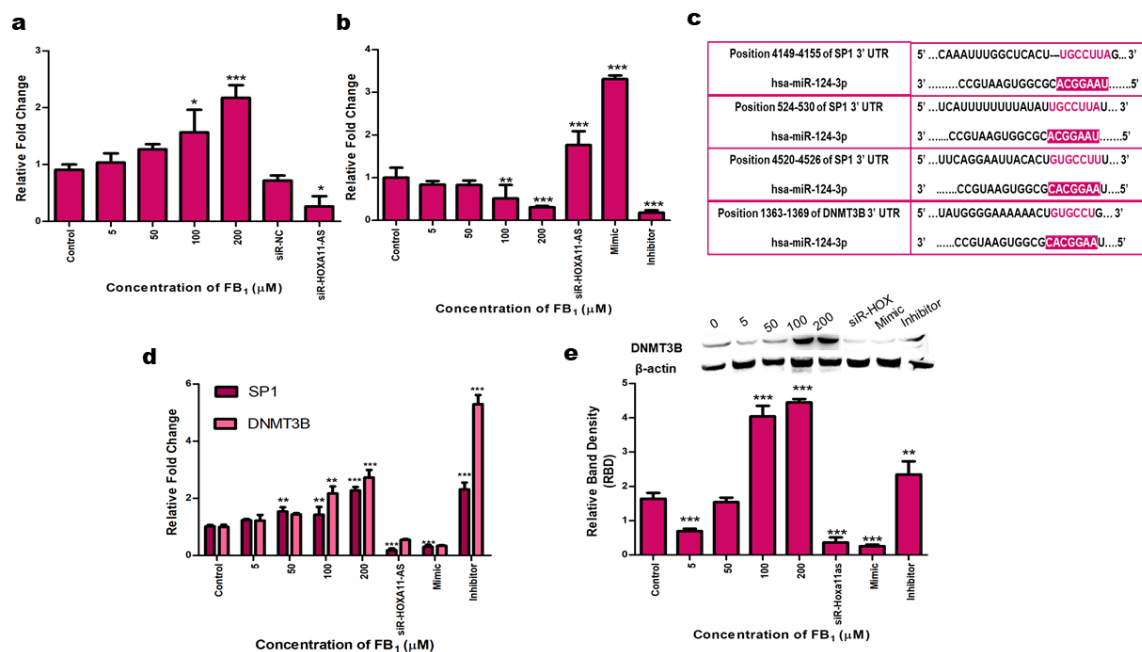
4884 *FB₁-induced HOXA11-AS sponges miR-124, regulating SP1 and DNMT expression*

4885 The RT² lncRNA PCR Array Human IncFinder (LAHS-001Z, Qiagen, Hilden, Germany) was used to
4886 identify differentially expressed lncRNA in HepG2 cells exposed to 200 μ M FB₁ [IC₅₀ (Arumugam et
4887 al., 2020)]. HOXA11-AS was identified as one of the most upregulated lncRNA (Supplementary Figure
4888 S6.1). The expression of HOXA11-AS was then validated in HepG2 cells using a range of FB₁
4889 concentrations (5, 50, 100 and 200 μ M) and the downstream effects of HOXA11-AS was determined.

4890 HOXA11-AS expression was increased in response to increasing concentrations of FB₁ ($p \leq 0.001$;
4891 Figure 6.1a). To validate the relationship between FB₁ and HOXA11-AS, HepG2 cells were transfected
4892 with siRNA against HOXA11-AS. Cells were transfected with silencing RNA against HOXA11-AS
4893 which acted as a negative control and used to gain insight into potential downstream effects of
4894 HOXA11-AS. Cells were also transfected with siR-NC to test the efficiency of transfection. HOXA11-
4895 AS expression was effectively knocked down in cells treated with siR-HOXA11-AS ($p \leq 0.05$; Figure
4896 6.1a); however, expression for the siR-NC treated cells was similar to the control, suggesting that
4897 transfection was successful (Figure 6.1a).

4898 It was previously shown that HOXA11-AS acts as a ceRNA for miR-124 (Lu et al., 2017). This was
4899 confirmed using online bioinformatics prediction algorithm software, starBase v2.0 (Li et al., 2014).
4900 MiR-124 was reduced at all FB₁ concentrations, but significantly reduced at 100 μ M and 200 μ M FB₁
4901 (Figure 6.1b; $p \leq 0.01$). Furthermore, we found miR-124 to be significantly upregulated in cells treated
4902 with siR-HOXA11-AS confirming the relationship between these 2 RNA species ($p \leq 0.001$; Figure

4903 6.1b). In addition to siRNA, HepG2 cells were transfected with a mimic and inhibitor against miR-124
 4904 which acted as a positive and negative control, respectively. The expression of miR-124 in HepG2 cells
 4905 treated with the mimic and inhibitor were increased and decreased, respectively (Figure 6.1b; $p \leq 0.001$).
 4906 TargetScan (version 7.1), an online bioinformatics prediction software that predicts miRNA-mRNA
 4907 interactions was used to determine possible targets of miR-124 (Agarwal et al., 2015). MiR-124 was
 4908 shown to potentially regulate DNA methylation as it was found to have complementary base pairs with
 4909 the DNA methyltransferase, *DNMT3B* at positions 1363-1369 and the DNMT1 transcription factor, *SP1*
 4910 at positions 524-530, 4149-4155 and 4520-4526 (Figure 6.1c).
 4911 Due to the decreased expression in miR-124 observed by FB₁, we then evaluated the expression of SP1
 4912 and DNMT3B. FB₁ significantly increased gene expression of *SP1* (Figure 6.1d; $p \leq 0.001$) and
 4913 *DNMT3B* (Figure 6.1d; $p \leq 0.001$). DNMT3B protein expression (Figure 6.1e; $p \leq 0.001$) was increased
 4914 in response to 50-200 μM FB₁; yet, it was reduced at 5 μM FB₁. *SP1* gene and DNMT3B gene and
 4915 protein expression was also significantly increased in cells treated with miR-124 inhibitor and
 4916 significantly reduced in miR-124 mimic and siR-HOXA11-AS treated cells; confirming the relationship
 4917 between HOXA11-AS and miR-124 with SP1 and DNMT1.



4918
 4919 **Figure 6.1.** FB₁ upregulated HOXA11-AS levels (a; $***p \leq 0.001$) which negatively regulated miR-
 4920 124 (b; $***p \leq 0.001$). Bioinformatic prediction revealed that the 3' UTR of *SP1* and *DNMT3B*
 4921 contains binding sites for miR-124 (c). *SP1* gene (d; $***p \leq 0.001$) and *DNMT3B* gene (d; $***p \leq 0.001$) and
 4922 protein (e; $***p \leq 0.001$) expression was altered by FB₁ treatment.

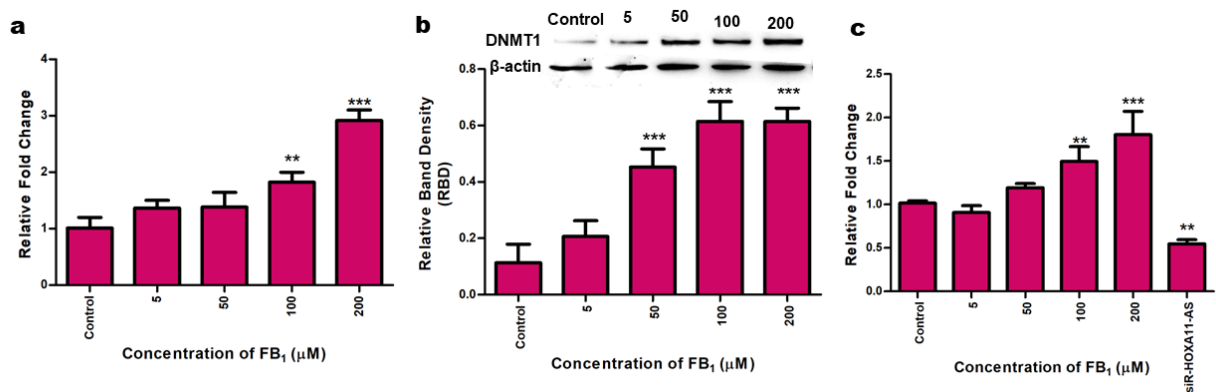
4923

4924

4925 ***FB₁ elevates DNMT1 expression and promotes HOXA11-AS-DNMT1 binding***

4926 SP1 activates the transcription of DNMT1 (Kishikawa et al., 2002), thus, DNMT1 expression was
4927 assessed. qPCR and western blotting analysis revealed a significant increase in DNMT1 mRNA (Figure
4928 6.2a; $p \leq 0.001$) and protein expression (Figure 6.2b; ≤ 0.001), respectively.

4929 In addition to its function as a ceRNA, HOXA11-AS acts as a scaffold for DNMT1 by recruiting it to
4930 gene promoters (Sun et al., 2016), therefore, HOXA11-AS-DNMT1 binding was evaluated by
4931 performing RNA immunoprecipitation. There was a slight reduction in the interaction at 5 μM FB₁,
4932 however, increased at the all other concentrations tested (Figure 6.2c; $p \leq 0.001$). HOXA11-AS-
4933 DNMT1 interactions were significantly reduced in siR-HOXA11AS treated cells ($p \leq 0.01$; Figure 6.2c).



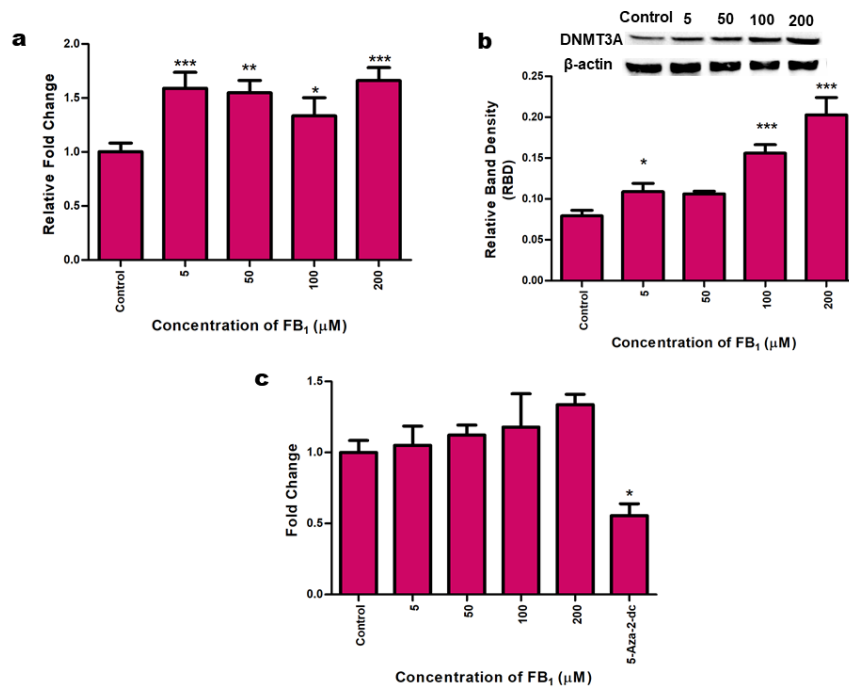
4934

4935 **Figure 6.2.** FB₁ significantly upregulated *DNMT1* mRNA (a; *** $p \leq 0.001$) and DNMT1 protein (b;
4936 *** $p \leq 0.001$) expression and altered HOXA11-AS-DNMT1 binding (c; *** $p \leq 0.001$) in HepG2 cells.

4937 ***FB₁ altered DNMT3A expression and global DNA methylation status of HepG2 cells***

4938 Although DNMT3A is not regulated by HOXA-11AS or miR-124, it does play an important role in
4939 DNA methylation., FB₁ significantly increased *DNMT3A* gene (Figure 6.3a, $p \leq 0.001$) and protein
4940 (Figure 6.3b; $p \leq 0.001$) expression at all concentrations investigated.

4941 Since FB₁ differentially regulated DNMT expression, we next determined whether FB₁ affected global
4942 DNA methylation levels (Figure 6.3c). Along with FB₁ treatments, cells were treated with 5-Aza-2-dc,
4943 a known DNA methylation inhibitor. Naturally, 5-Aza-2-dc treatment significantly reduced total
4944 methylation levels in HepG2 cells ($p \leq 0.05$; Figure 6.3c). In contrast, FB₁ increased total methylation
4945 of DNA; however, these results were not significant at any of the tested concentrations ($p > 0.05$; Figure
4946 6.3c).



4947

4948 **Figure 6.3.** qPCR and western blot quantification revealed that *DNMT3A* gene (a; *** $p \leq 0.001$) and
 4949 *DNMT3A* protein (b; *** $p \leq 0.001$) expression was significantly elevated in FB₁-exposed HepG2 cells.
 4950 Methylation of cytosine in the DNA of HepG2 cells were also increased following FB₁ treatment (c; *
 4951 $p \leq 0.05$).

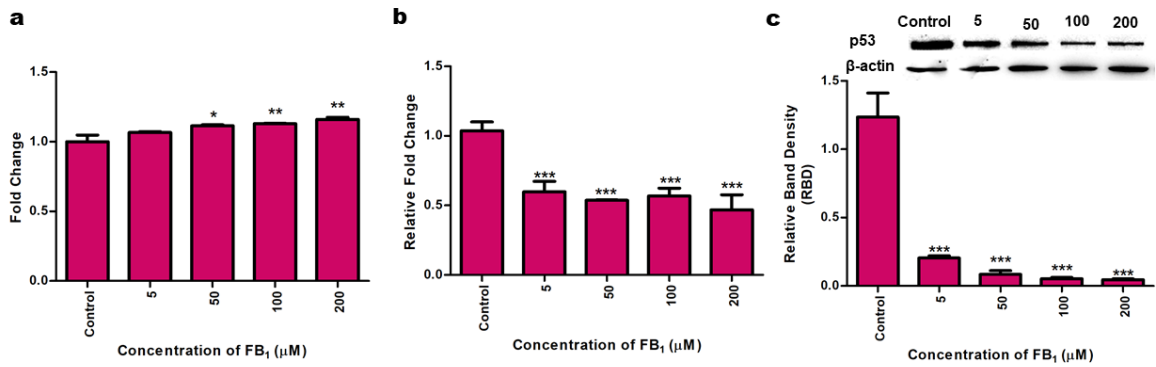
4952 ***FB₁ reduced p53 expression via hypermethylation of gene promoter***

4953 In addition to global methylation levels, we evaluated gene-specific methylation in HepG2 cells.
 4954 Methylation of specific CpG islands on gene promoters silences their transcription. We assessed
 4955 promoter methylation of the tumour suppressor, p53. p53 promoters of HepG2 cells were significantly
 4956 hypermethylated in response to FB₁ (Figure 6.4a; $p \leq 0.001$). This led to significant decreases in *p53*
 4957 gene (Figure 6.4b; $p \leq 0.001$) and p53 protein (Figure 6.4c; $p \leq 0.001$) expression.

4958

4959

4960

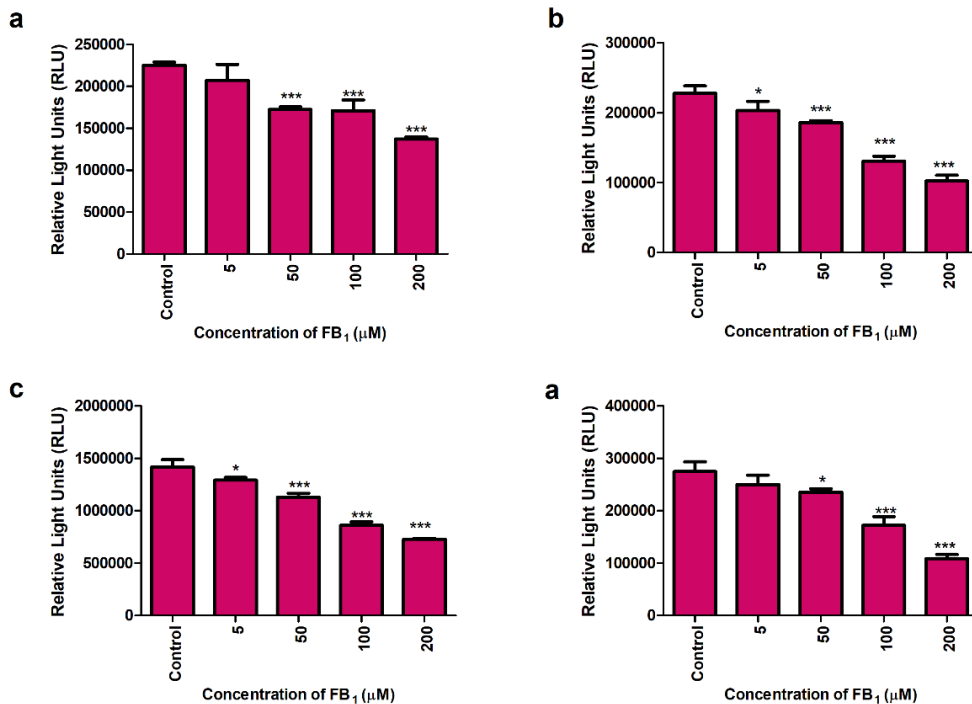


4961

4962 **Figure 6.4.** Increasing doses of FB₁ led to increasing hypermethylation at *p53* promoter regions (a; ***
 4963 $p \leq 0.001$) in HepG2 cells. This led to a significant dose-dependent decrease in *p53* gene (b; *** $p \leq$
 4964 0.001) and *p53* protein (c; *** $p \leq 0.001$) expression.

4965 ***FB₁ inhibits caspase dependent apoptosis***

4966 The *p53* tumour suppressor protein plays a major role in apoptosis. One of the mechanisms by which it
 4967 does this is through caspase activation (Schuler et al., 2000). There was a significant dose-dependent
 4968 decline in the activity of caspases -3/7 (Figure 6.5a; $p \leq 0.001$), -6 (Figure 6.5b; $p \leq 0.001$), -8 (Figure
 4969 6.5c; $p \leq 0.001$) and -9 (Figure 6.5d; $p \leq 0.001$) in the presence of FB₁.



4970

4971 **Figure 6.5.** The activity of caspases -3/7 (a; *** $p \leq 0.001$), -6 (b; *** $p \leq 0.001$), -8 (c; *** $p \leq 0.001$)
 4972 and -9 (d; *** $p \leq 0.001$) were decreased in FB₁ treated HepG2 cells.

4973 **Discussion**

4974 The epigenetic landscape is critical in modulating functional pathways such as apoptosis, proliferation
4975 and differentiation; however, it is continuously changing in response to external stimuli such as
4976 mycotoxin insult (Marczylo et al., 2016, Huang et al., 2019). FB₁ is regarded as one of the most
4977 important mycotoxins as it abundantly contaminates agricultural staples and adversely affects human
4978 and animal health (Idahor, 2010, Kamle et al., 2019). FB₁ impacts the epigenetic landscape of humans
4979 and animals which may play a role in its toxicity (Mobio et al., 2000, Chuturgoon et al., 2014a,
4980 Chuturgoon et al., 2014b, Demirel et al., 2015, Sancak and Ozden, 2015, Gardner et al., 2016,
4981 Arumugam et al., 2020). One mechanism studied is the alteration of DNA methylation patterns which
4982 contributes to genomic instability as well as effects the expression of genes regulating protein and DNA
4983 synthesis, cell cycle, proliferation and apoptosis (Mobio et al., 2000, Kouadio et al., 2007, Chuturgoon
4984 et al., 2014a, Demirel et al., 2015). Thus, in this study we evaluated the anti-apoptotic effects of FB₁ by
4985 assessing the epigenetic regulation of p53 via the HOXA11-AS/miR-124/DNMT axis.

4986 Once considered irrelevant, lncRNAs are gaining increasing advertece due to our new understanding
4987 of the functional role they play (Kung et al., 2013). Although over 146,000 lncRNAs have been
4988 documented to date; most have only been predicted and studied via computational analysis (Volders et
4989 al., 2015). To determine if FB₁ affected lncRNA profiles of HepG2 cells, we used a lncRNA array and
4990 evaluated changes in the expression of 84 lncRNA using an untreated control and IC₅₀ [200 µM FB₁;
4991 (Arumugam et al., 2020)]. We found that FB₁ significantly dysregulated the lncRNA profiles of HepG2
4992 cells and HOXA11-AS was amongst the most upregulated lncRNA (Supplementary Figure S6.1). Thus,
4993 we validated HOXA11-AS expression and further investigated its downstream effects following FB₁
4994 exposure.

4995 HOXA11-AS has mainly oncogenic functions, influencing the proliferation, invasion and migration of
4996 various cancers such as hepatocellular carcinomas, oesophageal cancer, renal cancer and melanomas
4997 (Lu et al., 2017, Yu et al., 2017a, Sun et al., 2018b, Yang et al., 2018a, Liu et al., 2019, Zhang et al.,
4998 2019). Conversely, it has tumour suppressor capabilities in epithelial ovarian cancer (Richards et al.,
4999 2015). In addition to its carcinogenic effects, HOXA11-AS influences gene expression by modulating
5000 epigenetic modifications by functioning as a ceRNA and molecular scaffold (Sun et al., 2016, Wang et
5001 al., 2017).

5002 As a ceRNA or RNA “sponge”, HOXA11-AS is able to bind to certain miRNAs blocking the interaction
5003 between the miRNA and its target mRNA. This reduces the negative regulatory impact that miRNAs
5004 have on their target mRNA. For instance, Lu et al. (2017) demonstrated that HOXA11-AS positively
5005 regulated enhancer of zeste homolog 2 (EZH2) expression by sequestering miR-124 and preventing
5006 miRNA-124 degradation of EZH2 mRNA. We confirmed the relationship between HOXA11-AS and
5007 miR-124 in the liver by using an online bioinformatics prediction algorithm, starBase v2.0

5008 (Supplementary Figure S6.2) (Li et al., 2014). We further validated the ceRNA capabilities of
5009 HOXA11-AS by determining the expression of HOXA11-AS and miR-124 in HepG2 cells treated with
5010 various concentrations of FB₁ (0, 5, 50, 100 and 200 μM). HOXA11-AS was significantly upregulated
5011 in the presence of FB₁ which resulted in the concurrent decrease in miRNA-124 levels (Figure 6.1a, b).
5012 This relationship was confirmed using relevant controls as miR-124 expression was significantly
5013 elevated in cells where HOXA11-AS was knocked down.

5014 To explore the downstream targets of miR-124, the online bioinformatics tool Targetscan (version 7.2)
5015 was employed (Agarwal et al., 2015). We found that miR-124 may influence DNA methylation as we
5016 uncovered complementary binding sites between miR-124 and the 3'UTR of *SP1* at positions 524-530,
5017 4149-4155 and 4520-4526 and the 3'UTR of *DNMT3B* at positions 1363-1369 (Figure 6.1c).

5018 DNMT3B directly regulates DNA methylation (Okano et al., 1998, Hervouet et al., 2018); while SP1
5019 indirectly influences DNA methylation as it binds to the cis-element of *DNMT1* gene promoter,
5020 activating its transcription (Kishikawa et al., 2002). FB₁-induced HOXA11-AS prevented the
5021 degradation of miR-124 targets as DNMT3B gene and protein expression (Figure 6.1d, e) as well as
5022 *SP1* gene expression (Figure 6.1d) were significantly upregulated. The use of appropriate controls
5023 confirmed this relationship as miR-124 knockdown resulted in a significant increase of its targets; while
5024 the use of miR-124 mimic and siR-HOXA11-AS independently downregulated DNMT3B and SP1
5025 expression. Furthermore, several other studies confirmed that HOXA11-AS sequesters miR-124 with
5026 one study revealing that HOXA11-AS positively regulates SP1 by sponging miRNA-124 (Cui et al.,
5027 2017, Xu et al., 2017, Yu et al., 2017b, Yang et al., 2018b, Jin et al., 2019, Zhang et al., 2019). Since
5028 FB₁ altered the expression of *SP1*, we determined if DNMT1 expression was also altered. In agreement
5029 with the upregulation of *SP1*, DNMT1 expression was also elevated both at the gene and protein levels
5030 (Figure 6.2a, b). Apart from its ceRNA capability, HOXA11-AS can also serve as a molecular scaffold
5031 that recruits chromatin modifying proteins such as EZH2, LSD1 and DNMT1 to the promoter region of
5032 genes thus modulating their transcription (Wei et al., 2020). For example, HOXA11-AS interacts with
5033 DNMT1 and EZH2, recruiting these proteins to the promoter regions of miR-200b and mediating
5034 methylation silencing of miR-200b in non-small cell lung cancer cells (Chen et al., 2017). Using RNA
5035 immunoprecipitation, we determined if FB₁ influences HOXA11-AS-DNMT1 binding and found that
5036 HOXA11-AS-DNMT1 interactions were significantly higher in the presence of FB₁ and reduced with
5037 HOXA11-AS knockdown (Figure 6.2c). However, this interaction should be further investigated at
5038 specific gene promoters.

5039 Four members make up the DNMT family with DNMT1, -3A and -3B having catalytic capabilities
5040 (Hervouet et al., 2018). Seeing as FB₁ altered the expression of DNMT1 and DNMT3B, we determined
5041 if FB₁ affects DNMT3A and found the mRNA and protein expression to be significantly upregulated
5042 (Figure 6.3a, b). DNMTs are responsible for the transferring methyl groups from S-adenosyl-
5043 methionine (SAM) to the 5-position of cytosine residues in DNA (Hervouet et al., 2018). We found that

5044 the increase in DNMT expression corresponded with an increase in total DNA methylation levels
5045 (Figure 6.3c); however, our results were not significant and opposed the results of another study which
5046 investigated in the effects of 200 μ M FB₁ in HepG2 cells (Chuturgoon et al., 2014a). Chuturgoon et al.
5047 (2014a) found that FB₁ reduced the expression of DNMTs which resulted in global hypomethylation,
5048 however similar to our study, DNA hypermethylation occurred in human intestinal Caco-2 cells and rat
5049 C6 glioma cells after 24 hours (Mobio et al., 2000, Kouadio et al., 2007).

5050 While several studies have investigated the effects of FB₁ on global DNA methylation only one other
5051 study has looked at its effects on gene-specific methylation (Demirel et al., 2015). Demirel et al. (2015)
5052 assessed CpG promoter methylation of tumour suppressor genes in rat liver (clone 9) cells and kidney
5053 epithelial (NRK-52E) cells. CpG islands of *VHL* and *e-cadherin* promoters were methylated in both
5054 cell lines; while, the *c-Myc* promoter was methylated exclusively in Clone 9 cells and methylation of
5055 the *p16* gene occurred in NRK-52E cells. Thus, we investigated the role of DNA methylation on the
5056 tumour suppressor p53.

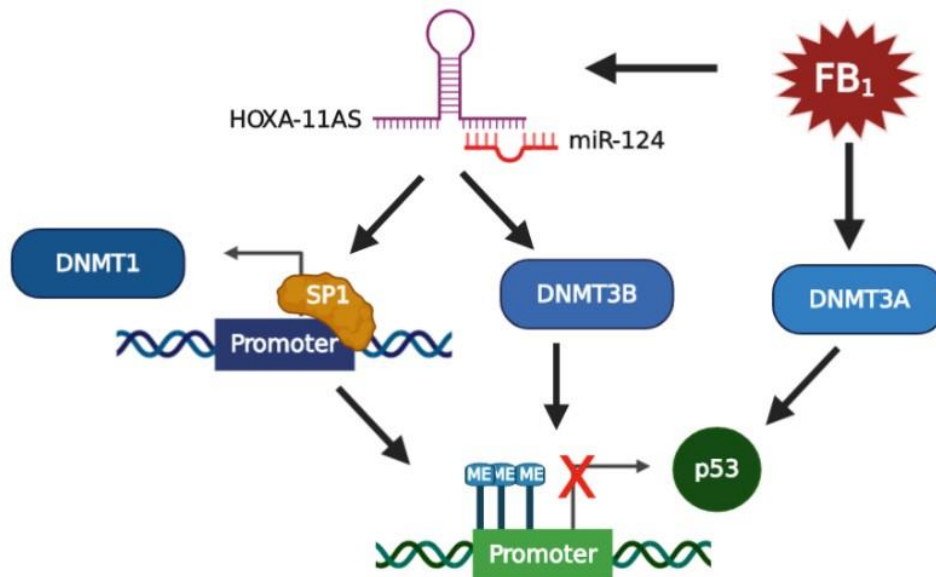
5057 p53 responds to cellular stress such as DNA damage, oxidative stress and cell cycle abnormalities by
5058 inducing cell cycle arrest, apoptosis or autophagy (Shieh et al., 1999, Yin et al., 1999, Vousden and
5059 Prives, 2009). FB₁ is a known inducer of oxidative stress, DNA damage and altered cell cycle
5060 checkpoint regulation (Mobio et al., 2000, Galvano et al., 2002, Stockmann-Juvala et al., 2004, Domijan
5061 et al., 2007, Kim et al., 2018, Arumugam et al., 2019, Arumugam et al., 2020). Furthermore, HOXA11-
5062 AS is known to repress p53 expression; however, the mechanism is unknown (Connell et al., 2009).
5063 Therefore, we evaluated CpG island methylation at *p53* promoters and subsequently p53 expression.
5064 We found that the promoter region of *p53* was significantly hypermethylated (Figure 6.4a), leading to
5065 the subsequent decrease in p53 transcription and translation (Fig. 4b, c). It is possible that p53 activity
5066 may be also be disrupted by FB₁. p53 is activated via a host of post-translational modifications,
5067 including phosphorylation (Sakaguchi et al., 1998). FB₁ was shown to inhibit checkpoint kinase 1
5068 (Arumugam et al., 2020), a kinase responsible for p53 phosphorylation and activation (Ou et al., 2005).

5069 One mechanism by which p53 initiates apoptosis is through the activation of the caspase cascade. p53
5070 activates initiator caspases (caspase- 8 and -9) and subsequently downstream effector caspases (caspase-
5071 3/7) (Ding et al., 1998, Schuler et al., 2000). p53 is also responsible for the transactivation of effector
5072 caspase-6 (Ehrnhoefer et al., 2014). We found a significant decrease in the activity of all 4 of the above-
5073 mentioned caspases (Figure 6.5). Taken together, our results suggest that FB₁ inhibits p53-dependent
5074 cell death. FB₁ was also found to inhibit apoptosis in HepG2 cells through the upregulation of anti-
5075 apoptotic Birc-8/ILP-2 and decrease in apoptotic Smac/DIABLO (Chuturgoon et al., 2015). Together
5076 the inhibition of p53 and activation of Birc-8 prevents caspase-dependent apoptosis in the presence of
5077 FB₁. However, several other studies have observed stress-induced apoptosis in response to FB₁ exposure
5078 (Tolleson et al., 1996, Tolleson et al., 1999, Seefelder et al., 2003). The difference could be due to the
5079 models used to examine toxicity. The HepG2 cell line is a cancerous model and thus prefers pro-survival

5080 mechanisms. It is possible that inhibition of p53-dependent apoptosis via the HOXA11-AS/miR-
 5081 124/DNMT axis may be responsible for promoting FB₁-induced carcinogenesis. However, further
 5082 studies using cancerous and primary liver cell lines should be conducted to test this hypothesis.
 5083 Nevertheless, this study provides novel insight into the relationship between HOXA11-As, DNA
 5084 methylation and p53 expression, which was previously unknown and adds to our understanding on the
 5085 impact of FB₁ on the human epigenome.

5086 **Conclusion**

5087 This study revealed that FB₁ upregulated the lncRNA, HOXA11-AS, which in turn sequesters and
 5088 inhibits miR-124, leading to an increase in SP1, DNMT1, DNMT3A and DNMT3B expression. The
 5089 increase in DNMTs not only elevated global methylation of FB₁ exposed HepG2 cells but also
 5090 hypermethylation of *p53* promoters. This led to a decrease in p53 expression and ultimately diminished
 5091 caspase activity. Therefore, FB₁ inhibits p53-dependent cell death via the HOXA11-AS/miR-
 5092 124/DNMT axis (Figure 6.6).



5093 **Figure 6.6.** FB₁ inhibits p53 via HOXA11-AS/miR-124/DNMT axis. FB₁ enhances HOXA11-AS levels.
 5094 HOXA11-AS inhibits miR-124, thus preventing the interaction between miR-124 and its target mRNAs (SP1 and
 5095 DNMT3B). The resulting upregulation of SP1 promotes DNMT1 expression. Moreover, FB₁ enhances DNMT3A
 5096 levels. The increase in DNMT expression facilitates promoter hypermethylation of p53, reducing p53 transcription
 5097 and expression.

5099 **Declarations**

5100 *Funding*

5101 The authors acknowledge the National Research Foundation (NRF) of South Africa and College of
 5102 Health Science (University of Kwa-Zulu Natal) for funding this study.

5103 *Conflicts of interest*

5104 The authors declare that they have no conflicts of interest.

5105 *Ethics approval*

5106 EthicS was received from the University of Kwa-Zulu Natal's Biomedical Research Ethics Committee.

5107 Ethics number: BE322/19.

5108 *Availability of data and material*

5109 All datasets generated in this study are available from the corresponding author on reasonable request.

5110 *Author Contributions*

5111 TA, TG, and AC conceptualised and designed the study. TA conducted all laboratory experiments,

5112 analysed the data and wrote the manuscript. TG and AC revised the manuscript. All authors have read

5113 the manuscript prior to submission.

5114

5115 **Supplementary Information**

5116 **Supplementary Table S6.1: Antibodies with dilutions used for western blotting**

Antibody	Dilution	Catalogue number (Cell Signaling Technologies)
Primary Antibodies		
Rabbit-Anti-DNMT1	1:250	5032S
Rabbit-Anti-DNMT3A	1:250	3598S
Rabbit-Anti-DNMT3B	1:250	57868S
Mouse-Anti-p53	1:500	2524S
Secondary Antibodies		
Goat-Anti- Rabbit	1:5000	#7074S
Goat-Anti-Mouse	1:5000	#7076P2

5117

5118

5119

5120

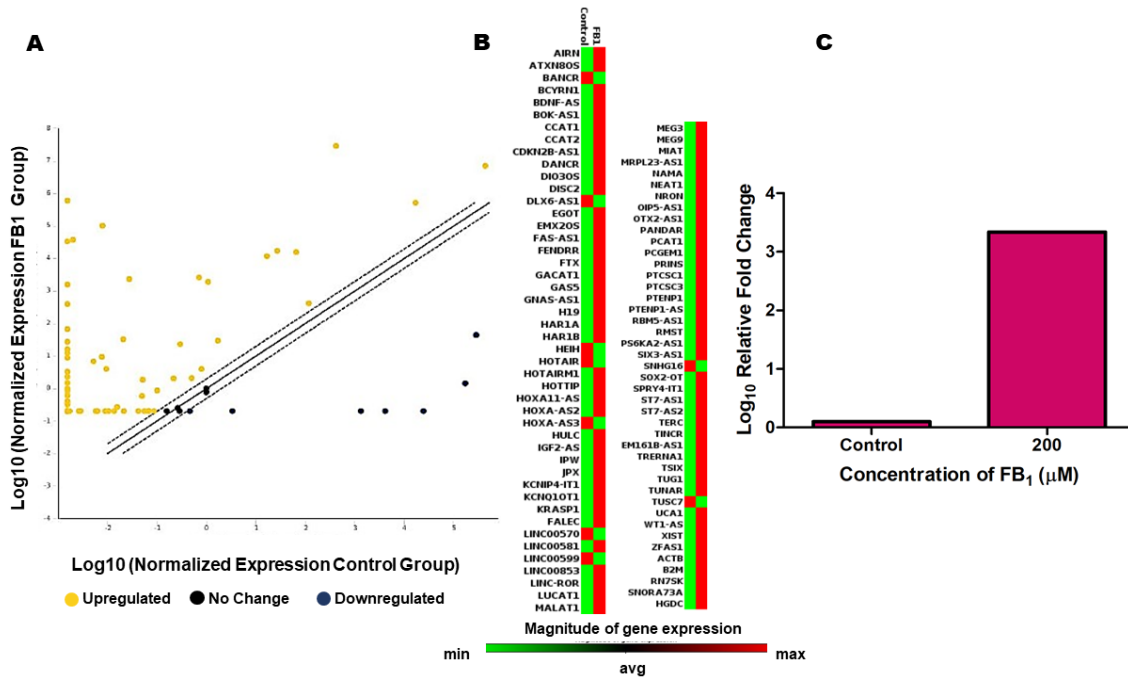
5121

5122 **Supplementary Table S6.2: Primer sequences and annealing temperatures used in qPCRs**

Gene	Sense Primer 5' → 3'	Anti-sense Primer 5' → 3'	Annealing Temperature (°C)
qPCR			
<i>DNMT1</i>	ACCGCTTCTACTTCCTCGAGGCCTA	GTTGCAGTCCTCTGTGAACACTGTGG	60
<i>DNMT3A</i>	GGGGACGTCCGCAGCGTCACAC	CAGGGTTGGACTCGAGAAATCGC	58
<i>DNMT3B</i>	CCTGCTGAATTACTCACGCCCC	GTCTGTGTAGTGCACAGGAAAGCC	58
<i>SPI</i>	CTTGGTATCATCACAAGCCAGTT	TCCCTGATGATCCACTGGTAGTA	56
<i>p53</i>	ACTTGTCGCTCTTGAAGCTAC	GATGCGGAGAATCTTTGGAACA	58
<i>GAPDH</i>	TCCACCACCCTGTTGCTGTA	ACCACAGTCCATGCCATCAC	Same as gene of interest
Promoter Methylation			
<i>p53</i>	GTGGATATTACGGAAAGT	AAAATATCCCCGAAACC	54
RNA Immunoprecipitation			
<i>HOXA11-AS</i>	GAGTTTGAAGCCGTGGATGT	AGATGAGGGGAGAGGTGGAT	56

5123

5124



5125

5126 **Supplementary Figure S6.1.** FB₁ alters lncRNA profiles in HepG2 cells. **A:** Scatter plot showing
 5127 normalized expression of lncRNA in FB₁ treated HepG2 cells. Yellow dots represent upregulated
 5128 lncRNA, blue dots represent downregulated lncRNA and black dots represent unchanged lncRNA in
 5129 FB₁ treated cells compared to the control. **B:** Heatmap showing expression profile of all lncRNA
 5130 assessed using the array. **C:** Normalized expression of HOXA11-AS using the lncRNA array.

5131

miRNA	GeneID	GeneName	GeneType	TargetSite	Alignment	Class	AgoExpNum	CleaveExp
hsa-miR-124-3p	ENSG00000240990	HOXA11-AS	antisense	chr7:27225522-27225542[+]	Target: 5' cogaagCGCUUUAGUGCCUUC 3' miRNA: 3' ccguaaGUGGCG-CACGAAU 5'	7mer-m8	1	0

5132

5133 **Supplementary Figure S6.2.** starBase v2.0 analyses of HOXA11-AS interaction humans.

	Predicted consequential pairing of target region (top) and miRNA (bottom)
Position 524-530 of SP1 3' UTR	5' ...UCAUUUUUUUUAUUAUGCCUUAU...
hsa-miR-124-3p.1	3' CCGUAAGUGGCGCACGGAAU
Position 4520-4526 of SP1 3' UTR	5' ...UUCAGGAAUACACUGUGCCUUU...
hsa-miR-124-3p.1	3' CCGUAAGUGGCGCACGGAAU
Position 4149-4155 of SP1 3' UTR	5' ...CAAUUUGGCUCACU---UGCCUUAG...
hsa-miR-124-3p.1	3' CCGUAAGUGGCGCACGGAAU

	Predicted consequential pairing of target region (top) and miRNA (bottom)
Position 1363-1369 of DNMT3B 3' UTR	5' ...UAUGGGGAAAAACUGUGCCUUG...
hsa-miR-124-3p.1	3' CCGUAAGUGGCGCACGGAAU

5134

5135 **Supplementary Figure S6.3.** TargetScan analyses of miR-124 to the 3' UTR of *SP1* and *DNMT3B* in
5136 humans. MiR-124 has complementary base pairs with the 3' UTR of *SP1* at positions 524-530, 4149-
5137 4155 and 4520-4526 and *DNMT3B* at positions 1363-1369 in humans.

5138 References

5139 Agarwal V, Bell GW, Nam J-W & Bartel DP 2015. Predicting effective microRNA target sites in
5140 mammalian mRNAs. *eLife*, 4, e05005.

5141 Ahn EY, Kim JS, Kim GJ & Park YN 2013. RASSF1A-mediated regulation of AREG via the Hippo
5142 pathway in hepatocellular carcinoma. *Mol Cancer Res*, 11, 748-758.

5143 Alberts J, Rheeder J, Gelderblom W, Shephard G & Burger H-M 2019. Rural Subsistence Maize
5144 Farming in South Africa: Risk Assessment and Intervention models for Reduction of Exposure to
5145 Fumonisin Mycotoxins. *Toxins*, 11, 334.

5146 Arumugam T, Pillay Y, Ghazi T, Nagiah S, Abdul NS & Chuturgoon AA 2019. Fumonisin B(1)-
5147 induced oxidative stress triggers Nrf2-mediated antioxidant response in human hepatocellular
5148 carcinoma (HepG2) cells. *Mycotoxin Res*, 35, 99-109.

5149 Arumugam T, Ghazi T & Chuturgoon A 2020. Fumonisin B 1 Epigenetically Regulates PTEN
5150 Expression and Modulates DNA Damage Checkpoint Regulation in HepG2 Liver Cells. *Toxins*, 12, 2-
5151 15.

5152 Atkinson SR, Marguerat S & Bähler J 2012. Exploring long non-coding RNAs through sequencing.
5153 *Seminars in Cell & Developmental Biology*, 23, 200-205.

5154 Bai Y, Lang L, Zhao W & Niu R 2019. Long Non-Coding RNA HOXA11-AS Promotes Non-Small
5155 Cell Lung Cancer Tumorigenesis Through microRNA-148a-3p/DNMT1 Regulatory Axis. *Oncotargets Ther*, 12, 11195-11206.
5156

- 5157 Bennett JW 1987. Mycotoxins, mycotoxicoses, mycotoxicology and Mycopathologia. *Mycopathologia*,
5158 100, 3-5.
- 5159 Bennett JW & Klich M 2003. Mycotoxins. *Clin Microbiol Rev*, 16, 497-516.
- 5160 Chen J-H, Zhou L-Y, Xu S, Zheng Y-L, Wan Y-F & Hu C-P 2017. Overexpression of lncRNA
5161 HOXA11-AS promotes cell epithelial–mesenchymal transition by repressing miR-200b in non-small
5162 cell lung cancer. *Cancer Cell International*, 17, 64.
- 5163 Chen Z, Liu S, Tian L, Wu M, Ai F, Tang W, Zhao L, Ding J, Zhang L & Tang A 2015. miR-124 and
5164 miR-506 inhibit colorectal cancer progression by targeting DNMT3B and DNMT1. *Oncotarget*, 6,
5165 38139-38150.
- 5166 Chuturgoon A, Phulukdaree A & Moodley D 2014a. Fumonisin B1 induces global DNA
5167 hypomethylation in HepG2 cells - An alternative mechanism of action. *Toxicology*, 315, 65-69.
- 5168 Chuturgoon A, Phulukdaree A & Moodley D 2015. Fumonisin B1 inhibits apoptosis in HepG2 cells by
5169 inducing Birc-8/ILP-2. *Toxicology letters*, 235.
- 5170 Chuturgoon AA, Phulukdaree A & Moodley D 2014b. Fumonisin B₁ modulates expression of human
5171 cytochrome P450 1b1 in human hepatoma (Hepg2) cells by repressing Mir-27b. *Toxicology letters*, 227,
5172 50-55.
- 5173 Connell KA, Guess MK, Chen HW, Lynch T, Bercik R & Taylor HS 2009. HOXA11 promotes
5174 fibroblast proliferation and regulates p53 in uterosacral ligaments. *Reprod Sci*, 16, 694-700.
- 5175 Cui M, Wang J, Li Q, Zhang J, Jia J & Zhan X 2017. Long non-coding RNA HOXA11-AS functions
5176 as a competing endogenous RNA to regulate ROCK1 expression by sponging miR-124-3p in
5177 osteosarcoma. *Biomedicine & Pharmacotherapy*, 92, 437-444.
- 5178 Demirel G, Alpertunga B & Ozden S 2015. Role of fumonisin B1 on DNA methylation changes in rat
5179 kidney and liver cells. *Pharmaceutical Biology*, 53, 1302-1310.
- 5180 Ding HF, McGill G, Rowan S, Schmaltz C, Shimamura A & Fisher DE 1998. Oncogene-dependent
5181 regulation of caspase activation by p53 protein in a cell-free system. *J Biol Chem*, 273, 28378-28383.
- 5182 Domijan A-M, Želježić D, Milić M & Peraica M 2007. Fumonisin B1: Oxidative status and DNA
5183 damage in rats. *Toxicology*, 232, 163-169.
- 5184 Ehrnhoefer DE, Skotte NH, Ladha S, Nguyen YT, Qiu X, Deng Y, Huynh KT, Engemann S, Nielsen
5185 SM, Becanovic K, et al. 2014. p53 increases caspase-6 expression and activation in muscle tissue
5186 expressing mutant huntingtin. *Hum Mol Genet*, 23, 717-729.
- 5187 Eskola M, Kos G, Elliott CT, Hajšlová J, Mayar S & Krska R 2020. Worldwide contamination of food-
5188 crops with mycotoxins: Validity of the widely cited ‘FAO estimate’ of 25%. *Critical Reviews in Food*
5189 *Science and Nutrition*, 60, 2773-2789.

- 5190 Ferrigo D, Raiola A & Causin R 2016. Fusarium Toxins in Cereals: Occurrence, Legislation, Factors
5191 Promoting the Appearance and Their Management. *Molecules*, 21, 627.
- 5192 Fung F & Clark R 2004. Health Effects of Mycotoxins: A Toxicological Overview. *Journal of*
5193 *toxicology. Clinical toxicology*, 42, 217-234.
- 5194 Galvano F, Russo A, Cardile V, Galvano G, Vanella A & Renis M 2002. DNA damage in human
5195 fibroblasts exposed to fumonisin B1. *Food and Chemical Toxicology*, 40, 25-31.
- 5196 Gardner NM, Riley RT, Showker JL, Voss KA, Sachs AJ, Maddox JR & Gelineau-van Waes JB 2016.
5197 Elevated nuclear sphingoid base-1-phosphates and decreased histone deacetylase activity after
5198 fumonisin B1 treatment in mouse embryonic fibroblasts. *Toxicology and applied pharmacology*, 298,
5199 56-65.
- 5200 Han P & Chang C-P 2015. Long non-coding RNA and chromatin remodeling. *RNA Biol*, 12, 1094-
5201 1098.
- 5202 Hervouet E, Peixoto P, Delage-Mourroux R, Boyer-Guittaut M & Cartron P-F 2018. Specific or not
5203 specific recruitment of DNMTs for DNA methylation, an epigenetic dilemma. *Clinical Epigenetics*, 10,
5204 17.
- 5205 Hu W, Yuan B, Flygare J & Lodish HF 2011. Long noncoding RNA-mediated anti-apoptotic activity
5206 in murine erythroid terminal differentiation. *Genes & development*, 25, 2573-2578.
- 5207 Huang D, Cui L, Sajid A, Zainab F, Wu Q, Wang X & Yuan Z 2019. The epigenetic mechanisms in
5208 Fusarium mycotoxins induced toxicities. *Food and Chemical Toxicology*, 123, 595-601.
- 5209 Idahor K 2010. Global distribution of Fumonisin B 1 – A review. *acta SATECH*, 3, 25 – 32.
- 5210 Jin J, Zhai H-F, Jia Z-H & Luo X-H 2019. Long non-coding RNA HOXA11-AS induces type I collagen
5211 synthesis to stimulate keloid formation via sponging miR-124-3p and activation of Smad5 signaling.
5212 *American Journal of Physiology-Cell Physiology*, 317, C1001-C1010.
- 5213 Kamle M, Mahato D, Devi S, Lee K, Kang SG & Kumar P 2019. Fumonisin: Impact on Agriculture,
5214 Food, and Human Health and their Management Strategies. *Toxins*, 11, 238.
- 5215 Kanherkar RR, Bhatia-Dey N & Csoka AB 2014. Epigenetics across the human lifespan. *Front Cell*
5216 *Dev Biol*, 2, 49-49.
- 5217 Kim SH, Singh MP, Sharma C & Kang SC 2018. Fumonisin B1 actuates oxidative stress-associated
5218 colonic damage via apoptosis and autophagy activation in murine model. *Journal of Biochemical and*
5219 *Molecular Toxicology*, 32, e22161.
- 5220 Kim Y-A, Park K-K & Lee S-J 2020. LncRNAs Act as a Link between Chronic Liver Disease and
5221 Hepatocellular Carcinoma. *International Journal of Molecular Sciences*, 21, 2883.

- 5222 Kishikawa S, Murata T, Kimura H, Shiota K & Yokoyama KK 2002. Regulation of transcription of the
5223 Dnmt1 gene by Sp1 and Sp3 zinc finger proteins. *Eur J Biochem*, 269, 2961-2970.
- 5224 Kouadio JH, Dano SD, Moukha S, Mobio TA & Creppy EE 2007. Effects of combinations of Fusarium
5225 mycotoxins on the inhibition of macromolecular synthesis, malondialdehyde levels, DNA methylation
5226 and fragmentation, and viability in Caco-2 cells. *Toxicon*, 49, 306-317.
- 5227 Kung JT, Colognori D & Lee JT 2013. Long noncoding RNAs: past, present, and future. *Genetics*, 193,
5228 651-669.
- 5229 Li J-H, Liu S, Zhou H, Qu L-H & Yang J-H 2014. starBase v2.0: decoding miRNA-ceRNA, miRNA-
5230 ncRNA and protein-RNA interaction networks from large-scale CLIP-Seq data. *Nucleic acids research*,
5231 42, D92-D97.
- 5232 Li Q, Zhang J, Su D-M, Guan L-N, Mu W-H, Yu M, Ma X & Yang R-J 2019. lncRNA TUG1 modulates
5233 proliferation, apoptosis, invasion, and angiogenesis via targeting miR-29b in trophoblast cells. *Human
5234 Genomics*, 13, 50.
- 5235 Liu Y, Zhang Y-M, Ma F-B, Pan S-R & Liu B-Z 2019. Long noncoding RNA HOXA11-AS promotes
5236 gastric cancer cell proliferation and invasion via SRSF1 and functions as a biomarker in gastric cancer.
5237 *World Journal of Gastroenterology*, 25, 2763.
- 5238 Livak KJ & Schmittgen TD 2001. Analysis of relative gene expression data using real-time quantitative
5239 PCR and the 2(-Delta Delta C(T)) Method. *Methods*, 25, 402-408.
- 5240 Lu Q, Zhao N, Zha G, Wang H, Tong Q & Xin S 2017. LncRNA HOXA11-AS exerts oncogenic
5241 functions by repressing p21 and miR-124 in uveal melanoma. *DNA and Cell Biology*, 36, 837-844.
- 5242 Marczylo EL, Jacobs MN & Gant TW 2016. Environmentally induced epigenetic toxicity: potential
5243 public health concerns. *Crit Rev Toxicol*, 46, 676-700.
- 5244 Mashinini K & Dutton MF 2006. The incidence of fungi and mycotoxins in South Africa wheat and
5245 wheat-based products. *J Environ Sci Health B*, 41, 285-296.
- 5246 Mobio TA, Anane R, Baudrimont I, Carratú MR, Shier TW, Dano SD, Ueno Y & Creppy EE 2000.
5247 Epigenetic properties of fumonisin B(1): cell cycle arrest and DNA base modification in C6 glioma
5248 cells. *Toxicology and applied pharmacology*, 164, 91-96.
- 5249 Nötzold L, Frank L, Gandhi M, Polycarpou-Schwarz M, Groß M, Gunkel M, Beil N, Erfle H, Harder
5250 N, Rohr K, et al. 2017. The long non-coding RNA LINC00152 is essential for cell cycle progression
5251 through mitosis in HeLa cells. *Scientific Reports*, 7, 2265.
- 5252 Okano M, Xie S & Li E 1998. Cloning and characterization of a family of novel mammalian DNA
5253 (cytosine-5) methyltransferases. *Nat Genet*, 19, 219-220.

5254 Ou Y-H, Chung P-H, Sun T-P & Shieh S-Y 2005. p53 C-terminal phosphorylation by CHK1 and CHK2
5255 participates in the regulation of DNA-damage-induced C-terminal acetylation. *Mol Biol Cell*, 16, 1684-
5256 1695.

5257 Phokane S, Flett B, Ncube E, Rheeder J & Rose L 2019. Agricultural practices and their potential role
5258 in mycotoxin contamination of maize and groundnut subsistence farmin. *South African Journal of*
5259 *Science*, 115.

5260 Prensner JR & Chinnaiyan AM 2011. The emergence of lncRNAs in cancer biology. *Cancer discovery*,
5261 1, 391-407.

5262 Rheeder JP, Marasas WFO & Vismer HF 2002. Production of Fumonisin Analogs by Fusarium Species.
5263 *Applied and Environmental Microbiology*, 68, 2101-2105.

5264 Richards EJ, Permuth-Wey J, Li Y, Chen YA, Coppola D, Reid BM, Lin H-Y, Teer JK, Berchuck A &
5265 Birrer MJ 2015. A functional variant in HOXA11-AS, a novel long non-coding RNA, inhibits the
5266 oncogenic phenotype of epithelial ovarian cancer. *Oncotarget*, 6, 34745.

5267 Ross P, Nelson P, Richard J, Osweiler G, Rice L, Plattner R & Wilson T 1990. Production of fumonisins
5268 by *Fusarium moniliforme* and *Fusarium proliferatum* isolates associated with equine
5269 leukoencephalomalacia and a pulmonary edema syndrome in swine. *Applied and Environmental*
5270 *Microbiology*, 56, 3225-3226.

5271 Ross PF, Rice LG, Osweiler GD, Nelson PE, Richard JL & Wilson TM 1992. A review and update of
5272 animal toxicoses associated with fumonisin-contaminated feeds and production of fumonisins by
5273 *Fusarium* isolates. *Mycopathologia*, 117, 109-114.

5274 Sakaguchi K, Herrera JE, Saito Si, Miki T, Bustin M, Vassilev A, Anderson CW & Appella E 1998.
5275 DNA damage activates p53 through a phosphorylation–acetylation cascade. *Genes & development*, 12,
5276 2831-2841.

5277 Sancak D & Ozden S 2015. Global histone modifications in Fumonisin B1 exposure in rat kidney
5278 epithelial cells. *Toxicology in vitro : an international journal published in association with BIBRA*, 29,
5279 1809-1815.

5280 Schuler M, Bossy-Wetzel E, Goldstein JC, Fitzgerald P & Green DR 2000. p53 induces apoptosis by
5281 caspase activation through mitochondrial cytochrome c release. *J Biol Chem*, 275, 7337-7342.

5282 Seefelder W, Humpf H-U, Schwerdt G, Freudinger R & Gekle M 2003. Induction of apoptosis in
5283 cultured human proximal tubule cells by fumonisins and fumonisin metabolites. *Toxicology and applied*
5284 *pharmacology*, 192, 146-153.

5285 Shieh S-Y, Taya Y & Prives C 1999. DNA damage-inducible phosphorylation of p53 at N-terminal
5286 sites including a novel site, Ser20, requires tetramerization. *The EMBO Journal*, 18, 1815-1823.

- 5287 Stępień L, Koczyk G & Waśkiewicz A 2011. Genetic and phenotypic variation of *Fusarium*
5288 proliferatum isolates from different host species. *J Appl Genet*, 52, 487-496.
- 5289 Stockmann-Juvala H, Mikkola J, Naarala J, Loikkanen J, Elovaara E & Savolainen K 2004. Oxidative
5290 stress induced by fumonisin B1 in continuous human and rodent neural cell cultures. *Free radical*
5291 *research*, 38, 933-942.
- 5292 Sun M, Nie F, Wang Y, Zhang Z, Hou J, He D, Xie M, Xu L, De W & Wang Z 2016. LncRNA
5293 HOXA11-AS promotes proliferation and invasion of gastric cancer by scaffolding the chromatin
5294 modification factors PRC2, LSD1, and DNMT1. *Cancer research*, 76, 6299-6310.
- 5295 Sun SF, Tang PMK, Feng M, Xiao J, Huang XR, Li P, Ma RCW & Lan HY 2018a. Novel lncRNA
5296 Erbb4-IR Promotes Diabetic Kidney Injury in *db/db* Mice by Targeting miR-29b. *Diabetes*,
5297 67, 731-744.
- 5298 Sun X, Wang X, Cui Y, Cao X, Zhao R, Wei H, Cao W & Wu W 2018b. Expression level and clinical
5299 significance of LncRNA HOXA11-AS in esophageal squamous cell carcinoma patients. *Zhonghua*
5300 *zhong liu za zhi [Chinese journal of oncology]*, 40, 186-190.
- 5301 Tang L, Liu L, Li G, Jiang P, Wang Y & Li J 2019. Expression Profiles of Long Noncoding RNAs in
5302 Intranasal LPS-Mediated Alzheimer's Disease Model in Mice. *BioMed Research International*, 2019,
5303 9642589.
- 5304 Tolleson WH, Melchior Jr WB, Morris SM, McGarrity LJ, Domon OE, Muskhelishvili L, James SJ &
5305 Howard PC 1996. Apoptotic and anti-proliferative effects of fumonisin B1 in human keratinocytes,
5306 fibroblasts, esophageal epithelial cells and hepatoma cells. *Carcinogenesis*, 17, 239-249.
- 5307 Tolleson WH, Couch L, Melchior W, Jenkins GR, Muskhelishvili M, Muskhelishvili L, McGarrity L,
5308 Domon O, Morris S & Howard P 1999. Fumonisin B1 induces apoptosis in cultured human
5309 keratinocytes through sphinganine accumulation and ceramide depletion. *International journal of*
5310 *oncology*, 14, 833-876.
- 5311 Volders PJ, Verheggen K, Menschaert G, Vandepoele K, Martens L, Vandesompele J & Mestdagh P
5312 2015. An update on LNCipedia: a database for annotated human lncRNA sequences. *Nucleic Acids Res*,
5313 43, D174-180.
- 5314 Vousden KH & Prives C 2009. Blinded by the Light: The Growing Complexity of p53. *Cell*, 137, 413-
5315 431.
- 5316 Wang X, Zhang L, Cui X, Wang M, Zhang G & Yu P 2017. lncRNA HOXA11-AS is involved in
5317 fracture healing through regulating mir-124-3p. *Eur Rev Med Pharmacol Sci*, 21, 4771-4776.

5318 Wei C, Zhao L, Liang H, Zhen Y & Han L 2020. Recent advances in unraveling the molecular
5319 mechanisms and functions of HOXA11-AS in human cancers and other diseases (Review). *Oncol Rep*,
5320 43, 1737-1754.

5321 Xu C, He T, Li Z, Liu H & Ding B 2017. Regulation of HOXA11-AS/miR-214-3p/EZH2 axis on the
5322 growth, migration and invasion of glioma cells. *Biomedicine & Pharmacotherapy*, 95, 1504-1513.

5323 Yang FQ, Zhang JQ, Jin JJ, Yang CY, Zhang WJ, Zhang HM, Zheng JH & Weng ZM 2018a. HOXA11-
5324 AS promotes the growth and invasion of renal cancer by sponging miR-146b-5p to upregulate MMP16
5325 expression. *Journal of cellular physiology*, 233, 9611-9619.

5326 Yang J, Liu B, Yang B & Meng Q 2018b. Long non-coding RNA homeobox (HOX) A11-AS promotes
5327 malignant progression of glioma by targeting miR-124-3p. *Neoplasia*, 65, 505.

5328 Yang Q, Wan Q, Zhang L, Li Y, Zhang P, Li D, Feng C, Yi F, Zhang L, Ding X, et al. 2018c. Analysis
5329 of LncRNA expression in cell differentiation. *RNA Biol*, 15, 413-422.

5330 Yin Y, Solomon G, Deng C & Barrett JC 1999. Differential regulation of p21 by p53 and Rb in cellular
5331 response to oxidative stress. *Molecular Carcinogenesis: Published in cooperation with the University*
5332 *of Texas MD Anderson Cancer Center*, 24, 15-24.

5333 Yu J, Hong J, Kang J, Liao L & Li C 2017a. Promotion of LncRNA HOXA11-AS on the proliferation
5334 of hepatocellular carcinoma by regulating the expression of LATS1. *Eur Rev Med Pharmacol Sci*, 21,
5335 3402-3411.

5336 Yu W, Peng W, Jiang H, Sha H & Li J 2017b. LncRNA HOXA11-AS promotes proliferation and
5337 invasion by targeting miR-124 in human non-small cell lung cancer cells. *Tumor Biology*, 39,
5338 1010428317721440.

5339 Zhang W-l, Zhao Y-n, Shi Z-z, Gu G-y, Cong D, Wei C & Bai Y-s 2019. HOXA11-AS promotes the
5340 migration and invasion of hepatocellular carcinoma cells by inhibiting miR-124 expression by binding
5341 to EZH2. *Human cell*, 32, 504-514.

5342 Zhu S, Li W, Liu J, Chen C-H, Liao Q, Xu P, Xu H, Xiao T, Cao Z, Peng J, et al. 2016. Genome-scale
5343 deletion screening of human long non-coding RNAs using a paired-guide RNA CRISPR-Cas9 library.
5344 *Nat Biotechnol*, 34, 1279-1286.

5345

5346

5347

5348

5349

CHAPTER 7

CONCLUSION

7.1. General conclusions

Epigenetic modifications are necessary for normal development and health; however, environmental factors such as mycotoxin exposure disrupts the epigenome of cells often leading to toxicity (Huang et al., 2019). Many studies have focused on the health implications of FB₁ as well as molecular mechanisms involved in its toxicity (Wang et al., 1991, Yin et al., 2016, Kouzi et al., 2018, Arumugam et al., 2019, Arumugam et al., 2020, Liu et al., 2020). Furthermore, some studies have evaluated epigenetic changes that occur due to FB₁ exposure but these studies mainly focused on DNA methylation and histone modifications and most failed to assess the downstream implications of these epigenetic changes (Mobio et al., 2000, Kouadio et al., 2007, Pellanda et al., 2012, Chuturgoon et al., 2014a, Chuturgoon et al., 2014b, Demirel et al., 2015, Sancak and Ozden, 2015, Gardner et al., 2016).

This study, for the first time, demonstrates that FB₁ not only alters the epigenetic landscape in HepG2 cells; but that these epigenetic modifications affect cellular responses to FB₁ mediated stress. Furthermore, it is the first study to evaluate the effect of FB₁ on the m⁶A epitranscriptome and lncRNAs.

FB₁ induced oxidative damage to DNA of HepG2 cells. PTEN is vital in maintaining genomic stability and DNA repair, while its inactivation or downregulation promotes DNA instability and damage (Ming and He, 2012, Bassi et al., 2013). Downregulation of PTEN activates PI3K/AKT signaling which inhibits CHK1 activity and DNA damage checkpoint signaling (Puc et al., 2005, Puc and Parsons, 2005). Therefore, epigenetic modifications that affect PTEN expression were evaluated in the presence of FB₁. FB₁ reduced the expression of histone demethylase, KDM5B which in turn resulted in the significant increase in global H3K4me₃. H3K4me₃ was also elevated at the promoter region of *PTEN*, where it activated *PTEN* transcription. While there was a significant increase in *PTEN* mRNA levels, FB₁ reduced the protein expression of PTEN. PTEN is post-transcriptionally regulated by miR-30c (Hu et al., 2019). FB₁ upregulated miR-30c, which inhibited the translation of *PTEN*, resulting in reduced PTEN protein expression. PTEN is a negative regulator of PI3K/AKT signaling (Cantley and Neel, 1999). The downregulation of PTEN permitted PI3K/AKT signaling to proceed undisturbed, resulting in the inhibitory phosphorylation of serine-280-CHK1. Inhibition of CHK1 prevents DNA repair and promotes genomic instability. This may contribute to the toxicity and carcinogenicity of FB₁.

Alterations to the m⁶A epitranscriptome have been linked to the toxic effects of some *Fusarium* mycotoxins (Ghazi et al., 2020, Zhengchang et al., 2020). Furthermore, m⁶A is influenced by cellular stresses such as oxidative stress and may in turn regulate responses to oxidative stress (Zhao et al., 2020). Intracellular ROS and global m⁶A levels were both elevated in HepG2 cells exposed to FB₁. Furthermore, FB₁ upregulated m⁶A methyltransferases (*METTL3* and *METTL14*) and downregulated m⁶A demethylases (*FTO* and *ALKBH5*); contributing to the elevation of global m⁶A levels observed.

5385 FB₁-induced increases in m6A levels may lead to the altered expression of important genes involved in
5386 its toxicity. Considering that there was an accumulation of intracellular ROS, the effect of m6A on
5387 Keap1/Nrf2 signaling was determined. Additional epigenetic changes to Keap1/Nrf2 were also
5388 evaluated. FB₁ induced hypermethylation of the *Keap1* promoter region, which inhibited *Keap1*
5389 transcription; 29 possible m6A sites with the consensus motifs: GGACU and AGACU, were predicted
5390 on *Keap1* transcripts. M6A-*Keap1* levels were upregulated; however, Keap1 protein expression was
5391 reduced. FB₁ increased the m6A reader *YTHDF2*, which may be responsible for inhibiting Keap1
5392 translation. Hypomethylation of Nrf2 promoters together with decreased miR-27b upregulated *Nrf2*
5393 mRNA levels in HepG2 cells exposed to FB₁; 54 possible m6A sites with the consensus motif GAACU
5394 were predicated on *Nrf2* transcripts. FB₁ elevated m6A-*Nrf2* and Nrf2 protein expression. The increase
5395 in m6A readers *YTHDF1*, *YTHDF3* and *YTHDC2* may be responsible for promoting Nrf2 translation.
5396 The downregulation of Keap1 and upregulation of Nrf2 activates antioxidant responses, which was
5397 previously observed (Arumugam et al., 2019). However, severe cellular injury occurred in cells exposed
5398 to FB₁, suggesting that the activation of Nrf2 antioxidant signaling may not be sufficient to counter the
5399 accumulation of ROS. Furthermore, prolonged activation of Nrf2 by epigenetic changes may support
5400 the cancerous phenotype observed in some models exposed to FB₁.

5401 The tumor suppressor, p53 is activated by cellular stress such as genotoxic and oxidative stress. When
5402 activated, p53 regulates several stress responses such as cell cycle arrest, DNA repair and apoptosis
5403 (Fridman and Lowe, 2003). However, p53 inactivation by epigenetic modifications inhibits its response
5404 to stress and promotes carcinogenesis (Saldaña-Meyer and Recillas-Targa, 2011, Chmelarova et al.,
5405 2013). FB₁ elevated the expression of the lncRNA, HOXA11-AS. HOXA11-AS sequestered miR-124,
5406 inhibiting its regulation of DNMT3B and SP1. Therefore, FB₁ upregulated the expression of DNMT3B
5407 and the DNMT1 transcription factor, SP1 as well as the expression of DNMT1 and DNMT3A. The
5408 increase in DNMT expression facilitated global DNA hypermethylation and *p53* promoter
5409 hypermethylation. This led to the decrease in both p53 gene and protein expression. p53 is known to
5410 activate caspase-dependent apoptosis during cellular stress. The decrease in p53 inhibited caspase-
5411 mediated apoptosis as observed by the decrease in the activity of initiator caspases-8 and -9 as well as
5412 executioner caspases-3/7 and -6. It is possible that the inhibition of p53-dependent apoptosis via the
5413 HOXA11-AS/miR-124/DNMT axis may be responsible for promoting FB₁-induced carcinogenesis.

5414 Taken together, this study suggests that FB₁ induces hepatotoxicity in the form of DNA damage and
5415 oxidative stress. FB₁ also alters the epigenome of liver cells by affecting DNA methylation, m6A RNA
5416 methylation, H3K4me3, miRNA (miR-30c, miR-27b and miR-124) and lncRNA (HOXA11-AS).
5417 These epigenetic changes in turn disrupt the DNA damage and anti-oxidant response mechanisms
5418 further exacerbating FB₁-induced hepatotoxicity. Furthermore, the epigenetic downregulation of the
5419 tumor suppressor proteins PTEN and p53, together with inhibition of DNA repair, activation of Nrf2

5420 and dysregulation of apoptosis, provides a potential mode of action by which FB₁ may induce or
5421 promote hepatocellular carcinomas.

5422 **7.2. Limitations, shortcomings and recommendations**

5423 This study provides novel mechanisms for FB₁-induced hepatotoxicity at the epigenetic level using an
5424 *in vitro* model that was acutely exposed (24 hours) to FB₁. However, the following limitations and
5425 shortcomings were found:

- 5426 • *In vitro* models usually consist of a single cell type (in this study, HepG2 cells) grown in
5427 monolayer and are therefore not exact dissociated replicates of their *in vivo* counterparts. This
5428 limits our interpretations of epigenetic patterns and interactions between the various cell types
5429 found in a multicellular organism. The use of *in vivo* models may express different patterns of
5430 epigenetic changes with different outcomes on stress response signaling that may be more
5431 accurate than the use of an *in vitro* model.
- 5432 • Maize is considered a staple in many developing countries and thus may be consumed on a daily
5433 basis. Humans and animals that are heavily reliant on maize are recurrently exposed to FB₁. The
5434 use of an acute model such as the one used in this study (24 hours) may not provide realistic
5435 epigenetic patterns. Additionally, while HepG2 cells were exposed to a range of FB₁
5436 concentrations (0-200 µM) which included an IC₅₀, it may not provide realistic results that are
5437 pertinent to humans.
- 5438 • While we can conclude that hepatotoxicity induced by FB₁ may be a result of its epigenetic
5439 properties, we cannot say with confidence that epigenetic mechanisms identified in this study also
5440 contribute to the carcinogenic nature of FB₁. This is because a cancerous cell line was used in this
5441 study. The use of a primary cell line along with a cancerous cell line should be used to evaluate
5442 whether these FB₁-induced epigenetic alterations to stress responses contributes to its
5443 carcinogenicity.

5444 Taking the limitations of this study into consideration, chronic exposure (greater than 24 h) to FB₁ or
5445 the use of an *in vivo* model may exhibit different patterns of epigenetic changes with different outcomes
5446 on stress response signaling. The outcomes observed may provide more realistic results than the ones
5447 found in the current study. Furthermore, the concentration of FB₁ used in experiments should be
5448 calculated based on the average daily intake of FB₁ and not a range based on the IC₅₀. Hence this study
5449 provides insight for future epigenetic studies using longer exposure times to FB₁, more accurate
5450 concentrations or *in vivo* models.

5451 **7.3. Final remarks**

5452 Collectively, this study suggests that FB₁ possesses epigenetic properties which dysregulate cellular
5453 responses to FB₁-induced stress, further exacerbating its toxicity and possibly carcinogenicity.

5454 **References**

- 5455 Arumugam T, Pillay Y, Ghazi T, Nagiah S, Abdul NS & Chaturgoon AA 2019. Fumonisin B(1)-
5456 induced oxidative stress triggers Nrf2-mediated antioxidant response in human hepatocellular
5457 carcinoma (HepG2) cells. *Mycotoxin Res*, 35, 99-109.
- 5458 Arumugam T, Ghazi T, Sheik Abdul N & Chaturgoon AA 2020. A review on the oxidative effects of
5459 the fusariotoxins: Fumonisin B1 and fusaric acid. *In: PATEL, V. B. & PREEDY, V. R. (eds.)*
5460 *Toxicology*. Academic Press.
- 5461 Bassi C, Ho J, Srikumar T, Dowling RJ, Gorrini C, Miller SJ, Mak TW, Neel BG, Raught B & Stambolic
5462 V 2013. Nuclear PTEN controls DNA repair and sensitivity to genotoxic stress. *Science (New York,*
5463 *N.Y.)*, 341, 395-399.
- 5464 Cantley LC & Neel BG 1999. New insights into tumor suppression: PTEN suppresses tumor formation
5465 by restraining the phosphoinositide 3-kinase/AKT pathway. *Proceedings of the National Academy of*
5466 *Sciences*, 96, 4240-4245.
- 5467 Chmelarova M, Krepinska E, Spacek J, Laco J, Beranek M & Palicka V 2013. Methylation in the p53
5468 promoter in epithelial ovarian cancer. *Clinical and Translational Oncology*, 15, 160-163.
- 5469 Chaturgoon A, Phulukdaree A & Moodley D 2014a. Fumonisin B1 induces global DNA
5470 hypomethylation in HepG2 cells - An alternative mechanism of action. *Toxicology*, 315, 65-69.
- 5471 Chaturgoon AA, Phulukdaree A & Moodley D 2014b. Fumonisin B1 modulates expression of human
5472 cytochrome P450 1b1 in human hepatoma (Hepg2) cells by repressing Mir-27b. *Toxicology Letters*,
5473 227, 50-55.
- 5474 Demirel G, Alpertunga B & Ozden S 2015. Role of fumonisin B1 on DNA methylation changes in rat
5475 kidney and liver cells. *Pharmaceutical Biology*, 53, 1302-1310.
- 5476 Fridman JS & Lowe SW 2003. Control of apoptosis by p53. *Oncogene*, 22, 9030-9040.
- 5477 Gardner NM, Riley RT, Showker JL, Voss KA, Sachs AJ, Maddox JR & Gelineau-van Waes JB 2016.
5478 Elevated nuclear sphingoid base-1-phosphates and decreased histone deacetylase activity after
5479 fumonisin B1 treatment in mouse embryonic fibroblasts. *Toxicol Appl Pharmacol*, 298, 56-65.
- 5480 Ghazi T, Nagiah S & Chaturgoon AA 2020. Fusaric acid decreases p53 expression by altering promoter
5481 methylation and m6A RNA methylation in human hepatocellular carcinoma (HepG2) cells.
5482 *Epigenetics*, 1-13.
- 5483 Hu W, Duan Z, Wang Q & Zhou D 2019. The suppression of ox-LDL-induced inflammatory response
5484 and apoptosis of HUVEC by lncRNA XIAT knockdown via regulating miR-30c-5p/PTEN axis.
5485 *European review for medical and pharmacological sciences*, 23, 7628-7638.

5486 Huang D, Cui L, Sajid A, Zainab F, Wu Q, Wang X & Yuan Z 2019. The epigenetic mechanisms in
5487 Fusarium mycotoxins induced toxicities. *Food and Chemical Toxicology*, 123, 595-601.

5488 Kouadio JH, Dano SD, Moukha S, Mobio TA & Creppy EE 2007. Effects of combinations of Fusarium
5489 mycotoxins on the inhibition of macromolecular synthesis, malondialdehyde levels, DNA methylation
5490 and fragmentation, and viability in Caco-2 cells. *Toxicol*, 49, 306-317.

5491 Kouzi S, Wright N, Dirks-Naylor A & Uddin M 2018. Fumonisin: Effects on human and animal health
5492 and mechanisms of toxicity. *EC Pharmacol. Toxicol*, 6, 187-208.

5493 Liu X, Zhang E, Yin S, Zhao C, Fan L & Hu H 2020. Activation of the IRE1 α Arm, but not the PERK
5494 Arm, of the Unfolded Protein Response Contributes to Fumonisin B1-Induced Hepatotoxicity. *Toxins*
5495 (*Basel*), 12, 55.

5496 Ming M & He YY 2012. PTEN in DNA damage repair. *Cancer Lett*, 319, 125-129.

5497 Mobio TA, Anane R, Baudrimont I, Carratú MR, Shier TW, Dano SD, Ueno Y & Creppy EE 2000.
5498 Epigenetic properties of fumonisin B(1): cell cycle arrest and DNA base modification in C6 glioma
5499 cells. *Toxicol Appl Pharmacol*, 164, 91-96.

5500 Pellanda H, Forges T, Bressenot A, Chango A, Bronowicki JP, Guéant JL & Namour F 2012. Fumonisin
5501 FB1 treatment acts synergistically with methyl donor deficiency during rat pregnancy to produce
5502 alterations of H3- and H4-histone methylation patterns in fetuses. *Molecular nutrition & food research*,
5503 56, 976-985.

5504 Puc J, Keniry M, Li HS, Pandita TK, Choudhury AD, Memeo L, Mansukhani M, Murty VVVS,
5505 Gaciong Z, Meek SEM, et al. 2005. Lack of PTEN sequesters CHK1 and initiates genetic instability.
5506 *Cancer Cell*, 7, 193-204.

5507 Puc J & Parsons R 2005. PTEN loss inhibits CHK1 to cause double stranded-DNA breaks in cells. *Cell*
5508 *Cycle*, 4, 927-929.

5509 Saldaña-Meyer R & Recillas-Targa F 2011. Transcriptional and epigenetic regulation of the p53 tumor
5510 suppressor gene. *Epigenetics*, 6, 1068-1077.

5511 Sancak D & Ozden S 2015. Global histone modifications in Fumonisin B1 exposure in rat kidney
5512 epithelial cells. *Toxicol In Vitro*, 29, 1809-1815.

5513 Wang E, Norred WP, Bacon CW, Riley RT & Merrill AH, Jr. 1991. Inhibition of sphingolipid
5514 biosynthesis by fumonisins. Implications for diseases associated with Fusarium moniliforme. *J Biol*
5515 *Chem*, 266, 14486-14490.

5516 Yin S, Guo X, Li J, Fan L & Hu H 2016. Fumonisin B1 induces autophagic cell death via activation of
5517 ERN1-MAPK8/9/10 pathway in monkey kidney MARC-145 cells. *Archives of Toxicology*, 90, 985-
5518 996.

5519 Zhao T, Wang J, Shen L-J, Long C-L, Liu B, Wei Y, Han L-D, Wei Y-X & Wei G-H 2020. Increased
5520 m6A RNA modification is related to the inhibition of the Nrf2-mediated antioxidant response in di-(2-
5521 ethylhexyl) phthalate-induced prepubertal testicular injury. *Environmental Pollution*, 259, 113911.

5522 Zhengchang W, Chao X, Haifei W, Song G, Shenglong W & Wenbin B 2020. Transcriptome-wide
5523 assessment of the m6A methylome of intestinal porcine epithelial cells treated with deoxynivalenol.
5524 *Research Square*.

5525

5526

5527

5528

5529

5530

5531

5532

5533

5534

5535

5536

5537

ADDENDUM A

5538 The following study titled, “**Fumonisin B₁-induced oxidative stress triggers Nrf2-mediated**
5539 **antioxidant response in human hepatocellular carcinoma (HepG2) cells**” set the foundation for this
5540 study.

5541

5542

5543

5544

5545

5546
5547
5548
5549
5550
5551
5552
5553
5554
5555
5556
5557
5558
5559
5560
5561
5562
5563
5564
5565
5566
5567
5568
5569
5570
5571
5572

Mycotoxin Research, 35 (1), 99-109.

DOI: [10.1007/s12550-018-0335-0](https://doi.org/10.1007/s12550-018-0335-0)



Fumonisin B₁-induced oxidative stress triggers Nrf2-mediated antioxidant response in human hepatocellular carcinoma (HepG2) cells

Thilona Arumugam¹ · Yashodani Pillay¹ · Terisha Ghazi¹ · Savania Nagiah¹ · Naeem Sheik Abdul¹ · Anil A. Chaturgoon^{1,2}

Received: 20 June 2018 / Revised: 26 October 2018 / Accepted: 29 October 2018
© Society for Mycotoxin Research and Springer-Verlag GmbH Germany, part of Springer Nature 2018

Abstract

Fumonisin B₁ (FB₁), a causative agent for animal-related mycotoxicoses, has been implicated in human and animal cancer. FB₁ induces oxidative stress but the related survival responses are not well established. Central to this response is the transcription factor, nuclear factor erythroid 2 p45-related factor 2 (Nrf2). The effects of FB₁ on Nrf2-related survival responses in human hepatoma (HepG2) cells were investigated. HepG2 cells were treated with 200 μmol/l FB₁ (IC₅₀–24 h). Cellular redox status was assessed via the quantification of intracellular reactive oxygen species (ROS), lipid peroxidation, protein oxidation and the antioxidant glutathione (GSH). The protein expression of oxidative stress and mitochondrial stress response proteins [Nrf2, phosphorylated-Nrf2 (pNrf2), superoxide dismutase 2 (SOD2), catalase (CAT), sirtuin 3 (Sirt 3) and Lon-protease 1 (Lon-P1)] were quantified by western blotting, while gene expression levels of *SOD2*, *CAT* and *GPx* were assessed using quantitative polymerase chain reaction (qPCR). Lastly, the fluorometric, JC-1 assay was used to determine mitochondrial polarisation. FB₁ significantly increased ROS ($p \leq 0.001$), and induced lipid peroxidation ($p < 0.05$) and protein carbonylation ($p \leq 0.001$), which corresponded with the increase in GSH levels ($p < 0.05$). A significant increase in pNrf2, *SOD2*, *SOD2*, *CAT* ($p < 0.05$), *CAT* ($p \leq 0.01$) and *GPx* ($p \leq 0.001$) expression was observed; however, total Nrf2 ($p > 0.05$) was reduced. There was also a minor reduction in the mitochondrial membrane potential of HepG2 cells ($p < 0.05$); however, the expression of Sirt 3 and Lon-P1 ($p \leq 0.001$) were upregulated. Exposure to FB₁ induced oxidative stress in HepG2 cells and initiated Nrf2-regulated transcription of antioxidants.

Keywords Fumonisin B₁ · Oxidative stress · Reactive oxygen species · Antioxidants · Nuclear factor erythroid 2-related factor 2

Introduction

Maize forms a vital part of the African staple diet due to its high yields, adaptability to different climates, versatile uses and storage capabilities. However, it is commonly contaminated by fungi, which produce toxic secondary metabolites

known as mycotoxins (Fandohan et al. 2003). *Fusarium verticillioides* and *F. proliferatum* are amongst the most common maize-associated fungi and the most abundant producers of the fumonisin family of mycotoxins. Fumonisin B₁ (FB₁) is the most frequent and toxic of the 28 fumonisin analogues that have been identified (Rheeder et al. 2002).

✉ Anil A. Chaturgoon
chatur@ukzn.ac.za

Thilona Arumugam
cyborglona@gmail.com

Yashodani Pillay
yashodani@gmail.com

Terisha Ghazi
terishaghazi@gmail.com

Savania Nagiah
Nagiah.savania@gmail.com

Naeem Sheik Abdul
naeemsheik11@gmail.com

¹ Discipline of Medical Biochemistry, School of Laboratory Medicine and Medical Sciences, University of KwaZulu-Natal, Durban, South Africa

² Discipline of Medical Biochemistry and Chemical Pathology, School of Laboratory Medicine and Medical Sciences, College of Health Sciences, Howard College, University of KwaZulu-Natal, George Campbell Building, Durban 4041, South Africa

FB₁ exerts toxicity by disrupting the de novo biosynthesis of sphingolipids and altering plasma membrane composition, signal transduction and cell cycle regulation. As a structural analogue of sphingoid bases, FB₁ can competitively inhibit ceramide synthase, the enzyme responsible for the acetylation of sphingoid bases. This inhibitory action leads to the accumulation of sphinganine and sphingosine to cytotoxic levels (Riley et al. 2001).

The liver and kidney are major targets of FB₁ toxicity in almost all animal species tested (Riley and Voss 2006). Additional species specific effects such as equine leukoencephalomalacia, porcine pulmonary oedema and the development of carcinomas in rodents have also been reported (Marin et al. 2013; Ross et al. 1990). Furthermore, epidemiological studies in humans have shown a correlation between high consumption of maize and incidence of oesophageal and hepatocellular carcinomas (Rheeder 1992; Shephard et al. 2007; Sun et al. 2007). Exposure to FB₁ is also associated with the high prevalence of neural tube defects and the induction of oxidative stress leading to DNA, lipid and protein damage (Marasas et al. 2004; Mary et al. 2012; Stockmann-Juvala and Savolainen 2008).

Oxidative stress occurs when the balance between reactive oxygen species (ROS) and antioxidants shifts towards ROS. The electron transport chain (ETC), found within the mitochondria, leaks unpaired electrons into the mitochondrial matrix during respiration (Turrens 2003). These electrons react with molecular oxygen to form ROS (Lenaz and Genova 2010; Sena and Chandel 2012). FB₁ disrupts mitochondrial respiration by inhibiting complex I of the ETC, elevating ROS generation (Domijan and Abramov 2011). Previous studies have identified oxidative stress as a consequence of FB₁ exposure. However, the role of the ensuing antioxidant response in the context of FB₁ toxicology has not been well established (Khan et al. 2018; Mary et al. 2012; Wang et al. 2016).

The first line of defence against oxidative stress in cells is the induction of antioxidants, which scavenge ROS and dampen oxidative damage to macromolecules (Birben et al. 2012). Nuclear factor erythroid 2 p45-related factor 2 (Nrf2) is a transcription factor that activates the antioxidant response element (ARE), a regulatory element found in the promoters of several cytoprotective and antioxidant genes including glutathione peroxidase (GPx), superoxide dismutase (SOD) and catalase (CAT) (Nguyen et al. 2009). Under basal physiological conditions, Nrf2 is sequestered in the cytoplasm and undergoes constant degradation through Kelch-like ECH-associated protein 1 (Keap-1) ubiquitination. The Nrf2-ECH homologue h2 (Neh2) domain of Nrf2 contains several lysine residues that are targets for Keap-1 ubiquitination via cullin 3 (CUL3) ubiquitin ligase (Rojo de la Vega et al. 2016). This prevents Nrf2 from translocating to the nucleus and activating antioxidant transcription. When cells

experience oxidative stress, the Keap1-Nrf2 stress response pathway is activated. Elevated levels of ROS oxidise specific cysteine residues in Keap-1, weakening its ability as a ligase adapter. This leads to the dissociation of Keap-1 from the Neh2 domain, allowing the accumulation of Nrf2 in the cytosol. Nrf2 is thus free to enter the nucleus, where it dimerises with small Maf proteins and binds to the ARE; promoting the transcription of antioxidant genes (Fig. 1) (Bellezza et al. 2018; Buendia et al. 2016; Furukawa and Xiong 2005; Itoh et al. 1997; Itoh et al. 1999; Kensler et al. 2007; Ma 2013; Nguyen et al. 2003; Ray et al. 2012; Valko et al. 2007).

Considering that FB₁ inhibits the ETC, which may enhance the production of ROS within the mitochondria; survival responses related to the mitochondria may be noteworthy (Domijan and Abramov 2011; Stockmann-Juvala and Savolainen 2008). Sirtuin 3 (Sirt 3) and the mitochondrial Lon-protease 1 (Lon-P1) help maintain homeostasis within the mitochondria during oxidative stress (Bause and Haigis 2013; Pinti et al. 2015). Lon-P1 dampens the effects of oxidative stress by degrading oxidised proteins, while Sirt 3 deacetylates antioxidant proteins such as SOD2 and CAT, increasing their capacity to detoxify ROS (Ngo et al. 2013; Weir et al. 2013).

Although a number of studies have investigated, the effect of FB₁ on ROS production and oxidative damage, the Nrf2-antioxidant response has not been thoroughly investigated. This study focussed on the effect of FB₁ on Nrf2-related survival responses in human hepatoma (HepG2) cells.

Materials and methods

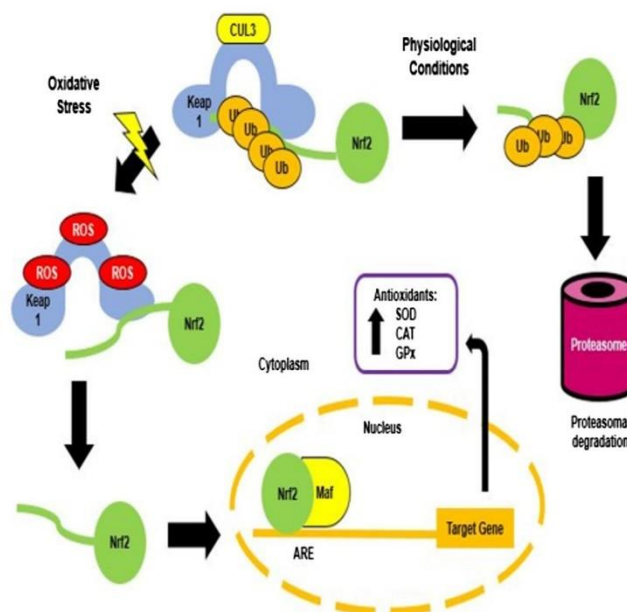
Materials

FB₁, isolated from *Fusarium verticillioides*, was obtained from Sigma-Aldrich (St Louis, MO, USA). The HepG2 cell line was acquired from Highveld Biologicals (Johannesburg, South Africa). Cell culture reagents and supplements were purchased from Lonza Bio-Whittaker (Basel, Switzerland). Western blot reagents were procured from Bio-Rad (Hercules, CA, USA) and anti-bodies were purchased from Abcam (Cambridge, UK), Sigma-Aldrich (St Louis, MO, USA), Cell Signalling Technologies (Danvers, MA, USA) and Santa Cruz (Dallas, TX, USA). All other reagents were purchased from Merck (Darmstadt, Germany) unless otherwise stated.

Cell culture

HepG2 cells were cultured in monolayer (10⁶ cells per 25 cm³ culture flask) with complete culture media [CCM: Eagle's Essential Minimal Media (EMEM) supplemented

Fig. 1 The Keap-1-Nrf2-mediated antioxidant response. Under physiological conditions, Nrf2 is ubiquitinated (Ub) by Keap-1-CUL3 system and degraded within the proteasome. Exposure to high levels of ROS disrupts Keap-1-CUL3 ubiquitination of Nrf2. This triggers the release and subsequent translocation of Nrf2 to the nucleus, where it dimerises with Maf and promotes the transcription of antioxidants such as SOD, CAT and GPx



with 10% foetal calf serum, 1% penstrepfungizone and 1% L-glutamine] at 37 °C in a humidified incubator. Cells were allowed to reach 80% confluence in 25 cm³ flasks before treatment with an IC₅₀ of 200 μmol/l FB₁ in CCM for 24 h (Chuturgoon et al. 2015). An untreated control, containing only CCM, was also prepared.

Reactive oxygen species analyses

Intracellular ROS was quantified using the fluorometric 2',7'-dichlorodihydrofluorescein-diacetate (H₂DCF-DA) assay. Control and treated cells (50,000 cells per treatment) were incubated in 500 μl of 5 μmol/l H₂DCF-DA stain (30 min, 37 °C). The stain was removed via centrifugation (400×g, 10 min, 24 °C) and cells were washed twice with 0.1 mol/l phosphate buffer saline (PBS). Cells were re-suspended in 400 μl of 0.1 mol/l PBS and seeded in triplicate (100 μl/well) in a 96-well opaque microtiter plate. A blank consisting of only 0.1 mol/l PBS was plated in triplicate as well. Fluorescence was measured with Modulus™ microplate luminometer (Turner Biosystems, Sunnyvale, CA) using a blue filter with an excitation wavelength (λ_{ex}) of 503 nm and emission wavelength (λ_{em}) of 529 nm. The fluorescence of each sample was calculated by subtracting the average fluorescence of the blank from the fluorescence of each sample.

Lipid peroxidation assessment

The thiobarbituric acid reactive substances (TBARS) assay measured lipid peroxidation by-products—malondialdehyde (MDA) and other TBARS as a measure of oxidative damage to lipids. TBARS assay was conducted as per the method described by Sheik Abdul et al. (2016). Absorbance of the samples was read using a spectrophotometer, λ = 532/600 nm. The TBARS content was expressed in terms of MDA-TBA adduct.

Protein isolation

Protein was isolated using 200 μl of cell lysis buffer (50 mmol/l HEPES, 1% Triton ×100, 10% glycerol, 50 mmol/l NaCl) for the protein carbonyl assay and 200 μl of Cytobuster™ (Novagen, USA) supplemented with protease and phosphatase inhibitors (Roche, 05892791001 and 04906837001, respectively) for western blotting.

Cells were incubated in the respective lysis solutions on ice for 10 min, then mechanically lysed and decanted into micro-centrifuge tubes. The cell lysate was centrifuged (13,000×g, 10 min, 4 °C) to obtain crude protein; which was quantified using the bicinchoninic acid (BCA) assay. Bovine serum albumin standards (0–1 mg/ml) were prepared and 25 μl of the standards and samples (triplicate) were dispensed into a 96-well microtiter plate. BCA working solution (196 μl BCA 4 μl

CuSO₄ per well) was dispensed into each well, followed by a 30 min incubation at 37 °C. The optical density of the samples was measured at 562 nm using a spectrophotometer (Bio-Tek µQuant, Winooski, VT, USA). The mean absorbance values of the standards were used to construct a standard curve, which determined the protein concentration of the samples. Quantified proteins were standardised to 1 mg/ml.

Protein carbonyl analysis

Protein oxidation was measured via the quantification of intracellular protein carbonyl groups. Standardised protein was incubated at room temperature (RT) for 1 h with 2,4-dinitrophenylhydrazine (DNPH) (800 µL). A blank, which consisted of standardised protein from control cells and 2.5 mol/l HCl (800 µl) was also prepared. Proteins were precipitated with 20% Trichloroacetic acid (1 ml), vortexed and centrifuged (2000×g, 10 min, 24 °C). The pellet was washed twice with 1 ml ethanol-ethyl acetate (1:1) and dissolved in 6 mol/l guanidine-HCl (1 ml). Samples were incubated (10 min, 37 °C) before any insoluble material was removed with centrifugation (2000×g, 10 min, 24 °C). The supernatant was collected and dispensed in triplicate in 96-well plate (100 µl/well). Absorbance was measured at λ = 370 nm with a spectrophotometer. The corrected absorbance was calculated by subtracting the mean absorbance of the blank from the absorbance of samples. The concentration of protein carbonyls was obtained by dividing the corrected absorbance by the absorption co-efficient of DNP (22,000 l mol⁻¹ cm⁻¹). Results were expressed in nanomoles per milligram.

Protein expression

The protein expressions of pNrf2, Nrf2, SOD2, CAT, Sirt 3 and Lon-P1 were determined by western blotting. Standardised protein samples were boiled in Laemmli buffer [dH₂O, 0.5 mol/l Tris-HCl (pH 6.8), glycerol, 10% sodium dodecyl sulphide (SDS), b-mercaptoethanol, 1% bromophenol blue] for 5 min. Proteins (25 µl) were separated by electrophoresis on SDS-polyacrylamide electrophoresis gels (4% stacking gel; 10% resolving gel) and electro-transferred to nitrocellulose membranes. Membranes were blocked with 5% BSA in Tween 20-Tris buffer saline (TTBS 150 mmol/l NaCl, 3 mmol/l KCl, 25 mmol/l Tris, 0.05% Tween 20, dH₂O, pH 7.5) for 1 h, and incubated with primary antibody [pNrf2 (ab76026); Nrf2 (ab31163); SOD2 (HPA001814); CAT (C0979), Sirt3 (C73E3), Lon-P1 (HPA002034)] in 5% BSA in TTBS (1:1000 dilution) overnight at 4 °C. Following overnight incubation, membranes were equilibrated to RT and washed with TTBS (5 times, 10 min). Membranes were subsequently probed with horseradish peroxidase-conjugated secondary antibody [Rabbit (sc-

2004); Mouse (sc-2005)] in 5% BSA in TTBS (1:10,000) for 1 h at RT. Thereafter, membranes were washed with TTBS (5 times, 10 min) and immunoreactivity was detected (Clarity Western ECL Substrate) with the Bio-Rad Chemidoc gel documentation system. After detection, membranes were quenched with 5% H₂O₂ for 30 min, incubated in blocking solution (5% BSA for 1 h at RT), rinsed thrice in TTBS, and probed with HRP-conjugated anti-β-actin (housekeeping protein). Protein expression was analysed by the Image Lab Software version 5.0 (Bio-Rad) and the results were expressed as relative band density (RBD). The expression of proteins of interest was normalised against β-Actin.

Glutathione analysis

The GSH status of HepG2 cells was measured using the GSH-Glo™ Glutathione assay. Cells were dispensed in an opaque microtiter plate (50 µl of 20,000 cells/well in 0.1 mol/l PBS) in triplicate. GSH standards (0–50 µmol/l) were prepared from a 5 mmol/l stock of GSH using 0.1 mol/l PBS and dispensed in triplicate. GSH-Glo reaction solution (50 µl) was added to each well and the plate was left in the dark (RT, 30 min). After the 30-min incubation, luciferin detection reagent (100 µl) was dispensed into each well and the plate was incubated (RT, 15 min). The luminescence emitted by the cells was measured by a Modulus™ microplate luminometer (Turner Biosystems, Sunnyvale, CA). The GSH standards were used to prepare a standard curve, which was used to facilitate conversion of luminescence (RLU) to GSH concentration (µmol/l).

RNA analysis

Total RNA was isolated according to the method described by Chuturgoon et al. (2014). Isolated RNA was quantified (Nanodrop 2000, ThermoScientific, Waltham, USA) and standardised to 1000 ng/µl. cDNA was synthesised from standardised RNA using the iScript cDNA synthesis kit (Bio-Rad). Thermocycler conditions for cDNA synthesis were 25 °C for 5 min, 42 °C for 30 min, 85 °C for 5 min and a final hold at 4 °C (Nagiah et al. 2015).

Gene expression was analysed using the SsoAdvanced™ Universal SYBR® Green Supermix kit (Bio-Rad). The mRNA expressions of *CAT*, *SOD2* and *GPx* were investigated using specific forward and reverse primers (Table 1). Reaction volumes which consisted of the following were prepared: SYBR green (5 µl), forward primer (1 µl), reverse primer (1 µl), nuclease free water (2 µl) and cDNA template (1 µl). All reactions were carried out in triplicate.

The samples were amplified using a CFX96 Touch™ Real-Time PCR Detection System (Bio-Rad). The initial denaturation occurred at 95 °C (4 min). Thereafter, 37 cycles of denaturation (15 s, 95 °C), annealing (40 s; temperatures—

Table 1 The annealing temperatures and primer sequences for the genes of interest

Gene	Annealing temperature	Primer	Sequence
CAT	58 °C	Forward	5'-TAAGACTGACCAGGGCATC-3'
		Reverse	5'-CAACCTTGGTGAGATCGAA-3'
GPx	58 °C	Forward	5'-GACTACACCCAGATGAACGAGC-3'
		Reverse	5'-CCCACCAGGAATTCTCAAAG-3'
SOD	57 °C	Forward	5'-GAGATGTTACACGCCAGAT
		Reverse	AGC-3'
GAPDH		Forward	5-AATCCCCAGCAGTGAATAAGG-3'
		Reverse	5'-TCCACCACCTGTTGCTGTA-3'
			5'-ACCACAGTCCATGCCATCAC-3'

Table 1) and extension (30 s, 72 °C) occurred. The method described by Livak and Schmittgen (2001) was employed to determine the changes in relative mRNA expression, where $2^{-\Delta\Delta Ct}$ represents the fold change relative to the untreated control. The expression of the gene of interest was normalised against the housekeeping gene, Glyceraldehyde 3-phosphate dehydrogenase (GAPDH), which was amplified simultaneously under the same conditions.

Mitochondrial membrane potential

The mitochondrial membrane potential ($\Delta\psi_m$) was measured by the JC-1 stain (Zheng et al. 2013). Control and treated cells (50,000 cells per treatment) were incubated in 200 μ l of 5 μ g/ml JC-1 stain (BD Biosciences, San Jose, NJ, USA) (20 min, 37 °C). The stain was removed via centrifugation (400 \times g, 10 min, 24 °C) and the cells were washed twice with JC-1 staining buffer. Cells were re-suspended in 400 μ l of JC-1 staining buffer and seeded in an opaque 96-well plate in triplicate (100 μ l/well). A blank, which consisted of only JC-1 staining buffer, was plated in triplicate as well (100 μ l/well). Fluorescence was quantified on a Modulus™ microplate reader (Turner Biosystems, Sunnyvale, CA). JC-1 monomers were measured with a blue filter (λ_{ex} = 488 nm, λ_{em} = 529 nm) and JC-1 aggregates were measured with a green filter (λ_{ex} = 524 nm, λ_{em} = 594 nm). The $\Delta\psi_m$ of the HepG2 cells was expressed as the fluorescence intensity ratio of JC-1 aggregates and JC-1 monomers (Zheng et al. 2013).

Statistical analysis

GraphPad Prism version 5.0 (GraphPad Software Inc., California) was used to perform all statistical analyses. The unpaired *t* test was used for all assays. All results were represented as the mean \pm standard deviation unless otherwise stated. A value of $p < 0.05$ was considered statistically significant.

Results

Assessment of oxidative stress

Oxidative stress parameters were quantified in HepG2 cells post-FB₁ exposure. The H₂DCF-DA assay revealed a highly significant ($p = 0.0002$) 3.34-fold increase (Fig. 2a) in intracellular ROS generated by FB₁ exposure (116,000 \pm 9020 RFU) compared to control cells (34,700 \pm 5740 RFU). As shown in Fig. 2b, the concentration of MDA-TBA adducts were significantly higher ($p = 0.0205$) in FB₁ exposed cells (FB₁ 0.186 \pm 0.007 μ mol/l) compared to the control (0.152 \pm 0.014 μ mol/l). FB₁ also induced protein oxidation (Fig. 2c),

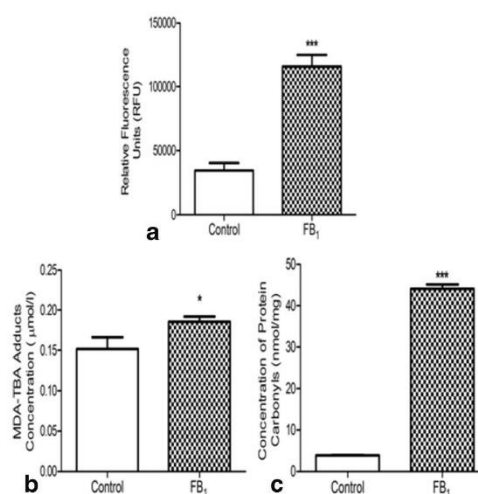


Fig. 2 Effects of FB₁ on cellular oxidation. **a** Intracellular ROS levels represented as relative light units (RLU) produced after H₂DCF-DA staining in control and FB₁-treated HepG2 cells. **b** Concentration (μ mol/l) of MDA-TBA adducts. **c** Concentration (ng/mol) of proteins carbonyls formed after 24 h-exposure to FB₁, where a single asterisk represents significance $p < 0.05$ and a triple asterisk represents significance $p < 0.001$

as evidenced by a significant ($p < 0.0001$) 11.3-fold elevation in the formation of protein carbonyls in FB₁ (44.1 ± 1.10 nmol/mg) exposed cells in relation to control cells (3.89 ± 0.120 nmol/mg). The observed increase in intracellular ROS and corresponding increase in lipid peroxidation and protein carbonylation indicated that oxidative stress was induced in HepG2 cells following FB₁ exposure.

The antioxidant response

Antioxidant regulation

Elevated ROS generated by FB₁ altered the antioxidant status in HepG2 cells. The transcription factor Nrf2 is the master regulator of endogenous antioxidants (Vomund et al. 2017). Western blot analysis revealed that the expression of total Nrf2 (Fig. 3a) was slightly reduced ($p = 0.111$) after a 24-h exposure to FB₁ (0.246 ± 0.037 RBD) when compared to control cells (0.371 ± 0.100 RBD). High concentrations of ROS normally activate phosphorylation pathways which in turn results in phosphorylation and nuclear translocation of Nrf2 (Bo et al. 2015). A significant 1.9-fold increase in the expression of active pNrf2 was observed in cells treated with FB₁ ($p = 0.0311$; control 7.24 ± 0.857 RBD vs FB₁ 13.7 ± 3.33 RBD—Fig. 3b).

Superoxide detoxification

The transcription of the mitochondrial detoxification enzyme, SOD2, is regulated by Nrf2 (Bo et al. 2015). SOD2 expression was significantly elevated at both mRNA ($p = 0.0172$; control $1.00 \pm 6.08 \times 10^{-6}$ fold vs FB₁ 1.76 ± 0.335 fold—Fig. 4a) and protein levels ($p = 0.004$; control 0.924 ± 0.083 RBD vs FB₁ 4.48 ± 0.848 RBD—Fig. 4b).

Detoxification of peroxides

Hydrogen peroxide is detoxified by CAT and GPx (Murphy 2009; Turrens 2003). CAT mRNA levels (Fig. 5a) were significantly ($p = 0.009$) upregulated 1.5-fold in FB₁ treatments.

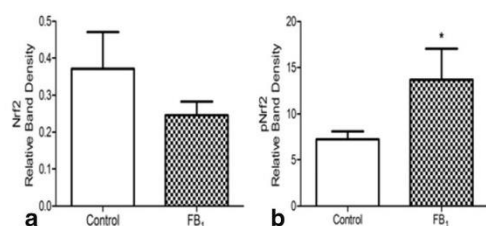


Fig. 3 Effect of FB₁ on Nrf2 and pNrf2. **a** Protein expression of total Nrf2. **b** Protein expression of pNrf2, where a single asterisk represents significance $p < 0.05$

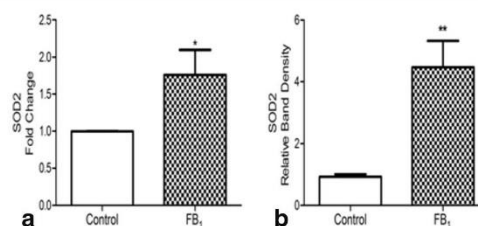


Fig. 4 Levels of SOD2 in HepG2 cells exposed to FB₁. **a** mRNA levels. **b** Protein expression, where a single asterisk represents significance $p < 0.05$ and a double asterisk represents significance $p < 0.01$

This was further confirmed by an increase in CAT protein expression after FB₁ exposure ($p = 0.073$; control 0.272 ± 0.092 RBD vs FB₁ 0.492 ± 0.128 RBD—Fig. 5b).

The qPCR results for GPx (Fig. 5c) showed a highly significant ($p = 0.0001$) 1.9-fold upregulation in FB₁-exposed cells. The concentration of GSH ($p = 0.012$; Fig. 5d), a cofactor for GPx, was 2.27-fold greater in FB₁-treated cells (17.5 ± 3.75 μ M) in relation to control cells (7.71 ± 1.14 μ M).

Mitochondrial stress responses

Mitochondrial health and function can be determined by measuring the mitochondrial membrane potential ($\Delta\psi$) (Sakamuru et al. 2016). The JC-1 assay was used to determine $\Delta\psi$ and found that it was slightly reduced in FB₁-treated

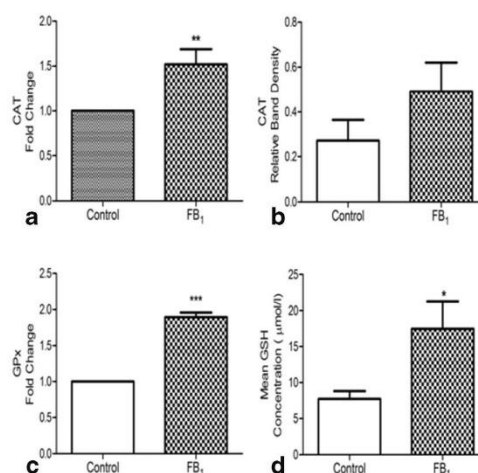


Fig. 5 Effects of FB₁ on the expression of antioxidants involved hydrogen peroxide detoxification. **a** CAT mRNA expression. **b** CAT protein expression. **c** GPx mRNA expression. **d** GSH concentration post-FB₁ exposure, where a single asterisk represents significance $p < 0.05$, a double asterisk represents significance $p < 0.01$ and a triple asterisk represents significance $p < 0.001$

cells ($p=0.205$; control 0.044 ± 0.01 JC-1 fluorescence ratio vs FB_1 0.027 ± 0.009 JC-1 fluorescence ratio—Fig. 6a).

Mitochondrial stress response proteins, Sirt 3 and Lon-P1, were highly expressed during oxidative and mitochondrial stress. Western blot analysis of Sirt 3 (Fig. 6b) revealed a significant ($p=0.0003$) 2.03-fold increase in FB_1 -treated cells (7.63 ± 0.003 RBD) relative to the control (3.76 ± 0.577 RBD). The protein expression of the protease, Lon-P1 (Fig. 6c), was significantly increased 1.72-fold in cells exposed to FB_1 ($p=0.0004$; control 0.189 ± 0.012 RBD vs FB_1 0.324 ± 0.017 RBD).

Discussion

The mycotoxin, FB_1 , is a world-wide contaminant of maize and maize-based products (Marasas 2001; Shephard et al. 1996). It is nephrotoxic, cytotoxic and hepatotoxic to both animals and humans (Ross et al. 1990). Although FB_1 is poorly absorbed in humans, a major portion of absorbed FB_1 is distributed to the liver (Voss et al. 2002). The liver is the oxidative hub for many metabolic and detoxification reactions. Hepatocytes have a high density of mitochondria, increasing the risk of oxidative insult (Johannsen and Ravussin 2009).

The primary function of the mitochondria is to generate ATP via the ETC (Brand et al. 2013). Normal mitochondrial metabolism contributes to the generation of ROS, by leaking unpaired electrons into the mitochondrial matrix (Turrens

2003). Unpaired electrons react with oxygen to form superoxide; which is converted to hydrogen peroxide (Apel and Hirt 2004). Unwarranted production of ROS from the ETC can be stimulated by a number of factors, including the inhibition of complex I of the ETC (Lenaz and Genova 2010; Sena and Chandel 2012). Domijan and Abramov (2011) have reported that FB_1 inhibits complex I of the ETC, resulting in the enhanced generation of ROS and mitochondrial depolarisation. Hence, complex I inhibition may explain the observed mitochondrial depolarisation and increased levels of intracellular ROS (Fig. 2a) following FB_1 exposure in HepG2 cells. Previous studies confirm that FB_1 triggered the generation of intracellular ROS in mouse GT1-7 hypothalamic cells, rat C6 glioblastoma cells, human U-118MG glioblastoma cells and human SH-SY5Y neuroblastoma cells (Domijan and Abramov 2011; Stockmann-Juvala et al. 2004a; Stockmann-Juvala et al. 2004b).

One consequence of uncontrolled production of ROS is the peroxidation of lipids, which yield by-products such as MDA (Ayala et al. 2014). FB_1 significantly increased extracellular MDA-TBA adducts in HepG2 cells as evidenced by the TBARS assay (Fig. 2b). This is supported by findings in a number of different studies involving human cell lines and animal *in vivo* and *in vitro* models (Bernabucci et al. 2011; Kouadio et al. 2005; Wang et al. 2016).

Additional downstream repercussions of elevated ROS include nucleic acid and protein oxidation. FB_1 has been implicated in both these outcomes as evidenced in a study by Mary et al. (2012), where a significant increase in the formation of protein carbonyls and mis-incorporation of 8-oxoG in the DNA of rat spleen mononuclear cells was observed after a 48-h incubation with FB_1 . A 24-h exposure to FB_1 in this study also resulted in significant increase in protein oxidation in form of protein carbonyls in HepG2 cells (Fig. 2c). This finding confirms protein oxidation is a biochemical hallmark of FB_1 exposure despite a significantly shorter exposure period.

The antioxidant defence system is responsible for detoxifying and neutralising the effects of excess intracellular ROS (Birben et al. 2012). Redox homeostasis relies on the disassociation of the antioxidant transcription factor, Nrf2, from Keap-1 (Bo et al. 2015). The cysteine residues of Keap-1 are targets for ROS (Schieber and Chandel 2014). Oxidative modification of these cysteine residues results in structural modifications to Keap-1, weakening its activity as a ligase adaptor (Sporn and Liby 2012). This leads to the dissociation of Keap-1 from the Neh domain, allowing the accumulation of Nrf2 in the cytosol. Modifications to Nrf2 such phosphorylation of the serine 40 residue also induce the dissociation of Nrf2 from Keap-1 (Nguyen et al. 2009). This study found that the expression of total Nrf2 was slightly reduced post- FB_1 exposure though the expression of Nrf2 with a phosphorylated serine 40 residue was significantly elevated (Fig. 3). Most transcription

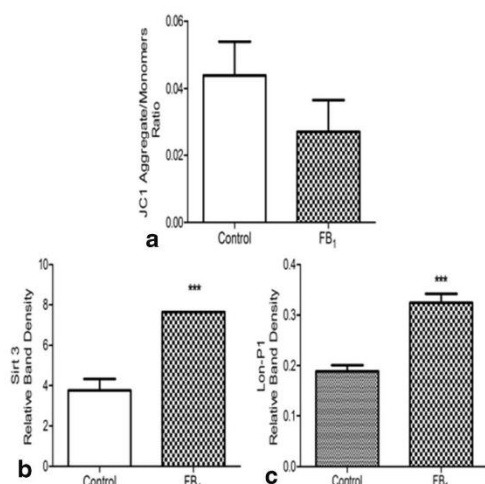


Fig. 6 Mitochondrial response to FB_1 . **a** $\Delta\psi_m$ represented as a ratio of JC-1 aggregates and JC-1 monomers. **b** Protein expression of Sirt 3. **c** Protein expression of Lon-P1, where a triple asterisk represents significance $p < 0.001$

factors—including Nrf2—are regulated by phosphorylation (Huang et al. 2002; Whitmarsh and Davis 2000). Excess ROS activates phosphorylation pathways such as mitogen-activated protein kinase (MAPK) and protein kinase c (PKC), which in turn participate in the phosphorylation and activation of the Nrf2-ARE (Bo et al. 2015). Phosphorylation of Nrf2 triggers its disassociation from Keap-1 ubiquitination, allowing translocation to the nucleus and subsequent transcription of antioxidant genes (Huang et al. 2002). Studies have shown that FB₁ activated both the MAPK and PKC pathways which may contribute further to Nrf2 phosphorylation (Pinelli et al. 1999; Yeung et al. 1996).

Nrf2 promotes the transcription of major antioxidants such as SOD2, CAT and GPx (Bo et al. 2015; Ma 2013). These antioxidant enzymes are the first line of defence against ROS (Wang et al. 2016). Surplus superoxide radicals, produced by dysregulated ETC, are detoxified to hydrogen peroxide by SOD2. Hydrogen peroxide is further detoxified by CAT and GPx to water and oxygen (Weir et al. 2013). The expression of SOD2 (Fig. 4), CAT and GPx (Fig. 5a–c) was all upregulated in HepG2 cells after exposure to FB₁. The expression of these antioxidants, however, were reduced in Balb/c mice and peripheral blood mononuclear cells (PBMC) exposed to FB₁ (Abbes et al. 2016; Bernabucci et al. 2011). Most cells in vivo are exposed to low oxygen concentrations; however, HepG2 cells were grown under 95% oxygen and 5% carbon dioxide. Therefore, more oxygen may have been available to react with electrons leaked from the mitochondria in HepG2 cells, which may have resulted in a higher production of ROS and more rigorous antioxidant response (Halliwell 2003).

An alternative non-enzymatic mechanism for hydrogen peroxide detoxification was also investigated. Glutathione is a major intracellular antioxidant in hepatocytes that protects against oxidative damage and is involved in detoxification of xenobiotics (Chen et al. 2013). This tripeptide is often referred to as the body's master antioxidant. It can be present in its reduced state—GSH or oxidised state (GSSG) (Filomeni et al. 2002). GSH directly quenches hydroxyl radicals and other oxygen-centred free radicals. It also acts a cofactor for the enzymatic antioxidant, GPx, in the detoxification of peroxides (Birben et al. 2012; Lushchak 2012).

After a 24-h incubation with FB₁, the concentration of GSH was significantly elevated in HepG2 cells (Fig. 5d). This is in agreement with results obtained by Domijan and Abramov (2011), who showed a significant increase in the concentration of GSH in SH-SY5Y cells after a 24-h incubation with FB₁. Long-term exposure to FB₁, however, lowered GSH concentration (Stockmann-Juvala et al. 2004a). Elevation of GSH could be a result of increased NADPH availability, a cofactor of GSH and component of GSH synthesis. Inhibition of sphingolipid synthesis by FB₁

distorts the structure of membrane receptors such as the folate receptor (Stevens and Tang 1997). Inhibition of folate uptake promotes the conversion of homocysteine to cysteine, a key amino acid required for the synthesis of GSH (Lu 2009; Stevens and Tang 1997).

As discussed previously, ROS produced by ETC resulted in the depolarisation of the mitochondria, which may have led to mitochondrial dysfunction. After observing a mild reduction in $\Delta\psi_m$ (Fig. 6a), mitochondrial stress responses to FB₁ was assessed.

Proteins within the mitochondrial matrix are at great risk to oxidative insult. The clearance of oxidised proteins within the mitochondria is essential as oxidised proteins form aggregates and crosslinks, resulting in mitochondrial toxicity (Ngo et al. 2013). Lon-P1 is responsible for degrading oxidised proteins such as protein carbonyls within the mitochondrial matrix (Gibellini et al. 2014). Several reports have indicated that Lon-P1 expression and activity increased in the presence of high levels of carbonylated proteins (Pinti et al. 2015). The 11.37-fold increase in protein carbonyls by FB₁ may have induced the upregulation in Lon-P1 expression in HepG2 cells (Fig. 6c) (Ngo et al. 2013).

Lon-P1 is post-transcriptionally activated by the mitochondrial deacetylase enzyme, Sirt 3 (Bota and Davies 2016). Sirt 3 expression may have been upregulated to counteract the highly oxidative environment induced by FB₁ (Fig. 6b). Sirt 3 does not have any direct antioxidant capabilities but is able to upregulate the mitochondrial antioxidant capacity via two methods. The first method involves activating the mitochondrial antioxidant, SOD2, via deacetylation. The second method involves the enhancing isocitrate dehydrogenase 2 (IDH2) activity through Sirt3-mediated deacetylation. The activity of IDH2 produces increased levels of NADPH, which facilitates regeneration of GSH from GSSG. Together, increased SOD2 and IDH activity increases the detoxification capacity of the mitochondria (Bause and Haigis 2013).

This study found that exposure to FB₁ induced oxidative stress, as noted by the increase in intracellular ROS and the corresponding increase in oxidative stress bio-markers (MDA and protein carbonyls). Cells responded to the highly oxidative environment created by FB₁, via the upregulation of the antioxidant transcription factor Nrf2 and its associated antioxidants—SOD2, CAT and GPx. Oxidative stress responses in the mitochondria (Sirt 3 and Lon-P1) were also upregulated in response to the elevated ROS induced by FB₁. Although there was an increase in the expression of all antioxidants and stress response proteins investigated, this may not be reflective of enzyme activity of these antioxidants. Further investigation into the enzymatic activities of these antioxidants should be carried to have a better understanding of the overall antioxidant capacity during exposure to FB₁.

Acknowledgments We thank Dr. D Moodley and Dr. A Phulukdaree for their assistance.

Funding information TA received financial support from the National Research Foundation (NRF) of South Africa and CHS (UKZN).

Compliance with ethical standards

Conflict of interest None.

References

- Abbes S, Ben Salah-Abbès J, Jebali R, Younes RB, Oueslati R (2016) Interaction of aflatoxin B₁ and fumonisin B₁ in mice causes immunotoxicity and oxidative stress: possible protective role using lactic acid bacteria. *J Immunotoxicol* 13:46–54. <https://doi.org/10.3109/1547691x.2014.997905>
- Apel K, Hirt H (2004) Reactive oxygen species: metabolism, oxidative stress, and signal transduction. *Annu Rev Plant Biol* 55:373–399. <https://doi.org/10.1146/annurev.arplant.55.031903.141701>
- Ayala A, Muñoz MF, Argüelles S (2014) Lipid peroxidation: production, metabolism, and signaling mechanisms of malondialdehyde and 4-hydroxy-2-nonenal. *Oxidative Med Cell Longev* 2014:1–31. <https://doi.org/10.1155/2014/360438>
- Bause AS, Haigis MC (2013) Sirt3 regulation of mitochondrial oxidative stress. *Exp Gerontol* 48:634–639. <https://doi.org/10.1016/j.exger.2012.08.007>
- Bellezza I, Giambanco I, Minelli A, Donato R (2018) Nrf2-Keap1 signaling in oxidative and reductive stress. *Biochim Biophys Acta* 1865:721–733. <https://doi.org/10.1016/j.bbamer.2018.02.010>
- Bernabucci U, Colavecchia L, Danieli PP, Basiricò L, Lacetera N, Nardone A, Ronchi B (2011) Aflatoxin B₁ and fumonisin B₁ affect the oxidative status of bovine peripheral blood mononuclear cells. *Toxicol in Vitro* 25:684–691. <https://doi.org/10.1016/j.tiv.2011.01.009>
- Birben E, Sahiner U, Sackesen C, Erzurum S, Kalayci O (2012) Oxidative stress and antioxidant defense. *World Allergy Organ J* 5:9–19. <https://doi.org/10.1097/WOX.0b013e3182439613>
- Bo C, Lu Y, Chen Y, Cheng J (2015) The role of Nrf2 in oxidative stress-induced endothelial injuries. *J Endocrinol:JOE-14-0662* doi:<https://doi.org/10.1530/JOE-14-0662>
- Bota DA, Davies KJ (2016) Mitochondrial Lon protease in human disease and ageing: including an etiologic classification of Lon-related diseases and disorders. *Free Radic Biol Med* 100:188–198. <https://doi.org/10.1016/j.freeradbiomed.2016.06.031>
- Brand MD, Orr AL, Perevoshchikova IV, Quinlan CL (2013) The role of mitochondrial function and cellular bioenergetics in ageing and disease. *Br J Dermatol* 169:1–8. <https://doi.org/10.1111/bjd.12208>
- Buendia I, Michalska P, Navarro E, Gameiro I, Egea J, Leon R (2016) Nrf2-ARE pathway: an emerging target against oxidative stress and neuroinflammation in neurodegenerative diseases. *Pharmacol Ther* 157:84–104. <https://doi.org/10.1016/j.pharmthera.2015.11.003>
- Chen Y, Dong H, Thompson DC, Shertzer HG, Nebert DW, Vasiliou V (2013) Glutathione defense mechanism in liver injury: insights from animal models. *Food Chem Toxicol* 60:38–44. <https://doi.org/10.1016/j.fct.2013.07.008>
- Chuturgoon A, Phulukdaree A, Moodley D (2014) Fumonisin B₁ induces global DNA hypomethylation in HepG2 cells – an alternative mechanism of action. *Toxicology* 315:65–69. <https://doi.org/10.1016/j.tox.2013.11.004>
- Chuturgoon AA, Phulukdaree A, Moodley D (2015) Fumonisin B₁ inhibits apoptosis in HepG2 cells by inducing Birc-8/ILP-2. *Toxicol Lett* 235:67–74. <https://doi.org/10.1016/j.toxlet.2015.03.006>
- Domijan A-M, Abramov AY (2011) Fumonisin B₁ inhibits mitochondrial respiration and deregulates calcium homeostasis—implication to mechanism of cell toxicity. *Int J Biochem Cell Biol* 43:897–904. <https://doi.org/10.1016/j.biocel.2011.03.003>
- Fandohan P, Hell K, Marasas W, Wingfield M (2003) Infection of maize by *Fusarium* species and contamination with fumonisin in Africa. *Afr J Biotechnol* 2:570–579. <https://doi.org/10.5897/AJB2003.000-1110>
- Filomeni G, Rotilio G, Ciriolo MR (2002) Cell signalling and the glutathione redox system. *Biochem Pharmacol* 64:1057–1064. [https://doi.org/10.1016/S0006-2952\(02\)01176-0](https://doi.org/10.1016/S0006-2952(02)01176-0)
- Furukawa M, Xiong Y (2005) BTB protein Keap1 targets antioxidant transcription factor Nrf2 for ubiquitination by the Cullin 3-Roc1 ligase. *Mol Cell Biol* 25:162–171. <https://doi.org/10.1128/mcb.25.1.162-171.2005>
- Gibellini L, Pinti M, Beretti F, Pierri CL, Onofrio A, Riccio M, Carnevale G, De Biasi S, Nasi M, Torelli F (2014) Sirtuin 3 interacts with Lon protease and regulates its acetylation status. *Mitochondrion* 18:76–81. <https://doi.org/10.1016/j.mito.2014.08.001>
- Halliwell B (2003) Oxidative stress in cell culture: an under-appreciated problem? *FEBS Lett* 540:3–6. [https://doi.org/10.1016/S0014-5793\(03\)00235-7](https://doi.org/10.1016/S0014-5793(03)00235-7)
- Huang H-C, Nguyen T, Pickett CB (2002) Phosphorylation of Nrf2 at Ser40 by protein kinase C regulates antioxidant response element-mediated transcription. *J Biol Chem* 277:42769–42774. <https://doi.org/10.1074/jbc.M206911200>
- Itoh K, Chiba T, Takahashi S, Ishii T, Igarashi K, Katoh Y, Oyake T, Hayashi N, Satoh K, Hatayama I, Yamamoto M, Nabeshima Y-i (1997) An Nrf2/small Maf heterodimer mediates the induction of phase II detoxifying enzyme genes through antioxidant response elements. *Biochem Biophys Res Commun* 236:313–322. <https://doi.org/10.1006/bbrc.1997.6943>
- Itoh K, Wakabayashi N, Katoh Y, Ishii T, Igarashi K, Engel JD, Yamamoto M (1999) Keap1 represses nuclear activation of antioxidant responsive elements by Nrf2 through binding to the amino-terminal Neh2 domain. *Genes Dev* 13:76–86. <https://doi.org/10.1101/gad.13.1.76>
- Johannsen DL, Ravussin E (2009) The role of mitochondria in health and disease. *Curr Opin Pharmacol* 9:780–786. <https://doi.org/10.1016/j.coph.2009.09.002>
- Kensler TW, Wakabayashi N, Biswal S (2007) Cell survival responses to environmental stresses via the Keap1-Nrf2-ARE pathway. *Annu Rev Pharmacol Toxicol* 47:89–116. <https://doi.org/10.1146/annurev.pharmtox.46.120604.141046>
- Khan RB, Phulukdaree A, Chuturgoon AA (2018) Fumonisin B₁ induces oxidative stress in oesophageal (SNO) cancer cells. *Toxicol* 141:104–111. <https://doi.org/10.1016/j.toxicol.2017.12.041>
- Kouadio JH, Mobio TA, Baudrimont I, Moukha S, Dano SD, Creppy EE (2005) Comparative study of cytotoxicity and oxidative stress induced by deoxynivalenol, zearalenone or fumonisin B₁ in human intestinal cell line Caco-2. *Toxicology* 213:56–65. <https://doi.org/10.1016/j.tox.2005.05.010>
- Lenaz G, Genova ML (2010) Structure and organization of mitochondrial respiratory complexes: a new understanding of an old subject. *Antioxid Redox Signal* 12:961–1008. <https://doi.org/10.1089/ars.2009.2704>
- Livak KJ, Schmittgen TD (2001) Analysis of relative gene expression data using real-time quantitative PCR and the 2^{-Delta-Delta CT} method. *Methods* 25:402–408. <https://doi.org/10.1006/meth.2001.1262>
- Lu SC (2009) Regulation of glutathione synthesis. *Mol Asp Med* 30:42–59. <https://doi.org/10.1016/j.mam.2008.05.005>
- Lushchak VI (2012) Glutathione homeostasis and functions: potential targets for medical interventions. *J Amino Acids* 2012:1–26. <https://doi.org/10.1155/2012/736837>

- Ma Q (2013) Role of Nrf2 in oxidative stress and toxicity. *Annu Rev Pharmacol Toxicol* 53:401–426. <https://doi.org/10.1146/annurev-pharmtox-011112-140320>
- Marasas WF (2001) Discovery and occurrence of the fumonisins: a historical perspective. *Environ Health Perspect* 109:239–243. <https://doi.org/10.2307/3435014>
- Marasas WF, Riley RT, Hendricks KA, Stevens VL, Sadler TW, Gelineau-van Waes J, Missmer SA, Cabrera J, Torres O, Gelderblom WC, Allegood J, Martinez C, Maddox J, Miller JD, Starr L, Sullards MC, Roman AV, Voss KA, Wang E, Merrill AH Jr (2004) Fumonisins disrupt sphingolipid metabolism, folate transport, and neural tube development in embryo culture and *in vivo*: a potential risk factor for human neural tube defects among populations consuming fumonisin-contaminated maize. *J Nutr* 134:711–716. <https://doi.org/10.1093/jn/134.4.711>
- Marin S, Ramos AJ, Cano-Sancho G, Sanchis V (2013) Mycotoxins: occurrence, toxicology, and exposure assessment. *Food Chem Toxicol* 60:218–237. <https://doi.org/10.1016/j.fct.2013.07.047>
- Mary VS, Theumer MG, Arias SL, Rubinstein HR (2012) Reactive oxygen species sources and biomolecular oxidative damage induced by aflatoxin B₁ and fumonisin B₁ in rat spleen mononuclear cells. *Toxicology* 302:299–307. <https://doi.org/10.1016/j.tox.2012.08.012>
- Murphy MP (2009) How mitochondria produce reactive oxygen species. *Biochem J* 417:1–13. <https://doi.org/10.1042/bj20081386>
- Nagiah S, Phulukdaree A, Chuturgoon A (2015) Mitochondrial and oxidative stress response in HepG2 cells following acute and prolonged exposure to antiretroviral drugs. *J Cell Biochem* 116:1939–1946. <https://doi.org/10.1002/jcb.25149>
- Ngo JK, Pomatto LC, Davies KJ (2013) Upregulation of the mitochondrial Lon protease allows adaptation to acute oxidative stress but dysregulation is associated with chronic stress, disease, and ageing. *Redox Biol* 1:258–264. <https://doi.org/10.1016/j.redox.2013.01.015>
- Nguyen T, Sherratt PJ, Pickett CB (2003) Regulatory mechanisms controlling gene expression mediated by the antioxidant response element. *Annu Rev Pharmacol Toxicol* 43:233–260. <https://doi.org/10.1146/annurev.pharmtox.43.100901.140229>
- Nguyen T, Nioi P, Pickett CB (2009) The Nrf2-antioxidant response element signaling pathway and its activation by oxidative stress. *J Biol Chem* 284:13291–13295. <https://doi.org/10.1074/jbc.R900010200>
- Pinelli E, Poux N, Garren L, Pipy B, Castegnaro M, Miller DJ, Pfohl-Leschkowitz A (1999) Activation of mitogen-activated protein kinase by fumonisin B₁ stimulates cPLA2 phosphorylation, the arachidonic acid cascade and cAMP production. *Carcinogenesis* 20:1683–1688. <https://doi.org/10.1093/carcin/20.9.1683>
- Pinti M, Gibellini L, Liu Y, Xu S, Lu B, Cossarizza A (2015) Mitochondrial Lon protease at the crossroads of oxidative stress, ageing and cancer. *Cell Mol Life Sci* 72:4807–4824. <https://doi.org/10.1007/s00018-015-2039-3>
- Ray PD, Huang BW, Tsuji Y (2012) Reactive oxygen species (ROS) homeostasis and redox regulation in cellular signaling. *Cell Signal* 24:981–990. <https://doi.org/10.1016/j.cellsig.2012.01.008>
- Rheeder J (1992) *Fusarium moniliforme* and fumonisins in corn in relation to human oesophageal cancer in Transkei. *Phytopathology* 82:353–357. <https://doi.org/10.1094/Phyto-82-353>
- Rheeder JP, Marasas WF, Vismar HF (2002) Production of fumonisin analogs by *Fusarium* species. *Appl Environ Microbiol* 68:2101–2105. <https://doi.org/10.1128/AEM.68.5.2101-2105.2002>
- Riley RT, Voss KA (2006) Differential sensitivity of rat kidney and liver to fumonisin toxicity: organ-specific differences in toxin accumulation and sphingoid base metabolism. *Toxicol Sci* 92:335–345. <https://doi.org/10.1093/toxsci/kfj198>
- Riley RT, Enongene E, Voss KA, Norred WP, Meredith FI, Sharma RP, Spitsbergen J, Williams DE, Carlson DB, Merrill AHJ (2001) Sphingolipid perturbations as mechanisms for fumonisin carcinogenesis. *Environ Health Perspect* 109(Suppl 2):301–308. <https://doi.org/10.1289/ehp.01109s2301>
- Rojo de la Vega M, Dodson M, Chapman E, Zhang DD (2016) Nrf2-targeted therapeutics: new targets and modes of Nrf2 regulation. *Curr Opin Toxicol* 1:62–70. <https://doi.org/10.1016/j.cotox.2016.10.005>
- Ross PF, Nelson PE, Richard JL, Osweiler GD, Rice LG, Plattner RD, Wilson TM (1990) Production of fumonisins by *Fusarium moniliforme* and *Fusarium proliferatum* isolates associated with equine leukoencephalomalacia and a pulmonary oedema syndrome in swine. *Appl Environ Microbiol* 56:3225–3226
- Sakamuru S, Attene-Ramos MS, Xia M (2016) Mitochondrial membrane potential assay. *Methods Mol Biol* 1473:17–22. https://doi.org/10.1007/978-1-4939-6346-1_2
- Schieber M, Chandel NS (2014) ROS function in redox signaling and oxidative stress. *Curr Biol* 24:R453–R462. <https://doi.org/10.1016/j.cub.2014.03.034>
- Sena LA, Chandel NS (2012) Physiological roles of mitochondrial reactive oxygen species. *Mol Cell* 48:158–167. <https://doi.org/10.1016/j.molcel.2012.09.025>
- Sheik Abdul N, Nagiah S, Chuturgoon AA (2016) Fusaric acid induces mitochondrial stress in human hepatocellular carcinoma (HepG2) cells. *Toxicol* 119:336–344. <https://doi.org/10.1016/j.toxicol.2016.07.002>
- Shephard GS, Thiel PG, Stockenstrom S, Sydenham EW (1996) Worldwide survey of fumonisin contamination of corn and corn-based products. *J AOAC Int* 79:671–687
- Shephard GS, Marasas WF, Burger HM, Somdyala NI, Rheeder JP, Van der Westhuizen L, Gatyeni P, Van Schalkwyk DJ (2007) Exposure assessment for fumonisins in the former Transkei region of South Africa. *Food Addit Contam* 24:621–629. <https://doi.org/10.1080/02652030601101136>
- Sporn MB, Liby KT (2012) Nrf2 and cancer: the good, the bad and the importance of context. *Nat Rev Cancer* 12:564–571. <https://doi.org/10.1038/nrc3278>
- Stevens VL, Tang J (1997) Fumonisin B₁-induced sphingolipid depletion inhibits vitamin uptake via the glycosylphosphatidylinositol-anchored folate receptor. *J Biol Chem* 272:18020–18025. <https://doi.org/10.1074/jbc.272.29.18020>
- Stockmann-Juvala H, Savolainen K (2008) A review of the toxic effects and mechanisms of action of fumonisin B₁. *Hum Exp Toxicol* 27:799–809. <https://doi.org/10.1177/0960327108099525>
- Stockmann-Juvala H, Mikkola J, Naarala J, Loikkanen J, Elovaara E, Savolainen K (2004a) Fumonisin B₁-induced toxicity and oxidative damage in U-118MG glioblastoma cells. *Toxicology* 202:173–183. <https://doi.org/10.1016/j.tox.2004.05.002>
- Stockmann-Juvala H, Mikkola J, Naarala J, Loikkanen J, Elovaara E, Savolainen K (2004b) Oxidative stress induced by fumonisin B₁ in continuous human and rodent neural cell cultures. *Free Radic Res* 38:933–942. <https://doi.org/10.1080/10715760412331273205>
- Sun G, Wang S, Hu X, Su J, Huang T, Yu J, Tang L, Gao W, Wang JS (2007) Fumonisin B₁ contamination of home-grown corn in high-risk areas for oesophageal and liver cancer in China. *Food Addit Contam* 24:181–185. <https://doi.org/10.1080/02652030601013471>
- Turrens JF (2003) Mitochondrial formation of reactive oxygen species. *J Physiol* 552:335–344. <https://doi.org/10.1113/jphysiol.2003.049478>
- Valko M, Leibfritz D, Moncol J, Cronin MT, Mazur M, Telser J (2007) Free radicals and antioxidants in normal physiological functions and human disease. *Int J Biochem Cell Biol* 39:44–84. <https://doi.org/10.1016/j.biocel.2006.07.001>
- Vomund S, Schafer A, Pamham MJ, Brune B, von Knethen A (2017) Nrf2, the master regulator of antioxidant responses. *Int J Mol Sci* 18(12). doi:<https://doi.org/10.3390/ijms18122772>

- Voss KA, Howard PC, Riley RT, Sharma RP, Bucci TJ, Lorentzen RJ (2002) Carcinogenicity and mechanism of action of fumonisin B₁: a mycotoxin produced by *Fusarium moniliforme* (*F. verticillioides*). *Cancer Detect Prev* 26:1–9. [https://doi.org/10.1016/S0361-090X\(02\)00011-9](https://doi.org/10.1016/S0361-090X(02)00011-9)
- Wang X, Wu Q, Wan D, Liu Q, Chen D, Liu Z, Martinez-Larranaga MR, Martinez MA, Anadon A, Yuan Z (2016) Fumonisin: oxidative stress-mediated toxicity and metabolism *in vivo* and *in vitro*. *Arch Toxicol* 90:81–101. <https://doi.org/10.1007/s00204-015-1604-8>
- Weir HJ, Lane JD, Balthasar N (2013) Sirt3: a central regulator of mitochondrial adaptation in health and disease. *Genes Cancer* 4:118–124. <https://doi.org/10.1177/1947601913476949>
- Whitmarsh AJ, Davis RJ (2000) Regulation of transcription factor function by phosphorylation. *Cell Mol Life Sci: CMLS* 57:1172–1183. <https://doi.org/10.1007/PL00000757>
- Yeung JM, Wang H-Y, Prelusky DB (1996) Fumonisin B₁ induces protein kinase C translocation via direct interaction with diacylglycerol binding site. *Toxicol Appl Pharmacol* 141:178–184. [https://doi.org/10.1016/S0041-008X\(96\)80023-8](https://doi.org/10.1016/S0041-008X(96)80023-8)
- Zheng J, Zhang Y, Xu W, Luo Y, Hao J, Shen XL, Yang X, Li X, Huang K (2013) Zinc protects HepG2 cells against the oxidative damage and DNA damage induced by ochratoxin A. *Toxicol Appl Pharmacol* 268:123–131. <https://doi.org/10.1016/j.taap.2013.01.021>

5628

5629

ADDENDUM B

5630 Ethical Approval Letter



29 May 2019

Ms T Arumugan (213531562)
 School of Laboratory Medicine and Medical Sciences
 College of Health Sciences
 cyborglona@gmail.com

Dear Ms Arumugan

Protocol: An investigation into the epigenetic and subsequent biochemical effects of Fumonisin B1 in human Liver (HepG2), oesophageal (SNO) and kidney (HEK293) cells.
 Degree: PhD BREC Ref No: BE322/19

EXPEDITED APPLICATION: APPROVAL LETTER

A sub-committee of the Biomedical Research Ethics Committee has considered and noted your application received 05 April 2019.

Please ensure that site permissions are obtained and forwarded to BREC for approval before commencing research at a site.

This approval is valid for one year from 29 May 2019. To ensure uninterrupted approval of this study beyond the approval expiry date, an application for recertification must be submitted to BREC on the appropriate BREC form 2-3 months before the expiry date.

Any amendments to this study, unless urgently required to ensure safety of participants, must be approved by BREC prior to implementation.

Your acceptance of this approval denotes your compliance with South African National Research Ethics Guidelines (2015), South African National Good Clinical Practice Guidelines (2006) (if applicable) and with UKZN BREC ethics requirements as contained in the UKZN BREC Terms of Reference and Standard Operating Procedures, all available at <http://research.ukzn.ac.za/Research-Ethics/Biomedical-Research-Ethics.aspx>.

BREC is registered with the South African National Health Research Ethics Council (REC-290408-009). BREC has US Office for Human Research Protections (OHRP) Federal-wide Assurance (FWA 678).

The sub-committee's decision will be noted by a full Committee at its next meeting taking place on 11 June 2019.

Yours sincerely



Prof V Rambiritch
 Chair: Biomedical Research Ethics Committee

cc: Postgrad Admin: dudhrajhp@ukzn.ac.za Supervisor: CHUTUR@stu.ukzn.ac.za Nagiah.savania@gmail.com

Biomedical Research Ethics Committee

Professor V Rambiritch (Chair)

Westville Campus, Govan Mbeki Building

Postal Address: Private Bag X54001, Durban 4000

Telephone: +27 (0) 31 260 2486 Facsimile: +27 (0) 31 260 4809 Email: brec@ukzn.ac.za

Website: <http://research.ukzn.ac.za/Research-Ethics/Biomedical-Research-Ethics.aspx>



100 YEARS OF ACADEMIC EXCELLENCE

Founding Campuses: ■ Edgewood ■ Howard College ■ Medical School ■ Pietermaritzburg ■ Westville

5631